Characterization of regulatory mechanisms by ^{V600E}BRAF

Thesis submitted for the degree of

Doctor in Philosophy

at the University of Leicester

By

Maria M. Aguilar Hernández (BSc, MSc, University of Leicester, UK)

Department of Biochemistry

University of Leicester

December 2012

ABSTRACT

Characterization of regulatory mechanisms by ^{V600E}BRAF

Maria Aguilar

More than 90% of *BRAF* mutations in human cancer are represented by a valine to glutamic acid mutation at residue 600 known as the ^{V600E}*BRAF* mutation. Our laboratory has generated mouse models expressing a conditional knock-in allele of *Braf*^{V600E} and in previous work we have shown that expression of the oncogene in a range of tissues including embryonic fibroblasts (MEFs), lung tissue, melanocytes and gastrointestinal crypts induces cell proliferation followed by senescence. Previous work from our laboratory showed that in the transition from proliferation to senescence, a decrease in Braf protein levels occurred in lung adenomas from *Braf*^{V600E} mice. I have further investigated the mechanisms underpinning this behavior in two different cellular systems: primary mice embryonic fibroblasts conditionally expressing endogenous ^{V600E}Braf and HEK293^{T} cells transiently expressing ^{V600E}BRAF. My findings show that in a similar way to *Braf*^{V600E} lung adenomas, a reduction in Braf expression is observed in both cellular systems in addition to a decrease in Craf protein levels. I found through qRTPCR experiments that *Braf* and *Craf* mRNA levels are not downregulated in *Braf*^{V600E} MEFs. However, a reduction in the stability of BRAF and CRAF proteins in the soluble fraction and a simultaneous accumulation of these proteins in the insoluble fractions was observed in both cellular systems. Inhibition of the Erk pathway at the level of Braf and Mek rescued Braf and Craf expression in Braf^{V600E} MEFs indicating that the expression of these proteins is dependent on Braf and Mek kinase activities. LC-MS/MS analysis of ectopic ^{WT}CRAF when co-expressed with ectopic ^{V600E}BRAF showed that the accumulation of ectopic ^{WT}CRAF in the insoluble fraction was associated with the phosphorylation of six novel serine residues in CRAF. The mutation of these phospho-residues to non-phosphorylatable alanines rescued ectopic ^{WT}CRAF expression in the soluble fraction and prevented the accumulation of this protein in the insoluble fraction. Although phosphorylation of Ser675 in ectopic ^{V600E}BRAF was also specifically detected in the insoluble fraction, mutation of this site did not alter the distribution of this protein. Thus, I propose that the post-translational regulation of BRAF and CRAF expression is an alternative mechanism for the regulation of the MAPK pathway output in cells expressing the ^{V600E}BRAF oncogene.

ACKNOWLEDGEMENTS

I would like to thank my supervisor Prof. Catrin Pritchard for her patience, continual support, encouragement and trust throughout the project. I am also very grateful to her for always being so approachable and for the constant effort she made in trying to understand my ideas and improve the communication between us. I would like to thank the members of the thesis committee, Dr. Sue Shackleton and Dr. Terry Herbert for their guidance and useful advice. I would like to thank those people who have helped me with experimental techniques described in the thesis, Dr. Nicholas Sylvius, Miss Reshma Vaghela and Mr. Thimma Reddy for their assistance in qRTPCR experiments; Bipin Patel for his assistance and invaluable advice with mass spectrometry analysis and site-directed mutagenesis; Dr. Neil Bate for his help with site-directed mutagenesis; Dr. Andrew Bottril and Miss Shairbanu Ibrahim for their assistance and useful discussions on mass spectrometry analysis; Miss Natallie Allock and Mr. Stefan Hayman for their assistance with electron microscopy; Dr. Kees for his assistance in the use of Image J software and Dr. Fiona Hey for her assistance in the design of the ribbon structures.

I would like to thank all the past and present members of the CAP lab. In special, I would like to thank, Dr. Tami Kamata for his invaluable guidance and useful discussions throughout the project; Dr. Catherine Noble for teaching me all the basic experimental techniques and being so patience; Dr. Hong Jin and Maggie Cheung for sharing their experimental data which gave direction to my project and for their useful technical advice and support; Susan Giblett for her assistance with mouse and cultural support.

I would like to specially thank, Susan Giblett, Maggie Cheung, Catherine Noble, Katerina Andreadi, Emma Stringer, Kimberly Snell, Ellie Karekla, Kath Clarke, Linda Carragher, Eilis Byrne, Pooyeh Farahmand, Samantha Carrera, Eric and Tami for their friendship and for making me feel like in home.

I wish to thank my parents, my brother, my sister, my two grandmothers and my uncle Manuel for their constant support, guidance and love throughout the project. For me, you will always be an example of faith and perseverance and a truth inspiration. I specially would like to thank Jianling Xie (“Alex”) for always being there for me and for his truth love and friendship. Finally, I would like to dedicate this work to God, who has being beside me all the time!

CONTENTS

ABBREVIATIONS

MAP3K	MAP kinase kinase kinase
MAP2K	MAP kinase kinase
MAPK	MAP kinase
RSK	p90 Ribosomal S6 kinases
MSK	Mitogen and stress-activated Kinases
MNK	MAPK-interacting kinases
MK	MAPK-activated protein Kinase
MAPKAPKs	MAPK-activated protein kinases
JNK	c-Jun N-terminal kinase
ERK	Extracellular signal regulated kinase
NLK	Nemo-like kinase
KSR	Kinase suppressor of Ras
MP	MEK-partner
IKAP	I·B Kinase complex-associated protein
JIP	JNK interacting proteins
TKD	Tyrosine kinase domains
RTKs	Receptor tyrosine kinases
ATP	Adenosine triphosphate
EGFR	Epidermal growth factor receptor
SH	Src homology
GRB	Growth factor receptor-bound protein
STAT	Signal transducer and activator of transcription
PLC	Phospholipase C
CBL	Casitas B-lineage lymphoma

JK	Janus kinase
GAB-1	GRB2-associated-binding protein 1
PTP	Protein tyrosine phopshatase
SOS	Son of Sevenless
GDP	Guanosine diphosphate
GTP	Guanosine-5'-triphosphate
PDGF	Platelet-derived growth factor
RAP	ribosomal acidic P protein
RHEB	Ras homolog enriched in brain
RAF	Rapidly accelerated fibrosarcoma
ERK	Endoplasmic reticulum
GEF	Guanine nucleotide exchange factors
GAP	GTPase activating proteins
DAG	Diacylglycerol
CR	Conserved region
CRD	Cystein rich domain
RBD	Ras binding domain
PEST	Proline (P), glutamic acid (E), serine (S), and threonine (T) rich sequence
PKA	Protein kinase A
PKC	Protein kinase C
AKT/PKB	Protein kinase B
PI3K	Phosphatidylinositol 3-kinases
PP5	Protein phosphatase 5
C-TAK	Cdc25C associated protein kinase

HSP	Heat shock protein
HIP	Hsp70-interacting protein
CDC	Cell division cycle proteins
CHIP	Carboxy terminus of Hsp70-interacting protein
HECT	homologous to E6-AP terminus
RING	Really interesting new gene
U-box	U-box protein
RNF149	RING finger protein 149
MEK	Mitogen-activated protein kinase
COSMIC	Catalogue of somatic mutations in cancer
CDK-1	Cyclin-dependent kinase
ELK-1	E twenty-six (ETS)-like transcription factor 1
SAP-1	SRF accessory protein 1
PDK1	Pyruvate dehydrogenase lipoamide kinase isozyme 1
IEG	Immediate early gene
CREB	cAMP response element binding protein
ETS	E-twenty six
SRF	serum response factors
BCL-2	B-cell lymphoma 2
MCL-1	Induced myeloid leukemia cell differentiation protein
BAX	Bcl-2-associated-X protein
BAK	bcl-2 homologous antagonist/killer
BOK	Bcl-2-related ovarian killer
BID	BH3 interacting-domain death agonist
BIM	BCL-2-interacting mediator of cell death

BLK	B Lymphocyte Kinase Protein
BAD	Bcl-2-associated death promoter
BMF	Bcl-2-modifying factor
HRK	Activator of apoptosis harakiri
PUMA	p53 upregulated modulator of apoptosis
NOXA/PMAIP1	PMA-induced protein 1
TNF	tumor necrosis factor
FADD	Fas-associated death domain protein
TRADD	TNFR-associated death domain protein
FOXO	Forkhead box
IAP	Inhibitor of apoptosis proteins
DISC	Death-inducing signalling complex
APAF-1	Apoptotic protease activating factor-1
TRAIL	TNF-related apoptosis-inducing ligand
ATG	Autophagy-related gene
PAS	pre-autophagosomal structure
ULK	Unc-51-like kinase
LC3	Microtubule-associated protein 1 light chain 3
GFP	Green fluorescent protein
mTOR	mammalian target of rapamycin
PIP2	Phosphatidylinositol (4,5)-bisphosphate
PIP3	Phosphatidylinositol (3,4,5)-trisphosphate
TSC	Tuberous sclerosis complex
S6K1	Ribosomal S6 kinase
4EBP1	Eukaryotic translation initiation factor 4E-binding protein 1

AMPK	5' AMP-activated protein kinase
GAIP	Ga-interacting protein
ROS	Reactive oxygen species
RNA	Ribonucleic acid
DNA	Deoxyribonucleic acid
UV	ultraviolet
pRB	retinoblastoma protein
SA b-gal	senescent-associated b-galactosidase
SASP	Senescence-Associated Secretory Phenotype
SAHF	Senescence-Associated Heterochromatic Foci
ATM	Ataxia telangiectasia mutated
BRCA1	breast cancer type 1 susceptibility protein
H2AX	Phosphorylated histone H2A
53BP1	p53 binding protein 1
GADD45	Growth Arrest and DNA Damage
CHK	Checkpoint kinase
MDM	Murine double minute
E2F	E2 promoter binding factor

CHAPTER 1 Introduction

1.1 Mammalian MAPK cascades

MAPK pathways are signaling platforms through which extracellular signals are routed from the plasma membrane to intracellular targets. This mechanism of signal transduction is able to unleash important cellular processes such as: growth, proliferation, differentiation, migration and apoptosis. Each cascade consists of 3 core kinases: MAP3K (MAP kinase kinase kinase), MAP2K (MAP kinase kinase), MAPK (MAP kinase) and often also additional upstream MAP4K or GTPases (Widmann et al. 1999). The signal is propagated by sequential phosphorylations which eventually lead to the activation of the MAPK proteins (Pearson et al. 2001).

Some of the cytoplasmic substrates of activated MAPKs are: p90 Ribosomal S6 Kinases (RSKs), Mitogen and Stress-activated Kinases (MSKs), MAPK-interacting kinases (MSKs), MAPK-activated protein Kinase 2/3 (MK2/3), and MK5. All of these kinases, which represent an additional amplification step in the MAPK catalytic cascade, belong to a family of proteins called the MAPK-activated protein kinases (MAPKAPKs) (Figure 1.1). In quiescent cells, generally the MAPKs are localized in the cytoplasm; however, upon stimulation, they shuttle to the nucleus where they directly phosphorylate other substrates.

In mammals, 14 MAPKs have been identified which are classified into two main groups: conventional and atypical MAPKs (Figure 1.1). Among the conventional MAPK cascades, four subgroups have been established: Extracellular signal Regulated Kinase 1 and 2 (ERK1/2) (Cobb, Boulton & Robbins 1991), c-Jun N-terminal Kinase (JNK) (Ip, Davis 1998), p38 MAPK and ERK5 (Zhou, Bao & Dixon 1995). The atypical MAPKs comprise three subgroups integrated by Extracellular signal Regulated Kinase 3 and 4 (ERK3/4), Extracellular signal Regulated Kinase 7 and 8 (ERK 7/8) and Nemo-Like Kinase (NLK)

Figure 1.1 The MAPK signaling pathways (Taken from Cargnello, Roux 2011b). Seven types of MAPKs have been detected, four of them are classified as conventional MAPKs and the remaining three are known as atypical MAPKs. MAP4Ks or GTPases (not shown in the diagram) activate MAP3Ks (MAPKKK) which in turn phosphorylate and activate MAP2Ks (MAPKK) which are responsible for the phosphorylation and activation of MAPKs. Among various substrates in the cytoplasm, the activated MAPKs are able to phosphorylate and activate five different subgroups of MAPKAPKs including: RSK, MSK, MNK, MK2/3 and MK5. Dotted lines indicate that, although reported, substrate regulation by the respective kinase remains to be thoroughly demonstrated. The γ and δ isoforms of p38 are in parentheses to indicate that they have not been shown to promote MAPKAPK activation.

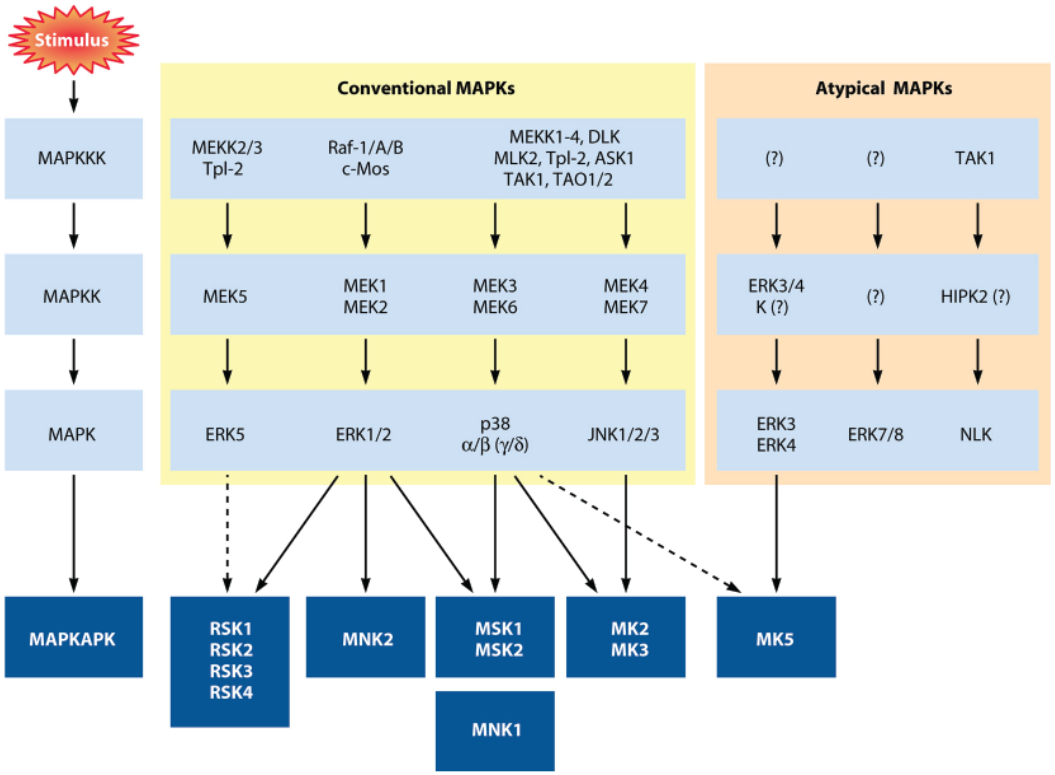

(Figure 1.1). The main characteristic of the atypical MAPKs is that they do not share the three-tiered cascade organization of the conventional MAPKs. For example, the phosphorylation of the conserved motif (TEY) needed for ERK7 activation appears to be catalyzed by ERK7 itself instead of the upstream MAPKK.

A common feature in the activation of the MAPK cascades is the key role played by the scaffold molecules. These proteins act as platforms in order to regulate the specificity of the MAPK cascades signaling (Harris et al. 2001, Park, Zarrinpar & Lim 2003). In the conventional MAPKs, the ERK pathway includes Kinase Suppressor of Ras (KSR), MEK-Partner 1 (MP-1) and β-arrestin 2 as their scaffold proteins while the JNK pathway depends on CrkII, filamin, I·B Kinase complex-Associated Protein (IKAP) and the JNK Interacting Proteins (JIP) family for this activity. Specifically, JIP-2 and JIP-4 act as scaffolds for the p38 pathway. In the ERK5 pathway, MEK5 has been recognized to bind to MEKK2 and ERK5 promoting the activation of the latter (Morrison, Davis 2003)

1.2 The RAS/RAF/MEK/ERK pathway

Although the ERK pathway can be activated by various stimuli such as hormones, cytokines, osmotic stress and microtubule disorganization, the role of growth factors in the activation of ERK has occupied main stage in cancer research (Robinson, Cobb 1997). In this pathway, the binding of growth factors or mitogens to receptor tyrosine kinases (RTKs) triggers GTP loading of the RAS GTPase. The RAS protein, which in most cases is attached to the plasma membrane, recruits cytosolic RAF kinases to this region and promotes their activation by unknown kinases. Then, RAF proteins phosphorylate and activate MEK kinases (MEK1 and MEK2), which in turn phosphorylate and activate ERK kinases (ERK1 and ERK2). Active ERK phosphorylates numerous cytoplasmic and

nuclear targets which regulation, influence processes such as proliferation, differentiation, survival, migration, angiogenesis and chromatin remodelling (Dhillon et al. 2007) (Figure 1.2).

Cancer is the result of various genetic changes that confer different types of growth advantage to normal cells. In 2000, Hanahan and Weinberg gathered these functional capabilities into six main alterations: self-sufficiency in growth signals, insensitivity to antigrowth signals, evasion of apoptosis, limitless replicative potential, sustained angiogenesis, and tissue invasion and metastasis (Hanahan, Weinberg 2000).

ERK pathway contains two of the oncogenes that are more commonly found in human cancers: *RAS* and *RAF*. Thus hyperactivation of ERK pathway as a result of activating mutations around the RAS-RAF axis suggests that this is a key regulatory point in cancer development (Dhillon et al. 2007).

1.2.1 Signal transduction through RTKs

Receptor Tyrosine Kinases (RTKs) are molecules localized in the extra-cellular region that allow the cell to sense its surrounding (Lemmon, Schlessinger 2010). The early observation that ligand binding to RTKs induced their autophosphorylation, implied an important role for these molecules in cellular proliferation (Hunter, Marais 2010, Hunter 2009). There are 58 types of RTKs in the human genome which have been classified according to their structures in 20 subfamilies as shown in Figure 1.3 (Robinson, Wu & Lin 2000). Specifically, the activation of the ERK pathway occurs upon the binding of EGF, PDGF, NFG and VEGF to their correspondent receptors.

Figure 1.2 Activation of the ERK signaling pathway (Taken from Nissan, Solit 2011b). ERK pathway activation can occur by the binding of growth factors to the correspondent RTK. SOS is recruited from the cytosol to the plasma membrane by GRB2. Then, SOS activates RAS by catalyzing the exchange of GDP for GTP which allows RAS interaction with RAF proteins. Incompletely defined membrane associated kinases activate RAF which in turn phosphorylate MEK. Activated MEK transmits the signal to ERK. The signaling cascade is negatively regulated by Sprouty proteins (SPRY) and dual-specificity phosphatases (DUSP).

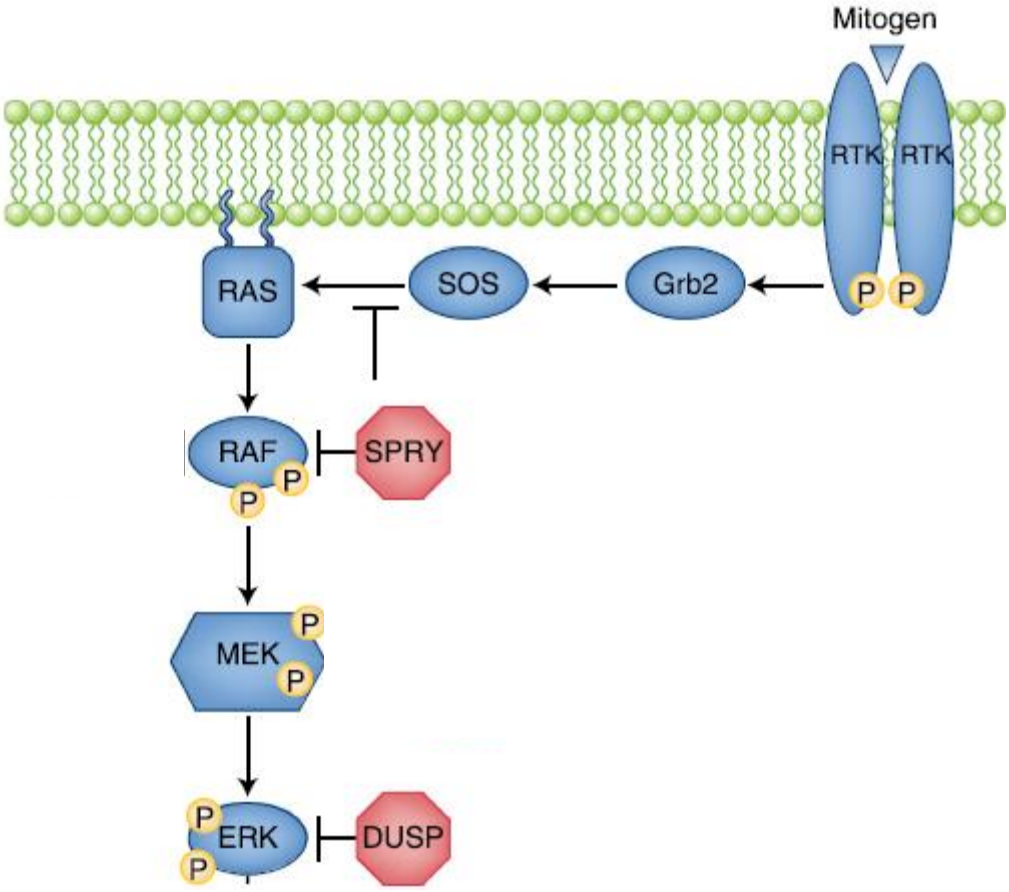

RTKs structure consists of a ligand binding domain, a single transmembrane helix and a tyrosine kinase domain plus the carboxy (C-) terminal and juxtamembrane regulatory regions (Hubbard 2004). Although the tyrosine kinase domains (TKDs) share the same structure consisting of a N´lobe which contains the αC helix, a C´terminal lobe which contains the activation loop and the hinge region which comprises the ATP pocket, the activation mechanism of each RTK dimer differs from each other (Lemmon, Schlessinger 2010).

In the case of EGFR, the bivalent ligand makes contact with two different domains within a single receptor molecule causing a conformational change in the extracellular region. The exposure of the previously occluded dimerization site results in the interaction with a second ligand bound receptor molecule. In the newly formed EGFR dimer, the C´lobe of one TKD called the “activator” makes intimate contact with the N´lobe of the other TKD called the “receiver”. This contact induces conformational changes in the N´lobe of the “receiver” kinase that disrupt the autoinhibitory state seen in the monomer. As a result the receiver kinase can adopt the characteristic active configuration without phosphorylation of its activation loop (Burgess et al. 2003, Bouyain et al. 2005, Garrett et al. 2002). At this point, the kinase activity of the EGFR receptor is enough to promote the autophosphorylation of multiple residues that act as binding sites for proteins containing SH2 or PTB domains (Pawson 2004, Schlessinger, Lemmon 2003). An alternative way to recruit these proteins is through docking proteins that are associated to the RTKs (Schlessinger 2000). The rest of the downstream signaling is integrated by two different types of proteins: proteins that interact with SH2 proteins and are characterized by the presence of SH3, WW and PDZ domains (Seet et al. 2006) and the second group that binds to phospholipids and contain the PX, C1, C2 and FYVE domains. In the case of EGFR, the SRC, GRB2, STAT3/35, PLC-γ (Rhee 1991), SHC (Pelicci et al. 1992), CBL,

Figure 1.3 Receptor Tyrosine Kinase subfamilies (Taken from Lemmon, Schlessinger 2010). The tyrosine kinase receptors are categorized into 20 subfamilies depending on their structure. Schematical representation of each family of receptors with members listed below. All of the receptors share in common very similar cytoplasmic tyrosine kinase domains (red rectangles) whereas their ectodomains are highly variable.

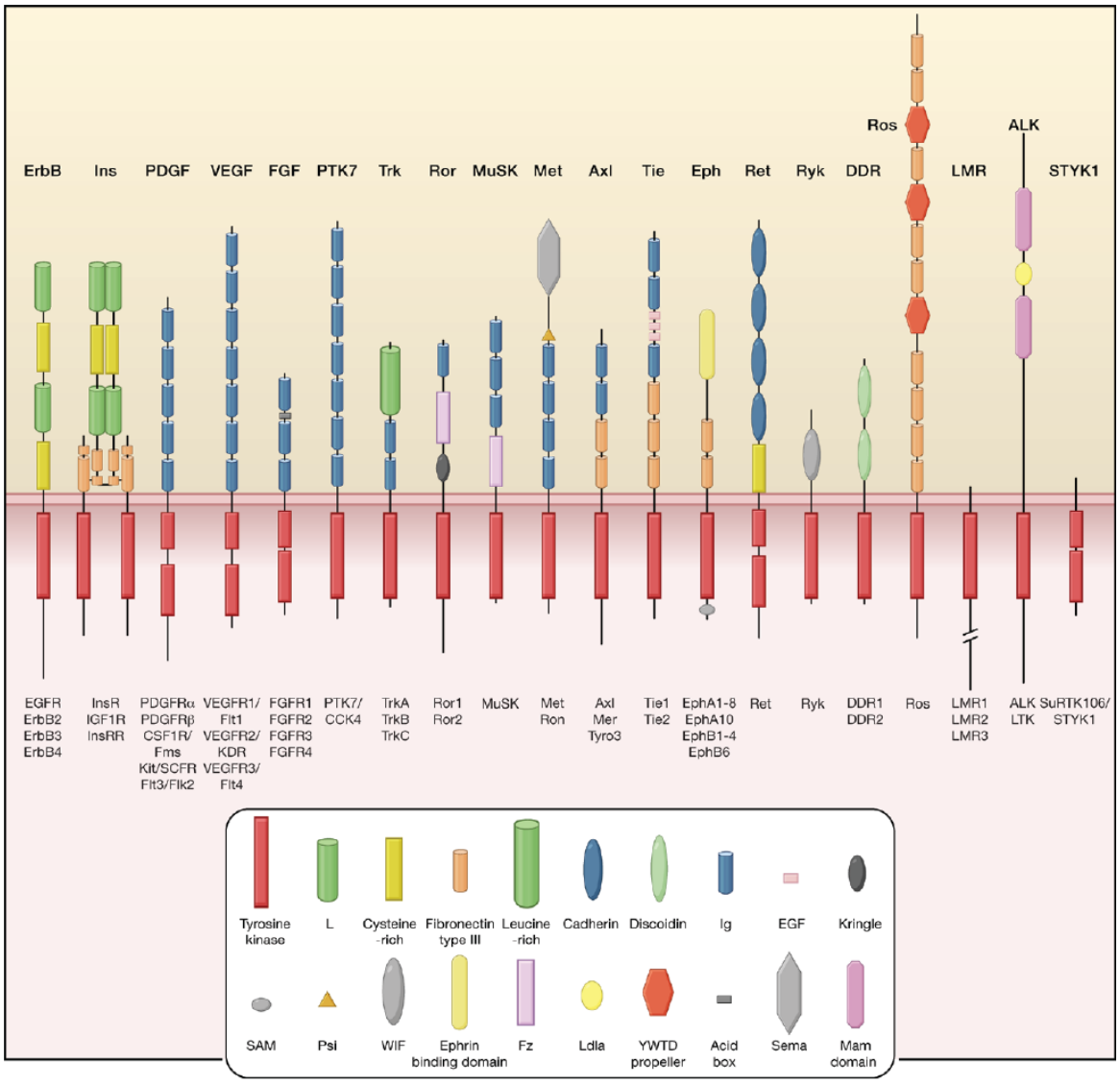

JAK2, GAB-1, SHP1 and PTP1 are some of the SH2 proteins that have been shown to directly bind the phosphotyrosine residues of EGFR. In the case of the Growth factor Receptor-Bound protein 2 (GRB2) (Skolnik et al. 1993), it can bind to the protein Son of Sevenless (SOS) through its SH3 domain (Wei et al. 1992, Bowtell et al. 1992). In this way, SOS is brought into close proximity with RAS proteins, inducing it to release a GDP molecule and bind instead to a GTP molecule (McCormick 1993) (Figure 1.2).

1.2.2 RTKs in cancer

Hyperactivated signaling by RTKs has been reported in many types of cancer (Robinson, Cobb 1997). EGF receptor overexpression has been shown in cancers such as lung, colorectal, pancreatic and squamous-cell carcinoma of the head and neck (Kwak et al. 2006, Rusch et al. 1993, Willmore-Payne, Holden & Layfield 2006). In normal conditions, EGF molecules bind as monomers to monomeric EGFR causing the exposure of the dimerization domain of each receptor which consequently associates with one another. The increase in the number of EGFR facilitates the receptor dimerization in the absence of EGF, resulting in transphosphorylation of each other and hyperactivation of ERK pathway (Grandis, Sok 2004). PDGF receptor, which signals through the ERK pathway, has been found overexpressed in ovarian, prostate, breast, lung, glioma, and bone tumors (Henriksen et al. 1993, Hofer et al. 2004, Carvalho et al. 2005, McGary et al. 2002, Rikova et al. 2007). Moreover, co-expression of PDGFα receptor and PDGFs has been observed in ovarian neoplasms, consistent with autocrine growth. The latter represents another mechanism for tumorigenesis consisting in the simultaneous expression of a growth factor and its correspondent receptor which is not normal.

1.2.3 RAS family of proteins

RAS is a small GTPase, downstream of many RTKs and upstream of the RAF kinases in the ERK cascade. RAS belongs to a family of small GTPases including R-RAS, RAP, RAL, RHEB, RIN and RIT protein (Colicelli 2004). There are four RAS proteins encoded by three different genes: *HRAS*, *NRAS*, *KRAS 4A* and *KRAS 4B* (Barbacid 1987, Lowy, Willumsen 1993). Although they share 85% of sequence identity, Voice et al. in 1999 showed that each of the RAS homologs have different ability to activate CRAF. When they transfected COS-1 cells with ^{WT}CRAF and constitutively active HRAS, KRAS 4A, KRAS 4B and NRAS plasmids, they observed that KRAS 4B was the most efficient in the activation of CRAF while KRAS 4A, NRAS and HRAS show progressively lower ability to activate CRAF (Voice et al. 1999). These data support the idea that the RAS isoforms are not functionally redundant.

The *RAS* oncogene was among the first oncogene to be discovered. In 1964 Jennifer Harvey observed that a preparation of murine leukaemia virus taken from leukaemic rat induced sarcoma in new-born rodents (Harvey 1964). The sequencing of the viral DNA in 1977 revealed a mix of retroviral DNA, rat cellular sequences of ancestral retroviral origin and rat cellular genes which stand for the Ras acronym. In 1982, Barbacid et al. demonstrated the similarity of the sequences between the retroviral oncogene *v-ras* and its human homologue *NRAS* (Shimizu et al. 1983). The molecular cloning of the normal human *HRAS* and its oncogenic allele showed that their functional difference was due to a single point mutation (Reddy et al. 1982). Three years later, the *KRAS* oncogene was detected in colorectal (Bos et al. 1987), lung (Rodenhuis et al. 1987) and pancreatic tumor biopsies (Almoguera et al. 1988).

RAS isoforms are targeted to the plasma membrane after a series of post-translational modifications aimed to create hydrophobic domains that facilitate this association. All

isoforms are modified by the addition of a farnesyl isoprenoid group in the cytosol, which are further modified in the Endoplasmic Reticulum (ER) by a cleavage and a carboxyl methylation. KRAS is sent to the plasma membrane whereas NRAS and HRAS are transported to the Golgi where they are palmitoylated and finally transferred to the plasma membrane (Clarke 1992, Clarke 1992, Clarke et al. 1988, Casey, Seabra 1996, Zhang, Casey 1996, Kim et al. 1999, Perez de Castro et al. 2004).

RAS proteins become activated when they are bound to a GTP molecule. The SOS protein, which functions as a GEF, catalyzes the release of GDP from the guanine nucleotide binding pocket allowing RAS to bind GTP. The binding of GTP to RAS is facilitated by the fact that GTP is 10-fold more abundant in the cytosol than GDP. The inactivation of RAS involves hydrolysis of GTP to GDP performed by the GTPase activity of RAS. Because this reaction is slow, RAS needs the action of the GTPase activating proteins (GAPs) to accelerate this process (Vetter, Wittinghofer 2001).

Activated RAS proteins have been shown to occupy dynamic plasma membrane nanodomains called nanoclusters or lipid rafts. These are lipid platforms composed of sphingomyelin and cholesterol that segregate membrane components within the cell. Their main role is to generate high local concentrations of all the ERK cascade members including scaffold proteins, resulting in high fidelity signal transmission (Tian et al. 2007).

It has been shown that RAS signaling is not only restricted to the plasma membrane. Recently, significant pools of NRAS and HRAS have been detected on the Golgi apparatus (Apolloni et al. 2000, Choy et al. 1999). Moreover, in 2002 through visualization of the CRAF-RBD domain fused to GFP, Chiu et al. showed that the recruitment of CRAF to the Golgi membrane occurs after growth factor stimulation (Chiu et al. 2002). Two models have been proposed for the explanation of ERK signaling from the Golgi: the first model suggests the activation of the RAS exchange factor (RASGRP) occurs through

diacylglycerol (DAG) and Ca^{+2} via activation of PLCγ (Bivona et al. 2003); the second model proposes the transport of an already active RAS-GTP from the plasma membrane to the Golgi (Rocks et al. 2005). There is some evidence suggesting that RAS can also signal from other cellular compartments such as: ER (Sobering et al. 2003) and mitochondria (Rebollo, Perez-Sala & Martinez-A 1999), but the physiologic consequences of this alternative signaling of RAS remained to be established.

1.2.4 Activating *RAS* mutations

RAS is the oncogene most frequently mutated in human cancer with approximately 20-30% of all tumors expressing activated *RAS* (Downward 2003). Most cancers with somatic *RAS* mutations harbour changes in *KRAS* (85%), whereas *NRAS* mutations represent 15% of overall mutations and *HRAS* mutations are rare (<1%) (Downward 2003). Each one of the *RAS* family members is mutated in specific types of human cancers: *KRAS* is commonly mutated in pancreatic, lung and colorectal cancers (Smit et al. 1988, Karapetis et al. 2008, Johnson et al. 2001); *NRAS* is found mutated in melanoma, liver and myeloid cancers (Platz et al. 2008, Hu et al. 1986) and *HRAS* mutations are commonly found in bladder cancer.

As mentioned in section 1.2.3, RAS molecules cycle between a switch-ON (GDP for GTP exchange) and a switch-OFF (GTP hydrolysis) state. For an effective transition from the switch-OFF to switch-ON state, the following mechanistic features are needed: i) positioning of the catalytically essential glutamine side chain (Gln61) from RAS and ii) positioning of the Arg789 residue provided by GAP, which main function is to stabilize charges in the transition state. The residue G12 is involved in the re-arrangement of Gln61 and Arg789 residues within the active site of RAS (Scheffzek et al. 1997, Prive et al. 1992,

Seeburg et al. 1984). Oncogenic RAS proteins are characterized by showing mutations in the residues mentioned before (Gly12, Gly13 and Gln61), which leads to the reduction of the RAS GTPase activity and GAP resistance (Scheffzek et al. 1997).

The use of mouse models conditionally expressing ^{G12D}Kras in pancreas and lung, demonstrated that this mutation is an initiating event in the development of these cancers (Hingorani et al. 2003). Also, it has been shown that ^{G12D}Kras expression in pancreas or lung of $p16^{INK4A}$/$p19^{INK4D/ARF}$ or p53 deficient mice accelerates the development of metastatic adenocarcinomas (Aguirre et al. 2003). In contrast, *Kras* mutation does not appear to be an initiating event in colon cancer. However, cooperation of ^{G12D}Kras with loss of APC resulted in colon cancer progression in a mouse model (Sansom et al. 2006). By comparing phenotypic differences between mouse models expressing ^{G12D} Kras or ^{G12D}Nras, it has been confirmed that the mutation confers a weaker oncogenic potential to Nras than to Kras.

Interestingly, *RAS* mutations occur in a mutually exclusive manner with the most common form of oncogenic BRAF known as ^{V600E}*BRAF* (Davies et al. 2002, Brose et al. 2002).

1.2.5 The RAF kinases

RAF proteins constitute a key point of regulation in the activation of the ERK pathway. These serine-threonine kinases are located downstream of RAS, which is frequently found disregulated in various human pathologies and upstream of ERK, which is known to influence cellular proliferation, differentiation, survival, migration, angiogenesis and chromatin remodelling (Robinson, Cobb 1997). The RAF proteins main role relies on the ability to enhance, attenuate or suppress signals from extracellular stimuli towards ERK (Garnett, Marais 2004).

1.2.5.1 Discovery of RAF kinases

In 1980, the RAF proteins were identified as oncogenes in murine and avian viruses:

The viral homolog of the *c-RAF* oncogene called *v-RAF*, was found incorporated in the genome of the B611-MSV mouse retrovirus that causes tumors in mice (Rapp et al. 1983).

ARAF protein was identified as the coding product of a 1.6 kb cDNA derived from mouse spleen. The kinase domain of ARAF was demonstrated to share an 85% homology with that of CRAF which allowed associating them as members of the same family. The incorporation of *ARAF* cDNA into the genome of murine leukemia virus revealed a strong potential for cell transformation of this gene, suggesting that the lost of the regulatory domain of ARAF is the cause of its constitutive enzymatic activity (Huleihel et al. 1986).

The oncogene responsible for the proliferation of infected neuroretina cells from chicken embryos was designated as *v-Rmil* (Marx et al. 1988). This novel oncogene was named after *v-mil* protein because the *v-Rmil* encoded protein()() and the *v-mil* protein shared an homology of 83.8% in their catalytic domain (Galibert et al. 1984). Importantly, at the N terminus, both proteins only shared 28.2% of homology which explained the poor regulation and oncogenic power of *v-Rmil*. Moreover, a striking similarity was found between *v-Rmil* encoded protein and human proteins CRAF (Jansen, Bister 1985) and ARAF (Beck et al. 1987). After Ikawa et al. in 1988 reported the identification of a third member of the *RAF* gene family (*BRAF*), a comparison between the DNA sequences of *BRAF* and *v-Rmil* suggested that these two proteins had the same genetic origin (Ikawa et al. 1988).

1.2.5.2 Specific functions of RAF isoforms

The RAF family consists of three members: ARAF, BRAF, and CRAF. Although they are similar in structure, the limited redundancy between these isoforms has been demonstrated at different levels of regulation:

In 1990, Storm et al. examined the RNA expression of each *raf* isoform in tissues from normal adult mice. They observed that *Craf* RNA was present in every tissue at consistent levels suggesting its involvement in cellular maintenance and viability. *Araf* was barely detectable in some organs but highly expressed in others specifically in tissues from the urogenital system such as: ovary, fallopian tubes, epididymis, seminal vesicle, kidney and bladder. The tighter control of *Araf* transcription suggests a more speciliazed role for this gene. In the case of *Braf*, most of the tissues examined exhibit undetectable or very low levels of transcripts corresponding to this gene. Neural tissues such as brain and spinal cord contained the highest level of *Braf* mRNA whereas tissues such as kidney, liver and thymus expressed lower levels of *Braf* transcripts (Storm, Cleveland & Rapp 1990).

In contrast to *Araf* and *Craf*, alternative splicing represents a regulatory mechanism for *Braf* activity (Storm, Cleveland & Rapp 1990). Originally the presence of two alternatively spliced exons in the mouse *Braf* gene were found: exon 8b and 10a (currently known as 9b) (Calogeraki et al. 1993). The *Braf* gene containing exon 8b, which is located between exon 8 and 9, is characterized by an additional 36 bp while exon 9b confers an extra 120 bp to *Braf* and is localized between exons 9-11. In 1995, Barnier et al. by using oligonucleotides specific to exons 8 and 11 of *Braf*, showed the possible combinations among these exons (Barnier et al. 1995). They detect four different *Braf* isoforms: B1 containing exons 8, 9 and 11(79 kDa); B2 containing exons 8, 8b, 9 and 11 (82 kDa); B3 containing exons 8, 9, 10 and 11 (90 kDa) and B4 including exons 8, 8b, 9, 10 and 11(96 kDa). They also found variants for each isoform differing by a couple of kDa from the

correspondent molecular weight (B1*: 86 kDa; B2*: 88 kDa; B3*: 94 kDa and B4*: 99 kDa). They proposed that these variants could be the result of an additional alternatively spliced exon as yet unidentified in *Braf* or they could be due to the presence of post-translational modifications such as phosphorylations (Barnier et al. 1995).

The existence of a 67 and a 69 kDa Braf protein was also detected in brain and liver extracts by antibodies directed against exon 11. Curiously, they could not detect these products by using antibodies that recognized exon 1 and 2, suggesting that short forms possibly lacking of exons 1 and 2 can be found in these specific tissues (Barnier et al. 1995).

In 1998, Papin et al. showed that the presence of exon 9b results in an increase basal kinase activity for BRAF while the presence of exon 8b had the opposite effect. They suggested that the presence of the exon 9b sequence elongates the linker region between CR1 and CR3, facilitating an open conformation for BRAF, while exon 8b, which is also localized at the linker region favours a more closed conformation which hides the kinase domain of BRAF (Papin et al. 1998).

There is evidence that the RAF isoforms differ in their kinase activity: Under comparable conditions the kinase activity of ARAF is approximately 20% of that shown in CRAF while BRAF has 15-20 times higher kinase activity than CRAF. In 1995, Pritchard et al. by using an estradiol regulated form of the raf kinases showed that Braf is the most efficient activator of Mek in comparison to Craf and Araf. In agreement with these data, Papin et al. in 1996 showed that BRAF displayed a stronger MEK-binding capacity than CRAF, confirming that BRAF is a strongest MEK activator (Papin et al. 1998, Papin et al. 1996).

1.2.5.3 Structure of RAF proteins

All three RAF isoforms share three conserved regions (CR1, CR2 and CR3) embedded in variable sequences. The CR1 and CR2 domains are located in the N terminus while the CR3 domain is localized at the C terminus (Figure 1.4). In CR1 domain there are two RAS-GTP binding sites: the RAS binding domain (RBD) (Scheffler et al. 1994) and the cystein-rich domain (CRD) (Mott et al. 1996). Both segments are responsible for RAF protein recruitment to the plasma membrane. In particularly CRD is responsible for interacting with the CR3 domain to maintain the RAF proteins in an autoinhibited state. The CR2 domain contains the phosphoserine 259 in CRAF (Ser365 in BRAF and Ser214 in ARAF) to which the 14-3-3 protein binds stabilizing the closed conformation of CRAF (Dhillon et al. 2002b). The CR3 domain contains the kinase domain which includes the negative-charge regulatory region (N-region), the glycine loop, catalytic loop and the activation segment. The residues Ser338 and Tyr341 in the negative-charge regulatory region (N-region) of CRAF (Ser299 and Ser302 in ARAF) must be phosphorylated in order to activate these proteins (Fabian, Daar & Morrison 1993, Mason et al. 1999a). In the case of BRAF, the equivalent residue Ser446, is constitutively phosphorylated, while the residue Ser449 is substituted by an aspartic acid which mimics the negative charge of the phosphate group (Mason et al. 1999a, Brummer et al. 2002, Carey et al. 2003) (Figure 1.4). Another critical requirement for the full activation of the three RAF isoforms is the phosphorylation of residues Ser491 and Ser494 located in the CRAF activation segment (Thr599 and Ser602 in BRAF; Thr452 and Thr455 in ARAF) (Zhang, Guan 2000). The glycine loop is important for localizing the phosphates of ATP and spans residues Gly356-Gly361 in CRAF, Gly464-Gly470 in BRAF and Gly317-Gly323 in ARAF (Johnson et al. 1998) (Figure 1.4).

Figure 1.4 Structure and main regulatory sites in the three RAF isoforms (Adapted from Mercer, Pritchard 2003a). (A) The table shows a summary of the key regulatory phosphorylations as well as the domains constituting the RAF proteins. **(B)** Primary structure of the RAF isoforms sharing three conserved regions: CR1 (blue box), CR2 (green box) and CR3 (purple box). CR1 and CR2 integrate the regulatory domain which is responsible for RAS interactions and the auto-inhibition of the protein. The CR3 contains the kinase domain which includes the N-region, the glycine rich loop or P-loop, catalytic segment and the activation segment.

A

Main segments	ARAF	BRAF	CRAF
RBD	13-93	150-230	51-131
CRD	98-143	234-279	139-184
PEST sequence	Poor probability	297-337	284-309
N-region	299-302	S446-D449	338-341
Glycine loop	317-323	464-470	356-361
Catalytic loop	427-434	574-581	473-483
Activation loop	447-476	594-623	496-515
Key phosphorylation sites	**ARAF**	**BRAF**	**CRAF**
14 - 3 -3 docking site	S214, E583	S365, S729	S259, S621
N-region	S299, Y302	S446, D449	S338, Y341
Activation segment	T452, T455	T599, S602	T491, S494
PKA	Not known	S365, S429	S43, S233, S59
PKC	Not known	Not known	S497, S499
ERK	Not known	S151, T401, S750, S753	S29, S43, S289, S301, S642
AKT	Not known	S365, S429	S259
Autophosphorylation	Not known	Not known	S621

B

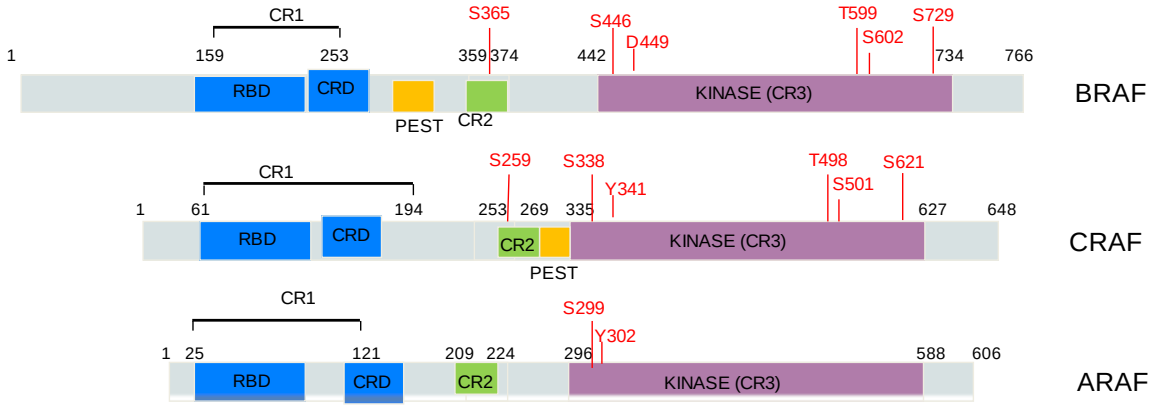

Crystal structures of the ^{WT}BRAF kinase domain complexed with the inhibitor BAY43-9006 were analysed to determine the structure of the protein (Wan et al. 2004a) (Figure 1.5). The kinase domain of BRAF adopted a similar conformation to other kinases:

The N´terminal lobe is comprised of five strands of anti-parallel β-sheets and a αC helix. The C-terminal lobe includes four α-helices (D,E,F,H) flanked by two additional helices (G and I) and two short antiparallel β-sheets (β7 with β8 and β6 with β9). The ATP binding site is situated at the interface of the two lobes. The N´terminus of the C´terminal lobe contains a negative-charge regulatory region (N-region) and the glycine rich loop or P loop which main function is to bind the phosphates from the ATP (Figure 1.5). The C´terminus of the C terminal lobe includes the activation segment which runs from the DFG segment to the APE segment. The aspartate residue (D) within the DFG sequence is responsible for chelating a Mg^{2+} that contributes to the positioning of the ATP phosphates for phosphotransfer. The phenylalanine residue (F), interacts with some residues of the αC helix which alters the interface between the N´ terminal lobe and the C´ terminal lobe. The β9 which is located beside the DFG sequence, needs to bind to the β6 sheet from the catalytic segment in order to maintain the active conformation. The activation loop, also located within the activation segment, contains one to three residues that need to be phosphorylated in order to displace the activation segment, allowing the substrate binding. Finally, the P+1 loop also contribute to substrate binding (Figure 1.5).

Figure 1.5 Structure of ^{WT}BRAF kinase domain (Taken from Wan et al. 2004a). Ribbon diagram of ^{WT}BRAF kinase domain in complex with BAY43-9006 (green molecule) is shown. The N lobe is in magenta, C lobe in marine blue, and P loop or Glycine rich loop is in orange. The positions of Asp593 and Phe594 of the DFG motif, Asn580 of the catalytic loop, and Glu585 are indicated. The DFG motif is represented in yellow as well as the APE motif. The rest of the activation segment and the N-region are in red. Residues 600–611 of the activation loop are disordered (dashed lines).

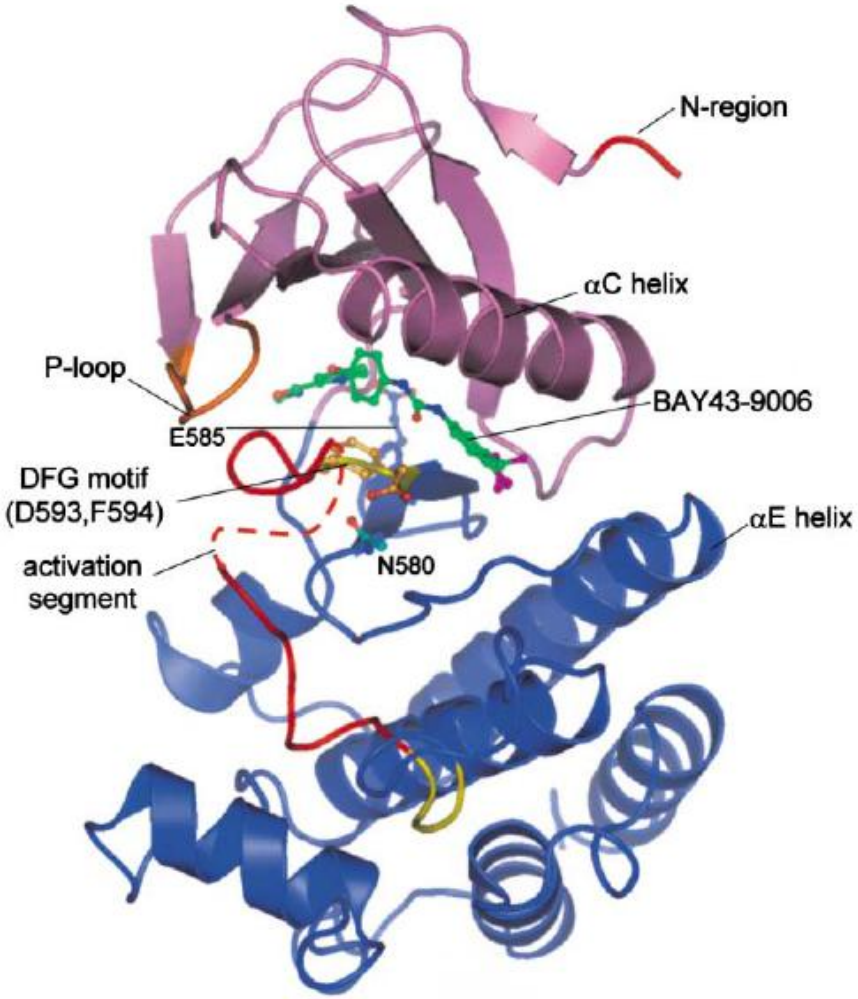

1.2.5.4 Model of activation of RAF proteins

In quiescent cells, inactive CRAF proteins normally reside in the cytoplasm in a “close conformation” (Figure 1.6). This state which is characterized by the interaction of the CRD domain with the kinase domain, is stabilized by 14-3-3 binding to residues Ser259 and Ser621 (Mercer, Pritchard 2003b, Niault, Baccarini 2010). Upon ligand stimulation, RAS recruits the CRAF-14-3-3 complex to the plasma membrane by binding to the RAS binding domain (RBD) of CRAF (Mercer, Pritchard 2003a, Baccarini 2002) (Figure 1.6). The dephosphorylation of residues Ser259 and Ser621 in CRAF (Ser365 and Ser729 in BRAF; Ser214 and Ser583 in ARAF) by protein phosphatase 1 and 2A (PP1/PP2A) (Hancock, Parton 2005) and the negatively charged membrane phospholipids, results in the displacement of the 14-3-3 protein from the N´-terminus of CRAF (Dhillon et al. 2002a, Abraham et al. 2000). This step enables the binding of RAS to the cysteine-rich domain (CRD).

As mentioned in section 1.2.5.3, CRAF phosphorylation occurs in two regions of the kinase domain; the N-region and the activation segment. In 1999, Mason et al. showed that only in the presence of both RAS-GTP and activated SRC, a high proportion of Craf molecules become phosphorylated at Ser338 and Tyr341 within the N-region (Mason et al. 1999b). They suggested that plasma membrane-localized kinases such as Pak3 might be responsible for S338 phosphorylation while SRC might phosphorylate Tyr341 (Mason et al. 1999c). Other yet undefined kinases are thought to phosphorylate residues Thr491 and Ser494 localized in the activation segment. The phosphorylation of these key residues in the activation segment destabilize the hydrophobic interactions between this segment and the glycine-rich loop, resulting in the open catalytic conformation, whereas the phosphorylation of key residues within the N-region help to disrupt the autoinhibitory

activity of the N-terminal domain (Wan et al. 2004a, Cutler et al. 1998, Tran, Wu & Frost 2005).

The inactivation of CRAF requires the phosphorylation of Ser259 which has been shown to occur in the presence of PI3K or PKA (Zimmermann, Moelling 1999). Another event controlling CRAF activation is the dephosphorylation of Ser338 by the protein phosphatase 5 (PP5) which paradoxically is the same enzyme that removes ERK feedback phosphorylations (von Kriegsheim et al. 2006) (Section 1.4.1) .

In quiescent cells, BRAF is similar to CRAF in being bound to the 14-3-3 protein through phosphorylated residues Ser364 and Ser728 (Mercer, Pritchard 2003a). However, inactive BRAF exists in the cytoplasm in an “open conformation” due to the presence of phospho-Ser446, Asp449 and the possible inclusion of amino acids encoded by exon 9b (Mercer, Pritchard 2003a) (Section 1.2.5.2). After RAS-GTP formation, BRAF is recruited to the membrane by binding to RAS through its CRD domain. Similarly to CRAF, PP1/PP2A may dephosphorylate residue Ser365, resulting in the release of 14-3-3 from the N-terminus facilitating the phosphorylation of Ser599 and Ser602 in the activation segment (Mercer, Pritchard 2003a). Serum and glucocorticoid-inducible kinase (SGK) (Zhang et al. 2001) or PI3K have been shown to negatively phosphorylate BRAF at Ser365 (Guan et al. 2000). The phosphorylation of residue Ser428 by PI3K has also been shown to inactivate BRAF, however the mechanism has not yet been established.

As mentioned briefly in section 1.1, KSR is a molecular scaffold that facilitates signal transmission through the ERK pathway (Morrison 2001). It has been shown that, when KSR is inactive, it is found in complex with various proteins in the cytosol (Figure 1.7). Among these proteins are the 14-3-3, C-TAK, the inactive form of the PP2A enzyme and MEK (Muller et al. 2001, Aitken 2006).

Figure 1.6 Mechanism of activation of CRAF (Taken from (Baccarini 2002)**. (A)** In the cytosol, CRAF is kept in a "closed conformation" characterized by the CRD domain- kinase domain interaction and by the binding of the 14-3-3 protein to Ser259 and Ser621 residues. **(B)** The dephosphorylation of Ser259 allows the opening of CRAF and the subsequent interaction with RAS. **(C)** The phosphorylation of key residues within the N-region and the activation segment of CRAF are performed by membrane-associated kinases. **(D)** and **(E)** CRAF adopts again its "close conformation" upon rephosphorylation of S259 subsequently binding to 14-3-3.

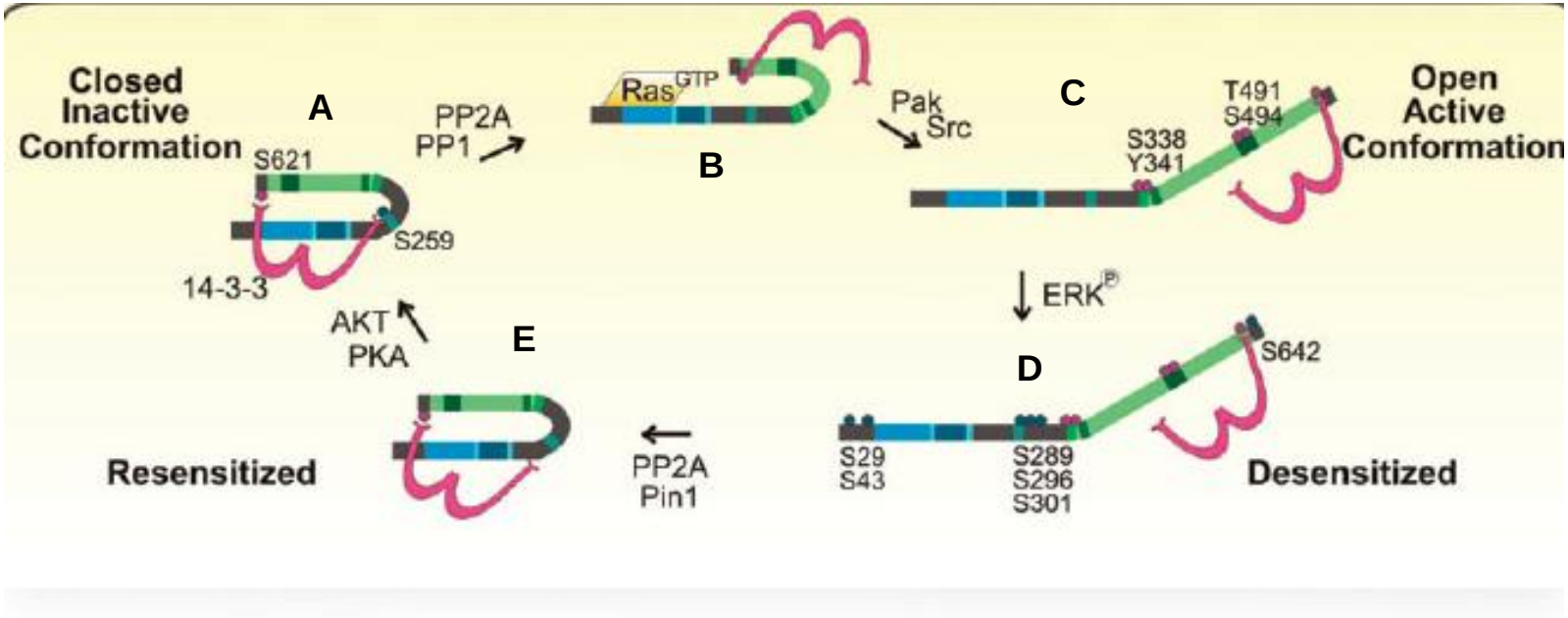

GTP-bound RAS can activate the PP2A, resulting in the dephosphorylation of S392 in KSR which is necessary for 14-3-3 binding (Aitken 2006, Kolch 2005). The release of KSR from the 14-3-3 protein allows its translocation to the membrane, the presentation of MEK to activated RAF and the subsequent binding of KSR with RAF and ERK (Aitken 2006, Kolch 2005) (Figure 1.7).

An alternative mechanism for the activation of RAF proteins requires the formation of dimers in response to RAS activation. The model that explains the formation of the CRAF-BRAF heterodimer suggests that CRAF can only bind to BRAF when the latter has been recruited to the plasma membrane and fully activated in a RAS-dependent manner. BRAF then contributes directly or indirectly to the phosphorylation of residues Thr491 and Ser494 in the CRAF activation segment (Rushworth et al. 2006a, Garnett et al. 2005a).

The formation of CRAF-BRAF heterodimers and their respective homodimers involve several sites of contact distributed along conserved and non-conserved domains within both proteins. The heterodimer arrangement is enhanced by the presence of the 14-3-3 protein which acts as a bridging molecule cross-linking CRAF to BRAF. This is supported by the fact that a mutated 14-3-3 docking site resulted in the prevention of heterodimer formation (Rushworth et al. 2006a, Garnett et al. 2005b).

Eventually, in 2006 Rushworth et al. reported that the phosphorylation of the 14-3-3 binding site on BRAF Ser729 is also essential for BRAF-CRAF heterodimerization (Rushworth et al. 2006a). In 2010, Ritt et al. also found that the heterodimer can be disrupted by ERK direct phosphorylation on residue Thr753 in BRAF (Ritt et al. 2010b).

Although the CRAF-BRAF heterodimer is thought to have higher kinase activity than monomers and homodimers, the proportion of BRAF and CRAF arranged in this manner is thought to be less than 1% of the total amount of BRAF and CRAF present in the cell. In

Figure 1.7 The role of KSR in CRAF activation (Taken from Aitken 2006). Inactive KSR is localized in the cytoplasm where it interacts with 14-3-3 dimers, the inactive form of PP2A, MEK and C-TAK1. Upon stimulation, RAS-GTP activates PP2A, resulting in the dephosphorylation of S392 and the release of the 14-3-3 protein. KSR1 binds to the membrane through its C1 domain where it associates with CRAF promoting the activation of MEK and ERK.

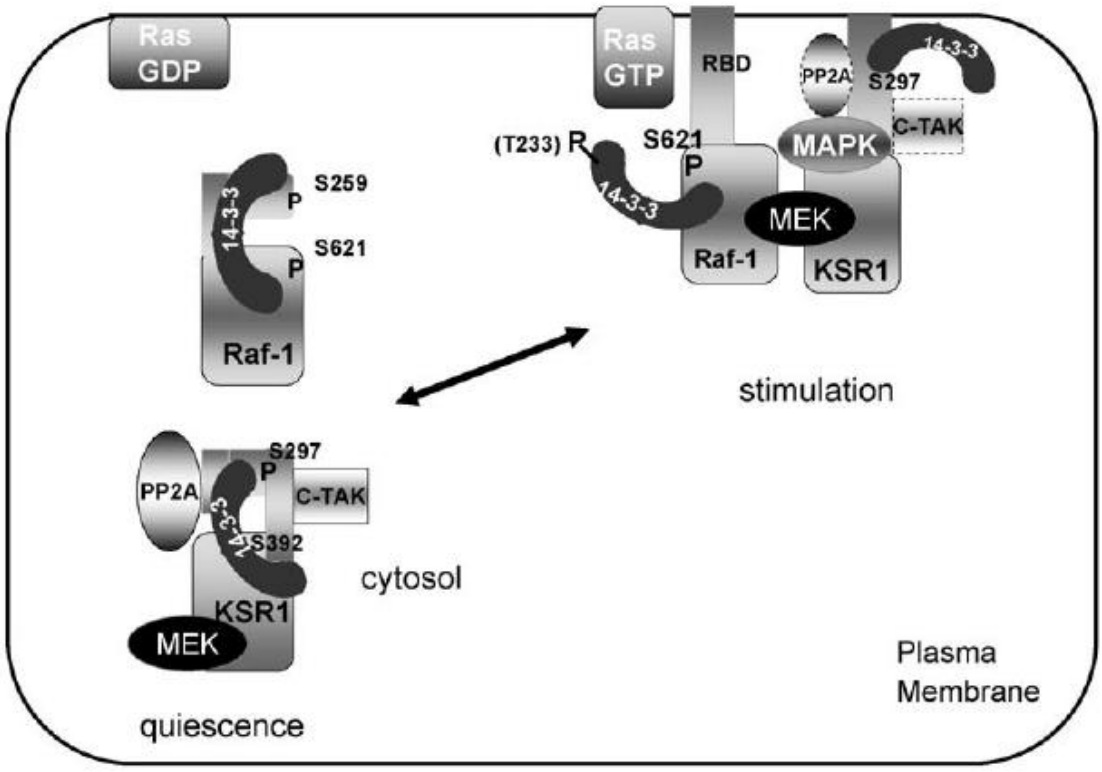

2006, Rushworth et al. demonstrated a limited impact of the heterodimer on global activation of ERK, proposing that the CRAF-BRAF heterodimer contributed to sustained activation of ERK leading to cell differentiation rather than transient activation (Rushworth et al. 2006b).

1.2.5.5 Stability of the RAF proteins

The chaperones HSP70 and HSP90 are required for the *de novo* folding and conformational maturation of several key signaling proteins including CRAF (Maloney, Workman 2002, Demand et al. 2001b).

Various studies have illustrated the assistance of molecular chaperones to the efficient folding and activation of CRAF (Powers, Workman 2006). Specifically, it is known that newly synthesized CRAF interacts with the HSP70/HSP40/HIP complex in order to reach its native conformation (Rudiger, Buchberger & Bukau 1997, Pellecchia et al. 2000, Hartl, Hayer-Hartl 2009b). Then, folded CRAF is transferred to the HSP90/CDC37/p23/immunophilins complex (Whitesell, Lindquist 2005, Sharp, Workman 2006). It is after the binding of CRAF to the latter complex that the protein becomes active and is able to bind to different ligands or become phosphorylated. The main function of CDC37 in the complex is to facilitate the loading of kinase clients (Roe et al. 2004)(Roe et al. 2004)(Roe et al. 2004)onto HSP90 (Roe et al. 2004) while p23 has been implicated in the stabilisation of the ATP-bound state of HSP90 which is the conformation required for client activation (Ali et al. 2006). It has been shown that CRAF requires prolonged chaperoning and in fact its binding to the complex persists whilst still active. If for some reason the HSP90/CDC37/p23/immunophilins complex cannot achieve the folding and activation of CRAF, the HSP90 interacts with the E3-ubiquitin ligase CHIP, incorporating it

into the heterocomplex which results in CRAF ubiquitylation and consequently proteasomal degradation (Demand et al. 2001b, Connell et al. 2001).

HSP90 is a ubiquitously expressed ATP-dependent chaperone that functions downstream of HSP70 during the folding of newly synthesized proteins (Terasawa, Minami & Minami 2005, Hartl, Hayer-Hartl 2009a). This chaperone has differential functions to those of HSP70 such as the prevention of non-specific aggregation of unfolded proteins and the induction of conformational changes in folded proteins that lead to their activation and stabilization (Wandinger, Richter & Buchner 2008). ARAF has also been found to exist in a cytosolic heterocomplex with the heat shock protein HSP90 and the co-chaperone CDC37 (Maloney, Workman 2002, Grbovic et al. 2006). In contrast, the binding of wild-type BRAF to HSP90 does not seem to be necessary for the stability of the protein (Grbovic et al. 2006).

1.2.5.6 Degradation of the RAF proteins

The proteasome is the most likely route by which the majority of cytoplasmic and nuclear proteins are turned over (Ciechanover 1998, Coux, Tanaka & Goldberg 1996). Its activity regulates the abundance of a multitude of proteins involved in differentiation, cell cycle, signal transduction and immunological events among others (Baumeister et al. 1998). The proteasome consists of a cylindrical structure known as 20S that contain six internal catalytic threonine sites for protein cleavage. A 19S regulatory complex binds to each end of the 20S proteasome to form the 26S proteasome which is required for ubiquitin-dependent degradation (Brannigan et al. 1995, Hershko 1997, Rivett, Gardner 2000). In this pathway, substrate proteins become marked for degradation by the attachment of multi-ubiquitin chains which are recognized by the 19S subunit (Hershko 1997). The

ubiquitylation reaction is performed by a three enzymatic cascade. Through an ATP-requiring step, the Gly residue of ubiquitin is activated by a E1 enzyme which charges an E2 ubiquitin-conjugating enzyme with ubiquitin (Pickart 2001, Dye, Schulman 2007). The E2 enzyme is bound to the substrate through the action of the E3 ligase. The latter is responsible to confer substrate specificity in the ubiquitylation reaction. There are three different types of E3 domains: RING, U-box and HECT (Pickart 2001, Dye, Schulman 2007).

In 2008, Noble et al. confirmed that misfolded CRAF is degraded by the proteasome and they suggested that this process is not dependent on CHIP, proposing that other E3 ligases are involved (Noble et al. 2008).

In 2006, Grbovic et al. also showed that ARAF and different BRAF mutants including V600E, V600D and G468A could be found ubiquitylated following simultaneous inhibition of HSP90 and the proteasome (Grbovic et al. 2006). A recent study showed a reduction in ^{WT}BRAF protein levels in colorectal cancer human samples after treatment with the anti-neoplastic agent simvastatin (Lee et al. 2011). Later studies confirmed that this drug was able to upregulate the expression of the E3 ligase: RNF149 which bound to BRAF causing its polyubiquitylation and consequently its degradation by the proteasome (Hong et al. 2012).

1.2.6 Oncogenic BRAF

BRAF mutations are present in approximately 7-8% of human cancers. In 2002, Davies et al. performed a screening for BRAF somatic mutations in 378 primary human cancer samples. They found single base substitutions distributed mainly in two regions of the kinase domain; the activation segment and the glycine-rich loop (Figure 1.8). Almost 90%

of the mutations were localized in the segment between DFG and APE motifs in the activation loop while the remaining 10% of the mutations occurred in the glycine residues within the GXGXXG motif. Importantly, a valine to glutamate substitution in the position 600 (V600E) accounted for approximately 92% of the mutations found in the activation segment (Figure 1.8). Large scale studies detected *BRAF* point mutations with high frequency in melanoma (39%), thyroid carcinoma (44%), colorectal carcinoma (10%) and biliary tract carcinoma (10%). At a lower frequency, *BRAF* mutations are found in oesophagus, stomach, pancreas, lung, urinary tract, prostate, breast, ovary and cervical carcinoma. Haematopoietic neoplasms and central nervous system tumors can also contained mutated *BRAF*. Other mutations such as chromosomal translocations and rearrangements affecting *BRAF* are detected in astrocytomas, melanomas, prostate and gastric cancer samples. Approximately 30 single site missense mutations have been reported in the BRAF kinase domain (Davies et al. 2002).

To determine the kinase activity of each mutant with respect to ^{G12V}RAS stimulated ^{WT}BRAF activity, Wan et al. in 2004 co-transfected a myc-epitope tagged version of each mutant to COS cells (Wan et al. 2004b). The phosphorylation of MEK was measured in the presence of physiological concentrations of ATP (5 mM). From the 22 mutants that they analyzed, they found 7 mutants (G469A, E586K, V600D, V600E, V600K, K601E) had a kinase activity between 1.3-7.3 fold higher than that found in ^{G12V}RAS stimulated ^{WT}BRAF. The 11 other mutants, which were classified as intermediate activity mutants, were characterized by having a kinase activity between that of basal ^{WT}BRAF and ^{G12V}RAS (R462I, I463S, G464E, G464V, G466A, G469E, N581S, F595L, L597V, T599I, A727V). The remaining 4 mutants retained 30-80% of the basal ^{WT}BRAF kinase activity for which they were called impaired activity mutants (G466E, G466V, G596R, D594V). When

Figure 1.8 Single-base substitutions in BRAF. Schematic illustration of BRAF depicting three conserved domains (CR1-CR3). The green bars represent the frequency at which the mutations were detected in the glycine-rich loop and the activation segment of BRAF kinase domain.

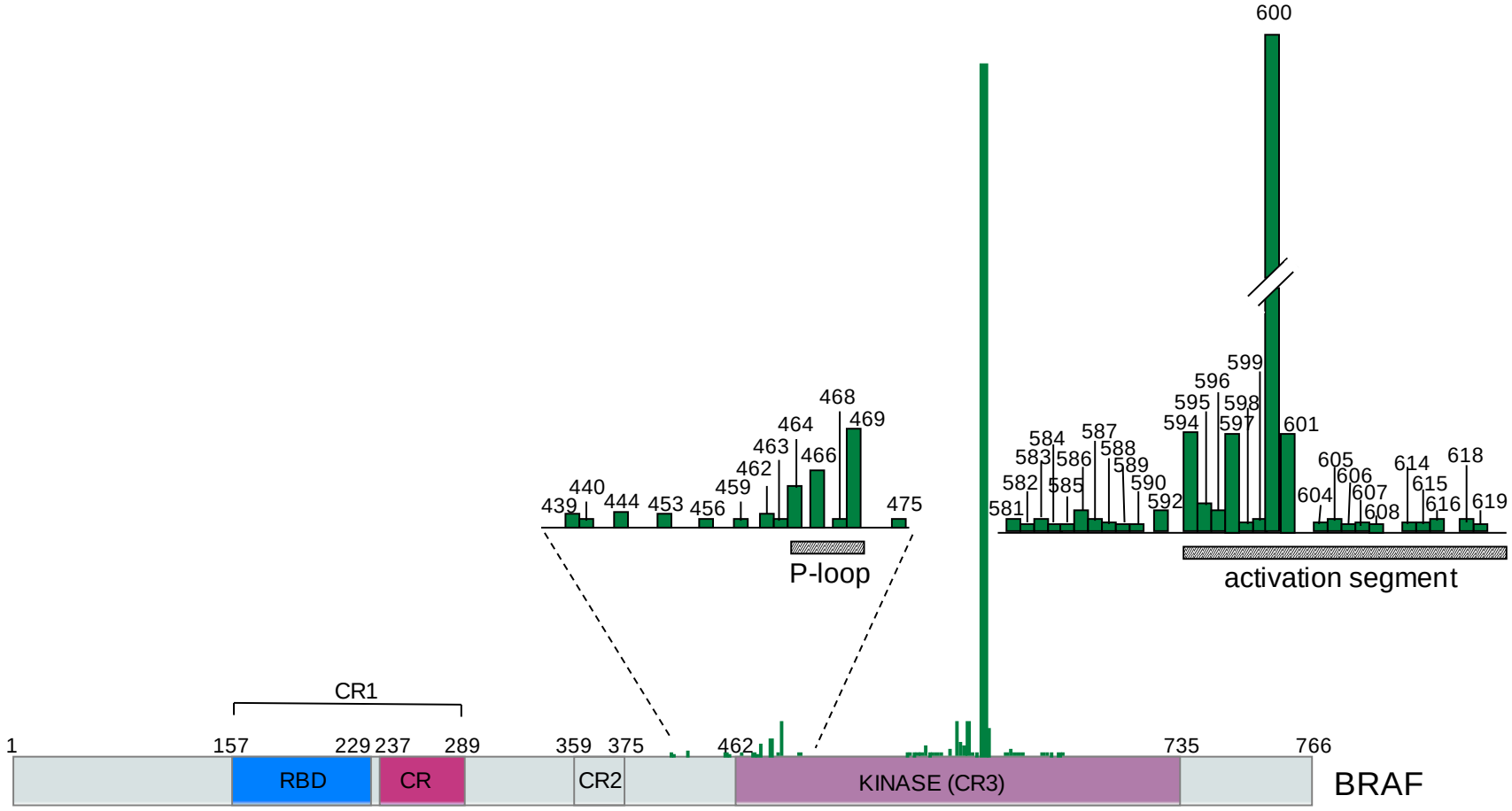

the structures of high and intermediate activity mutants were compared with that of inactive ^{WT}BRAF, a crucial difference was observed: In ^{WT}BRAF, a hydrophobic interaction between valine at position 600 in the activation segment and the phenylalanine at position 467 from the P loop was observed. This interaction caused the displacement of the DFG motif to a position inconvenient for phosphoryl transfer. This repositioning of the DFG motif is known as DFG "out" conformation. In oncogenic BRAF, the hydrophobic interaction was lost and DFG was properly positioned to catalyse activation (Wan et al. 2004b). In the case of impaired mutants G466E and G466V, the substitution of a glycine residue for a glutamic acid or valine, prevents the binding of the ATP phosphates to the P loop.

After Wan et al. transfected the G466E, G466V and G596R mutants into COS cells, they observed that they were still capable of activating endogenous ERK. In contrast, the *BRAF*^{D594V} mutant, in which an aspartic acid for valine substitution prevents Mg^{2+} chelation, was thought to be completely incapable of activating ERK. Garnett et al. found that the low kinase activity retained by G466E, G466V and G596R mutants was enough to transphosphorylate and activate CRAF which in turn was able to phosphorylate MEK (Wan et al. 2004b) (Figure 1.9). Moreover, when the ability to form heterodimers was blocked in cells expressing intermediate or impaired kinase activity mutants (G466A and D594G), the transformation potential was dramatically affected (Ritt et al. 2010b). Later studies performed by Kamata et al. in 2010 showed that mice expressing endogenous levels of impaired ^{D594A}BRAF are able to increase ERK activity through the formation of heterodimers with CRAF in the presence of ^{WT}RAS (Kamata et al. 2010).

The fact that *BRAF* somatic mutations associated to cancer are much more frequent than *CRAF* and *ARAF* relies on two main aspects: i) The mode of activation of BRAF, which depends only on the phosphorylation of key residues in the activation segment and does not required any phopshorylation at the N-region and ii) the increased affinity of BRAF

Figure 1.9 Impaired activity BRAF mutants activate MEK through CRAF kinase activity (Taken from Wan et al. 2004a). While high and intermediate activity mutants can directly activate MEK without CRAF intervention, the impaired activity BRAF mutants activate the MEK-ERK pathway through CRAF. The molecular mechanism consists in the hetero-oligomerisation of impaired BRAF mutant with CRAF followed by the transphosphorylation of the CRAF activation segment by the residual kinase activity of the BRAF mutant.

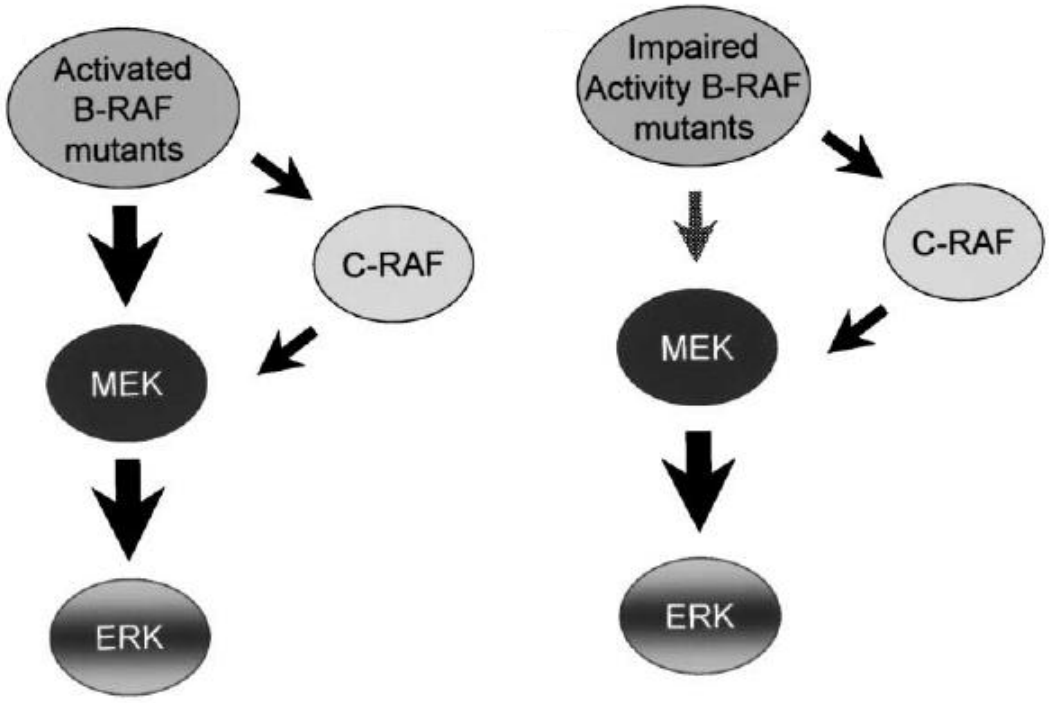

towards MEK, which is correlated with the ability of the RAF kinases to phosphorylate MEK1. As shown by Pritchard et al. in 1995, the activated kinase domain of BRAF (ΔBRAF:ER) phosphorylates Mek1 approximately 10 times more efficiently than ΔCRAF:ER and at least 500 times more efficiently than ΔARAF:ER.

1.2.7 CRAF as an effector of RAS and RAF proteins

In different types of cancers, CRAF has been shown to cooperate with driver-oncogenes such as RAS in tumor development (Blasco et al. 2011, Ehrenreiter et al. 2009). Moreover, its ablation in these scenarios not only suppresses tumorigenesis but confirms that its role cannot be compensated by ARAF or BRAF (Blasco et al. 2011, Takezawa et al. 2009).

After sequencing the *BRAF* and *CRAF* genes in 545 cancer cell lines, Emuss et al. in 2005 found that *BRAF* was mutated in 43 samples and *CRAF* was mutated in only 4 samples (Emuss et al. 2005). After measuring the kinase activity of mutant CRAF proteins, no difference was observed in comparison to ^{WT}CRAF. Currently, the COSMIC database shows other two point mutations in *CRAF* so far which confirms that this protein is rarely mutated in cancer.

The introduction of the equivalent mutation of ^{V600E}*BRAF* in *CRAF* (V492E), gave an increase of 45-fold more in the kinase activity of the mutant with respect to the wild-type protein, demonstrating the low tumorigenic potential of CRAF *per se* (Emuss et al. 2005). Although *CRAF* is not a driver oncogene, there is enough evidence to support its role as an important effector of RAS. In 2009, Takezawa et al. showed that in NSCLC cells expressing ^{G12V}KRAS, ERK activation depended more on CRAF signaling than on BRAF (Takezawa et al. 2009). Supporting these results, Blasco et. al showed that the conditional knockout of *Craf* from mice lungs expressing endogenous ^{G12V}Kras resulted in the

formation of less tumors and consequently in a longer survival rate in comparison to mice expressing only oncogenic Kras. In contrast, when Braf expression was lost from lungs of ^{G12V}Kras mice, the level of Erk activation was not altered. Moreover, in melanoma cell lines carrying activating mutations in RAS, a change from BRAF to CRAF signaling resulted in senescence evasion. This change in signaling was possible after the dysregulation of the cAMP dependent inhibition of CRAF by RAS (Dumaz et al. 2006).

1.2.8 Activation of MEK

As mentioned previously (Section 1.2), active RAF proteins are able to phosphorylate the dual-specificity protein kinases MEK 1 and MEK 2 (Alessi et al. 1994b). These kinases consist of an N-terminal domain, a kinase domain and a C-terminal domain. The N-terminal domain contains an ERK binding site, a nuclear localization sequence (NES) and an inhibitory sequence; the protein kinase domain includes the activation sequence and the proline-rich domain (Fischmann et al. 2009, Roskoski 2012). RAF proteins are able to phosphorylate MEK1 and MEK2 on two serine residues in the activation segment: Ser218 and Ser222 in MEK1 (Zheng, Guan 1994) and Ser222 and Ser226 in MEK2 (Roskoski 2012). The phosphorylation of residue Thr298 by PAK1, enhances the binding of MEK1 to ERK. Negative regulation sites have also been found in MEK such as: Ser212 (unknown protein) (Gopalbhai et al. 2003), Thr286 (Cdk5) (Rossomando et al. 1994), Thr292 (ERK) (Rossomando et al. 1994, Eblen et al. 2004) and Thr386 (Cdk5 and ERK).

In 2009, Catalanotti et al. showed that *Mek1* knock out embryos died around E9.5 as a result of placental defects. In the conditional knockout mice models, non-stimulated *Mek1*-/- fibroblasts showed a slower migration towards fibronectin in comparison to EGF or FGF stimulated *Mek1*$^{-/-}$ fibroblasts. Consistent with these data, the absence of Mek1 in stimulated MEFs resulted in an overall increase of Mek and Erk activation. They explained

this behaviour by showing that in wild-type cells Mek1 heterodimerizes with Mek2 in order to restrict its time of activation which results in Erk dephosphorylation. In the absence of Mek1, the prolonged phosphorylation of Mek2 and Erk is observed. In addition, the identification of a negative feedback loop from Erk to Mek1 showing the phosphorylation of Thr292 subsequently disrupting the heterodimer, gave support to this hypothesis (Catalanotti et al. 2009) (Section 1.4.1).

ERK1 and ERK2 are the only known substrates for MEK1/2 (Robbins et al. 1993) and their activation, as shown in section 1.2.5.4, is facilitated by the scaffold protein KSR which binds to the three members of the ERK cascade. ERK1 can be phosphorylated at residues Thr202 and Thr204 located within the Thr–Xaa–Tyr motif (Butch, Guan 1996) while in ERK2, the phosphorylation of residues Thr183 and Thr185 has been demonstrated (Aebersold et al. 2004, Gonzalez et al. 1993). It is worth mentioning that, depending on which cellular compartment the ERK cascade is located, there are different scaffold proteins assisting MEK activation: MEK partner 1 (MP1) promotes activation of MEK1 and ERK1 in the late endosomal stage (Schaeffer et al. 1998, Teis, Wunderlich & Huber 2002), PAXILLIN directs ERK activation at focal adhesions (Ishibe et al. 2003) and SEF which is a Golgi-localized scaffold recruits activated MEK to this particular organelle (Philips 2004).

There are three main factors contributing to ERK recognition of its unique substrates: the core consensus sequence (Ser/Thr) Pro, the docking sites and the scaffold proteins that bind to ERK and its substrates.

ERK selectively binds to its upstream regulators, scaffolds and downstream targets by surface interactions that are achieved through docking motif binding sites. Although these docking sites are common for more than one MAPK in the cell, the substrate specificity is dictated by the amino acid sequence (Chang et al. 2002, Heo et al. 2004, Zhou et al. 2006). One of the best described docking sites is the D domain or docking site for ERK

and JNK, LXL (DEJL) (Chang et al. 2002, Zhou et al. 2006, Lee et al. 2004, Callaway, Rainey & Dalby 2005). This docking site is found in ERK substrates such as the transcription factor ELK-1 (Dimitri et al. 2005), p90 Ribosomal S6 Kinase-1 (RSK-1) (Sharrocks, Yang & Galanis 2000), caspase 9 (Martin et al. 2008) and protein-tyrosine phosphatase HePTP (Zuniga et al. 1999). The D domain interacts with the common docking domain (CD) on ERK proteins (Bardwell 2006, Jacobs et al. 1999, Tanoue et al. 2000). Another well characterized docking site is the ERK FXFP (DEF) domain which is present in scaffold proteins such as the Kinase Suppressor of RAS (KSR) (Jacobs et al. 1999) and the transcription factors ELK-1 (Jacobs et al. 1999) and SAP-1 (Galanis, Yang & Sharrocks 2001).

Upon activation, ERK dissociates from the scaffold proteins and MEK and translocates to the nucleus. The phosphorylation of the Tyr190 residue on ERK by MEK causes a conformational change necessary for MEK and ERK dissociation. At least two different pathways for nuclear import of ERK have been reported: passive diffusion for ERK monomers and Ran-dependent active transport for ERK dimers which involve the importin-β family of proteins (Adachi, Fukuda & Nishida 1999).

1.3 Biological responses controlled by ERK

Depending on the duration, the magnitude and its subcellular localization, ERK activation can influence multiple processes including proliferation, apoptosis, senescence and autophagy (Yoon, Seger 2006, Zehorai et al. 2010, Pouyssegur, Volmat & Lenormand 2002) . The nuclear substrates of ERK include the transcription factors which activate the immediate-early genes (IEG). This group of genes are transcriptionally activated as a response of starved cells to the addition of growth factors within the first two hours of

exposure. ERK has also been involved in *de novo* synthesis of other transcription factors required for the expression of late genes. In the cytosol, ERK is able to phosphorylate RSK family members and MSK proteins (Murphy et al. 2002) (Figure 1.10). The human RSK family is integrated by four isoforms: RSK1, RSK2, RSK3 and RSK4 (Cargnello, Roux 2011a). Except from RSK4, which remains in the cytoplasm, all share the same mechanism of activation: In quiescent cells they form an inactive complex with ERK in the cytoplasm and, upon stimulation; they become phosphorylated by ERK at residues Thr359, Ser363 and Thr573 (Ranganathan et al. 2006, Dalby et al. 1998) which leads to Ser380 autophosphorylation creating a docking site for PDK1. In turn, PDK1 phopshorylates RSK, resulting in the full activation of the latter (Vik, Ryder 1997, Frodin et al. 2000). Activated RSK proteins translocate to the nucleus where they phosphorylate and activate various transcription factors involved in IEG such as serum response factor (SRF) (Rivera et al. 1993) and CREB (Ginty, Bonni & Greenberg 1994). The sustained activation of RSK results in the stabilization of early gene products such as c-FOS (Ginty, Bonni & Greenberg 1994), c-JUN and NUR77 (Davie, Spencer 1999, Davis et al. 1993). Other RSK substrates involved in transcriptional regulation are: the ETS transcription factor ER81 (Wu, Janknecht 2002)(Wu et al. 2003), microphthalamia (Park, Gilchrest 2002) and the estrogen receptor α (Joel et al. 1998). More substrates have been identified for RSK2 than for any other RSK; however studies supporting the isoform selectivity among substrates have not been generated (Cargnello, Roux 2011a).

Upon stimulation, ERK binds to MSK proteins and phosphorylates them at three different residues: Ser360, Thr581 and Thr700 (Deak et al. 1998, McCoy et al. 2007). This event fully activates MSK proteins which translocate to the nucleus where they phosphorylate various transcription factors such as: CREB, ATF1, NF-kβ, STAT3 and ER81 (Cargnello, Roux 2011a).

Figure 1.10 Regulation of transcription and translation by ERK (Taken from R&D systems). Activated ERK is able to phosphorylate the cytoplasmic kinases: RSK and MNK. Upon stimulation, ERK phosphorylates RSK facilitating its recruitment to the plasma membrane where it is phopshorylated by PDK1. Activated RSK is translocated to the nucleus by ERK where it can phosphorylate and activate several transcription factors such as FOS, CREB and SRF. After MNK becomes activated by ERK, it can phosphorylate components of the translational machinery such as eIF4E; however the biological meaning of this phosphorylation is not established yet. In the nucleus, MNK phosphorylates Histone H3 and HMG-14, resulting in chromatin relaxation and gene activation. Finally. ERK itself translocates to the nucleus where it phopshorylates various transcription factors such as: ELK-1, MYC, BRF1 and UBF. It is also able to directly phosphorylate c-FOS preventing its degradation allowing the formation of the AP-1 complex.

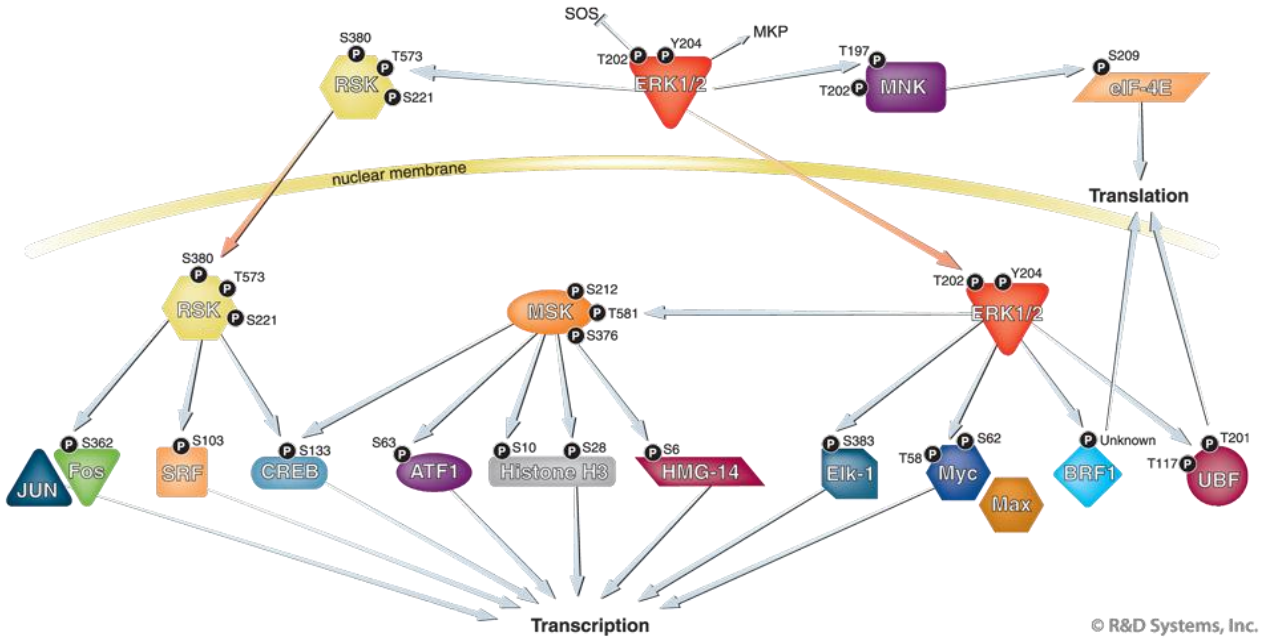

Also, MSK1 and MSK2 directly phosphorylate Histone H3 at S10 (Soloaga et al. 2003). The phosphorylation of this residue in addition to the acetylation of nearby lysine residues such as K9 or K14, allow the binding of 14-3-3 which is responsible for recruit other proteins necessary for transcriptional elongation (Clayton, Mahadevan 2003). The phosphorylation of Ser28 seem to function through the 14-3-3 recruitment as well; however more studies are needed to discard any functional difference between both phosphorylations (Winter et al. 2008) (Figure 1.10)

1.3.1 Proliferation

The progression through the cell cycle is dependent upon the combined actions of Cyclin/CDK complexes and CDK inhibitors (Chambard et al. 2007). A key step for quiescent cells to re-enter the cell cycle is the activation of Cyclin D-CDK4/6 complexes (Sherr et al. 1994, La Thangue 1994, Weintraub et al. 1995). Cyclin D is the only cyclin able to integrate receptor-mediated signals with the cell cycle machinery (Sherr 1994). It has been shown that ERK is able to regulate Cyclin D1 and Cyclin D2 transcription through direct phosphorylation and subsequent activation of the transcription factors ELK-1 and MYC (Figure 1.10). Activated ELK-1 binds to serum response factors (SRF) and the complex interacts with serum response elements (SRE) located in the *c-FOS* gene promoter (Whitmarsh et al. 1995). Transient activation of ERK results in an increased expression of the *c-FOS* gene but not in the accumulation of the c-FOS protein. In contrast, ERK sustained activation results in the phosphorylation of Thr325 and Thr331 on c-FOS which stabilizes and further accumulates the protein. The regulation of *c-FOS* expression levels by ERK has a direct influence in the formation of JUN and FOS heterodimers which constitute the AP-1 complex (Angel, Karin 1991). AP-1 is required for

the expression of cell cycle mediators such as Cyclin D1 (Albanese et al. 1995), p53, $p21^{CIP1}$, $p19^{INK4D/ARF}$ and $p16^{INK4A}$.

As mentioned above, ERK induce the transcription of Cyclin D2 through the action of MYC. The transcription factor MYC can also form heterodimers with the transcription factor Max, resulting in an increase in Cyclin D2 expression (Ayer, Eisenman 1993). In 2000, Sears et al. showed that the activation of the ERK pathway extends the half-life of the MYC protein through the phosphorylation of the Ser62 residue (Figure 1.10). However, it has not been defined as to whether ERK is the directly responsible for this event. Some evidence such as the matching consensus sequence of ERK and the inhibition of Ser62 phosphorylation by ERK inhibitor PD098059, suggests that ERK is a likely candidate (Sears et al. 2000).

Cells are able to respond to extracellular mitogens and inhibitory actions such as the removal of growth factors in the early phase of G1. After crossing the R point, which occurs almost at the end of G1, the cells take the commitment to advance through the remainder of the cell cycle. The degree of phosphorylation of the Rb protein acts as a sensor for the crossing of the R point. For the G0/G1 transition phase, Rb changes from a non-phosphorylated state to a hypophosphorylated state due to the action of Cyclin D-CDK4/6 complexes. This results in the disruption of Rb binding to E2F transcription factors which are responsible for Cyclin E expression. To achieve the hyperphosphorylated state, which is necessary for the G1/S phase transition, Cyclin E-CDK2 complexes have to phosphorylate the remaining residues in hypophosphorylated pRb.

It has been shown that ERK is able to regulate the expression of the chromatin associated receptor Cdc6 (Lunn, Chrivia & Baldassare 2010). The activated CDK2-Cyclin E complex binds to this receptor as a pre-requisite for DNA synthesis upon S-phase entry (Koff et al. 1992, Pagano et al. 1993). It has been proposed that ERK is also able to regulate Cyclin E

expression, nuclear translocation of the CDK2-Cyclin E complex and CDK2. phosphorylation of residue T160 which is essential for its activation (Lunn, Chrivia & Baldassare 2010, Keenan, Bellone & Baldassare 2001, Lents et al. 2002)

In cancer, the sustained activation of ERK promotes the phosphorylation and stable expression of *FOS*, *JUN*, *MYC* and *ELK-1* resulting in the accumulation of proteins required for cell cycle entry and the repression of genes which inhibit proliferation. Moreover, the disruption of anti-proliferative effects such as transforming growth factor beta (TGF-β) has also been observed. Kretzschmar et al. found that the hyperactivation of the MAPK pathway by ^{V12H}Ras caused the phosphorylation of Smad2 and Smad3 in ERK consensus sites (Kretzschmar et al. 1999). Later studies demonstrated that these phosphorylation events prevented the nuclear accumulation of SMAD2 and SMAD3 resulting in the blockage of $p15^{INK4B}$ and $p21^{CIP1}$ transcription (Seoane et al. 2001).

1.3.2 Apoptosis

Apoptosis or programmed cell death in mammalian cells is mediated through either the intrinsic pathway or the extrinsic pathway depending on the origin of the stimuli (Ashkenazi 2002, Li et al. 1997). ERK has been involved in the activation of both pathways as well as in anti-apoptotic responses (Cagnol, Chambard 2010).

The intrinsic pathway is activated by intracellular stress signals and is mediated by the BCL-2 proteins (Cory, Adams 2002a). Within the three subfamilies of BCL-2 related proteins there is a subfamily characterized by its anti-apoptotic activity known as BCL2. This family is integrated by BCL-2, BCL-XL, BCL-W, A1 and MCL1 proteins (Petros et al. 2001). The other two subfamilies, BAX and BH3-only have pro-apoptotic properties and are integrated by the following proteins: BAX, BAK and BOK in the case of BAX family and

BID, BIM, BLK, BAD, BMF, HRK, NOXA and PUMA constitute the BH3-only family (Cory, Adams 2002a). BH3 proteins act as damage sensors and direct antagonists of anti-apoptotic BCL-2 proteins (Oltvai, Milliman & Korsmeyer 1993). The binding of BH3 to BCL-2 and BCL-XL, results in the release of BAX or BAK from these anti-apoptotic proteins (Puthalakath, Strasser 2002) (Figure 1.11). BAX and BAK proteins have the main role of disrupting the mitochondrial membrane which leads to the Cytochrome c release (Madesh et al. 2002, Wei et al. 2000). The interaction between APAF-1 and Cytochrome C activates caspase 9 which in turn cleaves the effector caspase 3 (Li et al. 1997) (Figure 1.11). Finally, the latter caspase contributes to apoptotic chromatin condensation and DNA fragmentation (Porter, Janicke 1999).

The extrinsic pathway depends on the activation of death receptors from the tumor necrosis factor (TNF) receptor family that promote the recruitment and activation of initiator-caspase 8 via the adaptor protein FADD or TRADD (Ashkenazi 2002) (Figure 1.11). Activated caspase 8 cleaves effector caspase 3 which results in the formation of apoptotic bodies (Stennicke et al. 1998). A link between the extrinsic and intrinsic pathway has been established based on the activation of BID by caspase 8, resulting in the amplification of the apoptotic signal (Li et al. 1998).

One of the main lines of evidence showing that the activation of ERK promotes cell death comes from the interaction with p53. This tumor suppressor protein is a nuclear protein with a short half life regulated mainly through post-translational modifications (Levine 1997). After p53 concentration increases in response to certain physiologic signals, p53 is stabilized by phosphorylation and acetylation of specific residues (Chehab et al. 2000a, Buschmann et al. 2001, Itoh et al. 2000). This protein then is able to bind to the promoters of target genes implicated in apoptosis, particularly in the release of Cytochrome c such as BAX, FAS\APO1, KILLER/DR5, PIGS, IGF-BP3, PERP, NOXA, p53AIPI, p53DINP1,

PUMA, BID and caspase 6 (Vousden, Prives 2009). In a variety of systems, ERK has been shown to phsophorylate p53 in the Ser15 residue, which leads to stabilization and activation of p53 (Wang, Shi 2001).

ERK has also been shown to increase the expression of death ligands (TNFα or FASL) (Jo et al. 2005, Ulisse et al. 2000), death receptors (FAS, DR4, DR5) (Tewari et al. 2008, Drosopoulos et al. 2005, Shenoy, Wu & Pervaiz 2009) and FADD (Tewari et al. 2008, Cagnol, Van Obberghen-Schilling & Chambard 2006). ERK also contributes to the downregulation in the expression of BCL-XL and BCL-2 (Liu et al. 2008, Tang et al. 2002, DeHaan, Yazlovitskaya & Persons 2001, Li et al. 2007).

Paradoxically, there is some evidence showing that ERK pathway has a protective role from apoptosis. It has been shown that ERK phosphorylates FOXO3A promoting its degradation and preventing FOXO3A-depending BIM expression (Yang et al. 2008). Moreover, the BIM_{EL} has been demonstrated to be directly phosphorylated by ERK which contributes to its proteasomal degradation (Ley et al. 2003b, Weston et al. 2003, Ewings et al. 2007). The cytosolic ERK substrate p90RSK is able to regulate the binding of the pro-apoptotic protein BAD to 14-3-3 through a direct phosphorylation. This prevents the binding of BAD to other anti-apoptotic proteins and its inhibition. Moreover, this phosphorylation in BAD has been involved in the proteasome dependent turnover of the protein (Bonni et al. 1999, Shimamura et al. 2000).

A failure of cells to undergo apoptosis is a common feature in many types of cancers. ERK pathway has been shown to promote cell survival through the regulation of the BCL-2 proteins and other mechanisms as mentioned above. The importance of ERK in tumor survival or regression due to apoptosis will differ from one type of cancer to another depending on the driver oncogene and other factors (Balmanno, Cook 2009).

Figure 1.11 Two main pathways for apoptosis (Taken from Cory, Adams 2002b) The cell intrinsic pathway is regulated by the BCL-2 protein whose main role is to regulate the release of the Cytochrome C from the mitochondria. The association of APAF-1 with an ATP molecule and Cytochrome C results in the formation of the apoptosome which in turn activates pro-caspase 9. Finally the activated form of pro-caspase 9 (caspase-9) cleaves caspase 3 and 7. Omi and DIABLO proteins promote caspase activation through neutralizing the inhibitory effects of the IAP protein. In the extrinsic pathway or Death-receptor pathway, the binding of FASL ligand to FAS receptor recruits the adaptor protein FADD to the membrane which in turn recruits pro-caspase8. The activation of caspase 8 by DISC (not shown in the diagram) results in the cleavage and activation of caspase 3. Caspase 8 can also cleave the BID protein which acts as a signal on the mitochondrial membrane facilitating Cytochrome c release.

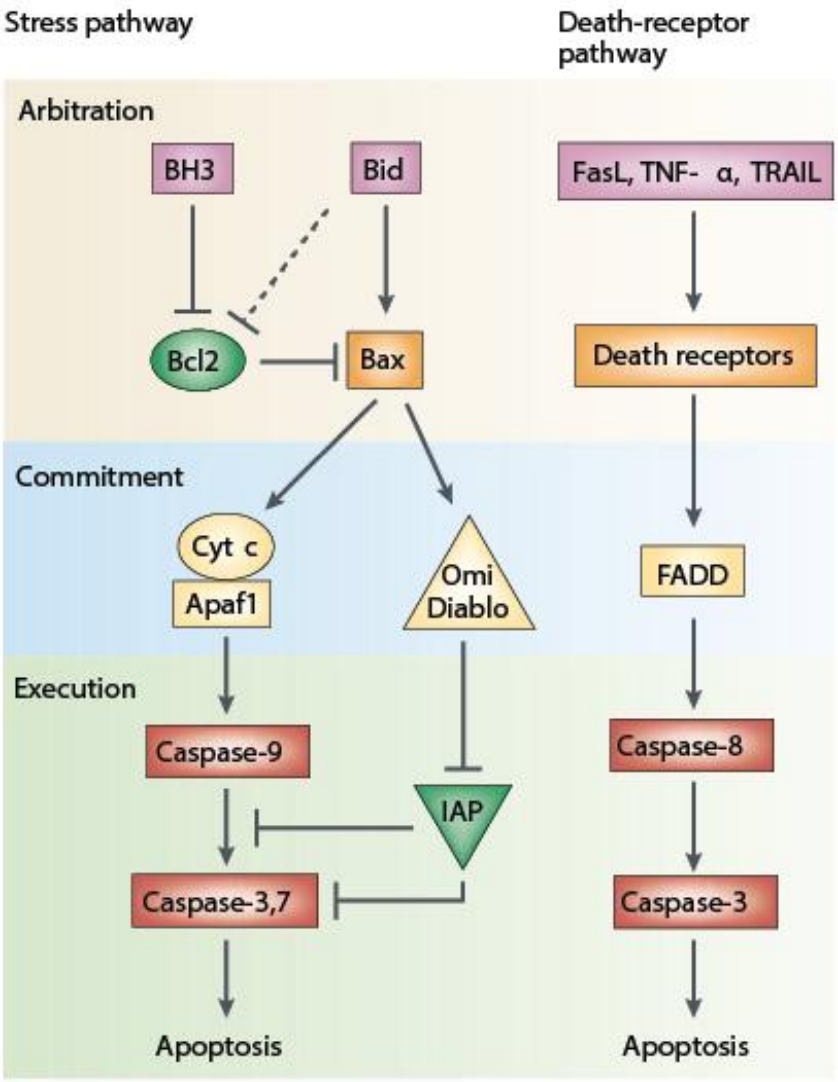

1.3.3 Autophagy

Autophagy, also known as macroautophagy, is a process by which cells capture intracellular proteins, lipids and organelles, and delivers them to the lysosomal compartment where they are degraded (Levine, Kroemer 2008, Mizushima 2010). The first step for this process is the formation of a double-vesicle termed autophagosome that sequesters cytoplasmic materials. Then, the fusion of the autophagosome with the lysosome takes place, resulting in the release of the internal membrane vesicles into the lumen of the lysosome (Liou et al. 1997, Berg et al. 1998). The single-membrane vesicles referred to as autophagic bodies and their contents are then degraded by hydrolases that reside in the lysosome (Rabinowitz, White 2010). The products of autophagic degradation are exported from the lysosome to the cytoplasm where they are recycled as building blocks for new proteins (Rabinowitz, White 2010).

Autophagy can occur at basal levels contributing to the removal of unfolded proteins and damaged organelles. However, increased autophagic activity can be induced by starvation or stress, resulting in bulk intracellular degradation (Rabinowitz, White 2010). Autophagy also can be selective or non-selective. The former uses ubiquitin as tags for the identification and selective elimination of the target proteins and organelles.The ubiquitylated products are recognized by autophagy receptors that link the cargo to the autophagosome machinery (Clague, Urbe 2010a).

Macroautophagy, which is a general response in eukaryotic cells, has been studied in detail through light microscopy in the yeast *Saccharomyces* cerevisiae (Takeshige et al. 1992, Cebollero, Reggiori 2009). In this organism two main cellular components have been confirmed to be essential in the autophagosome formation: the pre-autophagosomal structure (PAS) and the 16 *ATG* (autophagy-related) genes (Suzuki et al. 2001, Suzuki,

Ohsumi 2000). PAS is an isolation membrane to which the ATG proteins transitionally associate, resulting in the formation of a double-membrane vesicle.

Because the localization of the ATG proteins at the PAS is a hierarchic process, these proteins have been classified in two main groups: The first group consists of the ATG17-ATG29-ATG31 complex which acts as a scaffold for PAS organization. This group also includes ATG1, ATG13 and ATG9 (Nakatogawa et al. 2009, Suzuki, Ohsumi 2010). The latter has been shown to cycle between the peripheral puncta in the cytoplasm and the PAS, suggesting its involvement in the delivery of membrane necessary for the formation of the autophagosome. It has been shown that the deletion of any of these genes, except from ATG9, blocks the recruitment of most of the ATG proteins to the PAS. The second group is composed of the PtdIns(3) kinase complex I integrated by ATG14 and VPS30, the ATG2-ATG18 complex, the ATG12 system and the ATG8 system. PtdIns(3) kinase complex I is specifically involved in the double membrane vesicle formation and is required for the recruitment of other ATG proteins. ATG12 and ATG8 proteins are ubiquitin-like proteins. ATG12 is conjugated to ATG5 in an uniquitin-like reaction that requires ATG7 and ATG10 (E1 and E2-like enzymes respectively). ATG12-ATG5 conjugate interacts non-covalently with ATG16 to form a large complex. ATG8 is cleaved at the C´terminus by ATG4 protease to generate cytosolic ATG8-I. Then, ATG8-I is conjugated to a phospholipid, phosphatidylethanolamine (ATG8-II), by serial reactions where ATG7 (E1-like protein) and ATG3 (E2-like protein) are involved. ATG8 protein is engaged in membrane fusion events during the autophagosome formation which require the binding of the phosphatidylethanolamine to the autophagolysosome membrane (Nakatogawa et al. 2009, Suzuki, Ohsumi 2010).

The majority of the *ATG* genes are conserved in mammalian cells as well as the hierarchy of the ATG proteins during the autophagosme biogenesis (Meijer et al. 2007). ATG1

homologues in mammals are ULK1 and ULK2 whereas mATG13 and FIP2000 are the equivalent proteins of ATG13 and ATG17 in mammalian cells (Chan, Kir & Tooze 2007, Young et al. 2006, Ganley et al. 2009, Hosokawa et al. 2009b). The counterparts of the PtdIns(3) kinase complex I are: mVps34, Beclin 1 (homolog of yeast Atg6), p150 (homolog of yeast Vps15), and mATG14 (homolog of yeast Atg14) (Suzuki, Ohsumi 2010). Also the mammalian homolog of ATG8-II defined as LC3II has been reported.

In mammals as well as in yeasts, LC3 is initially synthesized as the non-processed form, pro-LC3, which is converted into LC3-I by the mammalian homologue of yeast ATG4 (mATG4) (Klionsky et al. 2008). LC3I is characterized by the lack of some amino acids from the C´terminus and is localized in the cytoplasm. LC3I is then conjugated to a phosphatidylethanolamine (LC3II) and recruited to the outer and inner membrane of the autophagosomes (Klionsky et al. 2008, Mizushima, Yoshimori & Levine 2010). After fusion with the lysosome, LC3II on the outer membrane is cleaved off by mATG4 and LC3II on the inner membrane is degraded by lysosomal enzymes, resulting in very low LC3 content in the autolysosome. LC3II is known to exist exclusively on autophagosomes and therefore serves as a widely used biomarker. Western blot can easily be used to monitor the changes in LC3 amounts: LC3II migrates faster than LC3I on SDS-PAGE giving an apparent mobility of 16 kDa while LC3I is retarded and identified by an 18 kDa band (Klionsky et al. 2008, Mizushima, Yoshimori & Levine 2010).

The correct analysis of autophagic activity in cells relies in the combination of two types of assays: those which monitor the number of autophagosomes and those that monitor autophagic flux (Mizushima, Yoshimori & Levine 2010). The first category includes: Electron Microscopy counting of autophagosomes, GFP-LC3 puncta formation assay and immunoblot analysis of of LC3II. The second group consists of LC3 turnover assay and selective substrate degradation assays (p62, GFP-LC3) (Klionsky et al. 2008). A common

misinterpretation is that the accumulation of autophagosomes is indicative of autophagy induction. This might not be truth as it also can represent a block in autophagosomal maturation. Thus, the use of several different methods to accurately measure autophagic activity should be considered (Klionsky et al. 2008).

1.3.3.1 Regulation of autophagy

Activated mTOR regulates several mammalian processes including angiogenesis, insulin sensitivity, mitochondrial metabolism, transcriptional responses and autophagy. mTOR is a large protein kinase related to PI3K which integrates nutrient and growth factor derived signals into the control of cell growth (Wullschleger, Loewith & Hall 2006, Foster, Fingar 2010) (Figure 1.12). mTOR can be found in two different complexes: mTORC1 (mTOR, Raptor, mLST8/G-protein β-subunit-like protein (GβL), PRAS40, and Deptor) and mTORC2 (mTOR, Rictor, mLST8/GβL, mSin1, PRR5/Protor, and deptor) (Zoncu, Efeyan & Sabatini 2011). When PI3K becomes activated by RTKs, growth factor receptors or insulin receptor, it catalyzes the generation of phosphatidylinositol-3,4,5-trisphosphate (PIP_3) from phosphatidylinositol-4,5-bisphosphate (PIP_2). PIP_3 recruits Akt to the membrane where it is phosphorylated by PDK1 and mTORC2 (Sengupta, Peterson & Sabatini 2010). Activated Akt inhibits the GTPase activity of TSC2 promoting Rheb-mediated activation of mTORC1 which in turn phosphorylates proteins such as S6K1, S6K1and Ulk-1. In contrast, when genotxic stress, energy deficit and oxygen deprivation promote TSC1-TSC2 GTPase activity, it causes inhibition of Rheb and mTOR leading to an increase in autophagy levels (Inoki et al. 2003) (Figure 1.12). In the case of mTORC2, it has been shown to repress the expression of some *ATG* genes and other autophagy regulators through suppression of the transcription factor FOXO3 (Mammucari et al. 2007).

Figure 1.12 A simplified view of the mTORC1 pathway (Taken from Laplante, Sabatini 2009). Activated PI3K phosphorylates AKT which is able to inhibit the GTPase activity of TSC2. Rheb-GTP then activates mTORC1, resulting in autophagy inhibition. In contrast, AMPK mediated phosphorylation of TSC2 enhances its GTPase activity, resulting in Rheb inactivation and mTORC1 inhibition. AMPK is also able to phosphorylate Raptor causing its dissociation from the mTORC1 leading to high autophagic activity.

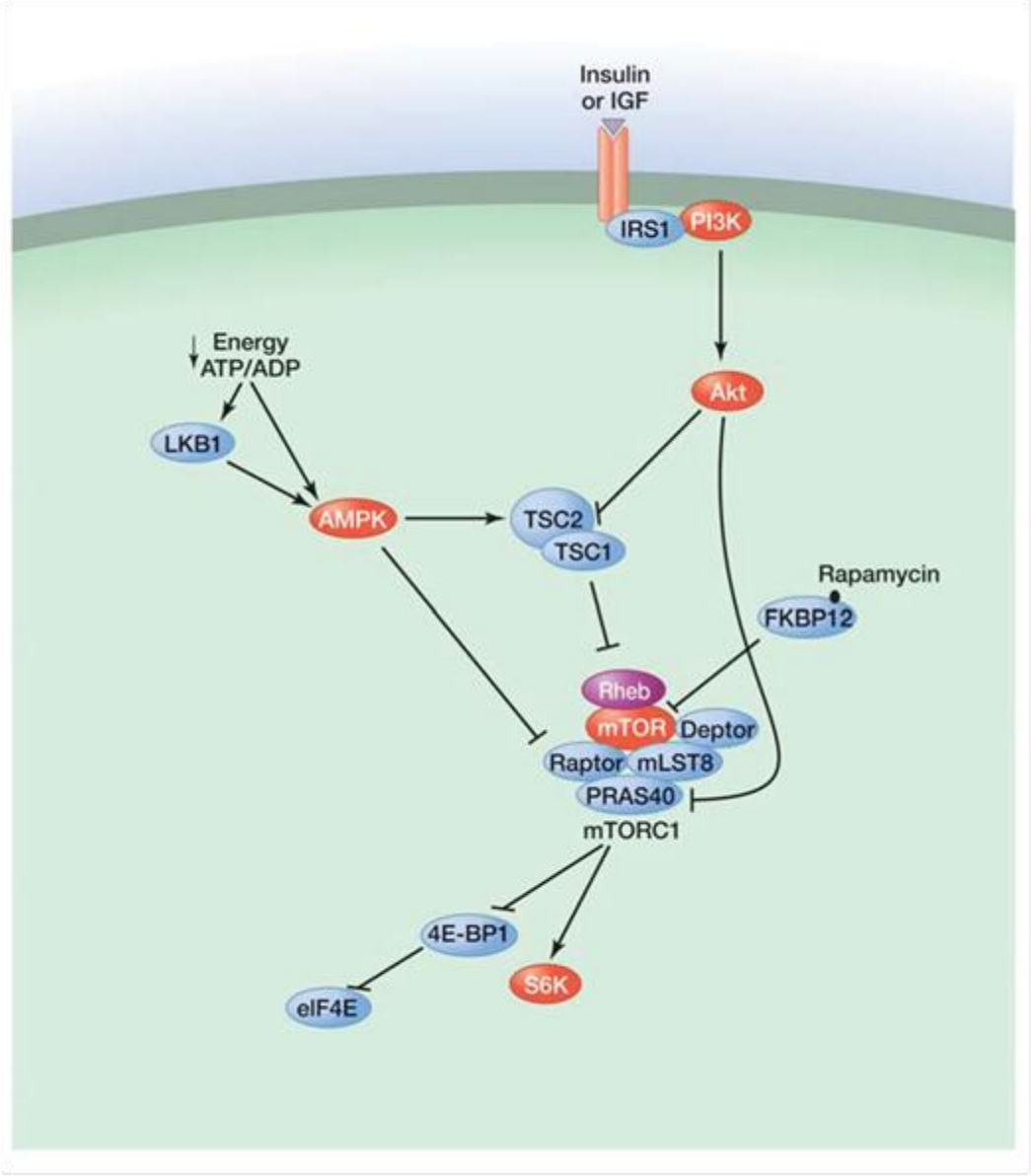

Yeast TOR and its mammalian homolog mTOR are negative regulators of autophagy. In yeasts, the phosphorylation of ATG13 from the ATG17-ATG29-ATG31-ATG1-ATG13 complex by TORC1 results in the dissociation of the complex and the inhibition of the autophagosome formation (Hosokawa et al. 2009a). However, recent studies performed in mammalian cells have confirmed that under nutrient sufficiency activated mTOR phosphorylates S757 from ULK-1 preventing its activation and association with the rest of the ATG proteins whereas the lack of glucose results in ULK-1 phosphorylation by AMPK facilitating the formation of the ATG17-ATG29-ATG31-ATG1-ATG13 complex and consequently autophagy (Kim et al. 2011) (Figure 1.13). AMPK acts as a cellular sensor of the energy status in the cell. If ATP levels are low, AMPK suppresses cell growth and biosynthetic processes through mTORC1 inhibition (Hardie 2007). Previously, two different modes of mTOR regulation by AMPK were reported: AMPK directly phosphorylates TSC2 and raptor (Inoki, Zhu & Guan 2003, Gwinn et al. 2008). The positive phosphorylation of ULK-1 shows the molecular mechanism for autophagy induction by AMPK (Kim et al. 2011) (Figure 1.13).

1.3.3.2 Cross-talk between the ERK and mTORC1 pathways

The RAS/RAF/MEK/ERK pathway cross-activates the PI3K-mTORC1 signaling by regulating PI3K, TSC2 and mTORC1 (Mendoza, Er & Blenis 2011). At the level of TSC2, ERK can phosphorylate residues Ser540 and Ser664 of this protein, which inhibits its GTPase activity, resulting in the permanent binding of Rheb to GTP and consequently mTOR activation and autophagy inhibition (Ma et al. 2005). The downstream effector of ERK, p90 Ribosomal S6 Kinase (RSK), has also been found to negatively phosphorylate TSC2 by phosphorylating Ser1798 and, to a lesser extent, the two conserved AKT sites

Figure 1.13 ULK1 regulation by AMPK and mTOR (Taken from Kim et al. 2011). Under glucose-rich conditions AMPK is maintained in an inactive state and consequently high mTOR activity is observed. The latter is able to prevent ULK-1 activation by phosphorylating the Ser757 residue, resulting in the lack of association with ATG13 and FIP200. In contrast, energy limited conditions causes AMPK activation leading to mTOR inhibition and ULK-1 phosphorylation on residues Ser317 and Ser777. The AMP-phosphorylated ULK-1 is active to initiate autophagy.

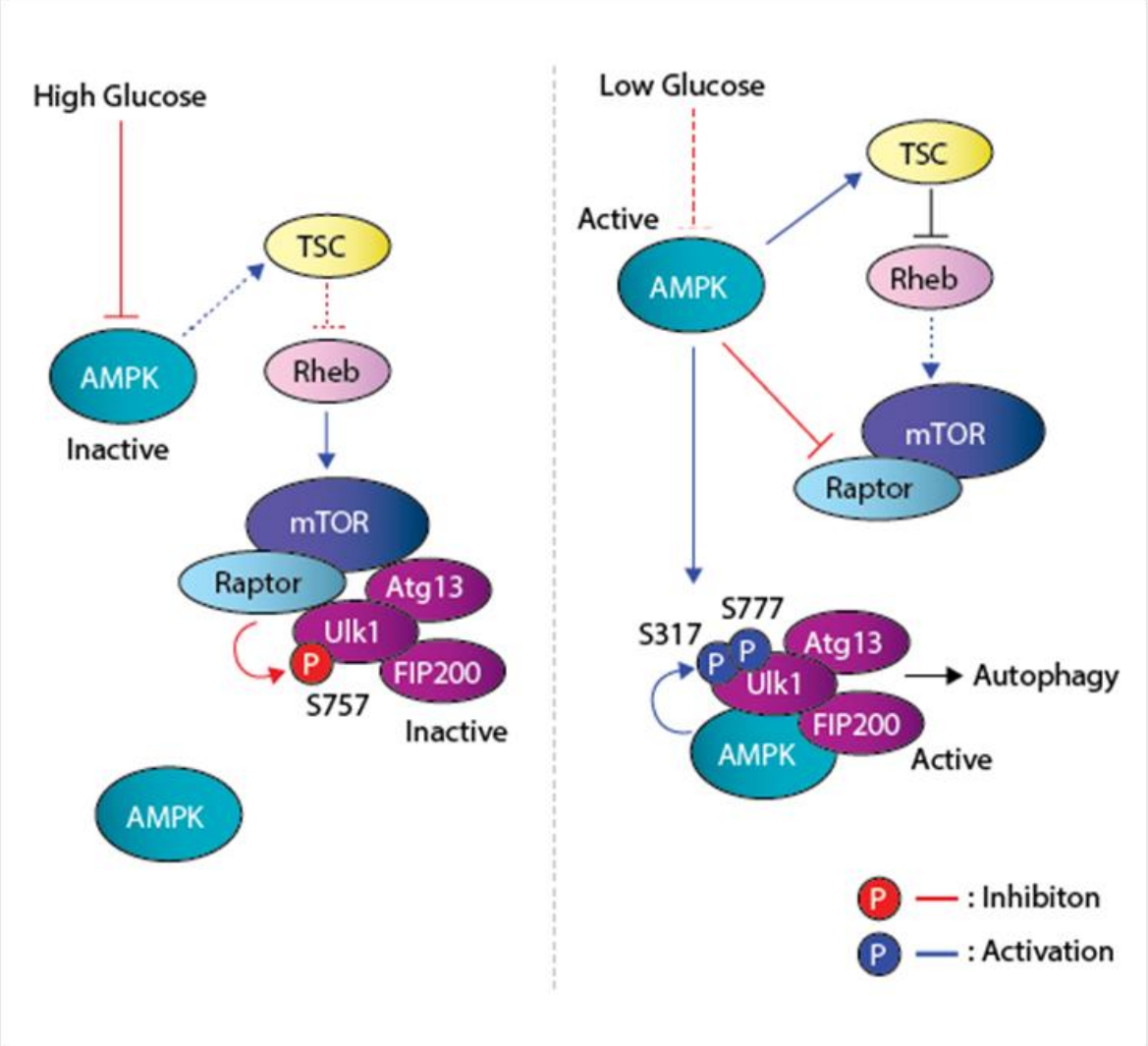

Ser939 and Ser1462 (Roux et al. 2004). At the level of mTORC1, ERK has been shown to phosphorylate Raptor at Ser8, Ser696 and Ser863 causing mTOR activation and autophagy inhibition while RSK1 and RSK2 have been shown to positively regulate mTOR by phosphorylating Raptor at Ser719, Ser721 and Ser722 (Carriere et al. 2008, Carriere et al. 2011).

Importantly, Wang et al in 2009 showed that in response to autophagy stimuli MEK-ERK activation occurs simultaneously with an increase in autophagic activity and Beclin-1 expression in rat hepatoma H4IIE and human erythroleukemia K562 cells. They were able to demonstrate that in this non-canonical MEK-ERK pathway, the main activator of MEK was AMPK and not the RAF proteins. The activation of TSC2 by MEK caused mTORC1 and mTORC2 inhibition and high autophagy levels (Wang et al. 2009).

1.3.3.3 ERK induces autophagy independently of the mTORC1 pathway

It has been shown that the RAF/MEK/ERK pathway is also able to modulate autophagic activity: high concentrations of free amino acids can stimulate the phosphorylation of S259 in CRAF causing its binding to 14-3-3 and the inactivation of MEK (Pattingre, Bauvy & Codogno 2003). The lack of TSC2 activation by MEK results in Rheb binding to GTP and mTOR stimulation which results in autophagy inhibition (Wang et al. 2009). An alternative mechanism for macroautophagy stimulation by ERK is one involving the phosphorylation of the Gα-interacting protein (GAIP) by activated ERK. Activated GAIP shows high GTPase activity, resulting in Gα_{13} activation thereby promoting its association with $\beta\gamma$ dimer and the initiation of the signaling pathway controlling the lysosomal-autophagic route (De Vries et al. 2000, Ogier-Denis et al. 1997, Ogier-Denis et al. 2000).

In cancer cells with impaired autophagy, an accumulation of abnormal mitochondria that result in increased levels of reactive oxygen species (ROS) and consequently, acquisition of genome mutations has been observed (Karantza-Wadsworth et al. 2007, Mathew et al. 2007). Paradoxically, autophagy has also been shown to limit tumor necrosis and inflammation which induces angiogenesis and tumor growth (Vakkila, Lotze 2004, Zeh, Lotze 2005). The fact that ERK has been implicated in the promotion and suppression of autophagy suggests a tumorigenic role for this kinase that is context-specific.

1.3.4 Senescence

Hayflick and Moorhead defined senescence as the state in which the cells are incapable of entering into cell division cycle no matter what growth factors and nutrients are added. They observed that primary human diploid fibroblasts cultured *in vitro* become permanently arrested after 60-80 population doublings (Hayflick, Moorhead 1961).

Later studies confirmed that senescent cells entered into an irreversible growth arrest in the G1 phase of the cell cycle being no longer able to divide regardless of being viable and metabolically active (Campisi 2005, Herbig, Sedivy 2006, Kuilman et al. 2010b, Sharpless, DePinho 2005).

The senescent response is controlled by the shortening of telomeres which acts as a cell division counting mechanism (Harley, Futcher & Greider 1990). The telomeres are composed of TTAGGG repeats and are located at the end of the eukaryotic chromosomes (Meyne, Ratliff & Moyzis 1989). These chromosomal regions are maintained by telomerase which is a ribonucleoprotein complex that includes RNA template and a reverse transcriptase catalytic subunit (Bodnar et al. 1998). Because the telomerase is not expressed in somatic cells, each round of DNA replication is accompanied by telomere

shortening which eventually leads to permanent growth arrest better known as replicative senescence (Wright et al. 1996). It has been shown that normal cells can go more rapidly into senescence when they are exposed to potential oncogenic stimuli such as: UV radiation (Chainiaux et al. 2002), ionising radiation (Sedelnikova et al. 2004), oxygen stress (Ramirez et al. 2001, Parrinello et al. 2003) or activation of certain oncogenes (Serrano et al. 1997, Courtois-Cox et al. 2006a, Dankort et al. 2007, Sarkisian et al. 2007).

1.3.4.1 Hallmarks of senescent cells

Some of the hallmarks shown by cells undergoing replicative senescence includes the loss of proliferative capacity involving the $p16^{INK4A}$-Rb pathway, the presence of the persistent DNA damage response dependent on p53, morphological changes, induction of senescent-associated β-galactosidase (SA β-gal) activity, changes in the secretome defined as Senescence-Associated Secretory Phenotype (SASP) and alterations in chromatin structure reflected in the formation of Senescence-Associated Heterochromatic Foci (SAHF) (Rodier, Campisi 2011) (Figure 1.14). All of these senescence biomarkers are described in more detailed in the following subsections.

a) Cell cycle arrest

Many senescent cells harbour genomic DNA damage at other regions different from telomeres generating a persistent DNA Damage Response (DDR) (Nakamura et al. 2009). When severe or irreparable DNA damage occurs such as DNA double strand breaks, the MRN complex is recruited to the damaged site (Lee, Paull 2005). This complex apart from being engaged in the repair mechanism of the DNA double strand break, it associates with an ATM dimer resulting in ATM autophosphorylation and the formation of catalytically

active ATM monomers (Lee, Paull 2005, Bakkenist, Kastan 2004, Bakkenist, Kastan 2003, Sun et al. 2005). BRCA1 protein, which is also recruited to the site along with the MRN complex, is involved in the repair mechanism of the DNA double strand break either by non-homologous end joining or homology-directed repair (Aglipay et al. 2006). Activated ATM is able to phosphorylate the histone H2AX (Burma et al. 2001) and the p-53 binding protein-1 (53BP1) (Ward et al. 2003). The former is a variant of histone H2A that, when phosphorylated at Ser139 by ATM, creates a binding site for other proteins involved in the recognition or repair of the double strand break (Rogakou et al. 1998). 53BP1 protein binds to the central DNA-binding domain of p53 enhancing p-53 mediated transcription (Iwabuchi et al. 1998). The tumor suppressor p53 is a transcription factor that plays a central role in the response of mammalian cells to genotoxic stress. After p53 concentration increases in response to DNA damage-related signals, p53 is stabilized by phosphorylation and acetylation of specific residues (Chehab et al. 2000a, Buschmann et al. 2001, Itoh et al. 2000). This protein then is able to bind to the promoters of target genes implicated in growth arrest such as: $p21^{CIP1}$, GADD45, 14-3-3 and BAX (Di Leonardo et al. 1994, Carrier et al. 1999, Hermeking et al. 1997). Other downstream target substrates phosphorylated by ATM are CHK2, CHK1, MDM2 and E2F1. Activated CHK2 phosphorylates p53 inhibiting the interaction of this protein with Mdm2, resulting in p53 stabilization and sustained cell cycle arrest (Takai et al. 2002, Chehab et al. 2000b). CHK2 is also able to phosphorylate CDC25A and CDC25C inducing their degradation and consequently the inhibition of Cyclin E-CDK2 kinase activity leading to S phase arrest (Falck et al. 2001). The persistent DNA damage response has been shown to initiate a p53-independent cytokine response through ATM, NBS1 and CHK2, suggesting that, in addition to coordinate cell-cycle checkpoints and DNA repair, the DNA damage response is involve in the production of IL-6 and IL-8 and through their action in the communication of the cells with their surrounding tissue (Rodier et al. 2009).

b) Increase in $p16^{INK4A}$ expression

The growth arrest state during senescence can also be reached through p53-independent mechanisms. In this response, the tumor suppressor Rb plays a crucial role (Shay, Pereira-Smith & Wright 1991). When pocket proteins, pRb, p107 and p130, are in their non-phosphorylated or hypophosphorylated state, they bind E2F transcription factors, resulting in the blockage of their transcription activating domain (Classon, Dyson 2001). The binding of the Rb family members to E2F transcription factors also causes the recruitment of proteins that modify the chromatin structure leading to transcriptional repression (Magnaghi-Jaulin et al. 1998). However, if the Rb family members are phosphorylated by the Cyclin-dependent kinases (CDKs) they cannot bind to E2F transcription factors, resulting in gene transactivation and cell cycle progression (Chen et al. 1989, Hinds et al. 1992, Lundberg, Weinberg 1998). The activities of the CDKs are regulated by the binding of CDK inhibitors which are categorized into two different groups: the KIP/CIP family integrated by $p21^{CIP1}$, $p27^{KIP1}$ and $p57^{KIP2}$ and the INK4 family composed by $p15^{INK4B}$, $p16^{INK4A}$, $p18^{INK4C}$ and $p19^{INK4D/ARF}$ (Sherr, Roberts 1999).

The INK4 family protein specifically inhibits the Cyclin D-CDK4/CDK6 complexes. The binding of any of these proteins to the cyclin binding site of CDK6, reduces its affinity for Cyclin D (Sherr, Roberts 1999). At the same time, they distort the ATP binding site compromising the catalytic activity of the CDK4/CDK6 proteins (Russo et al. 1998). $P19^{INK4D}/^{ARF}$ has been shown to mediate senescence in murine cells (Xue et al. 2007) while in human cells, its equivalent $p14^{ARF}$ protein does not play a crucial role in this process (Michaloglou et al. 2005a). $P19^{INK4D/ARF}$ protein binds to MDM2 and sequesters it in the nucleolus. Because MDM2 is responsible for the ubiquitylation of p53 that allows its degradation, the action of $p19^{INK4D/ARF}$ results in p53 accumulation and cell cycle arrest (Honda, Yasuda 1999).

The KIP/CIP family inhibits a broad range of CDK, specifically the protein $p21^{CIP1}$ acts as a CDK inhibitor able to bind to CyclinE-CDK2, CyclinA-CDK2, CyclinA-CDC2 and Cyclin B-CDC2 complexes (Harper et al. 1993, Xiong et al. 1993). Its binding causes the obstruction of the ATP binding site in the catalytic cleft of the CDK (Russo et al. 1996). This results in the maintenance of hypophosphorylated pRb which remains attached to E2Fs, repressing the expression of genes implicated in the cell cycle (Ezhevsky et al. 1997) (Figure 1.14).

c) Increase in Senescent associated β-galactosidase (SA β-gal) activity

β-galactosidase enzyme is expressed exclusively by senescent cells during *in vitro* and *in vivo* conditions. This enzyme, histochemically detectable at pH = 6, has been found in senescent fibroblasts and keratinocytes in culture as well as in skin samples from human donors in an age-dependent pattern. β-galactosidase is considered to be an alternative spliced form of the lysosomal β-galactosidase whose presence is explained by the elevated lysosomal activity detected during senescence (Dimri et al. 1995b) (Figure 1.14)

d) SASP

It has been shown that senescent cells increase the expression of genes encoding different types of secreted proteins such as inflammatory cytokines and chemokines. In 2008, Kuliman et al. showed that IL-6 and IL-8 are not only secreted during the senescent response induced by DNA damage but also in response to oncogene-induces senescence (OIS) (0). They discovered that high levels of IL-6 and IL-8 are due to increased activation of the C/EBPβ transcription factor by IL-6 itself. Moreover, they showed that IL-6 is able to

increase $p15^{INK4B}$ expression and in conjunction with an IL-6 autocrine signaling effect, this can instigate cell cycle arrest (Kuilman et al. 2010a).

e) Heterochromatin foci

In senescent cells, DNA is organized as a new type of facultative heterochromatin denominated (SAHF). This heterochromatin has a different appereance from that of the constitutive heterochromatin. SAHF is characterized by the presence of histone methyl-transferases and the HP1 protein. This new arrangement of DNA observed in senescent cells is caused by the binding of the Rb protein to the E2F promoter which results in the recruitment of histones deacetylases (HDACs) (Brehm et al. 1998, Chen, Wang 2000, Luo, Postigo & Dean 1998). These enzymes deacetylate the nearby histones, causing chromatin remodelling and transcriptional repression (Rayman et al. 2002). The further recruitment of histone methyl-transferases and HP1 protein to the E2F promoter helps to spread this chromatin remodelling throughout the genome originating the observed foci (Narita et al. 2003b) (Figure 1.14).

f) Morphological changes in senescent cells

Hayflick and Moorhead observed a distinctive phenotype in senescent fibroblasts characterized by elongated shape, flat cell size and vacuolated morphology. Later studies confirmed that senescent fibroblasts show a 3-fold increase in the expression of Vimentin, a type of intermediate filament that constitutes the cytoskeletal network. The overproduction of this protein results in the formation of unusually large bundles of filaments causing a greater mechanical rigidity to the cells which negatively influence the formation of focal adhesions and their proliferation (Nishio et al. 2001).

Figure 1.14 Hallmarks of senescent cells (Taken from Rodier, Campisi 2011). The investigation of cellular senescence generated over the last 40 years has allowed establishment of specific features that characterize the senescent phenotype. These hallmarks include an irreversible growth arrest, the expression of $p16^{INK4A}$ and SA β–gal, secretion of inflammatory cytokines, chemokines or matrix remodeling factors (SASP), nuclear foci containing DNA damage response (DDR) proteins or heterochromatin foci (SAHF).

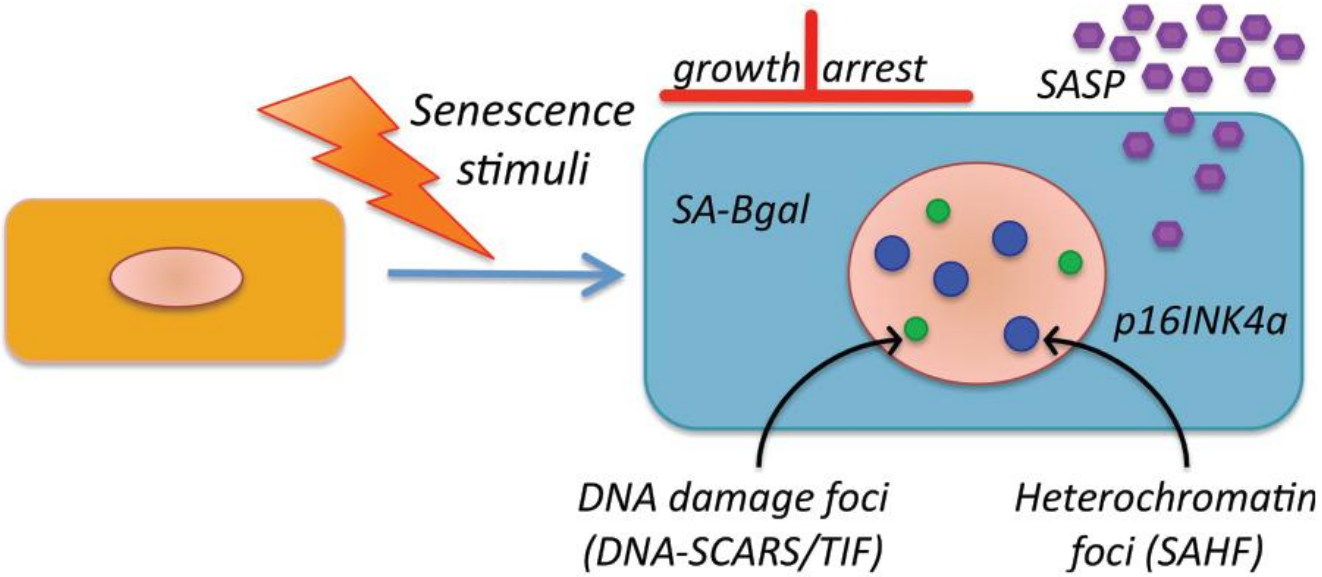

A senescent state that is independent of telomere shortening and that shares some of the hallmarks of replicative senescence discussed above, has been associated to cancer suppression. This type of senescence, known as oncogene-induced senescence (OIS), is present in several pre-neoplastic lesions in mice and humans (Bennett 2003, Mooi, Peeper 2006). In the following section, the relation between the activation of ERK pathway and OIS induction will be discussed.

1.3.4.2 Oncogene-induced senescence

Although aberrant activation of the RAS/RAF/MEK/ERK pathway promotes oncogenic transformation of immortalized cells, it is also tightly associated with senescence in primary cells (Courtois-Cox et al. 2006b). The constitutive activation of RAS, RAF and MEK has been shown to promote OIS in human and rodent primary fibroblasts (Michaloglou et al. 2005a, Collado et al. 2005). This condition is characterized by permanent growth arrest in primary cells cultures, non-responsiveness to mitogenic growth factors, increased expression of the cyclin inhibitors: p21, $p16^{INK4A}$ and $p19^{INK4D/ARF}$ and a distinctive phenotype similar to the one described by Hayflick and Moorhead (Michaloglou et al. 2005a, Collado et al. 2005).

The first evidence due to an oncogenic stimulus comes from a study performed by Serrano et al in 1997. In this study, the ^{G12V}HRAS oncogene was transduced into primary human diploid fibroblasts, primary mice embryonic fibroblasts (MEFs) and immortalized REF52 cells. After ^{G12V}HRAS expression, human and mice fibroblasts showed very similar morphological characteristics to the senescent phenotype described by Hayflick and Moorhead. ^{G12V}HRAS expression also caused cell cycle arrest which was related to increased levels of p53, $p16^{INK4A}$ and $p21^{CIP1}$. Importantly, in rodent fibroblasts the disruption of either p53 or $p16^{INK4A}$ alone was sufficient to prevent oncogenic Ras induced

arrest (Serrano et al. 1997). Later studies performed by this same group using an identical expression system for ^{G12V}HRAS oncogene, added another requisite for RAS-induced senescence in normal human fibroblasts: the constitutive activation of MEK (Lin et al. 1998).

In 2004, a study performed by Tuveson et al. questioned the physiological relevance of the senescent response observed in *in vitro* systems. By using mice that conditionally express ^{G12D}Kras at physiological levels, they observed an increase in proliferation of Kras$^{+/Lox\text{-}G12D}$ MEFs in contrast to the growth arrested state suggested by previous studies. They also found low levels of phosphorylated Erk in Kras$^{+/Lox\text{-}G12D}$ in contrast to the high phosphorylation levels observed in oncogenic-ras overexpressing MEFs. Moreover, when they compared the levels of cell cycle regulatory components in Kras$^{+/Lox\text{-}G12D}$ MEFs and oncogenic-ras overexpressing MEFs, they observed high levels of Cyclin D1 and p16^{INK4A} in both systems but low levels of Cyclin A and Cyclin E in the ^{G12D}Kras overexpressing system which may explain why cell cycle arrest only happens in MEFs ectopically expressing ^{G12D}Kras (Tuveson et al. 2004).

In 2005, Collado et al. demonstrated the upregulation of senescent markers in pre-malignant lesions (adenoma) from mice conditionally expressing ^{G12V}Kras in the lung. In contrast to adenocarcinomas, they also observed an increased presence of proliferation markers in lung adenomas. These observations were extended to mice exclusively expressing ^{G12V}Kras in the pancreas and oncogenic Hras in the skin (Collado et al. 2005).

By employing transgenic mice in which the expression of oncogenic ^{G12V}HRas could be titrated, Sarkisian et al. in 2007 showed that low Ras-GTP levels results in an increased of cellular proliferation. In contrast, the mice expressing high Ras-GTP levels showed an Ink4a-Arf-dependent senescent growth arrest which had the potential to be avoided by inactivation of the p53 pathway. Based on this study and previous reports they concluded

that the Ras activation *in vivo* depends on Ras signal intensity, proposing a three stage model for Ras induced tumorigenesis: the need of an initial activating *Ras* mutation, the overexpression of the activated Ras allele and the evasion of p53-Ink4a-Arf dependent senescence (Sarkisian et al. 2007).

Traditional indicators such as β-galactosidase (Dimri et al. 1995a), senescence-associated heterochromatin foci (SAHF) (Narita et al. 2003a) and $p16^{INK4A}$ (Lowe, Cepero & Evan 2004) have been used to monitor senescence. In 2005, Collado et al. identified novel biomarkers of senescence in lung tissue conditionally expressing ^{G12V}*Kras* oncogene. The DNA microarray analysis of these samples showed increased expression of the following genes: $p15^{INK4B}$, differentiated embryo-chondrocyte expressed gene 1 (*Dec1*) and Decoy Receptor 2 (*DcR2*) (Collado et al. 2005). Since then, various other biomarkers such as the presence of senescence associated secretory phenotype (SASP) (Rodier et al. 2009) and increased autophagic activity have been proposed (Young et al. 2009). It is important to take into account that different senescent lesions may be characterized by different biomarker (Kuilman et al. 2010a). It is advisable not to rely in one single biomarker and to use them in addition with proliferation markers (Kuilman et al. 2010a).

The first evidence of ^{V600E}BRAF inducing senescence *in vitro* came from a study performed by Michaloglou et al in 2005. They transduced human fibroblasts with a mixture of retrovirus containing ^{V600E}*BRAF* or a short hairpin (sh) RNA targeting endogenous ^{WT}*BRAF* and ectopic ^{V600E}BRAF (Michaloglou et al. 2005b). The balance between expression and repression of BRAF resulted in similar levels to those observed in melanoma. After ^{V600E}BRAF expression they observed an upregulation of $p16^{INK4A}$, accumulation of senescence associated heterochromatin foci (SAHF) and inhibition of DNA replication reflected in the absence of BrdU incorporation. The presence of these markers showed the ^{V600E}BRAF expression induces a senescent-like cell cycle arrest phenotype in primary

human cells (Michaloglou et al. 2005b). The induction of OIS *in vivo* by ^{V600E}BRAF has been observed in nevi or common moles, which are melanocytic lesions that frequently contained ^{V600E}BRAF and remained growth-arrested for decades (Michaloglou et al. 2005a). Murine models for the study of senescence are described in more detail in section 1.5.2.

1.4 Negative feedbacks in the RAS/RAF/MEK/ERK pathway

In 2006, Curtois et al. observed that the inactivation of NF1 (RAS-GAP) in human fibroblasts resulted in an increased phosphorylation of ERK followed by the rapid inactivation of this protein. They found that ERK inhibition was caused by negative feedback loops involving SPROUTY, SPREDs and DUSPs. Moreover, they observed that because of RAS inactivation, the inhibition of the PI3K pathway resulted in p53 and Rb activation leading to growth arrest. Overall, Curtois et al. proposed that negative feedback loops are mechanisms through which the cell activates p53 and Rb that are essential for the establishment of senescence (Courtois-Cox et al. 2006a) (Section 1.3.4).

1.4.1 Direct feedback phosphorylations by ERK

Physiologic activation of ERK is negatively feedback-regulated at multiple levels both downstream and upstream of MEK (Miyoshi et al. 2004, Tsavachidou et al. 2004, Bloethner et al. 2005, Fong et al. 2006). Here are some examples of regulatory mechanisms involving from ERK:

COS1 cells were transiently transfected with hSOS1 and treated with phorbol esters to stimulate the ERK pathway. This activation resulted in a decreased electrophoretic mobility of SOS, suggesting its phosphorylation. Further incubation of this protein with pre-

activated ERK confirmed the direct feedback from ERK to hSOS. This negative regulation causes the uncoupling of SOS/GRB2 complex from tyrosine kinases substrates (Porfiri, McCormick 1996).

Oncogenic and wild-type BRAF are feedback phosphorylated by ERK in 4 different S/TP sites: Ser151, Thr401, Ser750 and Ser753. The phosphorylation of these residues was observed in ^{WT}BRAF cells after 30 minutes of PDGF stimulation and could be blocked by MEK inhibitors. The feedback phsophorylation of BRAF by ERK prevented its interaction with active RAS, disrupted the formation of wild-type BRAF-CRAF heterodimers and inhibited the heterodimerization of oncogenic BRAF with CRAF. When the physiological impact of this feedback was evaluated in ^{V600E}BRAF-expressing cells, no difference in its potential to induce cellular transformation was observed. In contrast, intermediate or impaired BRAF mutants showed a non-transformed morphology of the cells and a decrease in focus formation (Ritt et al. 2010b) (Figure 1.15).

ERK is also able to regulate CRAF activation through a negative feedback loop. After quiescent 3T3 cells were treated with PDGF for 5 minutes, Dougherty et al. measured a peak in Craf kinase activity. Fifteen minutes post-treatment, Craf inactivation occurred simultaneously to a change in its electrophoretic mobility. This difference in Craf migration was caused by the phosphorylation of 5 different S/TP residues: Ser29, Ser43, Ser289, Ser301 and Ser642. By blocking the activation of these sites with Mek inhibitors and through isolated incubation of Erk and Craf, it was concluded that Erk was directly phosphorylating these residues. This Erk-dependent negative phosphorylation resulted in the disruption of the Ras-Craf interaction and consequently a reduction of Craf kinase activity (Dougherty et al. 2005) (Figure 1.15). Finally, it has been shown that ERK is able to phosphorylate MEK1 at residue Thr292. This event disrupts MEK1-MEK2 heterodimers,

resulting in a prolonged activation of MEK2 and ERK (Catalanotti et al. 2009) (Section 1.2.6).

1.4.2 GAPs, SPROUTYs, SPREDs and DUSPs

Several feedback regulators controlling the RAS/RAF/MEK/ERK pathway at multiple levels have been discovered. Although the Sprouty (Spry) protein was discovered initially in *Drosophila* (dSpry) (Hacohen et al. 1998), four mammalian dSpry homologs have been reported: Spry1-4 (Guy et al. 2003). *SPROUTY* gene transcription is regulated by the ERK pathway, supporting their role as negative feedback regulators and consequently tumor suppressors. SPRY proteins become activated after various growth factor stimuli such as: Fibroblast Growth Factor (FGF), Vascular-Endothelial Growth Factor, Platelet Derived Growth Factor (PDGF), Hepatocyte Growth Factor, glial-derived growth factor, and Nerve Growth Factor (NGF) (Lee et al. 2004, Mason et al. 2006, Li et al. 2004). SPRY mechanism of action has been demonstrated to be cell and ligand specific. In NIH3T3 stable cell lines conditionally expressing Spry1 and Spry2, it has been shown that the latter is able to prevent Ras activation by disrupting the signal downstream to the formation of the Grb2-Sos complex (Hanafusa et al. 2002). In 2005, Ozaki et al. studied the interactions between various members of the ERK pathway (GRB2, SOS1, RAS, RAS-GAP and CRAF) and SPRY isoforms in HEK293^{T} cells. They transfected these cells with expression vectors encoding SPRY 1-4, stimulated the cells with FGF or EGF and through co-immunoprecipitation experiments, validated two interactions: SPRY1 with GRB2 and SPRY4 with SOS1(Figure 1.15). They proposed that the binding of SPRY1 to GRB2 and the association of SPRY4 to SOS1 prevented the formation of the GRB2-SOS1 complex, resulting in RAS inactivation. Moreover, they showed that SPRY1 and SPRY4 can form heterodimers causing a stronger inhibition of the ERK pathway (Ozaki et al. 2005).

High levels of Spry2 have been found in mice conditionally expressing ^{G12D}Kras in the lung (Shaw et al. 2007). Moreover, the knockout of *Spry2* in ^{G12D}Kras heterozygous mice showed an increase in the number and size of tumors simultaneously with high levels of phospho-ERK. These results confirm the role of Spry2 as a tumor suppressor gene (Shaw et al. 2007).

Another potential mechanism for ERK signaling inhibition by SPRY proteins occurs at the level of CRAF (Figure 1.15). In 2011, Sasaki et al. showed that SPRY4 and SPRY2 are able to suppress VEGF-induced activation of CRAF but are incapable of inhibiting CRAF after EGF stimulation (Sasaki et al. 2001). It is known that, in endothelial cells VEGF binds to VEGFR activating Phospholipase Cγ (PLCγ) which in turn activates PKC. The latter is able to phsophorylate CRAF, resulting in a RAS-independent activation of the pathway. Only after VEGF stimulation, SPRY4 and SPRY2 bound to the kinase domain of CRAF and blocked the phosphorylation of key residues such as Ser338 (Takahashi et al. 2001).

It has also been shown that SPRY2 is able to bind endogenous BRAF in melanoma cell lines, resulting in decreased phospho-ERK levels (Tsavachidou et al. 2004). In contrast, when Brady et al. in 2009 transfected HEK293 cells with *SPRY2* and *BRAF^{V600E}*, a slower migrating form of SPRY2 characterized by the inability to associate with ^{V600E}BRAF was detected. By mass spectrometry analysis, it was determined that SPRY2 was phosphorylated on 6 different residues: Ser7, Ser42, Ser140, Ser167 and previously reported Ser111 and Ser120 (DaSilva et al. 2006). The simultaneous mutation of all residues caused a significant increase between SPRY2 and ^{WT}BRAF association but it did not affect ^{V600E}BRAF binding to SPRY2. These results showed that the resistance of oncogenic BRAF to SPRY2 inhibition can be explained by post-translational phosphorylation of SPRY2 and BRAF kinase conformation. Also the fact that SPRY2 has been found down-regulated in ^{WT}BRAF melanoma and up-regulated in ^{V600E}BRAF

melanoma cell lines, confirms its tumor suppressor role only in the wild-type melanomas (Brady et al. 2009) (Figure 1.15).

The Sprouty-related Ena/VASP homology 1(EVH1) domain containing proteins (SPRED) belong to the SPRY family of proteins (Bundschu, Walter & Schuh 2007). There are four SPRED proteins in mammals: SPRED 1-3 and EVE-3 (Bundschu, Walter & Schuh 2007). SPRED 1 and SPRED 2 have been found to inhibit the ERK pathway after NGF and FGF stimulation (Wakioka et al. 2001). Moreover, as well as SPRY4, SPRED 1/2 are able to repress VEGFA induced ERK activation via VEGFR2 (Taniguchi et al. 2007). It is unclear if SPREDs use the same inhibitory mechanisms as SPRYs because no interacting partner has been yet identified for these proteins (Guy et al. 2009).

MAPKs phosphatases (MKPs) belong to the dual-specificity phosphatase (DUSP) family and can be divided into three groups: DUSP1, 2, 4 and 5 which dephosphorylate ERK (Jeffrey et al. 2007) (Figure 1.15), JNK and p38 MAPK; DUSP6, 7 and 9 which are considered ERK-specific and those targeting JNK and p38 MAPK only such as DUSP 8, 10 and 16 (Caunt et al. 2008). DUSPs are regulated by ERK at the transcriptional and post-translational level (Brondello, Pouyssegur & McKenzie 1999, Ekerot et al. 2008). Special attention has been paid to DUSP6 in relation to cancer progression and resistance. Although the expression of DUSP6 has been found down-regulated in pancreatic (Furukawa et al. 1998) and lung cancer tissue (Zhang et al. 2010) supporting its role as tumor supressors, other reports show DUSP6 upregulation in melanoma cells harbouring ^{V600E}BRAF or mutant NRAS (Li et al. 2012). In 2009, Pratilas et al. gave an answer to this contradiction by showing that in tumors containing mutated or overexpressed RTKs, ERK activation is observed as well as direct negative feedback from ERK to RAF proteins. This regulatory loop results in the attenuated activation of ERK and low expression of DUSPs. In the case of ^{V600E}BRAF tumors, mutant BRAF has shown to be

resistant to ERK negative feedback, resulting in ERK hyperactivation and increased transcription of DUSPs (Pratilas et al. 2009) (Figure 1.15).

1.5 The role of ^{V600E}BRAF in cancer development

The expression of ^{V600E}BRAF in cultured melanocytes results in the constitutive activation of ERK and cellular transformation (Wellbrock et al. 2004). However, this mutation can also be found in approximately 80% of benign naevi which suggests a link between ^{V600E}BRAF and senescence (Pollock et al. 2003a).

1.5.1 Senescence in human tumors

To analyse if the senescent response induced by ^{V600E}BRAF expression in cultured cells could be reproduced *in vivo*, Michaloglou et al. in 2005, employed samples from human congenital nevi (Michaloglou et al. 2005b). Nevi or common moles are a particularly useful model for the study of senescence because they are formed after an initial phase of melanocyte proliferation followed by a growth arrest state that can be maintained for decades (Gray-Schopfer, Wellbrock & Marais 2007). A high proportion of these naevi were characterized by the presence of the ^{V600E}*BRAF* mutation (Pollock et al. 2003b). Therefore, it is conceivable that ^{V600E}BRAF could be driving the senescent process in this scenario, constituting a perfect model for OIS *in vivo*. This study confirmed that the ^{V600E}BRAF positive human naevi were growth arrested supported by the absence of immunostaining for the proliferation marker Ki67. Moreover, they showed an increase activity of SA β–galactosidase and a mosaic expression of $p16^{INK4A}$ in these samples.

Figure 1.15 Negative regulators of the ERK pathway **(Taken from Karreth, Tuveson 2009).** Receptor activation of the ERK pathway results in an increased expression of SPRYs, SPREDs and DUSPs which inhibit the ERK signaling pathway by acting on ERK and other members of the cascade.

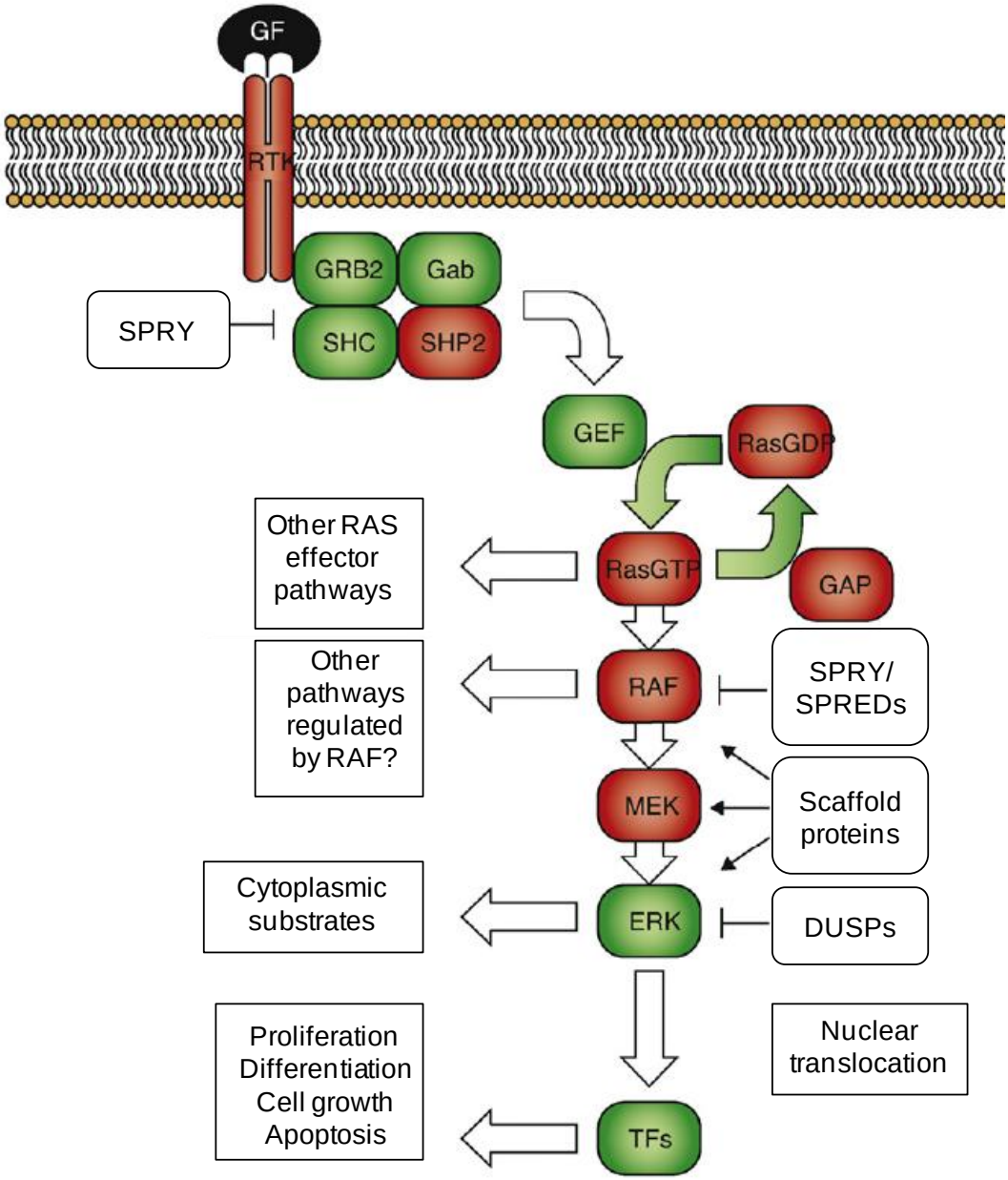

Importantly, the pattern of expression for $p16^{INK4A}$ was also observed in naevi where the ^{V600E}*BRAF* mutation was absent, indicating that $p16^{INK4A}$ is not essential for maintaining the growth arrest in the ^{V600E}BRAF naevi (Michaloglou et al. 2005b).

1.5.2 Mouse models for the study of ^{V600E}Braf

Genetically engineered mouse models (GEMs) in which endogenous Braf *gene* was genetically modified have been developed. These models allow the expression of oncogenic Braf at physiological levels. As discussed in section 1.3.5.2, small differences in oncogene activity can result in quiescence, proliferation or senescence. The creation of mice that are heterozygous mutant for a particular oncogene is definitely a reliable model for the study of senescence *in vivo*.

1.5.2.1 The Cre/LoxP system

Currently, transgenic mice are primarily generated by injection of genetically engineered embryonal stem (ES) cells into mouse blastocysts (Schwartzberg, Goff & Robertson 1989). Through natural homologous DNA recombination, the manipulated transgene substitutes the endogenous allele, contributing to the mouse germ line. Further manipulation of the transgene can be achieved *in vivo* by the use of a site-specific recombination system such as the Cre-lox system (Schwartzberg, Goff & Robertson 1989).

The Cre-lox recombination system was initially observed in the P1 bacteriophage replication cycle as a step needed for the circularization of its DNA (Hamilton, Abremski 1984) (Schwartzberg, Goff & Robertson 1989)(Schwartzberg, Goff & Robertson 1989).

Because of the simplicity of this system, it has been exploited as a technology for genome manipulation in mouse models.

The requirements for the Cre/LoxP system are: a Cre recombinase and two loxP sites flanking the DNA segment of interest (Figure 1.16). The loxP site is 34 bp sequence integrated by a core sequence of 8 bp and two palindrome flank sequences of 13 bp. The orientation of the loxP sites determines the outcome of the recombination: for obtaining the inversion of the target sequence, the loxP sites have to be oriented in opposite directions, flanking the sequence to be inverted; if the deletion of the target sequence is required, the loxP sites have to be oriented in the same direction and finally, if the lox P sites are located in different chromosomes, the translocation between those chromosomes will occurred (Voziyanov, Pathania & Jayaram 1999) (Figure 1.16).

Because the loxP sites and the Cre gene are not native to the mouse genome, they are contained in vectors that are introduced to the ES cells by electroporation (Tompers, Labosky 2004).

1.5.2.2 Generation of *Braf*$^{+/LSL\text{-}V600E}$ mice

For the study of the role of Braf in tumorigenesis, the strain called *Braf*$^{+/LSL\text{-}V600E}$ was developed. Normal Braf expression occurs prior to Cre-mediated recombination but after Cre expression, the *Braf*^{V600E} knockin mutation is expressed. This model mimics the situation in human cells, where one copy of normal *Braf* is converted by somatic mutation to *Braf*^{V600E}. The *Braf*$^{+/LSL\text{-}V600E}$ mice were generated as follows: An LSL vector was constructed consisting of a left arm spanning exon 14, a middle arm containing a mini-cDNA encoding wild-type exons 15-18 of *Braf* and a right arm containing exon 15 with the *Braf*^{V600E}mutation. The middle arm also contained a *neo*^{R} gene which helped in the

Figure 1.16 Structure of the LoxP site (Taken from Nagy 2000). The LoxP site is composed of a 8 bp core sequence where recombination takes place and two flanking 13 bp inverted repeats, resulting in a 34 bp site. When the LoxP sites are oriented in the same direction on a chromosome segment, the Cre recombinase mediates a deletion of the floxed segment.

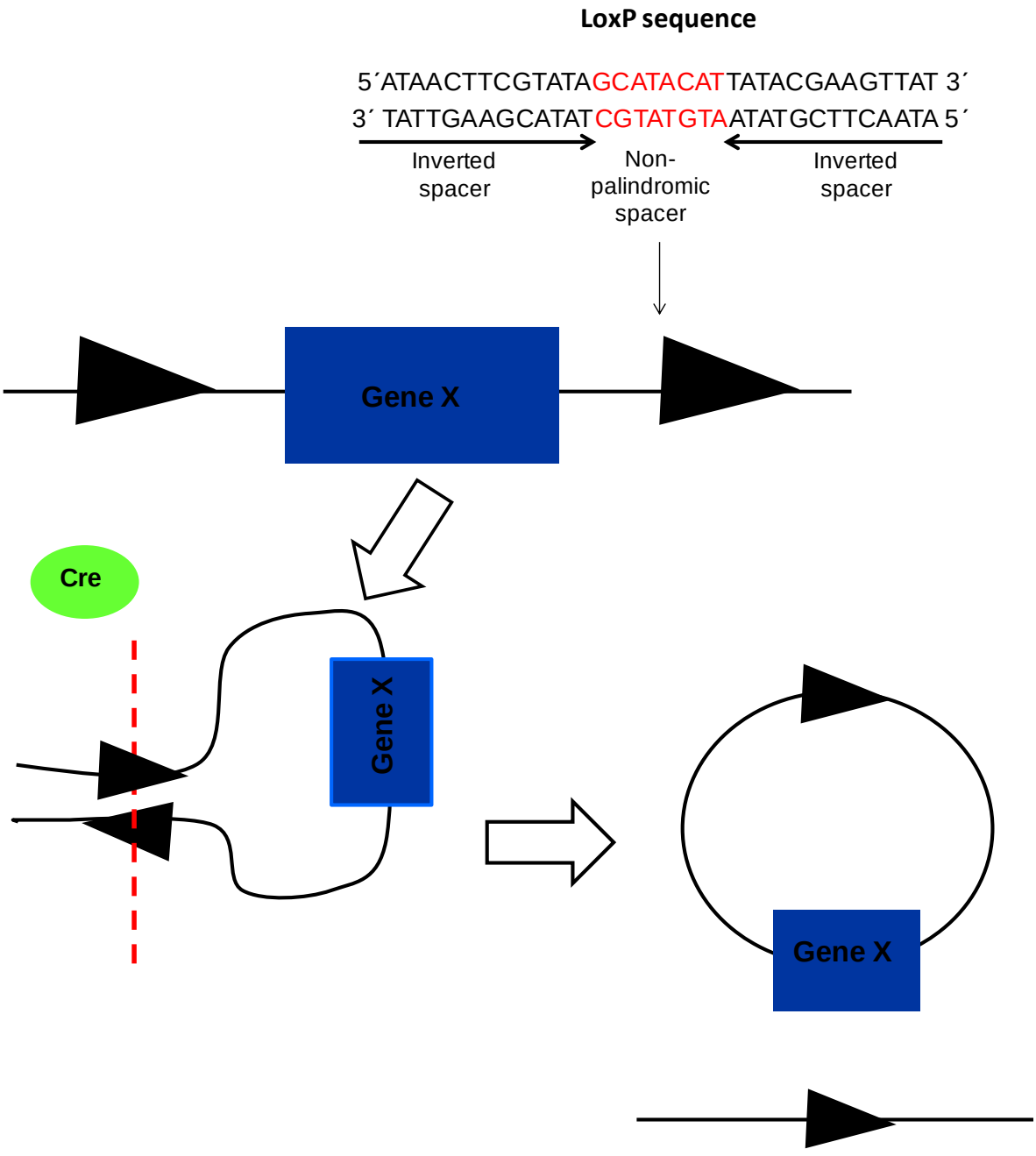

selection of positive clones containing the vector after the electroporation process. Both the mini-cDNA and the *neo*^{R} gene were flanked by loxP sequences and were added with polyadenylation signals at the end of each gene (Mercer et al. 2005) (Figure 1.17).The LSL vector was electroporated into embryonic stem cells (ES) belonging to an albino coat colour mouse. The ES cells were subsequently injected into a 3.5 dpc black coat colour blastocyst (wild-type C57BL6) which was re-implanted into the surrogate female.

Chimeric pups were produced containing cells derived from both, the original injected ES cells and the host blastocyst. In order to generate a breeding colony of *Braf*$^{+/LSL\text{-}V600E}$ mice, chimeric mice were backcrossed with wild-type mice. The offspring showing an agouti phenotype where examples of successful germline transmission (Mercer et al. 2005).

Heterozygous CMV-Cre mice in which the Cre recombinase was constitutively expressed, were crossed to *Braf*$^{+/LSL\text{-}V600E}$ mice generating offspring that showed permanent expression of ^{V600E}Braf in all tissues (*Braf*$^{+/Lox\text{-}V600E}$). The expression of the *Lox-Braf*^{V600E} allele during embryonic development resulted in the death of the embryo approximately after 7.5 days *post-coitum* (dpc) showing that constitutive expression of ^{V600E}Braf is not compatible with survival (Mercer et al. 2005).

As the constitutive expression of ^{V600E}Braf demonstrated incompatibility with mice survival, the mutation had to be acquired somatically. For this purpose several different Cre strains were developed.

One example of this inducible system is represented by the Cre recombinase fused to the binding domain of the estrogen receptor (CreER). Naturally, the estrogen receptor binds to the 17β-estradiol, translocating into the nucleus where it acts as a transcription factor enhancing RNA synthesis (Fawell et al. 1990). In 1993, Danielian et al. observed that the mutation of the glycine residue at position 525 and the mutation of the methionine and/or

Figure 1.17 Generation of conditional knockin *Braf*^{V600E} mouse (Adapted from Mercer et al. 2005). An illustration of the LSL (Lox-Stop-Lox) cassette placed in intron 14 of *Braf* gene is shown here. This cassette contains three *lox*P sites (red arrows), a mini gene (yellow box) encoding exons 15-18 of *Braf*^{WT} with a splice acceptor sequence at the 5´end (SA) and a stop sequence at the 3´end (PA). The vector also contains a *neo*^{R} cassette for the selection of positive clones. In the absence of Cre recombinase, Braf^{WT} is expressed with exons 15-18 being encoded by the mini gene (*LSL-Braf*^{V600E} allele), whereas, in the presence of the Cre recombinase, deletion of the cassette occurs such that ^{V600E}Braf is expressed (*Lox-Braf*^{V600E} allele).

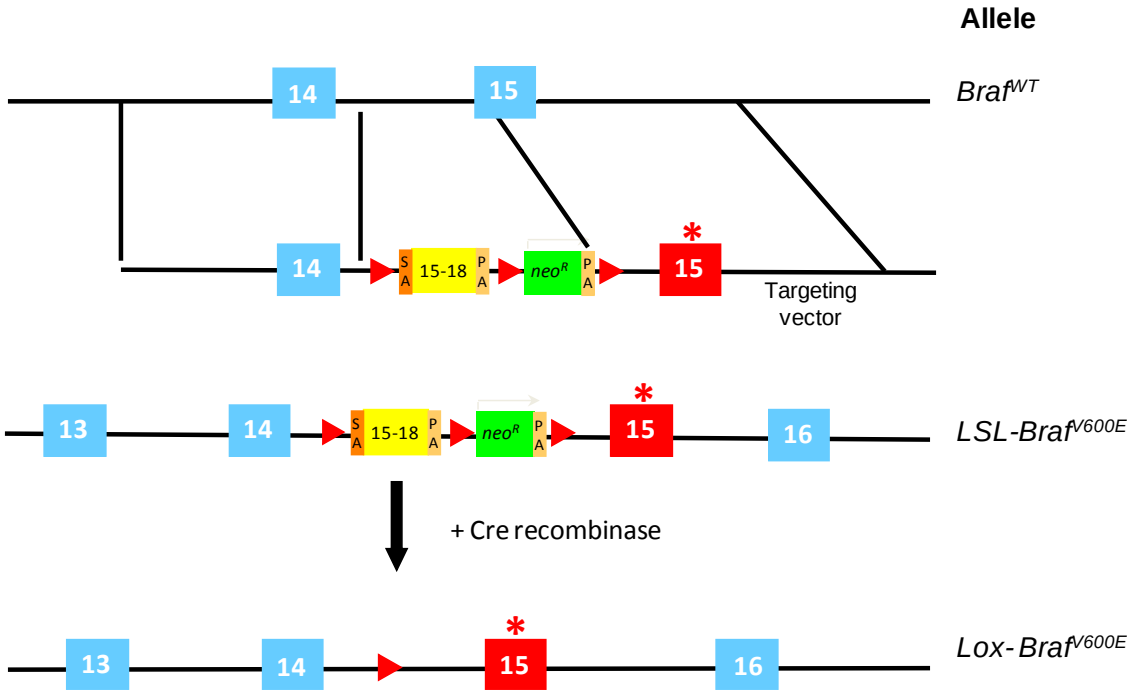

serine at position 521/522 on the estrogen receptor abolished its ability to bind to 17β-estradiol (Danielian et al. 1993). Surprisingly, the mutant estrogen receptor retained the ability to bind its agonist 4-hydroxytamoxifen (4-OHT) and to translocate into the nucleus (Danielian et al. 1993, Littlewood et al. 1995). Because of the advantage of having a nuclear localization sequence in the estrogen receptor, Danielian et al fused the Cre recombinase to the hormone binding domain of this receptor ($CreER^T$). After the mouse was injected with 4OHT, the Cre-mediated recombination was detected (Danielian et al. 1998). Cell specific expression of $CreER^T$ in transgenic mice has been achieved by placing the Cre fusion protein under the control of a tissue specific promoter (Indra et al. 1999). To study the role of the *Braf*^{V600E} oncogene in melanoma development, transgenic *Braf*$^{+/LSL\text{-}V600E}$ mice were crossed to mice expressing a tamoxifen (TM)-activated version of Cre recombinase ($CreER^{T2}$) placed under the control of a tyrosinase promoter (Dhomen et al. 2010). Because the tyrosinase enzyme is a key regulator of melanogenesis and is exclusively expressed in melanocytes, the expression of ^{V600E}Braf was restricted to these types of cells (Ferguson, Kidson 1997).

In 2007, Dankort et al. showed the efficient Cre mediated recombination of a different *LSL-Braf*^{V600E} allele by infecting mice with an adenovirus containing the gene for the *Cre recombinase* (AdCre). In order to restrict the expression of ^{V600E}Braf to the lung, they introduced the virus by intranasal instillation. Some of the advantages of using adenovirus as vehicles for Cre delivery are: their capability to accommodate up to 8 kbp of foreign DNA, their ability to infect a wide variety of cell types (epithelial and endothelial cells, fibroblasts, stromal and hepatocytes, etc) without replicating and the property of growing at high titers.

1.5.2.3 Oncogenic Braf mouse models

Mouse models were developed to explore the role of ^{V600E}Braf in the initiation and progression of tumors and have contributed enormously to characterize the senescence response.

The presence of the *Braf^{V600E}* mutation in melanocytes results in an initial burst in proliferation that lead to the formation of naevus or common mole. These hyperproliferative melanocytes can become growth arrested and remain dormant for decades. In some rare cases, naevi can progress to metastatic malignant melanoma (Gray-Schopfer, Wellbrock & Marais 2007).

The fact that the *Braf^{V600E}* mutation has been found in a high proportion of microdissected naevi samples, raises the question of whether ^{V600E}Braf contributes to the establishment of senescence and to melanoma progression (Michaloglou et al. 2005a). Because of the limited accessibility to human early cancer lesions of melanoma, transgenic mice models expressing *Braf^{V600E}* oncogene have been employed. *Braf$^{+/LSL\text{-}V600E}$* mice were crossed to mice containing a tamoxifen (TM)-activated version of Cre recombinase (CreER^{T2}) placed under the control of a tyrosinase promoter. This technology allowed the expression of heterozygous ^{V600E}Braf, restricting its presence to melanocytes. ^{V600E}Braf expression was induced under two schemes of tamoxifen treatment: 8 treatments over 8 days versus 4 treatments over 7 days at two different doses: 20 mg or 1 mg. The tamoxifen treatment resulted in the increased proliferation of melanocytes represented by areas of hyperpigmented skin and the formation of nevi (Figure 1.18). Positive staining for β-galactosidase and the lack of Ki67 were observed in all nevi. Around 60-70% of mice developed hypopigmented tumors that had remnants of nevi in the periphery and were characterized by increased amounts of mitotic figures and high Ki67 staining (Figure 1.18). Although it cannot be determined whether the tumors in the mice emerged directly out of

Figure 1.18 Timeline of changes in the mouse skin after ^{V600E}Braf expression (Taken from Dhomen et al. 2009). Timeline illustrating the phenotypic changes showed by *Braf*$^{+/LSL-V600E}$ mice after 4-OHT application on the skin. Two months after Cre activation, an increase proliferation of melanocytes was reflected in the hyperpigmentation of specific sections of the skin such as: snouts, tails, ears and paws. Melanocytic lesions in eyelids were detected after 3-5 months in approximately 80% of mice whereas these same type of lesions in the perianal region were evident after 6-10 months in mice treated with the maximum dose of 4-OHT. The appearance of nevi was observed in all animals approximately after 6 months of 4-OHT treatment. These lesions were positively stained for SA β–gal and lacked Ki67 staining. The presence of hypopigmented tumors in approximately 60-70% of mice was observed within 14 months of 4-OHT treatment. The melanoma lesions were characterized by its asymmetry, destructive growth pattern and ulceration. Remnants of blue nevi contiguous to the tumors were detected.

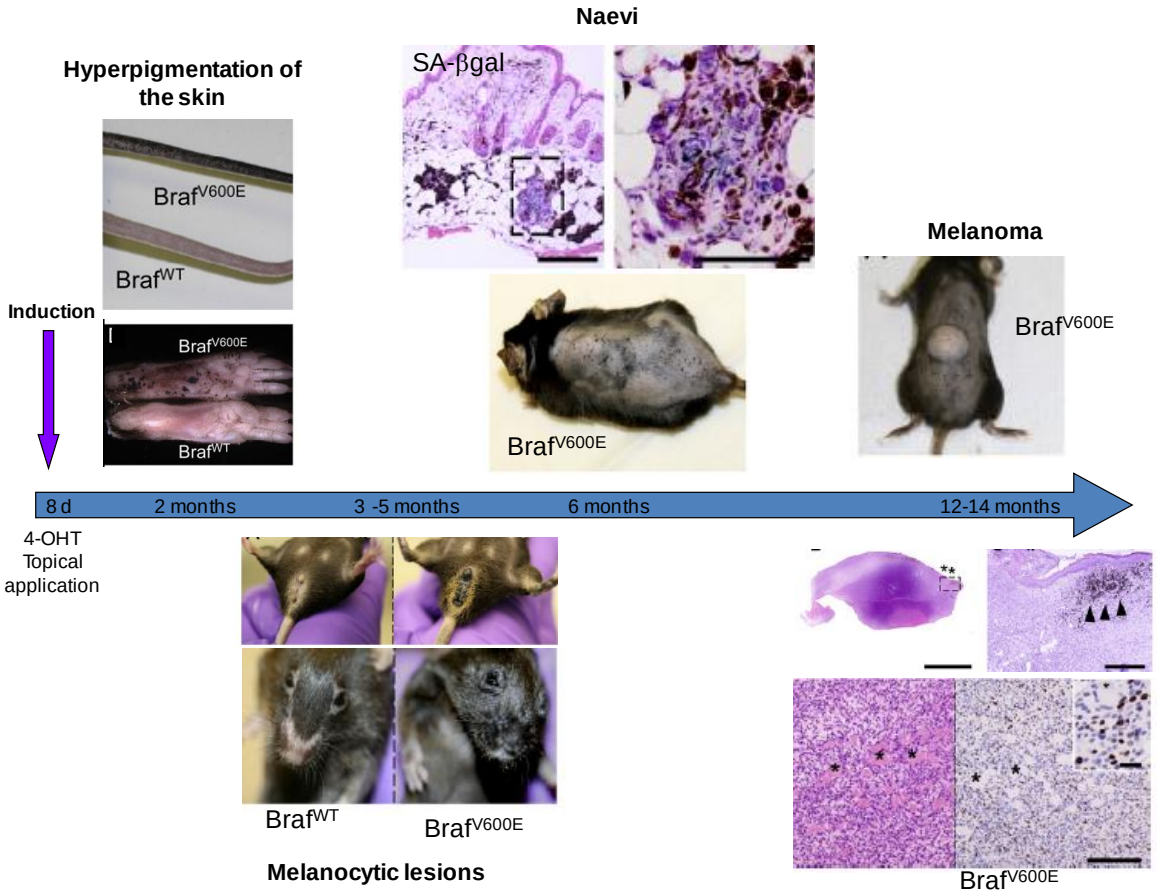

the nevi, this model shows that ^{V600E}Braf is capable of stimulating proliferation, senescence, and in conjunction with naturally occurring additional mutations, melanoma progression. In addition this model showed that p16^{INK4A} is not an essential requirement for the induction of the senescence response and its suppression is not required for escaping senescence (Dhomen et al. 2009). When Dankort et al. in 2007 analyzed lung tissue from mice conditionally expressing ^{V600E}Braf they observed that after 4 weeks of induction, an increase in cellular proliferation was taking place. Moreover, they detected the presence of adenomas at 6 to 8 weeks post-induction. During this period, samples were positively stained for proliferation markers such as Ki67, phospho-histone (H3) and BrdU incorporation. At later time points, approximately 14 weeks post-induction, ^{V600E}BRAF adenomas expressed oncogene induced senescence markers (OIS) such as p19$^{INK4D/ARF}$ and Dec1 but all samples were negative for SA β–gal. Some mice expressing ^{V600E}Braf in an Ink4a/Arf$^{lox/lox}$ or a TP53$^{lox/lox}$ background were the only that developed adenocarcinomas indicating that a mutation in a tumor suppressor gene is required to overcome senescence (Dankort et al. 2007).

In a colorectal cancer model, *Braf*$^{+/LSL\text{-}V600E}$ mice were crossed with mice containing a tamoxifen (TM)-activated version of the Cre recombinase placed under the control of Cyp1A1 promoter (Kemp et al. 2004). The expression of this promoter is exclusive to the stem cells and transit amplifying cells contained in the intestinal crypts. Tamoxifen was administered by intraperitoneal injection to 8-12 weeks old mice. Full recombination of the *LSL-Braf*^{V600E} allele was detected throughout the small intestine after 1 week of tamoxifen treatment (Figure 1.19). Initially, an augment in cell proliferation was detected in the ^{V600E}Braf expressing crypts as well as an increase of proliferation markers such as: phospho-Erk, Ki67, phospho-histone H3, BrdU and the number of mitotic cells (Figure 1.19). After 6 weeks of tamoxifen treatment, the crypts entered into a growth arrest phase

Figure 1.19 Timeline of changes in the small intestine of mice after ^{V600E}Braf expression (Taken from Carragher et al. 2010a). Timeline illustrating the phenotypic changes showed by *Braf*$^{+/LSL\text{-}V600E}$ mice after 4-OHT was injected intraperitoneally. Three days after 4-OHT application, an increase in the number of cells was measured in ^{V600E}Braf-expressing crypts. This hallmark was accompanied by high levels of phospho-Erk. After 1 week of 4-OHT treatment, an increase in the number of cells within the ^{V600E}Braf-expressing villi was detected, resulting in the formation of the serrated epithelium. In contrast, a clear suppression in cell growth was observed at 6 weeks post-treatment in ^{V600E}Braf-expressing crypts. This arrest in proliferation occurred concomitantly with the expression of senescent markers such as: SA β–gal and p16^{INK4A}. Twelve weeks after 4-OHT application approximately 76% of the mice developed tumors.

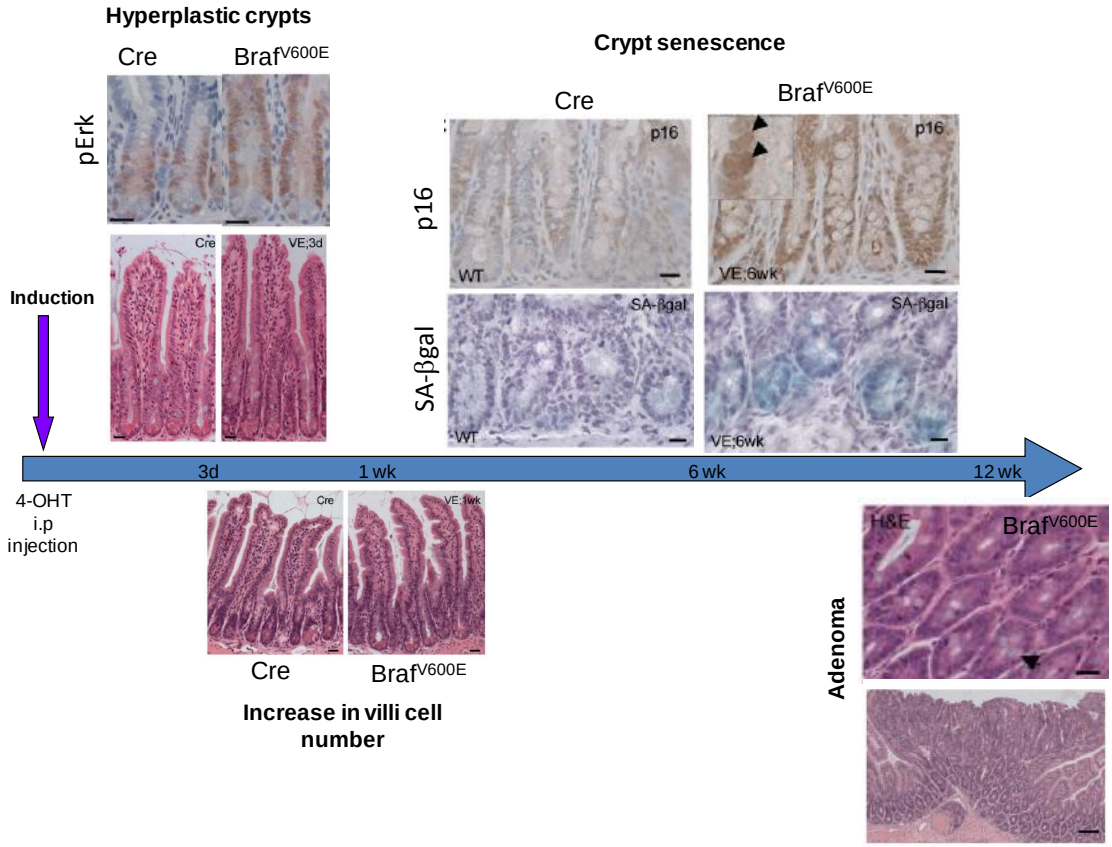

characterized by an accumulation of β-galactosidase and $p16^{INK4A}$. Approximately 12 weeks after tamoxifen treatment, the senescent state was overcome and the formation of adenomatous lesions was observed in 76% of the mice. These lesions showed high content of phospho-histone H3 and lack of β-galactosidase staining. Finally, these lesions evolved into more advanced dysplastic tumors which were present in 12% of the mice (Carragher et al. 2010b) (Figure 1.19).

1.6 BRAF inhibitors

Because of the high incidence of RAS and BRAF alterations in human tumors, intense efforts have been made to generate selective inhibitors of the ERK pathway (Nissan, Solit 2011b). The first RAF inhibitor to entered clinical testing was Sorafenib (Adnane et al. 2006). This inhibitor has shown to block the kinase activity of CRAF, ^{WT}BRAF and mutant BRAF. However, it was demonstrated that Sorafenib could also inhibit VEGFR-2, VEGFR-3 and PDGF which demonstrates its low selectivity (Adnane et al. 2006). Recently, more potent and specific RAF inhibitors have been synthesized which show promising clinical activity in melanoma patients whose tumors express ^{V600E}BRAF (Nissan, Solit 2011a). Recently more potent and selective RAF inhibitors have been clinically tested demonstrating to improve survival of patients with V600E-driven melanoma.

1.6.1 Pre-clinical studies of PLX4720

PLX is a ATP competitive inhibitor of RAF that binds to ^{V600E}BRAF and ^{WT}BRAF with IC_{50} values of 13 and 160 nM respectively (Tsai et al. 2008a). Its analogue PLX4032, inhibits ^{V600E}BRAF with an IC_{50} of 31 nM and ^{WT}BRAF with an IC_{50} of 100 nM.

PLX4720 and the adenine rings of the ATP molecule bind to the same region in the ATP pocket; however the tail of PLX4720 specifically fits into the "RAF selective pocket". This pocket is shared with very few kinases giving PLX4720 selectivity towards RAF proteins. In the case of ^{V600E}BRAF, this "RAF selective pocket" shows a different orientation of the Cα helix in comparison to that in ^{WT}BRAF increasing PLX4720 preference to oncogenic BRAF (King et al. 2006). Finally, it has been demonstrated that PLX4720 binds more efficiently to the active conformation of BRAF. In this state, the sulphonamide of the PLX4720 molecule interacts with the phenylalanine of the DFG motif which helps direct the PLX4720 tail into the "RAF selective pocket", stabilizing PLX4720 binding and resulting in 100% of compound occupancy. Although PLX4720 can bind to the inactive conformation of BRAF, the position of the DFG segment in BRAF allows no interaction with the PLX4720 molecule disfavouring its binding and resulting in 60% of occupancy (Tsai et al. 2008b).

For the study of the anti-cancer effects of PLX4720, athymic mice were implanted with cells containing the *Braf* ^{V600E} mutation. After tumor formation, mice were given orally daily doses of PLX4720 which resulted in tumor regression for 44% of the treated mice. The results obtained from the *in vivo* models supported the progression of PLX4720 to human clinical trials (Tsai et al. 2008b).

In 2010, Heidorn et al. observed that the expression of endogenous ^{D594A}BRAF in the presence of endogenous ^{G12D}RAS in melanocytes caused increased MEK-ERK signaling which resulted in the formation of rapidly growing oligo-pigmented tumors. In contrast, mice expressing ^{G12D}RAS or ^{D594A}BRAF by its own did not developed nevi or any tumor. This group proposed that the tumorigenic phenotype observed in mice containing the ^{D594A}*BRAF* and ^{G12D}*RAS* alleles was caused by the constitutive binding of ^{D594A}BRAF to CRAF observed only in the presence of oncogenic RAS. They suggested that the

formation of the ^{D594A}BRAF -CRAF complex occurs because of the lost of BRAF kinase activity and consequently the ability to maintain itself in an inhibited state. The resulting "open conformation" BRAF is recruited to the plasma membrane by mutant RAS. Another mutant RAS molecule recruits CRAF to the plasma membrane as well. The association between ^{D594A}BRAF and CRAF takes place. Because of the impaired kinase activity of BRAF, this protein acts only as a scaffold enhancing CRAF activation (Heidorn et al. 2010). The clinical implications of this finding are profound. If BRAF inhibitors such as PLX4720 are administered to patients containing a population of cells harbouring pre-existing mutations in *RAS* or suddenly acquired *RAS* mutations, the treatment will promote tumor growth in these patients (Su et al. 2012).

Another model that explains the enhanced ERK signaling found in ^{WT}BRAF cells after PLX4720 treatment has been suggested by Poulikakos et al in 2010. This group proposed that the PLX4720 molecule itself is causing the transactivation of the RAF proteins. They observed that, when PLX4720 is administered at low doses to these cells, the inhibitor binds to one of the RAF proteins within the dimer transactivating the non-drug bound protein. At higher doses, PLX4720 is able to bind to both members of the dimer, inhibiting RAF transactivation and consequently ERK phosphorylation. In the case of ^{V600E}BRAF cells, low levels of RAS activity due to negative feedback loops and consequently low levels of RAF dimers results in ERK inactivation (Poulikakos et al. 2010).

In agreement with the model of paradoxical activation of CRAF by BRAF, Marais et al. in 2012 showed that approximately 60% of squamous cell carcinoma (SCC) and keratoacanthomas lesions developed by vemurafenib (PLX4720) treated patients, contained pre-existing mutations in *HRAS* (Su et al. 2012).

1.6.2 Mechanism of resistance to RAF inhibitors

A high percentage of patients with *BRAF*^{V600E} mutant melanomas initially respond to vemurafenib but resistance eventually emerges.

Among the mechanisms of resistance that have been identified so far are: mutations in *MEK1* (C121S) (Wagle et al. 2011) and *NRAS*, *COT1* (Johannessen et al. 2010) and CRAF overexpression (Montagut et al. 2008), hyperactivation of RTKs (PDGFRβ and IGF-1R) (Nazarian et al. 2010, Villanueva et al. 2010) and loss of PTEN simultaneously with AKT activation.

Recently, it has been shown that aberrant splicing of *BRAF*^{V600E} is a common mechanism of resistance to BRAF inhibitors. In 2011, Solit et al. identified the presence of splicing isoforms of *BRAF*^{V600E} in 6 of 19 melanoma patients that developed resistance to vemurafenib (Poulikakos et al. 2011). The shorter PCR products encoded *BRAF*^{V600E} transcripts lacking exons 4-10, 4-8, 2-8 or 2-10. Interestingly, the missing exons encode the RAS-binding domain (RBD) and the cysteine rich domain (CRD), all essential for RAS binding and negative regulation of the BRAF kinase domain. Specifically when exons 4-8 are deleted a 61 kDa variant form of *BRAF*^{V600E} is expressed. P61^{V600E}BRAF showed increased ability to form dimers in a RAS independent manner (Poulikakos et al. 2011).

1.6.3 Human clinical trials for Vemurafenib

Vemurafenib has been subjected to Phase I, II and III clinical trials known as BRIM-1, BRIM-2 and BRIM-3. The Phase I and II studies revealed that Vemurafenib is a safe potent inhibitor of ^{V600E}BRAF in patients with metastatic melanoma. The Phase III trial showed that after treatment with Vemurafenib, a 63% reduction in the risk of death and a

74% reduction in the risk of disease progression can be observed in comparison to the chemotherapeutic agent dacarbizine (Young, Minchom & Larkin 2012).

In the phase I trial for PLX4720 or Vemurafenib, a safe dosage range of 960 mg twice a day was established. The side effects observed in this study were: rash (68%), arthralgia (48%), photosensitivity (42%) and fatigue (32%) (Ascierto et al. 2011). As explained above, Vemurafenib is known to have the paradoxical effect of promoting cutaneous squamous cell carcinomas (CSCC) and keratoacanthomas in part explained by the inhibition of ^{WT}BRAF (Flaherty et al. 2010). In this study 23% of patients developed such neoplasms at the start of the therapy (Ascierto et al. 2011). In an international randomized open-label Phase III trial in patients with previously untreated metastatic or unresectable melanoma containing ^{V600E}BRAF, the survival of patients treated with Vemurafenib or the chemotherapy drug Dacarbizine was compared. A progression free survival of 6.2 months showing significant tumor shrinkage in 52% of the patients was reported. The median overall survival of patients receiving Vemurafenib had not been reached whereas the patients receiving Dacarbizine showed a median survival of 7.9 months (Ascierto et al. 2011). In August 2011, it was announced that the Food and Drug Administration (FDA) approved Vemurafenib tablets (ZELBORAF, made by Hoffmann-La Roche Inc.) for the treatment of patients with unresectable and metastatic melanoma containing ^{V600E}BRAF. (Chapman et al. 2011).

1.7 MEK inhibitors

1.7.1 Pre-clinical studies of MEK inhibitors

In contrast to the mutation-specific inhibition of BRAF obtained with Vemurafenib, the MEK inhibitors have shown to block MEK and ERK activity in all cells (Nissan, Solit 2011a).

However, cell lines containing a BRAF or RAS mutation have been shown high dependency on the ERK pathway for survival and consequently a particular sensitivity to MEK inhibition (Solit et al. 2006, Pratilas et al. 2008, Halilovic et al. 2010).

PD184352 is a non-ATP competitive, allosteric inhibitor of MEK1/2. This inhibitor locks MEK in the inactive conformation, impairing its catalytic activity but still allowing Ser218 and Ser222 phosphorylation by RAF proteins (Sebolt-Leopold et al. 1999) (Section 1.2.8). It has also been suggested that PD184352 binding might also interfere with the approaching of MEK phosphatases to the activation segment, resulting in MEK hyperphosphorylation (Shapiro, Ahn 1998).

Although in the experiments performed for this thesis, the inhibition of MEK1/2 was achieved after PD184352 treatment; the clinical development of this compound (CI-1040, Pfizer) was halted because of modest clinical activity and toxicity concerns. Other MEK inhibitors such as: AZD6244 (AstraZeneca) also have shown little benefit for patients (Nissan, Solit 2011a). In contrast, clinical studies for the MEK inhibitor GSK1120212 (GlaxoSmithKline) showed better results. This compound not only stops MEK-dependent ERK phosphorylation but it also prevents MEK activation. After GSK1120212 treatment, the phosphorylation of Ser217 is lost in contrast to Ser221 in the activation segment of MEK. This monophosphorylated MEK has increased binding affinity to GSK1120212 which results in a prolonged inhibition of phospho-ERK (Gilmartin et al. 2011). However, when comparing the response rate of this compound to that of PLX4720 in melanoma patients, the GSK1120212 inhibitor achieved a lower response rate (Nissan, Solit 2011a).

1.8 Combinatorial therapies

The combination of vemurafenib with a MEK inhibitor results in the prevention of SCC. A phase IB/II study testing the combination of the BRAF inhibitor GSK2118436 with the MEK inhibitor GSK1120212 is currently being performed. A disadvantage of MEK inhibitors in comparison to BRAF inhibitors is their ability to block the T-cell immune response. Therefore, immunotherapy in combination to BRAF selective inhibitors is also being considered as a powerful combinatorial therapy.

1.9 Aims of the project

The aim of this project was to investigate the regulation of BRAF and CRAF in the presence of ^{V600E}BRAF. This was accomplished by:

a) Establishing an *in vitro* cellular system in which ^{V600E}BRAF could be expressed and the behaviour of endogenous BRAF and CRAF could be examined.
b) Determining if the regulation of BRAF and CRAF expression by ^{V600E}BRAF occurs at the transcriptional or post-transcriptional level.
c) Elucidating the mechanism behind this regulatory event
d) Characterising the signaling pathways that cooperate with ^{V600E}BRAF in the regulation of BRAF and CRAF.

CHAPTER 2 Materials and Methods

2.1 Materials

2.1.1 Reagents

All chemicals and reagents are supplied by SIGMA unless otherwise stated. The H_2O in all methods was MiliQ water in sterile containers.

Reagent	Supplier
Dulbecco´s Modified Eagle Medium ([+] 4.5 g/L Glucose; [+] L-Glutamine; [-] Pyruvate; [+] Penicillin/Streptomycin; (+) FBS. Penicillin [10,000 U/ml]-Streptomycin [10,000 mg/ml], 10x Trypsin-EDTA, Hank's Buffered Salt Solution (HBSS), Lipofectamine 2000, 1 kb Plus DNA ladder, Superscript III Reverse Transcriptase kit, Hydrochloric acid, Acetic acid, NaCl, APS, NaCl, EDTA, EGTA, APS, etc checarle, Primers	Invitrogen
Ethanol, Methanol, Isopropanol	Department of Chemistry
Restriction enzymes: DbnI, BclII and SalI	NEB
Primers from PROTEX	Eurofin
KOD Hot start DNA polymerase	MERCK
Protein marker	Fermentas
Bacto-agar, Bacto-tryptone, Yeast extract	Oxoid
Agarose	Bioline
Coomassie Reagent, Supersignal WestPico Chemiluminescent substrate, BCA protein assay kit	Pierce
Plasmid Purification kit (Maxi-prep, Mini-prep)	QIAGEN
SYBR Green I	BioRad
Adenoviral Cre recombinase	University of Iowa
Ready mix reagent	Thermoscientific

2.1.2 Drugs

Inhibitor 885-A was a gift from Professor Richard Marais (Cancer Research UK Centre for Cell and Molecular Biology, The Institute of Cancer Research, London, UK).

The PD184352 inhibitor was a gift from Dr. Simon Cook at Babraham Institute. Inhibitors MG132 and Epoxomicin were purchased from EMD4 Biosciences. Rapamycin was a gift from Dr. Terry Herbert (Department of Cell Physiology and Pharmacology, University of Leicester). Cloroquine was purchased from SIGMA.

2.1.3 Vectors and Constructs

Vector	Tag	Application	Supplier
pEFm/BRAF.6	Myc	Eukaryotic protein expression	Prof. Richard Marais (ICR, London)
pEFm/RAF-1	Myc	Eukaryotic protein expression	Prof. Richard Marais (ICR, London)
pEGFP/CRAF^{WT}	Myc-GFP	Eukaryotic protein expression	Dr. Neil Bate (Leicester, UK)
pEGFP/BRAF^{V600E}	Myc-GFP	Eukaryotic protein expression	Dr. Simon Cook (Babraham Institute, Cambridge)
pEGFP	-GFP	Eukaryotic protein expression	Clontech

2.1.4 Antibodies

		1° antibody	Mol. Weight (kDa)	Diluent	Dilution	2° antibody	Company
MEFs	Soluble fraction	Braf	95	5% milk	1:1000	M	SC-5284
		Craf	74	TBS	1:2000	M	BD 610152
		Erk2	42	5% milk	1:2000	M	SC-154
		Gapdh	37	5% milk	1:6000	M	Millipore MAB374
		LC3	14, 16	5% milk	1:1000	R	Abcam
		pErk1/2	42, 44	5% BSA	1:1000	R	CS 9101
		pMek1/2	45	5% BSA	1:500	M	CS 9121
		pS6K (Thr 389)	70, 85	5% BSA	1:1000	R	NEB
		P-rpS6 (Ser240/Ser244)	32	5% BSA		R	NEB
	Insoluble fraction	Braf	95	5% milk	1:500	M	SC-5284
		Craf	74	TBS	1:200	M	BD 610152
		Actin	45	5% milk	1:16,000	R	S-A2103
HEK293^T	Soluble fraction	Ectopic BRAF	105 (Myc), 140 (GFP)	5% milk	1:10,000	M	SC-5284
		Endogenous CRAF	74	TBS	1:200	M	BD 610152
		Ectopic CRAF	110 (GFP)	TBS	1:4000	M	BD 610152
		9B11 (myc tag)	105 (BRAF)	5% milk	1:10,000	M	CS 2276
		GFP	36	5% milk	1:1000	R	06-896 Millipore
		GAPDH	37	5% milk	1:6000	M	Millipore MAB374
		LC3	14, 16	5% milk	1:1000	R	Abcam
		pERK1/2	42, 44	5% BSA	1:1000	R	CS 9101
		pS6K (Thr 389)	70, 85	5% BSA	1:1000	R	NEB
	Insoluble fraction	Ectopic BRAF	105 (Myc), 140 (GFP)	5% milk	1:10,000	M	SC-5284
		Endogenous CRAF	74	TBS	1:200	M	BD 610152
		9B11 (myc tag)	105 (BRAF)	5% milk	1:10,000	M	CS 2276
		GFP	36	5% milk	1:1000	R	06-896 Millipore
		ACTIN	45	5% milk	1:5000	R	S-A2103

M = mouse; R = rabbit; SC = Santa Cruz; BD = BD biosciences; CS = Cell Signaling; NEB = New England Biolabs; S = Sigma.

2.2 Methods

2.2.1 Animal Cell culture

2.2.1.1 *Isolation of MEFs*

The E14.5 embryos arised from the crossing of a *Braf*$^{+/LSL\text{-}V600E}$ heterozygous mouse and a wild type C57BL6 mouse were employed for isolating mouse embryonic fibroblasts (MEFs). The embryos were transferred to a Petri dish containing cold PBS (1 tablet dissolved in 100 ml of deionized H_2O yields 5 mM phosphate buffer, 1.35 mM potassium chloride and 68.5 mM sodium chloride pH = 7.4). Under the microscope, the embryos were separated from their placenta and their liver. A sample of the tail of each embryo was taken for genotyping purposes. The head and body from each embryo were placed in a separate Petri dish containing cold PBS and subsequently sliced with a sterile blade. The tissue was transferred to a centrifuge tube containing 3 ml of cold PBS. The PBS was replaced by 2 ml of 5x Trypsin/EDTA (50% [v/v] in PBS) and incubated for 5 hours at 4°C. After the incubation period, the tissue was placed in a new tube containing 1 ml of Dulbecco´S modified Eagle´s medium (DMEM) ([+] 4.5 g/L Glucose; [+] L-Glutamine; [-] Pyruvate; [+], 10% [v/v] Foetal Bovine serum (FBS); 1% [v/v] Penicillin-Streptomycin (P/S)). The tissue was disaggregated by pipetting up and down and then transferred into a 10 cm plate with 9 ml of growth medium (DMEM).

2.2.1.2 *Freezing and storage of cells*

Cells were trypsinized and the trypsin action was neutralized by adding the appropriate volume of growth medium (DMEM). The cells were transferred into sterile 15 ml conical tubes. The cells were centrifuged at 1200 rpm for 4 minutes at room temperature. The supernatant was removed and the pellet of cells was resuspended in 1 ml of freezing

media (10% [v/v] DMSO in FBS). The cells were transferred to labelled cryovials. In case of MEFs, the cells were stored in the -80°C freezer for a maximum of 3-5 days and then transferred to the liquid nitrogen tank for long term storage. In the case of HEK293^T cells, the cells were stored in the -80°C freezer for a maximum of 2 weeks and then transferred to the liquid nitrogen tank for long term storage.

2.2.1.3 *Thawing cells*

Cryovials were removed from the liquid nitrogen tank and immediately placed in a 37°C water bath. Cryovials were incubated for 1-2 minutes until the cells were completely defrosted. The content was placed in a sterile 15 ml conical tube containing 5 ml of pre-warmed growth medium (DMEM). The tube was inverted gently to disperse the cells in the growth medium and the sample was centrifuged at 1200 rpm for 4 minutes at room temperature. The supernatant was removed and the pellet of cells was resuspended in 1 ml of growth medium (DMEM). The entire volume or part of it, depending on the desired confluency, was placed in a 10 cm plate containing 9 ml of growth medium (DMEM). The cells were incubated in a 10% CO_2-buffered humidified incubator at 37°C.

2.2.1.4 *Growing MEFs and HEK293^T cells*

When MEFs or HEK293^T cells were grown to 80-90% confluency, the growth medium was aspirated from the plates and the cells were washed with a 5 ml aliquot of PBS at room temperature. The PBS was aspirated and a 1 ml aliquot of 1x Trypsin/EDTA (10% [v/v] 10x Trypsin/EDTA in PBS) was added to the cells. The plate was transferred into the 37°C incubator for 3-4 minutes. The plate was removed from the incubator and, after being observed under the microscope, the plate was gently tapped at the side for 3 times with

the purpose of detaching the cells from the plate. The plate was incubated for approximately 3 minutes more and then an aliquot of 10 ml of growth medium (DMEM) was added to the cells in order to neutralize the proteolytic action of the Trypsin/EDTA. An appropriate volume of resuspended cells was added to a new plate containing growth medium (DMEM).

2.2.1.5 *AdCre infection of MEFs*

Primary MEFs at passage 2-3 were split 24 hours after being thawed. Approximately, $2x10^5$ cells were seeded in a 6 cm plate, corresponding to each time point. After 24 hours of incubation (37°C, 10% CO_2) in growth medium (DMEM), the adenoviral infection was perfomed. An aliquot of AdCre containing $4x10^7$ PFU (plaque-forming units) was diluted in 2 ml of growth medium lacking FBS and P/S (DMEM [-] FBS; [-] P/S). Before adding the diluted AdCre to the plates, the original growth medium in which the cells were seeded was removed. The cells were rinsed twice with medium lacking FBS and P/S (DMEM [-] FBS; [-] P/S) and subsequently incubated with the adenovirus for 2 hours (37°C, 10% CO_2). At the end of the incubation period, a volume of 3 ml of growth medium (DMEM) was added to the plates which were incubated over a 96 hour time course.

2.2.1.6 *Transient transfection using Lipofectamine 2000*

$HEK293^T$ cells at 80-90% confluency were used for transfection. The cells were plated into 6 cm plates 18 to 24 hours before the procedure using growth medium (DMEM). Just before starting the transfection, the original growth medium (DMEM) was replaced with growth medium lacking FBS and P/S (DMEM [-] FBS; [-] P/S). The corresponding volumes of DNA and Lipofectamine 2000 were diluted in separate tubes containing Opti-

Mem. After mixing the contents of the tubes by gently inverting them twice, they were incubated for 10 minutes at room temperature. After the incubation period, the diluted DNA and the diluted Lipofectamine 2000 were combined. The content of the tubes were mixed by gently inverting them twice and they were incubated for 20 minutes at room temperature. The growth medium was removed from the cells and the DNA-Lipofectamine 2000 complexes were added to the plates drop by drop, dispensing them in a circular manner with the purpose of covering the entire plate surface. The cells were incubated for 4 hours (37°C, 10% CO_2). The Opti-Mem medium was replaced with growth medium (DMEM) and the cells were incubated for 48 hours (37°C, 10% CO_2) before being harvested. The concentration of the reagents needed for the transfection reaction varied depending on the size of the plates. The table below (Table 2.1) indicates the amount of each component optimized according to the surface area of the plate.

Table 2.1 Adjustment of the transient transfection conditions according to the relative surface area

Culture vessel	Surf. area per well (cm^2)	Vol. plating media (ml)	Vol. of OptiMem (ml)	DNA (μg)	Lipofectamine 2000 (μl)
6 cm	20	5	2 x 0.5	5	20
10 cm	60	15	2 x 1.5	24	60
15 cm	147.8	33	2 x 3.5	35	140

2.2.1.7 *Inhibitor treatments*

a) Proteasome inhibitors

MG132 was dissolved in DMSO to a concentration of 10 mM. A 9 μl aliquot was added to 6 cm plates with 3 ml of growth medium (DMEM) and a 15 μl aliquot was added to 6 cm plates containing 5 ml of growth medium (DMEM). The final concentration of MG132 in

MEFs and HEK293^T cells was 30 μM. The epoxomicin stock solution was prepared at a concentration of 1 mM in DMSO. A 1.5 μl aliquot was added to 6 cm plates with 3 ml of growth medium (DMEM) and a 2.5 μl aliquot was added to 6 cm plates containing 5 ml of growth medium (DMEM). The final concentration of epoxomicin employed for MEFs and HEK293^T treatment was 0.5 μM.

b) MEK1/2 inhibitor

For the stock solution, PD184352 was dissolved in DMSO at a concentration of 20 mM. Subsequently, the stock solution was further diluted in DMSO to a concentration of 5 mM. From this dilution, a 1 μl aliquot was added to 6 cm plates containing 5 ml of growth medium (DMEM) in the case of MEFs while a 0.6 μl aliquot was added to 6 cm plates containing 3 ml of growth medium (DMEM) in the case of HEK293^T cells. PD184352 was added to MEFs and HEK293^T cells at a final concentration of 1 μM.

c) BRAF inhibitor

For the stock solution, 885-A was dissolved in DMSO at a concentration of 10 mM. Subsequently, the stock solution was further diluted in DMSO to a concentration of 5 mM. From this dilution, a 1 μl aliquot was added to 6 cm plates containing 5 ml of growth medium (DMEM) in the case of MEFs while a 0.6 μl aliquot was added to 6 cm plates containing 3 ml of growth medium (DMEM) in the case of HEK293^T cells. 885-A was added to MEFs and HEK293^T cells at a final concentration of 1 μM.

d) Autophagosome inhibitor

Cloroquine stock solution was prepared at 50 mM in deionized H_2O. An aliquot of 6 μl was added to 6 cm plates containing 3 ml of growth medium (DMEM) while a 10 μl aliquot was added to 6 cm plates containing 5 ml of growth medium (DMEM). The final concentration of Cloroquine in the plate was 100 μM. For the stock solution, Bafilomycin was dissolved in DMSO to a concentration of 0.1 mM. Aliquots of 12 or 24 μl were added to 6 cm plates containing 3 ml of growth medium (DMEM) in order to reach a final concentration of 0.4 or 0.8 mM, respectively.

e) mTOR inhibitor

The mTOR inhibitor Rapamycin, which works as an autophagy inductor was dissolved in absolute ethanol to a concentration of 0.2 mM. A 12.5 μl aliquot was added to MEFs or HEK293^T cells giving a final concentration of 0.5 μM. The plates were incubated for 6 hours at 37°C.

i) Nutrient starvation

The growth medium (DMEM) from the plates was aspirated and cells were washed three times with 1xPBS. Hank´s balanced salt solution (HBSS) was added to the cells and the plates were incubated for 6 hours at 37°C before being harvested.

2.2.2 Molecular biology techniques

2.2.2.1 *Genomic DNA extraction*

After *Braf*$^{+/+}$ or *Braf*$^{+/LSL\text{-}V600E}$ MEFs were infected with AdCre and incubated for the appropriate time, the media was removed and the cells were washed twice with cold PBS. Depending on the confluency of the 6 cm plates, a 50 or 100 μl aliquot of DNA lysis buffer (50 mM Tris HCL [pH = 7.6], 100 mM NaCl, 0.2% [w/v] SDS and 0.1 mg/ml proteinase K) was added to the cells. The lysate was collected in a fresh centrifuge tube. The sample was incubated for 1 hour at 60°C. An aliquot of 130 μl of absolute ethanol was added to the tube and this was gently inverted several times until the DNA was precipitated. The sample was centrifuged at 10,000 rpm for 10 minutes at room temperature. The supernatant was removed and the DNA pellet was placed in a fresh centrifuge tube containing 200 μl of 70% [v/v] ethanol. The pellet was washed by pipetting up and down and then the sample was centrifuged at 10,000 rpm for 1 minute at room temperature. The supernatant was removed and the excess of ethanol was eliminated by incubating the tubes for 5 minutes at 60°C with the top open. The pellet was dissolved in 500 μl of sterile H_2O.

2.2.2.2 *PCR for genotyping*

The genotyping of primary isolated fibroblasts was done in a 22 μl reaction using: 16 μl of Ready Mix (0.625 U ThermoPrime Taq DNA Polymerase, 75mM Tris-HCl [pH 8.8 at 25°C], 20 mM $(NH_4)_2SO_4$, 1.5 mM $MgCl_2$, 0.01% mM [v/v] Tween 20, 0.2 mM each of dATP, dCTP, dGTP and dTTP), 2 μl of Primer 125 (diluted to 20 pmol/ml, final concentration in the reaction: 2 pmol/μl), 1 μl of Primer 137 (diluted to 20 pmol/ml, final concentration in the

reaction: 1 pmol/μl), 1 μl of Primer 143 (diluted to 20 pmol/μl, final concentration in the reaction: 1 pmol/μl) and 2 μl of DNA (Table 2.2).

The PCR conditions employed were: initial denaturation program (94°C for 5 min), denaturation, amplification and quantification program repeated 35 times (94°C for 1 min, 60°C for 1 min, 72°C for 1 min and a final extension step at 72°C for 5 min).

Table 2.2 Description of primers used for PCR genotyping

Primer	Sequence 5´ to 3´
OCP 125	GCCCAGGCTCTTTATGAGAA
OCP 137	GCTTGGCTGGACGTAAACTC
OCP 143	AGTCAATCATCCACAGAGACCT

2.2.2.3 *Agarose gel electrophoresis*

The agarose gel was prepared by dissolving the corresponding amount of agarose in 1xTAE buffer (40 mM Tris, 1 mM EDTA pH=8). The mixture was placed in the microwave oven and heated at full power for 45 second intervals initially and then in 10 seconds intervals until no visible particles were left. The mixture was cooled down to 50°C and ethidium bromide was added to a final concentration of 0.5 μg/ml. The mixture was poured into a mould with a comb already in place. The gel was chilled for 30 minutes before removing the comb and placed in the electrophoresis tank. DNA was combined with loading buffer (0.5% [w/v] Orange G, 30% [w/v] glycerol) in a 1:5 ratio [v/v]. The sample was loaded onto a 2% [w/v] agarose gel. The gel was electrophoresed at 100 volts until the required separation was achieved. For determining the size of the sample, this was compared to a DNA ladder containing DNA fragments from 100 bp to 12 kb. The DNA was visualized on a UV transilluminator.

2.2.2.4 *qRTPCR*

a) Nucleic acid preparation

Total RNA was purified from MEFs using the Qiagen RNeasy kit as described in the manufacturer´s manual. For removing contaminating DNA from the isolated RNA, DNase I was added. Rigorous DNase treatment was followed as indicated in the manufacturer´s manual. The amount of RNA was determined by spectrophotometry (Nanodrop 8000). An absorbance of 1 unit at 260 nm corresponds to 44 mg of RNA per ml. The sample purity ratio (260/280) was also determined. The RNA dissolved in H_2O was stored at -20°C.

Complementary DNA (cDNA) was synthesized as follows: A 20 μl reaction volume was used with 1 μg of RNA. The following components were added to a microcentrifuge tube: 250 ng of Random primers, 0.5 mM dNTPs mix, 1 μg of RNA and sterile distilled water to complete a 13 μl of volume. The mixture was heated at 65°C for 5 minutes and incubated on ice for 3 minutes. A second mixture was prepared by adding 4 μl of 5X First-stranded buffer, 1 μl of 0.1 M DTT, 1 μl of RNase OUT inhibitor (40 U/μl) and 1 μl of SuperScript III RT (200 U/μl) to a microcentrifuge tube. The contents of both tubes were mixed together by pipetting up and down. The final mixture was incubated at 25°C for 5 minutes and subsequently incubated for another 60 minutes at 50°C. The reaction was inactivated by heating at 70°C for 15 minutes. The negative controls for this process were a reaction without SuperScript III RT and a reaction without RNA. The synthesized cDNA was stored at -20°C.

b) Primer design

Table 2.3 Description of primers used for qRTPCR experiments.

Gene	Primer	Sequence 5´to 3´	Tm (°C)	%GC	Purification degree
Braf	OCP 255	GAA TGT GAC AGC ACC CAC AC	60	55	Desalted
	OCP 256	ATA AGC TGG AGC CCT CAC	55	55	Desalted
Craf	OCP 183	AAT ACT CAT CCG GGT TTT CTT GCC	65	45	Desalted
	OCP 184	GCG TGC TTT CTT ACC TTT GTGT	60	45	Desalted
Gapdh	OCP 174	AGG TCG GTG TGA ACG GAT TTG	64	52	Desalted
	OCP 175	TGT AGA CCA TGT AGT TGA GGT CA	57	43	Desalted

The Primer 3 Plus check service was used to verify that the sequences of the primers were not complementary to each other, do not form secondary structures or have repetitive sequences at the 3´end (Table 2.3). Primer 3 Plus website (http://www.bioinformatics.nl/cgi-bin/primer3plus/primer3plus.cgi).

c) Annealing temperature optimization

An annealing temperature gradient from 50-65°C was performed using *Braf* primers. The temperature was increased by 1.5°C within this range of temperatures and the amount of synthesized product was determined. The annealing temperature for *Gapdh* and *Craf* primers had been previously optimised by members of the laboratory, reporting maximum annealing temperatures of 57°C and 58°C, respectively. The highest amount of product for *Braf* primers was detected when using a temperature of 59°C for the annealing step in the PCR cycle.

d) Determination of PCR efficiency

Serial dilutions from the target and reference genes were made to determine the Cp value from each dilution (Figure 2.1 and 2.2). A 3-fold dilution series was performed containing five dilutions of cDNA in triplicate. The mean Cp value for each dilution was plotted versus the log concentration of the template to generate a standard curve (Figure 2.1 and Figure 2.2). The efficiency (E) was calculated from the slope of the standard curve using the following formula:

$$E = 10^{(-1/slope)}$$

The highest quality PCRs were run with an efficiency of 2, meaning that the number of target molecules doubled with every PCR cycle.

e) Light Cycler Real-Time PCR Systems

Quantitative RT-PCR was performed using the LightCycler 480 machine. The detection of the PCR product was based on the capacity of the SYBR Green I dye to intercalate into double stranded DNA. For the Light cycler the following master mix was prepared: 12.5 μl of SYBR Green I, 0.375 μl of forward primer (20 pmol/μl), 0.375 μl of reverse primer (20 pmol/μl) and sterile H_2O to 25 μl. The master mix was loaded (24 μl) into each well of a 96-well plate and 1 μl of cDNA (previously diluted to contain 10 ng) was added as PCR template. All volumes were dispensed with multichannel pipettes in order to avoid the individual pipetting of replicate samples. The following Light Cycler experimental run protocol was used: initial denaturation program (94°C for 5 min), denaturation, amplification and quantification program repeated 35 times (94°C for 30 sec, 59°C for 30

Figure 2.1 Standard curves for *Braf* and *Craf*. (A) The fluorescence values, which are proportional to the concentration of *Braf* or *Craf* genes, are plotted against the number of amplification cycle. **(B)** The Efficiency (E) value of the PCR reaction was obtained by plotting the amplification cycle for each dilution against the approximate estimate of the concentration of each dilution. The slope of the linear regression line corresponds to the E value of the reaction.

A

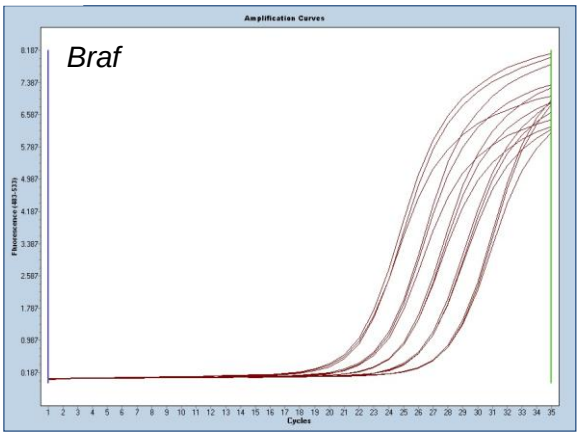

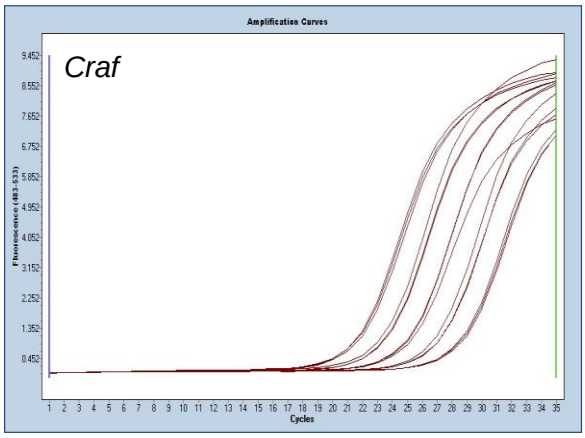

B

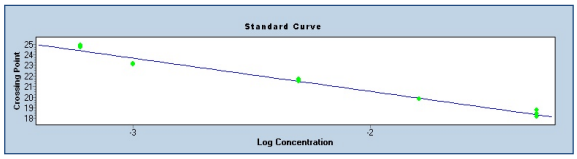

Error: 0.0464
Slope -3.096
Efficiency: 2

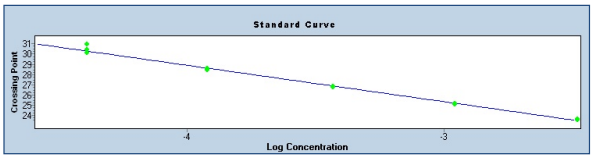

Error: 0.0374
Slope: -3.55
Efficiency: 1.86

Figure 2.2 Standard curve for *Gapdh*. (A) The fluorescence values, which are proportional to the concentration of *Gapdh* gene, are plotted against the number of amplification cycle. **(B)** The Efficiency (E) value of the PCR reaction was obtained by plotting the amplification cycle for each dilution against the approximate estimate of the concentration of each dilution. The slope of the linear regression line corresponds to the E value of the reaction.

A

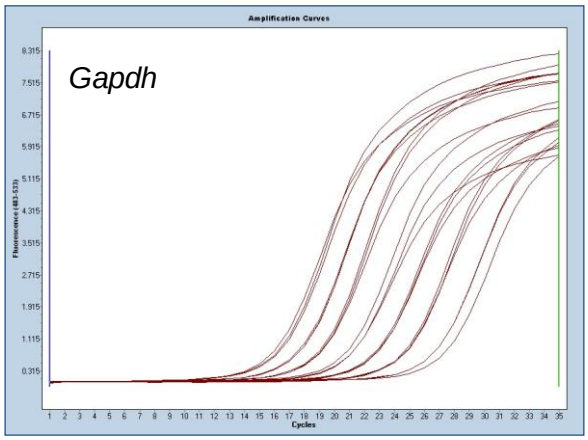

B

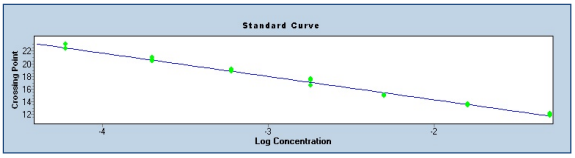

Error: 0.0788
Slope -3.69
Efficiency: 1.9

sec, 72°C for 30 sec), melting curve program (60-97°C, with 5°C increases) and a cooling step.

f) Controls

Negative controls consisted of a reaction where RNA was added to the master mix instead of cDNA and a second reaction in which sterille H_2O was added to the master mix instead of cDNA. These controls helped to determine the source of contamination when an unspecific product was detected. To verify that non-specific products were absent, post-PCR melting curve analysis was performed (Figure 2.3). A melting temperature analysis uses fluorescence measurements of the melting program to determine the melting temperature of each sample. The positive controls included serial dilutions from the standard curve. Because their Cp values have already been measured, they were an indicator of reproducibility between experiments.

g) Advanced Relative quantification

This type of analysis compared the levels of two different target sequences in a single sample and expresses the final result as a ratio of these targets. The crossing point (Cp) is the cycle at which fluorescence intensity exceeds background. The Cp value correlates with the amount of PCR product accumulating during the PCR. Second derivative method analysis was chosen for the determination of Cp values. This algorithm followed the mathematical model proposed by Pfaffl et al. where the relative expression ratio of a target gene is calculated based on E and the Cp value of an unknown sample versus a calibrator and expressed in comparison to a reference gene.

Figure 2.3 Fluorescent signal detection for negative control. (A) Melting curve chart was obtained by plotting fluorescence values against temperature. **(B)** Melting peak chart represented the first negative derivative of the sample fluorescent curves. The melting temperature for each sample appeared as a peak.

A

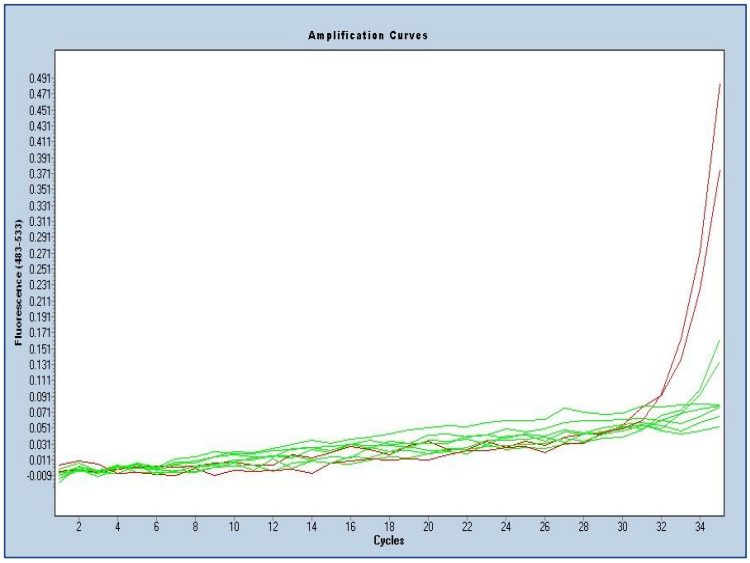

B

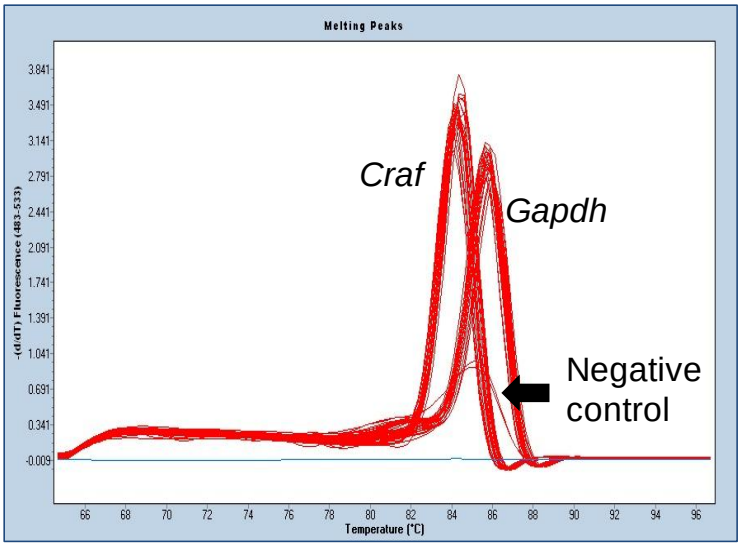

$$\text{Ratio} = \frac{E_{\text{target}}^{\text{DCp target (calibrator– sample)}}}{E_{\text{reference}}^{\text{DCp ref (calibrator– sample)}}}$$

The target was the DNA of interest, in this case *Braf* or *Craf*, while the calibrator was a sample with a stable ratio of target to reference gene in every time point over the time course (*Braf*$^{+/+}$ untreated sample). The reference gene was used for normalization of sample to sample differences having a similar function to a loading control (*Gapdh*).

h) Calculation of the fold change in *Braf* mRNA expression based on the Pfaffl method

The table in Figure 3.11 contains the Cp values for each replicate, the mean of these Cp values (Mean Cp) and their standard deviation (S.D.). The amplification cycles for *Gapdh* and *Braf* are also shown (Figure 2.4). The characterization of the PCR products was done by melting curve analysis. The melting temperature (Tm) can be estimated by slowly increasing the temperature until 95°C and determining the exact temperature at which 50% of the DNA has denatured resulting in the release of the SYBR Green. The Tm is plotted as the derivative melting curve (-dF/dT) where the peak corresponds to the Tm for each product (Figure 2.4). The peak detected at 83°C corresponds to the melting temperature for 50% of the product representing *Braf* while the peak at 86°C corresponds to the product amplified from the Gapdh sequence. The melting curve shows no primer dimers or the presence of any non-specific product amplified by these primers (Figure 2.4).

Figure 2.4 Relative quantification of *Braf* using *Gapdh* as the reference gene. (A) *Braf*$^{+/+}$ or *Braf*$^{+/LSL-V600E}$ MEFs were infected with AdCre or Adβgal over a 96 hour time course. RNA was extracted at each time point, the cDNA was reverse transcribed from mRNA and the expression of *Braf* and *Gapdh* was analyzed by qRT-PCR. Cp values for each sample were obtained in triplicate. The mean of these Cp values (Mean Cp) and their degree of dispersion (S.D.) was calculated. **(B)** Amplification curves for *Gapdh* and *Braf* genes. **(C)** The curves indicate the characteristic melting temperature of the product amplified by *Braf* primers (83°C) and *Gapdh* primers (86°C).

A

	***Braf*$^{+/+}$ MEFs**					***Braf*$^{+/LSL-V600E}$ MEFs**				
	Braf					***Braf***				
Sample	Cp1	Cp2	Cp3	Mean Cp	SD	Cp1	Cp2	Cp3	Mean Cp	S.D.
0	24.68	24.71	24.8	24.73	0.06	25.9	25.44	25.34	25.57	0.32
βgal	25.74	25.63	25.6	25.65	0.09	25.2	25.9	25.8	25.639	0.36
24	25.83	25.6	26	25.79	0.18	26	26.22	26.42	26.227	0.19
48	25.87	25.89	26	25.91	0.05	26.6	26.7	26.67	26.66	0.05
72	26.51	25.77	25.8	26.02	0.43	26	26.16	26.19	26.132	0.08
96	25.47	25.54	25.6	25.53	0.06	26.1	25.94	26.16	26.069	0.11
	Gapdh					***Gapdh***				
Sample	Cp1	Cp2	Cp3	Mean Cp	SD	Cp1	Cp2	Cp3	Mean Cp	S.D.
0	19.58	19.64	19.7	19.64	0.06	19.6	19.61	19.7	19.624	0.07
βgal	20.5	20.62	20.5	20.56	0.06	20.7	20.79	20.78	20.744	0.08
24	19.9	19.98	20	19.97	0.06	20.1	20.18	20.27	20.06	0.1
48	20.14	20.2	20.4	20.25	0.15	20.2	20.34	20.52	20.367	0.14
72	19.87	19.96	20	19.95	0.08	20	19.98	20.07	20.005	0.06
96	20.48	20.56	20.7	20.59	0.13	20.1	20.32	20.33	20.254	0.13

B

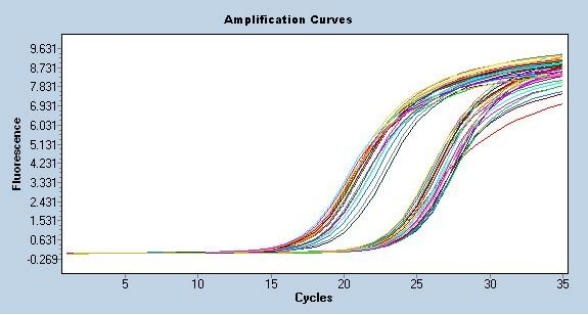

C

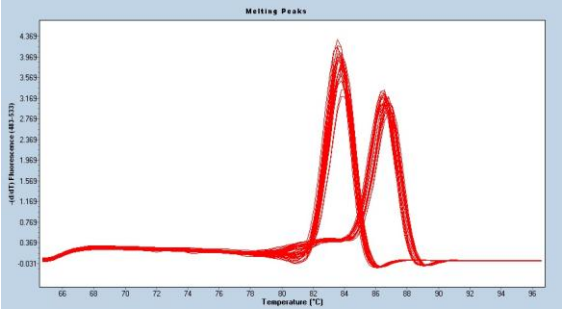

The normalized ratios for each time point were obtained based on the Pfaffl mathematical model (Pfaffl 2001), which is a function of PCR efficiency and of the Cp values as illustrated by the formula:

$$\text{Ratio} = \frac{E_{Braf}^{\Delta \text{Cp } Braf \text{ (calibrator– sample)}}}{E_{\text{Gapdh}}^{\Delta \text{Cp Gapdh (calibrator– sample)}}} \qquad \textbf{(Equation 1)}$$

As indicated in the Table from Figure 2.5, the values for E_{Braf} and E_{Gapdh} are 2 and 1.88 respectively. These values were calculated from the slope of the standard curve (Figure 2.1 and Figure 2.2). The ΔCp*Braf* is the difference between mean Cp (*Braf*) from the 0 sample obtained from *Braf*$^{+/+}$ MEFs (24.73) and the mean Cp (*Braf*) from any of the remaining samples (*Braf*$^{+/+}$ *and Brar*$^{+/LSL\text{-}V600E}$ MEFs). The ΔCp*Gapdh* is the difference between mean Cp (*Gapdh*) from the 0 sample obtained from *Braf*$^{+/+}$ MEFs (19.64) and the mean Cp (*Gapdh*) from any of the remaining samples (*Braf*$^{+/+}$ *and Bra*$^{+/LSL\text{-}V600E}$ MEFs). The final ratio represents the fold increase or decrease in *Braf* expression relative to the 0 sample from *Braf*$^{+/+}$ MEFs.

2.2.2.5 *Site directed mutagenesis*

The strategy involved the amplification of the GFP-BRAF^{V600E} vector (7 kb) by polymerase chain reaction (PCR) for introducing the mutation. This step was followed by digestion of the purified vector by the methylation sensitive enzyme DpnI. The purified vector was replicated using E.*Coli* competent cells and the antibiotic resistant colonies were selected for DNA preparation. The isolated DNA was sequenced to confirm the presence of the mutation.

Figure 2.5 Calculation of the fold change in *Braf* mRNA expression based on the Pfaffl model. The qRT-PCR efficiencies were calculated using the slope of the standard curve. The ΔCp is equal to the difference in mean Cp values for the calibrator and sample for *Braf* or *Gapdh* genes. The ratio results from dividing $E^{\Delta Cp}$(*Braf*) between $E^{\Delta Cp}$(*Gapdh*).

		Braf			***Gapdh***			
	Samples	E	ΔCp	EΔCp	E	ΔCp	EΔCp	ratio
Braf$^{+/+}$ MEFs	0 (calib)		-	-		-	-	-
	βgal		-0.92	0.528		-0.92	0.56	0.942
	24		-1.07	0.476		-0.33	0.811	0.586
	48	2	-1.19	0.439	1.88	-0.62	0.677	0.648
	72		-1.29	0.41		-0.31	0.82	0.499
	96		-0.8	0.575		-0.95	0.549	1.048
Braf$^{+/LSL\text{-}V600E}$ MEFs	0		-1.15	0.451		-1.1	0.498	0.906
	βgal		-0.61	0.657		0.015	1.009	0.651
	24		-1.5	0.353		-0.54	0.712	0.496
	48	2	-1.94	0.261	1.88	-0.73	0.63	0.415
	72		-1.4	0.378		-0.37	0.794	0.476
	96		-1.34	0.395		-0.61	0.678	0.582

a) Primer design

The alanine mutation of residue S675A was situated centrally in both primers. The sequence of the codon expressing the aminoacid serine (TCT) was substituted in the primer with the sequence (GCC) which codes for alanine (Table 2.4).

Table 2.4 Localization of the S675A mutation in overlapping primers.

Gene	Primer	Sequence 5´to 3´	Tm (°C)	%GC	Purification degree
BRAF	OCP_ 959 (F)	GGA TAC CTG GCC CCA GAC CTC AGT AAG GTA	72	56.7	Desalted
	OCP_ 958 (R)	GAG GTC TGG GGC CAG GTA TCC TCG TCC CAC	78	66.7	Desalted
		5´----------GGATACCTGGCCCCAGACCTCAGTAAGGTA3´ 3´CACCCTGCTCCTATGGACCGGGGTCTGGAG----------5´			

b) Polymerase Chain Reaction (PCR) for site directed mutagenesis

The reaction volume of the PCR reaction was 100 μl. Reactions contained 0.26 pmol/μl of each primer, 10 μl of the 10x KOD buffer, 2 mM each dNTP, 0.32 mM $MgSO_4$, 5 μl of DMSO, 2 U of KOD polymerase, 10 ng of GFP-$BRAF^{V600E}$ plasmid and enough deionized H_2O to complete a 100 μl reaction. PCR cycling parameters were as follows: initial denaturation at 95°C for 5 minutes; 30 cycles at 94°C for 30 seconds, 55°C for 30 seconds and 72°C for 10 minute; final extension was at 72°C for 10 minutes. After the amplification process, the samples were run on an agarose gel as described in Section 2.2.2.3.

c) Purification of DNA by extraction with Phenol-Chloroform

The PCR product was added to an equal volume of Phenol:Chloroform. The contents were mixed with a vortex until an emulsion was formed. After the sample was centrifuged at 13,000 rpm for 5 minutes at room temperature, the aqueous phase was transferred to a fresh tube. One tenth of the volume was added of 3M sodium acetate solution (pH=5). The same volume was added of absolute ethanol was. The contents of the tube were mixed by vortexing and then centrifuged at 13,000 rpm for 15 minutes at room temperature. The supernatant was removed and the pellet washed with 70% [v/v] ethanol. The tube was centrifuged at 13,000 rpm for 2 minutes at room temperature. The supernatant was removed and the ethanol excess was eliminated by placing the tube with the top open in the 37°C incubator for 30 minutes. The pellet was dissolved in 30 μl of sterile H_2O.

d) DNA quantification

A volume of 3 μl of the purified DNA and 0.7 μg of the 1 kb Plus DNA ladder were loaded in a 0.9% agarose gel stained with ethidium bromide (Section 2.2.2.3). The reference band of the DNA ladder (1650 bp) contained approximately 8% of the mass applied to the gel. The molecular weight of the PCR product was estimated by comparing the density of its band with that of the reference band contained in the DNA ladder using Image J software.

e) Restriction Enzyme digestión

- DpnI

For the elimination of the template vector which lacks the S675A mutation, the PCR product was digested with the restriction enzyme DpnI. For this reaction, 3 μl of 10x

Restriction buffer 4 (supplied by the manufacturer), 1 μg of PCR product, 10 U of DpnI and enough sterile H_2O to complete a 30 ml final volume were employed. The reaction was incubated at 37°C for 2 hours.

- BclII and SalI

After the bacterial replication of the plasmid and the mini-scale purification of the vector, this was digested with restriction enzymes BclII and SalI to characterize the purified vector. For this reaction, 3 μl of 10x Restriction buffer 3 (supplied by the manufacturer), 3 μl of BSA, 1 μg of DNA, 5 U of PstI, 5 U of BglII and enough sterile H_2O to complete a 30 μl final volume were employed. The reaction was incubated at 37°C for 2 hours.

f) Transformation of competent cells

A 50 μl aliquot of DH5α library competent cells (Invitrogen) was thawed on ice. Approximately 1-5 μg of plasmid was added to competent cells. The content of the tube was mixed gently and the tube was incubated on ice for 30 minutes. The bacteria were heat shocked by placing the tube for 2 minutes in a water bath. The tube was incubated on ice for 5 minutes and a volume of 200 μl of room temperature Luria Bertani medium (LB) (1% [w/v] bactotryptone, 0.5 [w/v] bactoyeast extract and 17 mM of NaCl) without antibiotic, was added to the tube under sterile conditions. The tube was placed in the shaking incubator at 37°C for 45 minutes (225 rpm). Three different aliquots (20, 50 and 100 μl) were spread onto LB agar plates (1.5% [w/v] agar bacteriological, 1% [w/v] bactotryptone, 0.5 [w/v] bactoyeast extract and 17 mM of NaCl) with 30 μg/ml kanamycin.

The plate was left on the bench for 10 minutes for the LB aliquots to be absorbed into the agar. The plates were inverted and incubated at 37°C for 16 hours.

g) Isolation of plasmid DNA by DNA miniprep

A minimum of 10 single colonies were selected from the LB agar plates and inoculated into a 5 ml LB culture with 30 μg/ml kanamycin. The cultures were placed in a shaking incubator at 225 rpm for 16 hours at 37°C. After the incubation period, a 1 ml aliquot of each culture was transferred into a fresh tube and centrifuged at 8000 rpm for 3 minutes at room temperature. The supernatants were removed and the pellets were resuspended in 100 μl of Buffer P1 (50 mM Tris HCl [pH = 8], 10 mM EDTA) by pipetting up and down. A 150 μl aliquot of Buffer P2 (200 mM NaOH, 1% [w/v] SDS) was added to the resuspended pellets and the tubes were inverted 6 times each. The tubes were incubated on the bench for 2 minutes while the lysis of the bacterial cells was taking place. An aliquot of 125 μl of Buffer P3 (3M CH_3COOK [pH=5.5]) was added to each of the tubes and thoroughly mixed by shaking them 6 times each. The tubes were incubated on ice for 5 minutes and then centrifuged at 13,000 rpm for 5 minutes. The supernatant was collected and every 375 μl of supernatant, an aliquot of 700 μl of absolute ethanol was added. The content of the tubes were mixed for a few seconds using the vortex. The tubes were centrifuged at 13,000 rpm for 5 minutes and the supernatants were discarded. The pellets were washed with 100 ml of 70% [v/v] ethanol and centrifuged at 13,000 rpm for 30 seconds. The supernatants were removed and the tubes were incubated for 30 minutes at 37°C with the top open. The pellet was dissolved in 50 μl of sterile H_2O. The purified vector was treated with bovine pancreatic ribonuclease A for selective removal of RNA and restriction enzymes. The reaction was performed by incubating 5 U of XhoI, 5 U of PstI, 3 μl of 10x

Restriction Buffer 3 (supplied by the manufacturer), 1 μl of RNase A (1 mg/ml) and enough sterile H_2O to complete a 30 μl final volume. The reaction was incubated for 2 hours at 37°C.

h) DNA sequencing

The PNACL service (http://www.le.ac.uk/mrctox/pnacl/dna.htm) was supplied with 0.2 mg/ml of the purified GFP-$BRAF^{V600E}$ (S675A) vector and 1 pmol/μl of forward and reverse primers covering the entire *BRAF* gene (Table 2.5). Automated sequencing was performed to verify the presence of the mutation.

Table 2.5 Characteristics of primers used for DNA sequencing.

Gene	Primer	Sequence 5´to 3´	Tm (°C)	%GC	Purification degree
BRAF	OCP_ 468 (F)	AAC TTT GTA CGA AAA ACG TTT TTC	72	56.7	Desalted
	OCP_465 (R)	CTC ACT GCA GTC AGT GGA CAG GAA ACG CAC	78	66.7	Desalted

i) Isolation of plasmid DNA by DNA maxiprep

DH5α competent cells were transformed with the purified plasmid and a colony was inoculated in 5 ml of selective LB medium. A 250 μl aliquot was diluted 1/1000 into selective LB medium. The flask containing the diluted culture was placed in the shaking incubator at 225 rpm for 16 hours at 37°C. The bacteria were harvested and the plasmid DNA extracted using an EndoFree Plasmid Maxi kit (Qiagen) according to the manufacturer´s manual.

2.3 Protein Analysis

2.3.1 Western Blot analysis

2.3.1.1 *Preparation of soluble and insoluble protein lysates*

Media was removed from plates and the cells were rinsed twice with ice cold PBS. The plates were placed on ice and the PBS remaining in the plate was aspirated. Cells were lysed by the addition of Gold Lysis Buffer (GLB) which consists of a stock solution of the following components: 1% [v/v] Triton-X100, 0.5% [v/v] NP-40, 50 mM Tris [pH = 7.5], 150 mM NaCl and 5 mM EDTA. The stock solution was adjusted to pH = 7 at room temperature and stored at 4°C. Immediately prior to use, protease and phosphatase inhibitors were added: 1 mM $NaVO_4$, 100 mM β-glycerophosphate, 5 mM EGTA, 10 mM NaF, 10 mM AEBSF, 10 μg/ml aprotinin and 10 μg/ml leupeptin. In the case of 6 cm plates with less than 70% confluency, the cells were lysed with an aliquot of 50 μl of GLB buffer. Plates that showed a higher confluency of cells were lysed with 100 μl of GLB buffer. Cells were scraped from the plate and collected in a fresh tube. Samples were incubated on ice for 10 minutes and then centrifuged at 13,000 rpm for 10 minutes at 4°C. Supernatant or soluble fractions were removed into a fresh tube and stored at -20°C. The insoluble fraction was obtained by treating the pellet with 1x Sample Buffer (1xSB) (0.05 mM Tris [pH = 6.8], 2% [v/v] SDS, 0.1% [v/v] Glycerol). The volume of 1xSB buffer added to the pellet was the same volume of GLB buffer employed to lyse the cells. Pellets were thoroughly shaken with a vortex until dissolved completely. Tubes were boiled for 5 minutes at 95°C and subsequently incubated on ice for 2 minutes. Samples were stored at -20°C.

2.3.1.2 *Quantification of proteins*

a) Bradford protein assay for quantification of soluble proteins

A volume of 1 ml of Coomassie Blue reagent (Pierce), which is a dye that binds to proteins in an acidic environment, was poured into appropriate cuvettes. For every experiment, a new standard curve was prepared by using five different dilutions of a Bovine Serum Albumin (BSA) standard. The standard curve covered a range of concentrations between 1 to 24 μg/μl which corresponds to an absorbance range of 0.05 to 0.9. The blank consisted of Coomassie reagent alone. A 1 μl aliquot of each sample was added into the cuvettes and mix with the coomassie reagent by pipetting up and down twice. The absorbance of all the samples was measured at 595 nm with the spectrophotometer. The absorbance value of the blank was subtracted automatically from all the samples and the final absorbance values were plotted against the concentration of each sample (mg/ml). The equation of the plot was used to calculate the samples unknown concentration.

b) BCA protein assay for quantification of insoluble proteins

An aliquot of 5 μl of each sample was diluted in 45 μl of 1xSB buffer. For every experiment, a new standard curve was prepared by using seven different dilutions of BSA standard. The standard curve covered a range of concentrations between 25-1500 mg/ml which corresponded to an absorbance range of 0.05 to 1.7. A volume of 50 μl of each standard and diluted sample was poured into appropriate cuvettes. An aliquot of 400 μl of the Working Reagent (1:50 [v/v] BCA Reagent A: BCA Reagent B; BCA Protein Assay kit) was added to each cuvette. The samples were covered and incubated for 30 minutes at 37°C. The blank consisted of a 50 μl aliquot of 1xSB buffer diluted in 400 μl of Working Reagent (Pierce) and incubated under the same conditions as the other samples. The absorbance

value of the blank was subtracted automatically from all the samples and the absorbance was measured at 562 nm. The final absorbance values were plotted against the concentration of each sample (mg/ml). The equation of the plot was used to calculate the samples unknown concentration.

2.3.1.3 *SDS polyacrylamide gel electrophoresis (SDS-PAGE)*

Protein samples were resolved on 7.5, 10 or 12% polyacrylamide gels by electrophoresis. The MiniProtean II polyacrylamide gel system from Bio-Rad was employed. For the resolving gel preparation, the reagents shown in Table 2.4 were thoroughly mixed. The resolving gel was poured between the glass plates leaving enough space for the comb to fit in. Immediately after pouring, the resolving gel was overlayed with a 750 μl aliquot of 0.1% SDS. The gel was incubated on the bench for 45 minutes to polymerize. Meanwhile the stacking gel was prepared according to Table 2.4. After polymerization of the resolving gel, the 0.1% SDS aliquot was discarded and the stacking gel mixture was poured between the plates. The comb was inserted between and, once the stacking gel was polymerized, the comb was removed and the gel cassette sandwich was placed into the tank filled with SDS-PAGE Running buffer (1x) (192 mM glycine, 25 mM Tris, 0.1% [w/v] SDS). All samples were prepared at the same concentration by adding the appropriate volumes of sample and GLB buffer. Before mixing the diluted samples in a 1:3 ratio with 3x Laemmli buffer, β-mercaptoethanol was freshly added to 3x Laemmli buffer aliquot at a final concentration of 17% [v/v]. After mixing the content of the tubes, the samples were boiled for 5 minutes at 95°C and then incubated on ice for 5 minutes. The samples were electrophoresed at 100 volts alongside with a 5 μl aliquot of a protein marker (10-250 kDa; Fermentas).

Table 2.6 Composition of resolving gel for SDS-PAGE

	Resolving gel			Stacking gel
	7.5% (x1)	10% (x1)	12% (x1)	5% (x1)
H_2O	3.75 ml	2.17 ml	4.2 ml	2 ml
Acrylamide	3 ml	2.66 ml	5 ml	0.5 ml
Tris pH = 8.8	4 ml	3 ml	3.15 ml	-
Tris pH = 6.8	-	-	-	0.37 ml
10% SDS	112.5 μl	80 μl	125 μl	30 μl
10% APS	112.5 μl	80 μl	125 μl	30 μl
TEMED	6.75 μl	3.2 μl	5 μl	3 μl

2.3.1.4 *Semi-dry transfer of proteins*

Proteins from the resolving gels were transferred to a nitrocellulose membrane by semi-dry transference. Briefly, two sheets of thick filter paper were pre-soaked in transfer buffer (192 mM glycine, 25 mM Tris, 0.01% [w/v] SDS), one of them was placed onto the anode. The air bubbles were rolled out with a pipette. The nitrocellulose membrane was soaked in transfer buffer and placed on top of the filter paper. The resolving gel was rinsed in transfer buffer and placed on top of the nitrocellulose sheets. Finally, a pre-soaked filter paper was placed on top of the gel. The air bubbles were rolled out with a pipette. The rest of the cell was assembled and connected to a power supply. Gels were transferred at 10 Volts for 70 minutes. Following transfer, membranes were soaked in Ponceau stain (Pierce), which is a protein dye specially applied to nitrocellulose membranes, to confirm that the loading and transfer was uniform in all areas of the membrane. The Ponceau stain was eliminated by rinsing the membrane with TBS (10 mM Tris HCl, 150 mM NaCl, pH=7.6).

2.3.1.5 *Treatment with antibodies*

Membranes were incubated in 5% [w/v] dried milk in TBS for 30 minutes and then incubated with the corresponding primary antibody overnight at 4°C with gentle shaking. The membrane was washed 3x10 minutes with TBS and then incubated with the appropriate secondary antibody. To eliminate unbound secondary antibody, membranes were rinsed 3x3 minutes with TBS. Target protein were detected by incubating membranes with chemiluminiscent substrate (Supersignal WestPico Chemiluminescent ubstrate) that reacts with horseradish peroxidase attached to a secondary antibody, for 40 seconds at room temperature. Membranes were placed into a cassette and exposed to an X-ray film for different lengths of time. The signal was developed using X-ray film processor.

2.3.1.6 *Quantification of proteins using the Image J software*

The Image J software was downloaded from the following website: http://rsbweb.nih.gov/ij/. The background of the blot was subtracted by adjusting the number of pixels with the option PROCESS from the tool bar. The band of interest was selected with the cursor and the optical density of all the bands of interest was measured using the same area. The inverse of the density values was obtained as well as that of the background. The value of the background was subtracted from each of the values corresponding to the bands of interest. The final values were divided by the density values from the loading controls such as GAPDH or ACTIN. The final density value which has no units was plotted against the time expressed in hours.

2.3.1.7 *Emetine treatment for determination of protein $t_{1/2}$*

Braf$^{+/+}$ and *Braf*$^{+/LSL\text{-}V600E}$ MEFs ($2x10^5$ cells) were plated onto 6 cm plates. Forty-eight hours after adenoviral Cre infection, emetine was added at a final concentration of 0.3 mM to each plate. The cells were harvested after 5, 10, 14 and 18 hours post-treatment. *Braf*$^{+/+}$ and *Braf*^{V600E} MEFs were lysed with GLB buffer.

HEK293^{T} cells were treated with 0.3 mM of emetine forty eight hours after the transfection complex was added to the cells. Treated cells were harvested after 5, 10, 14 and 18 hours.

2.3.1.8 *Calculation of the half-lives*

In this section, only the calculation of ectopic BRAF half-life will be explained; however, this example is representative of the method of calculation employed for endogenous Braf and Craf half-lives in HEK293T and MEFs (Figure 4.3.2). After immunoblotting, the optical density of each band on the X-Ray film was quantitated and expressed as [Myc-BRAF]. The concentration of Myc-BRAF^{WT} or Myc-BRAF^{V600E} at the end of each interval was expressed as a percentage of the initial value (Figure 2.6). In order to determine the half-life of ectopic BRAF ($t_{1/2}$) by using Equation 2, the rate constant of the reaction (k) was calculated by plotting ln [Myc-BRAF] against time (T). The slope of the resulting straight line was equivalent to the negative value of the rate constant (k) (Equation 1).

2.3.2 Mass spectrometry

In order to locate post-translational modifications specific to the GFP-BRAF^{V600E} protein recovered in the insoluble fraction, liquid chromatography coupled with tandem mass spectrometry (LC-MS/MS) analysis was performed.

Figure 2.6 Calculation of ectopic ^{V600E}BRAF half-life using the first order reaction. **(A)** The O.D. values which represent the concentration of BRAF protein in the sample are shown in the table [Myc-BRAF] as well as the natural logarithms of these values (ln [Myc-BRAF]). **(B)** The graph shows the natural logarithm of BRAF concentration (ln [Myc-BRAF]) plotted against time (T). The equations of the linear regression (Equation 1) and the first order reaction (Equation 2) are shown.

A

[Myc-BRAF]	437.7	360.7	164.82	144.12	88.11
% initial value	100	82.42	45.68	87.44	61.13
ln [Myc-BRAF]	6.08	5.88	5.1	4.97	4.47
T (h)	0	5	10	14	18

[Myc-BRAF]	86.24	55.43	49.64	14.8	8.9
% initial value	100	64.2	89.54	29.81	60.14
ln [Myc-BRAF]	4.45	4.015	3.9	2.69	2.18
T (h)	0	5	10	14	18

B

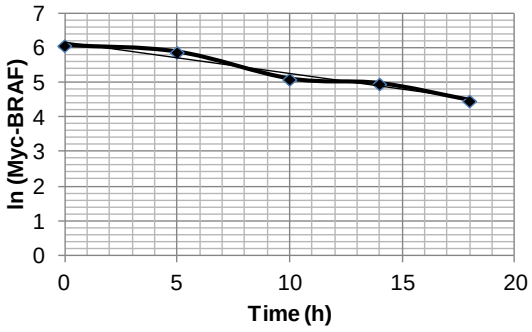

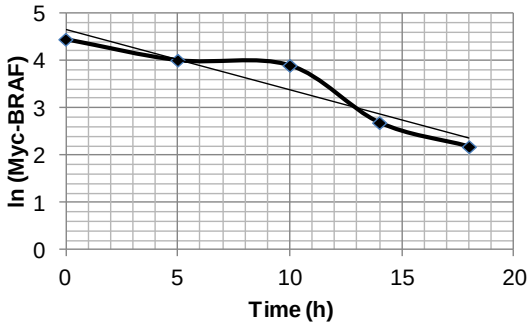

y = mx + b **Equation (1)**
y = -0.091 + 6.16
m = -k
k = 0.091
$t_{1/2}$ = ln2/k **Equation (2)**
$t_{1/2}$ = 0.69/0.091
$t_{1/2}$ = 7.55 h

y = mx + b **Equation (1)**
y = -0.128 + 4.65
m = -k
k = 0.128
$t_{1/2}$ = ln2/k **Equation (2)**
$t_{1/2}$ = 0.69/0.128
$t_{1/2}$ = 5.41 h

2.3.2.1 *GFP-trap*

The GFP-BRAF^{V600E} protein was immunoprecipitated from the soluble and insoluble fractions with a single domain antibody recognizing the GFP protein. For this experiment, 15 cm plates of HEK293^{T} cells transiently expressing GFP-BRAF^{V600E} were employed (Section 2.2.1.6). The soluble and insoluble fractions were obtained as indicated in section 2.3.1.1. Pellets were resuspended in 50 μl of 1xSB buffer and the suspensions were sonicated 3 times for a few seconds (0.5) until the pellet was not visible any more. Sample volumes were adjusted with dilution buffer (10 mM Tris/Cl pH = 7.5, 150 mM NaCl, 0.5 mM EDTA, 1 mM Na_2VO_4, 100 mM glycerophosphate, 5 mM EGTA, 10 mM NaF, 10 mM AEBSF, Aprotinin, Leupeptin) to 1300 μl. The volume of the supernatants was also adjusted to 1300 ml with dilution buffer. GFP beads were gently resuspended and a 20 μl aliquot was transferred to a new tube with 500 μl of cold dilution buffer. The tube was centrifuged at 2700g for 2 minutes at 4°C. GFP beads were washed 2 times more with dilution buffer. The diluted soluble and insoluble fractions were added to the washed GFP-beads and incubated with gentle end-over-end mixing for 4 hours at 4°C. At the end of the incubation period, tubes were centrifuged at 2000g for 2 minutes at 4°C and supernatants were removed. The GFP beads were washed twice with 500 μl of cold dilution buffer. GFP beads were resuspended in 100 μl of 2xSDS sample buffer (0.12 M Tris pH = 6.8, 2.6% SDS [w/v], 20% glycerol [v/v], 5% β-mercaptoethanol) and boiled for 10 minutes at 95°C in order to dissociate immunocomplexes from the beads. Samples were centrifuged at 2700g for 2 minutes at 4°C to collect the beads and bromophenol blue was added to the sample at a final concentration of 0.08% [w/v]. SDS-PAGE was performed with the supernatants.

2.3.2.2 *Visualization of proteins: Coomassie blue staining*

Resolving gels were immersed in fixing solution (7% [v/v] CH_3COOH, 40% [v/v] CH_3OH) for 1 hour with gently shaking. Gels were then soaked in (Wellbrock, Karasarides & Marais 2004)Coomassie Blue solution (20% [v/v] methanol in Coomassie blue reagent from Pierce) and incubated overnight with gently shaking at room temperature. Coomassie blue solution was replaced with destaining reagent (10% [v/v] CH_3COOH, 25% [v/v] CH_3OH) and gels were placed in the shaker for 30 seconds at room temperature. Gels were rinsed with a 25% [v/v] methanol solution.

2.3.2.3 *LC-MS/MS*

Mass spectrometry analysis was carried out by PNACL (Protein Nucleic Acid Laboratory http://www.le.ac.uk/mrctox/pnacl/lcmsms.htm) at the University of Leicester. Protein bands of size 120-220 kDa were excised from the gel. This region of the resolving gel was chosen because GFP-$BRAF^{V600E}$ has a molecular weight of 145 kDa. In the case of GFP-$CRAF^{WT}$, the region of the resolving gel that was excised was between 90-150 kDa because the molecular weight of this protein is approximately 110 kDa. In-gel trypsin or Glu C/Lys C digestion was performed and the fragmented peptides were separated by high pressure liquid chromatography (HPLC). Subsequently, the output of the reverse phase column was nanosprayed into the LTQ-Orbitrap-Velos mass spectrometer. Data obtained from each LC-MS/MS acquisition were processed using the Raw2MSM application. Each file was in turn searched using Mascot against the UniProtKB/Swissprot database. Fixed modifications were set as carbamidomethyl cysteine with variable modifications of phospho-serine, phospho-threonine, phospho-tyrosine and oxidised methionine. The enzyme was set to Trypsin/P and up to 3 missed cleavages were allowed.

A decoy database search was performed and the data was further processed using Scaffold software.

CHAPTER 3 Regulation of BRAF and CRAF expression by ^{V600E}BRAF

3.1 Introduction

Previous studies have shown that the strength and duration of signalling by Raf kinases has a direct impact on Erk pathway outcome leading to proliferation or cell cycle arrest (Sarkisian et al. 2007, Woods et al. 1997). Based on this fact it is easy to understand that the members of the RAF/MEK/ERK pathway are subjected to a tight regulation at the transcriptional and post-translational level as well as by control of their activation.

At the level of mRNA expression, tissue-specific patterns of transcription have been found for each Raf isoform (Storm, Cleveland & Rapp 1990). While *Araf* and *Craf* were found to be ubiquitously expressed in adult tissue from the mouse, *Braf* showed a more restricted pattern of expression limited to some organs such as: ovary, spleen, spinal cord and cerebellum. Interestingly, the amount of *Braf* mRNA found in these tissues was lower in comparison to *Araf* and *Craf* transcripts suggesting a very specialized role for the *Braf* gene. More recent studies using Western blot analysis have found ubiquitous expression of all Raf isoforms at the protein level (Wellbrock, Karasarides & Marais 2004). Different transcript sizes of *Braf* were also found in a tissue-specific distribution showing an additional level of regulation for this isoform, specifically differential splicing of exons 8-10 has been described. (Storm, Cleveland & Rapp 1990) (Section 1.2.5.2).

At the protein stability level, the Raf isoforms are not only subjected to phosphorylation by other proteins in the form of negative feedbacks (Dougherty et al. 2005, Brummer et al. 2003, Sasaki et al. 2003) (Sections 1.4.1 and 1.4.2) but they can also be regulated by autophosphorylation (Hekman et al. 2004). It is known that the phosphorylated forms of the residues Ser259 and Ser621 in CRAF, act as a binding site for the 14-3-3 dimer (Dhillon et al. 2002a). The analogous sites in ARAF (Ser214 and Ser582) and BRAF

(Ser365 and Ser729) have also been found to mediate 14-3-3 protein association (Papin et al. 1996). In 2004, Hekman et al. showed that after NFG stimulation of PC12 cells, the phosphorylation of S621 occurred prior to the phosphorylation of key residues from the N-region and the activation segment suggesting that the Ser621 phosphorylation is essential for CRAF activation. This same study showed that while the phosphorylation of Ser729 does not need the intrinsic kinase activity of BRAF, as shown in experiments using the kinase dead version of the protein, the phosphorylation of Ser621 in CRAF is the result of an autophosphorylation process (Hekman et al. 2004). In 2008, Noble et al. not only confirmed that CRAF autophosphorylation occurred *in cis* but that it had a main role in the proper folding and stability of the protein. In a kinase dead version of Craf that lacked of Ser621 autophosphorylation, the non-folding of the protein occurred. This protein could not be re-folded by the action of the chaperone protein Hsp90 leading to its degradation by the proteasome (Noble et al. 2008).

Regulatory mechanisms between BRAF and CRAF proteins have also been reported. As discussed in Section 1.2.5.4, the homodimers and heterodimers formed by the Raf isoforms have shown an increase kinase activity in respect to monomers (Rushworth et al. 2006a). However, when ^{V600E}BRAF associates with CRAF, the complex shows a reduced kinase activity resulting in low levels of ERK phosphorylation (Karreth et al. 2009). This negative regulation suggests a protective role for CRAF in the presence of ^{V600E}BRAF. In accordance to this observation, melanoma cell lines expressing ^{V600E}BRAF showed low levels of *CRAF* mRNA expression, which could be interpreted as a response of ^{V600E}BRAF to alleviate CRAF suppression (Karreth et al. 2009, Pavey et al. 2004). However, further studies are needed in order to rule out translational or post-translational processes (Karreth et al. 2009).

Data generated in our laboratory by Dr. Hong Jin prior to this project demonstrated a reduction in Braf protein levels in lung tissue expressing ^{V600E}Braf. For these experiments, *Braf*$^{+/LSL\text{-}V600E}$ mice were crossed to *CreER*$^{T+/0}$ mice to generate *Braf*$^{+/LSL\text{-}V600E}$*;CreER*$^{T+/0}$ double heterozygous mice. Unexpectedly, the *LSL-Braf*^{V600E} allele contained in the lung tissue from these mice was spontaneously recombined without the administration of 4-hydroxytamoxifen (4-OHT) (Section 1.5.2.2). This led to the generation of the *Lox-Braf*^{V600E} allele in the lung of these mice at 3 weeks post-partum. The development of adenomas was observed at the 3 week time point and continued to growth in a time-dependent manner until the tumours became growth-arrested at 8 weeks (Figure 3.2). Importantly, higher levels of Braf protein were present in control lungs in comparison to ^{V600E}Braf-expressing tissue over the time course (Figure 3.1). Moreover, concomitantly with low Braf protein levels in the *Braf*^{V600E} lung, a reduction in phospho-Erk levels beginning at the 6 week time point was observed (Figure 3.1)

3.2 Aims

The work described above was undertaken prior to my PhD studies. The aim of this chapter was to establish a cellular system in which the reduction in BRAF protein levels observed in the presence of ^{V600E}BRAF could be reproduced and further investigated. Also, I was interested to determine if the regulation of BRAF expression occurred at the transcriptional or post-transcriptional level.

Figure 3.1 Braf expression is downregulated in the lung expressing ^{V600E}Braf. Lung tissues were taken from *Braf*$^{+/+}$;*CreER*$^{T+/0}$ (WT) mice and *Braf*$^{+/LSL\text{-}V600E}$;*CreER*$^{T+/0}$ (VE) mice aged 3 weeks, 6 weeks, 8 weeks, and 10 weeks after birth. Protein levels of Braf, phospho-Erk and Actin (loading control) were assessed by immunoblotting. This blot was provided by Dr. Hong Jin.

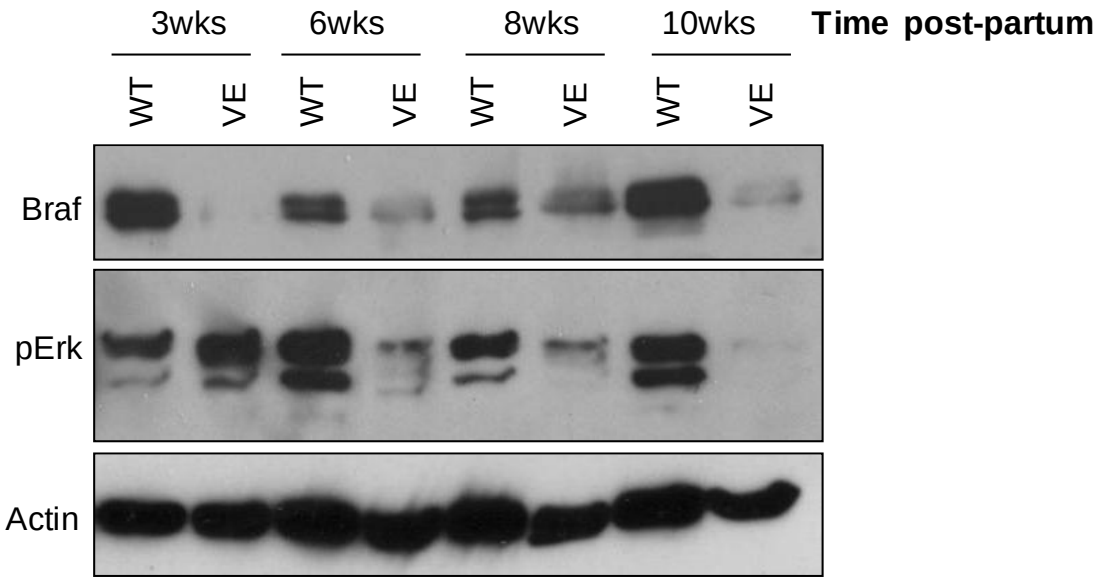

Figure 3.2 Expression of ^{V600E}Braf induces lung tumours in mice. Haematoxylin and eosin stained histological sections from lung tissue of *Braf*$^{+/LSL\text{-}V600E}$;*CreER*$^{T+/0}$ (VE) mice aged 3 weeks, 6 weeks, 8 weeks, and 10 weeks after birth. Data was provided by Dr. Hong Jin.

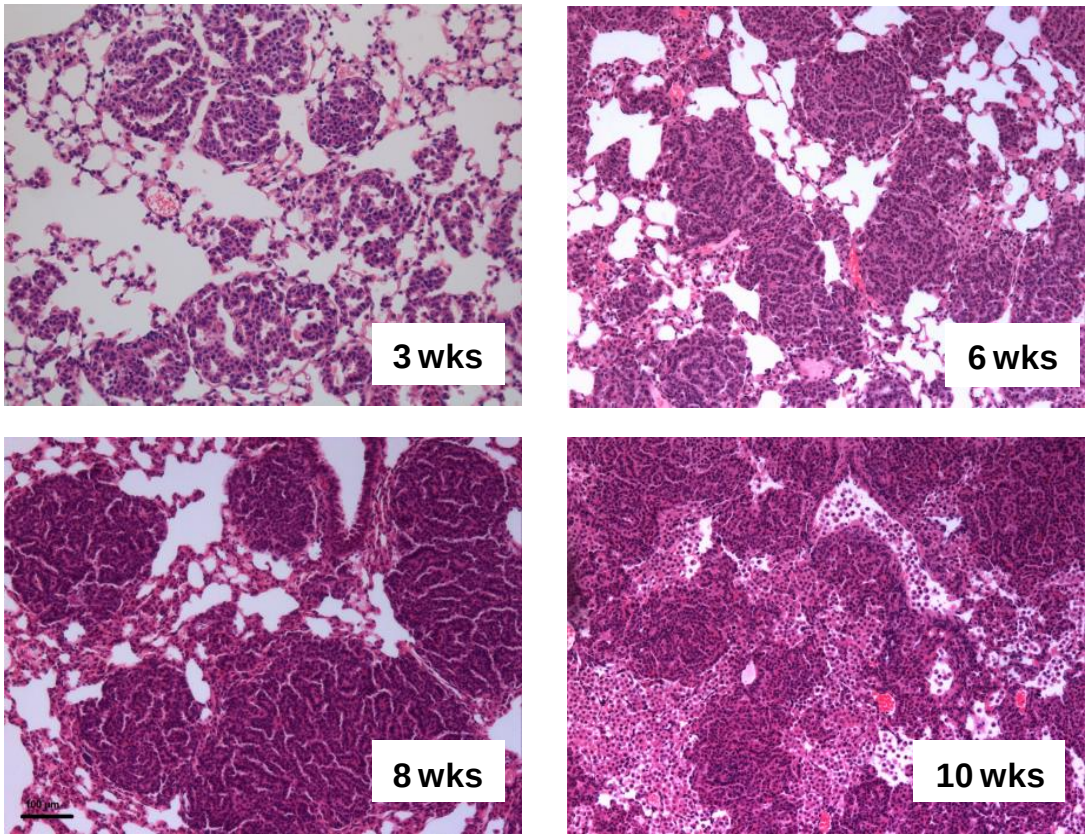

3.3 Results

3.3.1 Genotyping of *Braf*$^{+/LSL\text{-}V600E}$ MEFs after AdCre infection

The *Braf*$^{+/LSL\text{-}V600E}$ primary fibroblasts were chosen to study the regulatory mechanisms of Braf. Primary fibroblasts were isolated from 10.5-14.5d embryos arising from intercrosses between *Braf*$^{+/LSL\text{-}V600E}$ animals and wild-type C57BL6 animals (Section 1.5.2.2). Depending on each mouse, around 3 to 11 embryos were obtained from one mating. The MEFs isolated from each embryo were designated as a different MEF line. In order to assess the inheritance of the *LSL-Braf*^{V600E} allele, DNA was isolated from the tail of each embryo before being homogenized as described in section 2.2.1.1. The purified DNA was amplified by PCR using primers A, B and C which were necessary for the detection of the *Braf*^{WT} and *LSL-Braf*^{V600E} alleles (Figure 3.3).

After the embryos were homogenized and trypsinized, they were plated and cultured to establish the primary lines. With exception of the plate corresponding to the 0 time point, all the plates containing *Braf*$^{+/+}$ and *Braf*$^{+/LSL\text{-}V600E}$ MEFs were infected with $4x10^7$ plaque forming units (PFU) of AdCre (Section 1.5.2.2). DNA was extracted at each time point and amplified by PCR using primers A, B and C. A product of 466 bp was generated by primers A and C representing the *Braf*^{WT} allele while primers A and B amplified a 140 bp fragment corresponding to the *LSL-Braf*^{V600E} allele. The *Lox-Braf*^{V600E} allele, which preserves a LoxP site in intron 14, was characterized by a 518 bp fragment (Figure 3.3). PCR products were resolved on a 2% [w/v] agarose gel and the image of the gel is shown in (Figure 3.4).

The positive control consists of a MEF line, which recombination has been corroborated by previous experiments and was harvested at 48 hours post-AdCre infection (lane 6). As negative controls a non-infected plate of *LSL-Braf*^{V600E} MEFs harvested at the 96 hour time point (lane 1) and a MEF line isolated from a *Braf*$^{+/+}$ mouse were employed (lane 7).

Figure 3.3 Schematic representation of the conditional knockin allele for *Braf*^{V600E} . The LSL-cassette was placed in intron 14 of the endogenous *Braf* locus. The LSL-cassette consists of a mini-cDNA encoding exons 15-18 of *Braf*^{WT} (yellow box), a *neo*^{R} cassette (green box) and three LoxP sites indicated by the red arrows. On the 3´end of the LSL-cassette, the endogenous exon 15 containing the T1799A mutation, characteristic of *Braf*^{V600E}, is located (red asterisk). The expression of Cre recombinase converts the *LSL-Braf*^{V600E} allele into the *Lox-Braf*^{V600E} allele that encodes the ^{V600E}Braf protein. Primers used in PCR amplifications are indicated by a small black arrow and designated by (A-C). Using primers A and C, a fragment of 466 base pairs (bp) was amplified corresponding to the *Braf*^{WT} allele. Using primers A and B, a fragment of 140 base pairs (bp) was obtained, which represents the *LSL-Braf*^{V600E} allele. Finally, the primers A and C were employed to detect the *Lox-Braf*^{V600E} allele characterized by a 518 bp product due to the presence of an extra LoxP site in intron 14.

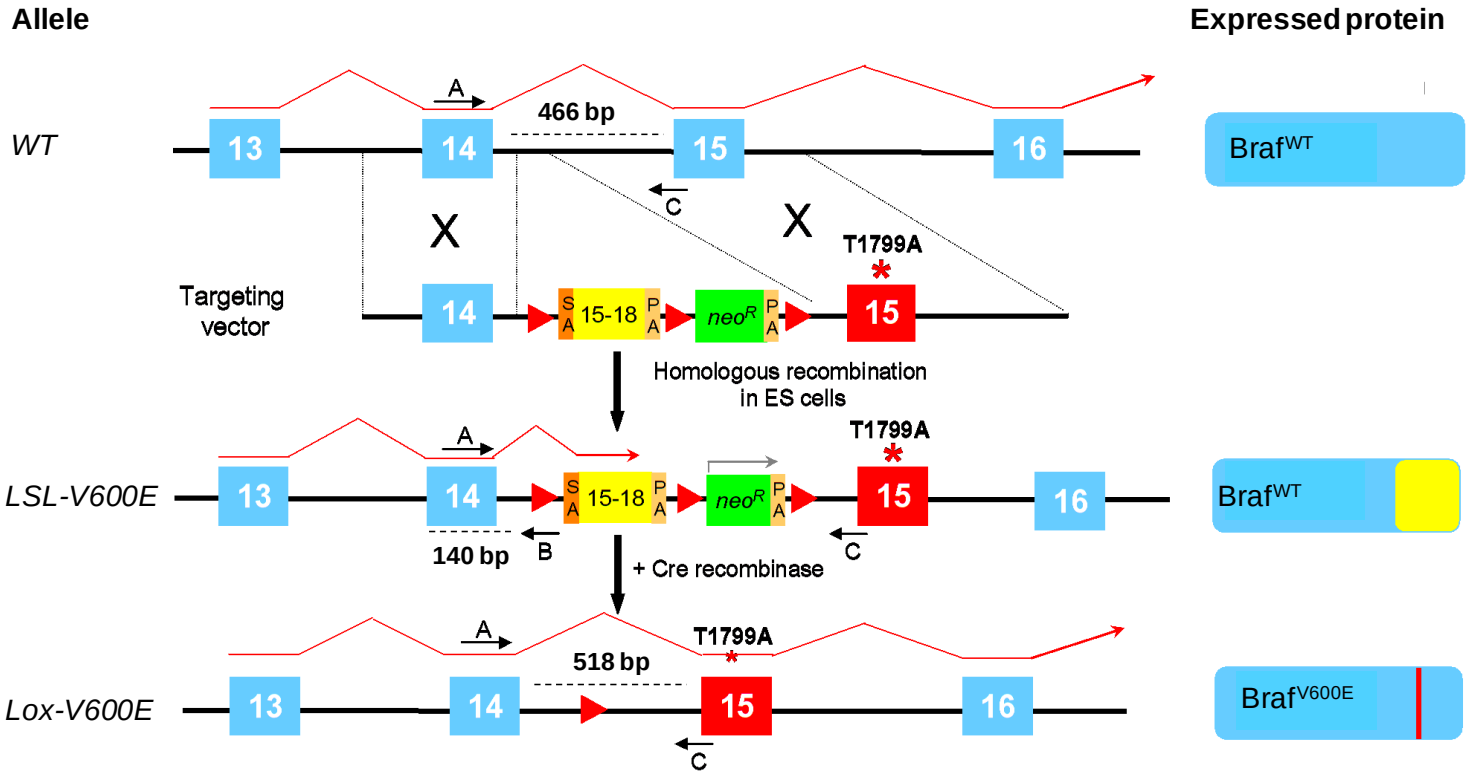

After 24 and 48 hours of AdCre infection, a 518 bp band representing the *Lox-Braf^{V600E}* allele was generated in the *Braf$^{+/LSL-V600E}$* MEFs (Figure 3.4). However, a high content of non-recombined *LSL-Braf^{V600E}* allele was still present in these samples as shown by the 150 bp band. At the 72 hour time point, the *LSL-Braf^{V600E}* band was lost meaning that the allele was completely recombined and existing in the form of *Lox-Braf^{V600E}* allele. The maximum recombination was sustained until 96 hour time point (Figure 3.4).

3.3.2 Morphological transformation of MEFs after ^{V600E}Braf expression

Hyperactivation of Erk has been related to the disruption of microtubule formation (Harrison, Turley 2001) and a decreased expression of various cytoskeletal proteins such as α-Actinin (Gluck, Kwiatkowski & Ben-Ze'ev 1993) and Vinculin (Rodriguez Fernandez et al. 1992) resulting in morphological transformation of cells. Moreover, oncogenic forms of Braf such as ΔBraf:ER has been shown to disrupt the morphology of 3T3 and rat1a cells through Erk activation (Pritchard et al. 1995).

In order to verify that the heterozygous knockin mutation of *Braf^{V600E}* can lead to alterations in the cellular shape and morphology, *Braf$^{+/LSL-V600E}$* MEFs were infected with AdCre over a 96 hour time course. It is important to mention that the media in the plates remained unchanged until the completion of the time course. As a negative control, *Braf$^{+/+}$* MEFs simultaneously infected with AdCre were employed. Images from non-infected plates (0) of both types of MEFs were taken at the 96 hour time point. Every 24 hours, the plates containing *Braf$^{+/+}$* or *Braf$^{+/LSL-V600E}$* MEFs were examined by light microscopy.

As shown in Figure 3.5 *Braf$^{+/+}$* MEFs infected with AdCre showed a typical non-transformed morphology throughout the time course. The non-infected *LSL-Braf^{V600E}* MEFs showed a very similar morphology to the *Braf$^{+/+}$* MEFs.

Figure 3.4 Detection of the *LSL-Braf^{V600E}* and the *Lox-Braf^{V600E}* alleles in MEFs. PCR genotyping to detect *LSL-Braf^{V600E}*, *Braf$^{+/+}$* and *Lox-Braf^{V600E}* alleles. Primers A, B and C were used in combination for the amplification of DNA obtained from *Braf$^{+/LSL-V600E}$* and *Braf$^{+/+}$* MEFs after AdCre infection over a 96 hour time course. The 140 bp band represents the *LSL-Braf^{V600E}* allele, the 466 bp band represents the *Braf^{WT}* allele and the 518 bp product indicates the presence of the *Lox-Braf^{V600E}* allele.

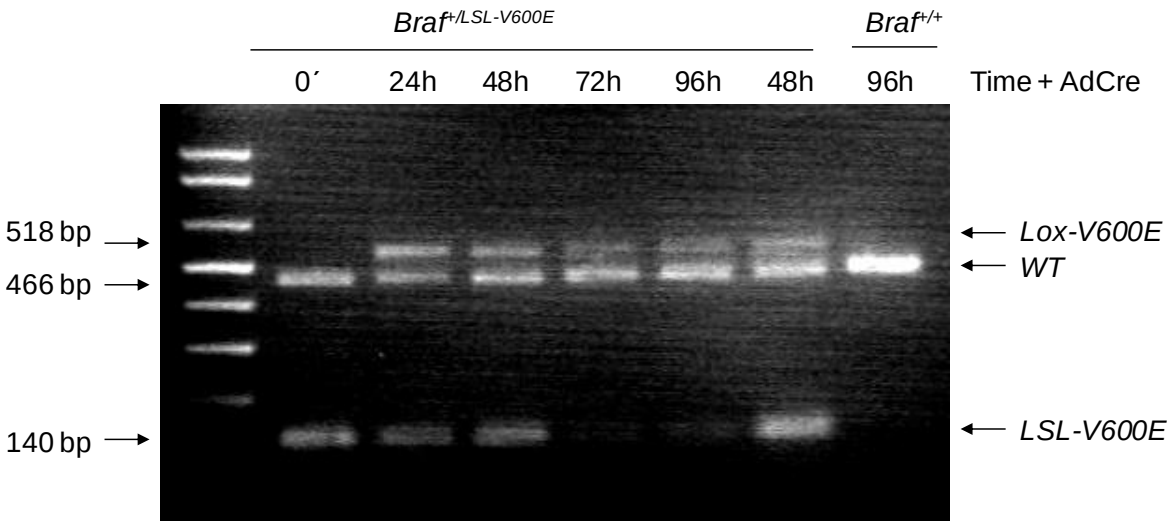

In contrast an elongated appearance was shown by the *Braf*$^{+/LSL\text{-}V600E}$ MEFs after 24 hours of being infected with AdCre. This morphological change progressively increased throughout the time course being more evident at the 96 hour time point. At this same time point the cells were also highly refractile (Figure 3.5).The morphological changes observed after ^{V600E} Braf expression in MEFs agrees with the rate of recombination of the *LSL-Braf*^{V600E} allele shown in Figure 3.4. The maximum expression of ^{V600E} Braf is reached between 48 and 72 hours post-AdCre infection leading to a strong morphological transformation evident from the 72 hour time point onwards (Figure 3.5).

In order to confirm that the morphological transformation observed in these cells was a result of Erk pathway activation, *Braf*$^{+/+}$ and *Braf*^{V600E} MEFs were treated with the MEK inhibitor U0126 (Figure 3.6). Both types of MEFs were plated in duplicate and infected with AdCre. The plates corresponding to the 72 and 96 hour time points were cultured with or without U0126 for the final 24 hours. The appearance of treated and non-treated MEFs was examined by light microscopy.

As shown in Figure 3.6, the *Braf*$^{+/+}$ MEFs showed no morphological transformation after 72 hours of AdCre infection with or without U0126. In contrast, the *Braf*$^{+/LSL\text{-}V600E}$ MEFs were evidently transformed after 72 and 96 hours of AdCre infection and the inhibition of Mek resulted in a less elongated appearance and a reduction in the brightness of the cells.

3.3.3 Braf and Craf protein levels are reduced in MEFs expressing ^{V600E}Braf

In order to analyse if a reduction in Braf and Craf protein levels could be happening within MEFs after ^{V600E}Braf expression, Braf and Craf protein levels were examined by western blot analysis.

Figure 3.5 Morphological characterization of *Braf*^{V600E} MEFs. *Braf*$^{+/+}$ and *Braf*$^{+/LSL-V600E}$ MEFs were infected with AdCre over a 96 hour time course. The morphology of the cells was examined by light microscopy at each time point. The cells were photographed at 40x magnification.

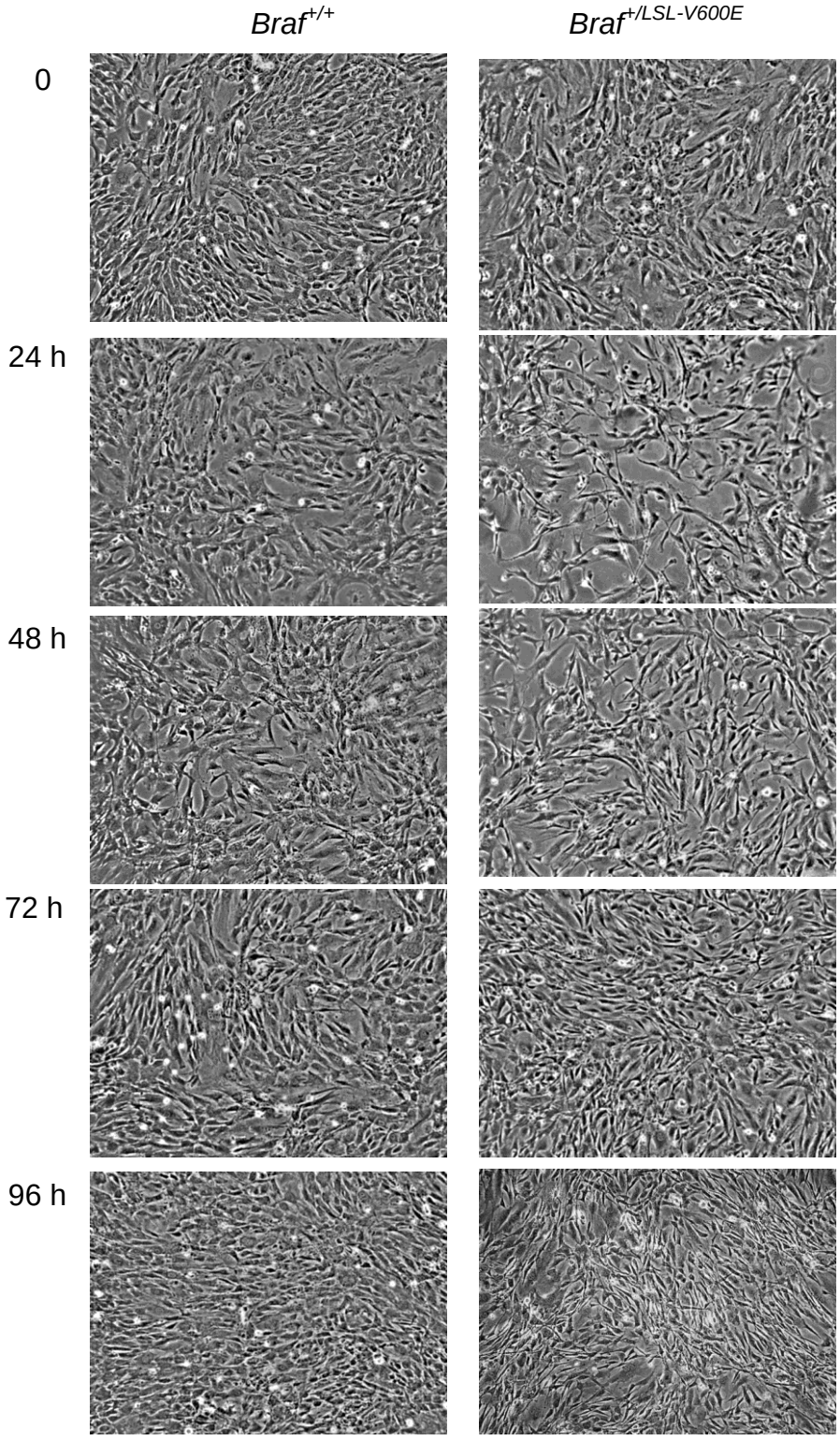

Figure 3.6 Morphological transformation of *Braf*^{V600E} MEFs depends on Erk pathway. *Braf*$^{+/+}$ and *Braf*$^{+/LSL\text{-}V600E}$ MEFs were infected with AdCre for 72 or 96 hours. *Braf*$^{+/+}$ and *Braf*^{V600E} MEFs were treated with DMSO (-) or 10 μM U0126 for the final 24 hours. The morphology of the cells was examined by light microscopy at each time point and cells were photographed at 40x magnification.

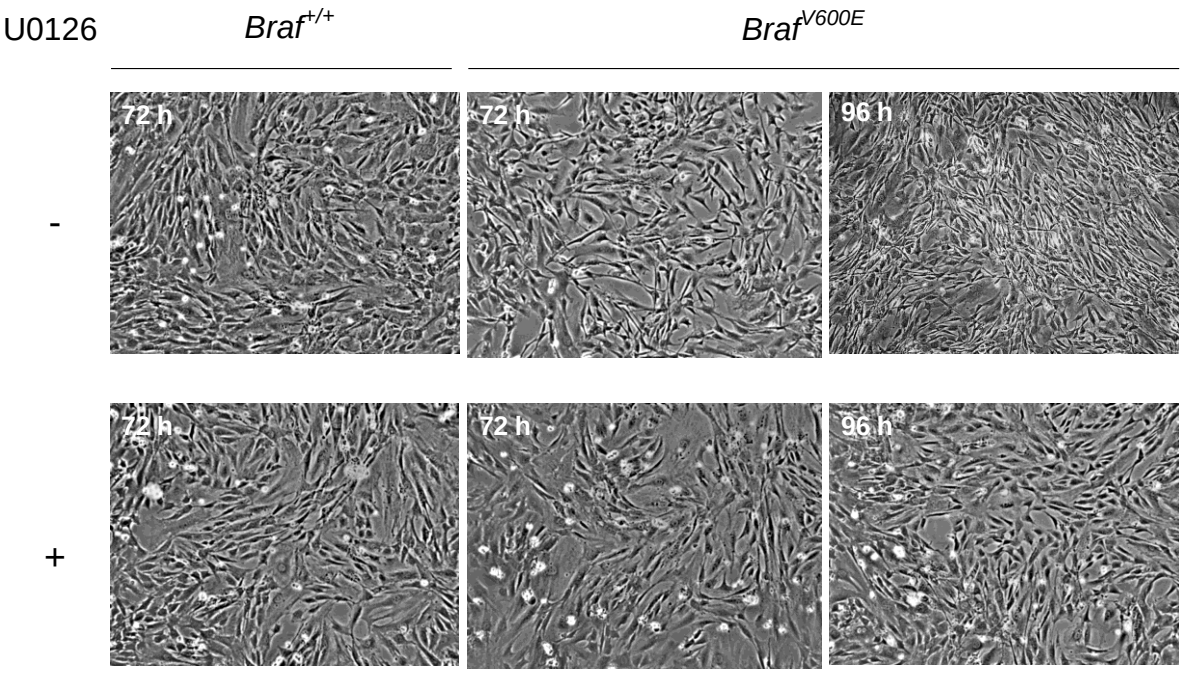

To do this, *Braf*$^{+/LSL\text{-}V600E}$ MEFs were infected with AdCre over a 96 hour time course. The cells were harvested every 24 hours using 1x Sample Buffer (1xSB) containing 2% SDS. Samples were resolved by SDS-PAGE and immunoblotted for Braf, Craf, phospho-Erk and Gapdh proteins. As negative controls, *Braf*$^{+/+}$ MEFs infected with AdCre over a 96 hour time course were employed.

As shown in Figure 3.7 and quantitated in Figure 3.8, Braf and Craf protein levels remained unchanged throughout the time course in *Braf*$^{+/+}$ MEFs. Also in these MEFs there was a progressive loss of Erk phosphorylation which began 72 hours post-AdCre infection. In contrast, *Braf*^{V600E} MEFs showed an increase in *Braf* expression at 24 and 48 hour time points followed by a noticeable decrease occurring at 72 and 96 hours post-infection. Craf behaved similarly to Braf by increasing its expression in the early time points and then showing a reduction at the later time points. In the case of Erk, its maximum level of phosphorylation was reached at the 24 hour time point and sustained until 48 hours post-AdCre infection; however a sudden suppression of Erk phosphorylation occurred at 72 and 96 hours post-infection.

The high levels of *Braf* protein observed at 24 and 48 hours post-infection in *Braf*^{V600E} MEFs could be explained by the fact that the *LSL-Braf*^{V600E} allele expresses Braf at approximately 20% the level of the *Braf*^{WT} allele and the generation of the *Lox-Braf*^{V600E} allele thus increases the overall Braf expression. Interestingly, the abrupt reduction in Braf and Craf protein levels occurred at the same time point as the maximum expression of *Braf*^{V600E} (Figure 3.4) suggesting that this behaviour is a response by the cell to the presence of ^{V600E}Braf. Although it is not possible to know if the response affects ^{WT}Braf or ^{V600E}Braf or both in these particular cells, it seems that the regulation is extended to Craf as well. The loss of Erk phosphorylation observed in *Braf*$^{+/+}$ MEFs at 96 hours post-AdCre

Figure 3.7 Decrease in Braf and Craf protein levels after ^{V600E}Braf expression in MEFs. (A) *Braf*$^{+/+}$ and **(B)** *Braf*$^{+/LSL\text{-}V600E}$ MEFs were infected with AdCre over a 96 hour time course. Cells were lysed with 1x Sample Buffer (1xSB) containing 2% SDS and the lysates were electrophoresed on a 7.5% SDS-PAGE gel. Expression of Braf, Craf, phospho-Erk and Gapdh (loading control) was analyzed by immunoblotting.

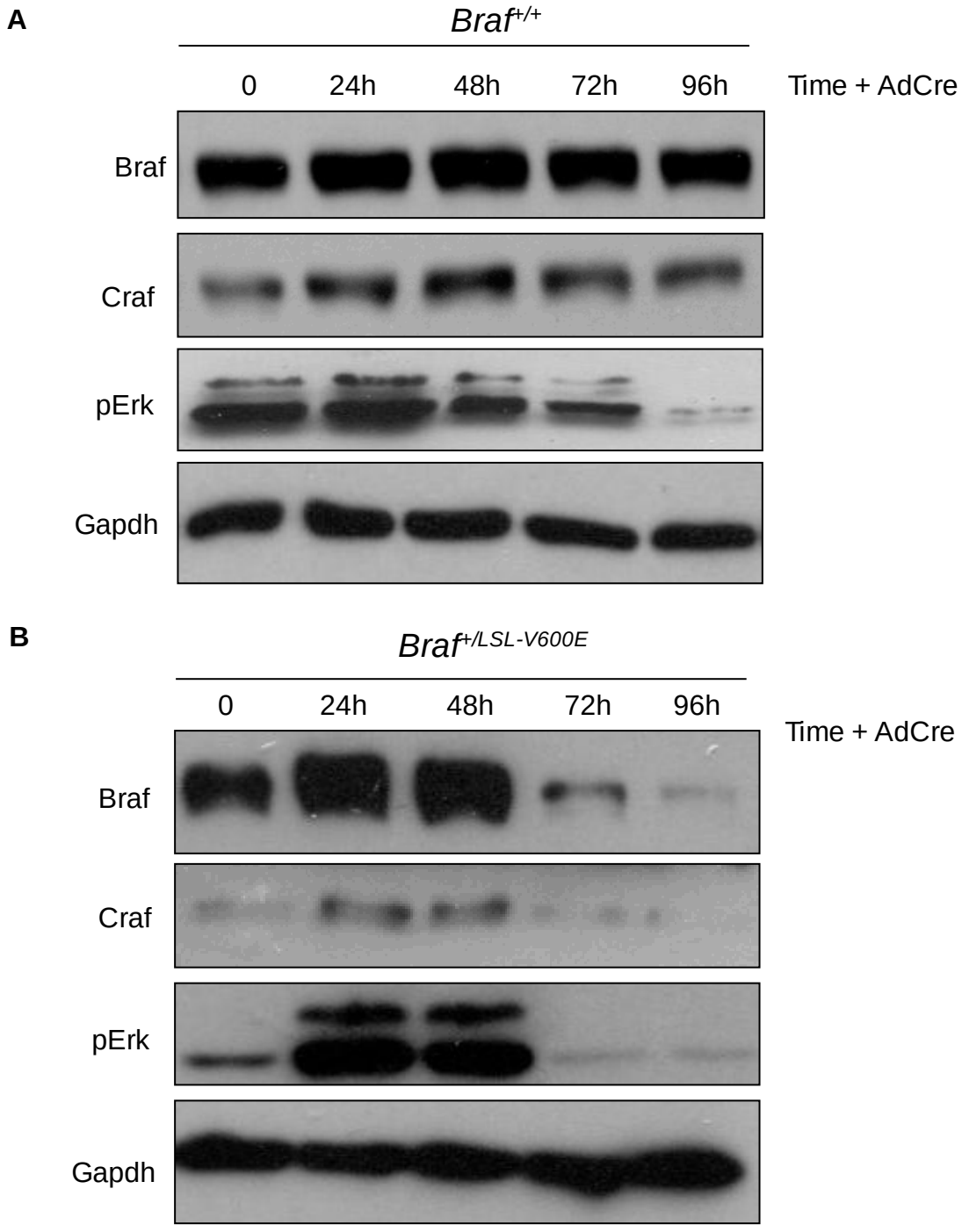

Figure 3.8 Quantification of Braf and Craf protein levels in *Braf*$^{+/+}$ and *Braf*^{V600E} MEFs. The X-ray films were scanned and the optical density (O.D.) of the bands was measured using Image J software. The optical density of the background was subtracted from every sample. The values plotted on the graphs correspond to the Braf/Gapdh **(A and C)** or Craf/Gapdh **(B and D)** ratio expressed in Arbitrary Units (A.U.) Except from graph (**B**), they all represent four independent experiments using four different MEF lines (Mean ± S.D. One asterisk, P< 0.05; two asterisks, P < 0.01; three asterisks, P < 0.001). Graph **(B)** shows the results from two independent experiments (mean).

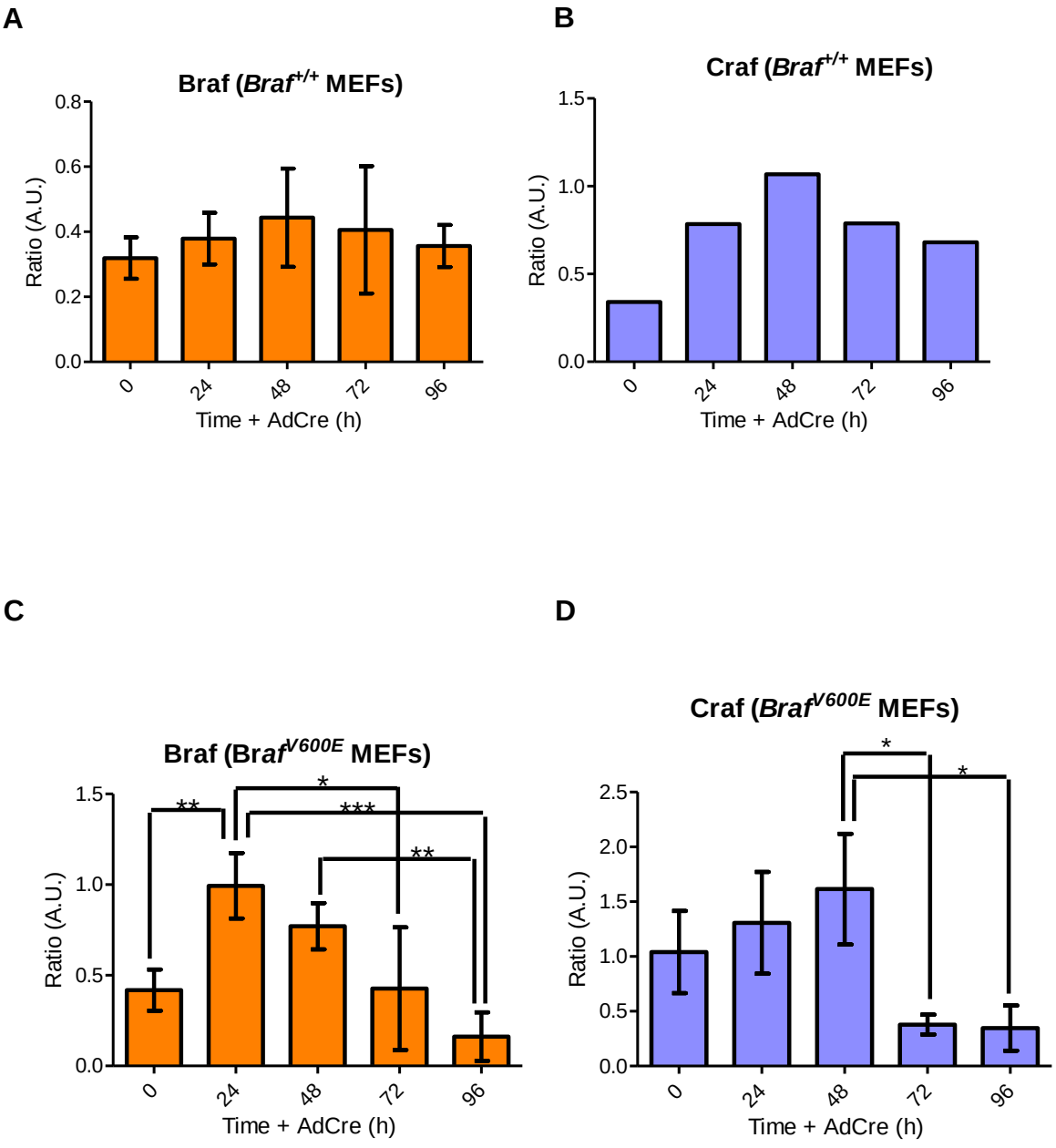

infection may be related to the fact that the cells have become confluent at this time point resulting in a depletion of growth factors since the culture media had not been replenished. However, there is an even further suppression of phospho-Erk in the *Braf*^{V600E} MEFs suggesting that the presence of oncogenic Braf has an additional effect presumably through the drop in Braf and Craf protein levels.

Braf and Craf protein levels were examined in various MEF lines coming from different *Braf*$^{+/LSL\text{-}V600E}$ mice. The reduction in the expression of Braf and Craf at 72 and 96 hours post-AdCre infection was repeatedly observed throughout the different time course experiments. Although the extent of the decrease differed among the MEF lines with respect to the non-infected sample, the reduction was found statistically significant in four different biological samples as shown in Figure 3.8.

3.3.4 Distribution of BRAF and CRAF in the NP-40/Triton X-100 soluble and insoluble fractions

Reduced protein levels of CRAF have been reported by other research groups under different conditions (Noble et al. 2008, Schulte et al. 1995, Schulte, An & Neckers 1997). In 2008, Noble et al. showed that the lack of phosphorylation of Ser621 in Craf, resulted in the accumulation of the unfolded protein in the Triton X-100 insoluble fraction (Noble et al. 2008). Other groups observed that, after the blockage of the proteasome, an accumulation of CRAF in the NP-40 insoluble fraction occurred (Grbovic et al. 2006, Noble et al. 2008). In 1997, Schulte et al. reported an accumulation of unfolded CRAF in the NP-40 insoluble fraction after treating the cells with Hsp90 inhibitor geldanamycin (Schulte, An & Neckers 1997).

In order to investigate whether, in our system, a movement to the NP-40 insoluble fraction was associated with the reduction in Braf and Craf expression, the NP-40/Triton X-100

soluble and insoluble fractions were obtained. To do this, *Braf*$^{+/+}$ and *Braf*$^{+/LSL\text{-}V600E}$ MEFs were infected with AdCre over a 96 hour time course. The cells were harvested every 24

hours post-AdCre infection with Golden Lysis Buffer (GLB) containing NP-40 and Triton X-100 as the main detergents (Section 2.3.1.1). After the lysates were centrifuged, the supernatant and the pellet were separated. The cell pellet was solubilised in 1x Sample buffer (1xSB), forming the NP-40/Triton X-100 insoluble fraction (Section 2.3.1.1). Both fractions were prepared at a concentration of 2 μg/μl and equal amounts of total protein from both fractions (15 μg) were loaded onto the SDS-PAGE gel. The samples were transferred from the gel to a membrane and immunoblotted with Braf, Craf, Gapdh and Actin antibodies.

Preliminary experiments have shown that Braf and Craf in the insoluble fraction represent approximately 5% and 3% of the total cellular content of these proteins, respectively. So when loading the same quantity of total protein from the soluble and insoluble fractions samples (15 μg), because of the lower abundance of Braf and Craf in the latter fraction, some adjustments to the immunoblotting protocol of these samples had to be made in order to enhance the chemiluminescence signal. These modifications consisted in increasing the concentration of the secondary antibody (from 1:2000 to 1:500) and the use of a more sensitive ECL detection system (Figure 3.9). Thus, Braf and Craf bands from the blots corresponding to the soluble and insoluble fraction should not be interpreted as a 1:1 ratio (Figure 3.9).

In agreement with Figure 3.8, an increase in Braf and Craf protein levels is observed at the 24 and 48 hour samples in comparison to the untreated sample (0) in the soluble fraction from both types of MEFs. However, while Braf and Craf protein levels remained constant at 72 and 96 hour time points in *Braf*$^{+/+}$ MEFs, a reduction in the expression of these

proteins was observed in *Braf*^{V600E} MEFs. Interestingly, in the latter cells, an accumulation of Braf and Craf occurred in the insoluble fraction simultaneously to the drop of these proteins in the soluble fraction. In *Braf*$^{+/+}$ MEFs, no clear pattern of accumulation was observed in the insoluble fraction. The level of Erk phosphorylation was constant throughout the time course in *Braf*$^{+/+}$ MEFs while an evident suppression of phospho-ERK occurred simultaneous to the reduction in Braf and Craf expression in *Braf*^{V600E} MEFs.

Overall the data from Figure 3.9 suggests that the expression of *Braf*^{V600E} causes a drop in Braf and Craf expression in the soluble fraction concomitantly to an accumulation of these proteins in the insoluble fraction. The experiments presented in the next chapters will attempt to determine the characteristics of Braf and Craf recovered from the insoluble fraction in Braf^{V600E}-expressing cells.

Figure 3.9 Increase expression of Braf and Craf in the NP-40/Triton X-100 insoluble fraction from Braf^{V600E} MEFs. *Braf*$^{+/+}$ and *Braf*$^{+/LSL-V600E}$ MEFs were infected with AdCre over a 96 hour time course. Cells were lysed with GLB buffer and soluble and insoluble fractions were prepared. Expression of Braf, Craf, Gapdh and Actin was analyzed by immunoblotting. Gapdh was used as a loading control for the soluble fraction while Actin was used as a loading control for the insoluble fraction. Data are taken from an experiment representative of three different experiments.

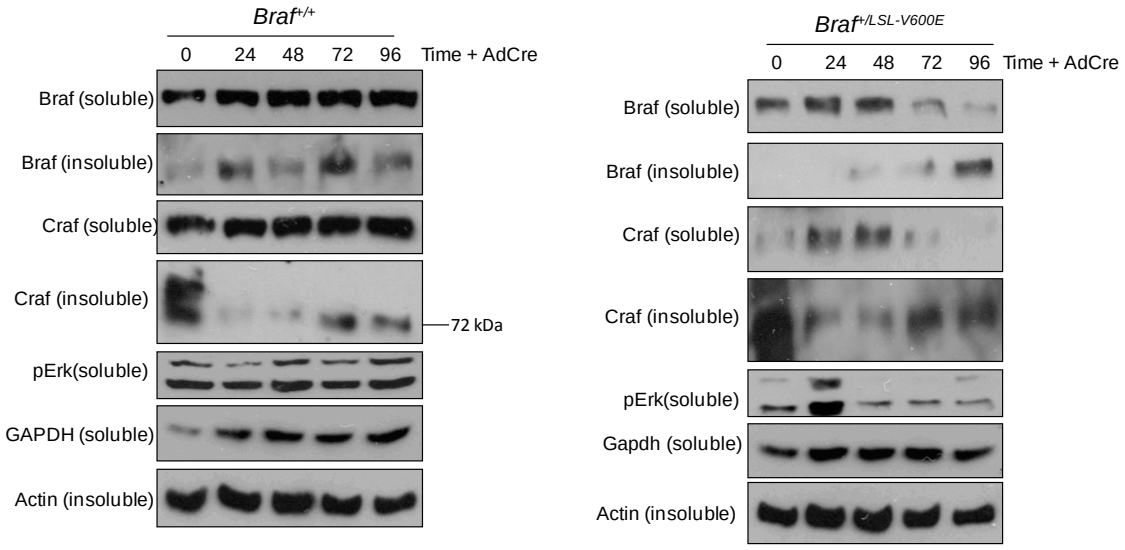

3.3.5 CRAF protein levels are reduced in cells expressing ectopic ^{V600E}BRAF

Although the MEFs have the advantage of a conditional expression of ^{V600E}Braf at physiological levels, they proved to be a difficult system to work with. Variances in experimental conditions and between MEF lines meant that reproducible data was difficult to acquire. For example, the passage number had a clear influence on the growth rate and the morphology of the primary MEFs. If the cells were plated more than 5-7 times, their speed of growth was reduced and they showed a flat and rounded appearance similar to senescent cells, which altered the Braf/Craf/phospho-Erk expression levels.

An alternative cellular system with less heterogeneity than MEFs in which ^{V600E}BRAF expression could be induced was pursued. HEK293^{T} cells transiently expressing ^{V600E}BRAF were tested. These cells were transfected with GFP-BRAF^{V600E} expression vector using Lipofectamine 2000 and harvested 48 hours post-transfection with GLB buffer. The soluble and insoluble fractions were obtained as stated in Section 2.3.1.1. In this experiment, the same quantity of total protein from the soluble and insoluble fraction was loaded into a SDS-PAGE gel; however, preliminary experiments have shown that endogenous CRAF recovered in the insoluble fraction represents approximately 18% of total cellular CRAF. Thus, BRAF and CRAF bands from the blots corresponding to the soluble and insoluble fraction should not be interpreted as a 1:1 ratio (Figure 3.10). The samples were transferred from the gel to a membrane and immunoblotted with BRAF, CRAF, pERK, GAPDH and ACTIN antibodies.

In Myc-BRAF^{V600E}-transfected samples, a reduced amount of ectopic ^{V600E}BRAF was observed in the soluble fraction compared to Myc-BRAF^{WT}-expressing cells (Figure 3.10). In contrast, a greater accumulation of ectopic ^{V600E}BRAFprotein was observed in the insoluble fraction. In Myc-BRAF^{WT} and Myc-BRAF^{V600E}-transfected samples, BRAF appeared as a shifted band in the insoluble fraction, which could be indicative of post-

translational modifications. The cells expressing Myc-BRAF^{WT} and Myc-BRAF^{V600E} showed a decrease in endogenous CRAF protein levels in the soluble fraction simultaneous to an accumulation of this protein in the insoluble fraction. However, as with MEFs, a greater accumulation of endogenous CRAF in the insoluble fraction occurred in ^{V600E}BRAF-expressing cells (Figure 3.10). The CRAF protein recovered in this fraction showed higher-molecular-weight forms suggesting that ubiquitylation or phosphorylation could be taking place. As expected, phospho-ERK levels were higher in cells expressing ectopic ^{V600E}BRAF compared to Myc-BRAF^{WT}-transfected cells.

Overall data from Figure 3.10 shows that the overexpression and consequently hyperactivation of BRAF causes a reduction in ectopic BRAF and endogenous CRAF protein levels in the soluble fraction. However, only cells expressing ectopic ^{V600E}BRAF, showed a greater accumulation of BRAF and CRAF in the insoluble fraction. In the case of HEK293^{T} cells, the reduction in ectopic ^{V600E}BRAF and endogenous CRAF results in high levels of phospho-ERK which is opposite to the behaviour observed in *Braf*^{V600E} MEFs.

Figure 3.10 Ectopic ^{V600E}BRAF expression induces an accumulation of endogenous CRAF protein levels in the NP-40/Triton X-100 insoluble fraction. (A) HEK293^{T} cells were mock transfected or transiently transfected with Myc-BRAF^{WT} or Myc-BRAF^{V600E}. The cells were lysed 48 hours post-transfection with GLB buffer and the soluble and insoluble fractions were obtained. Expression of BRAF, CRAF, pERK, GAPDH and ACTIN was analyzed by immunoblotting. (**B**) The X-ray films were scanned and the optical density (O.D.) of the bands was measured using Image J software. The optical density of the background was subtracted from every sample. The values plotted on the graphs correspond to the CRAF/GAPDH and CRAF/ACTIN ratio expressed in Arbitrary Units (A.U.). Data indicate the Mean ± S.D. of 3 different experiments.

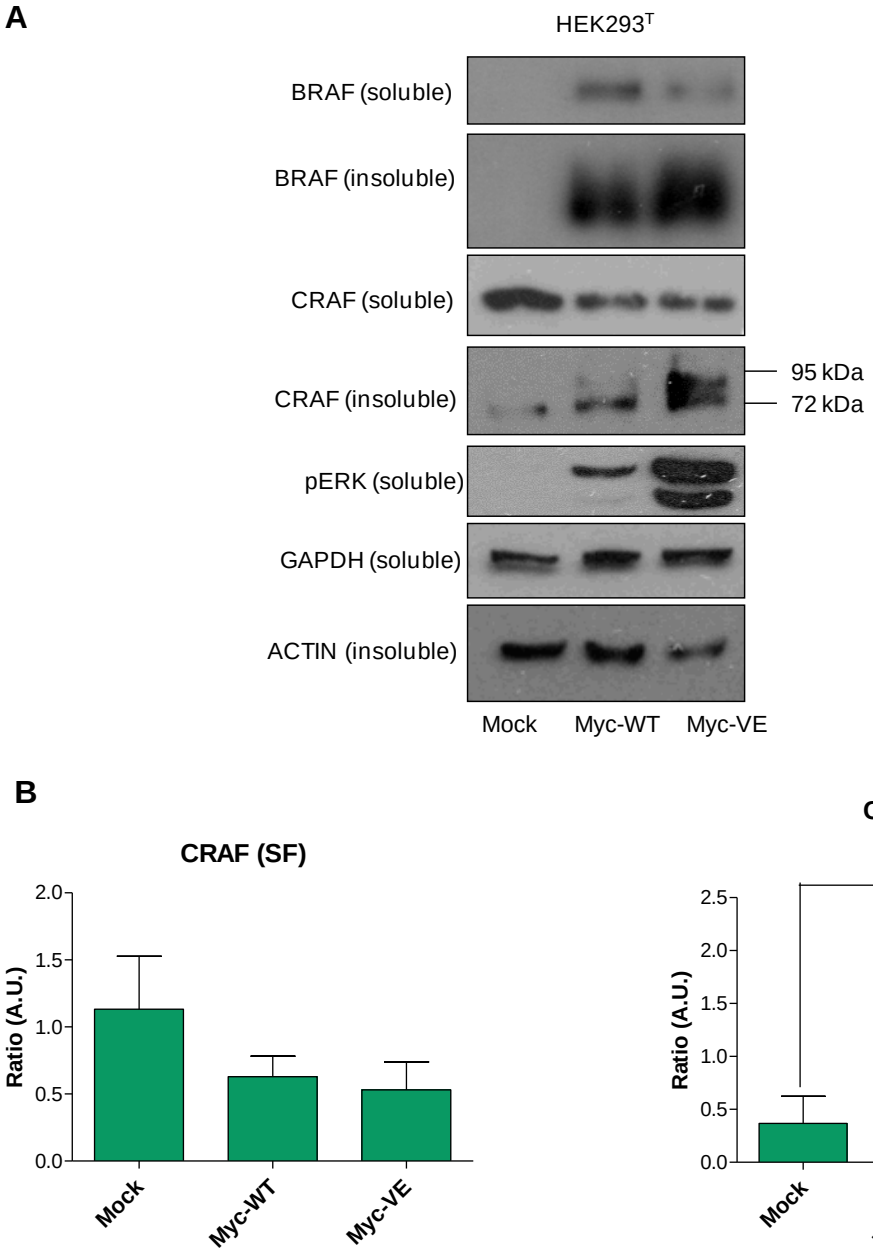

3.3.6 *Braf* and *Craf* mRNA levels are not reduced in *Braf*^{V600E} MEFs

3.3.6.1 qRT-PCR analysis of *Braf* expression in *Braf*^{V600E} MEFs

To investigate if the decrease of Braf protein levels could be explained by a transcriptional repression, the expression profile of *Braf* mRNA was analyzed by quantitative real time polymerase chain reaction (qRT-PCR). *Braf*$^{+/+}$ and *Braf*$^{+/LSL\text{-}V600E}$ MEFs were infected with AdCre over a 96 hour time course and RNA was isolated every 24 hours. cDNA was synthesized and qRT-PCR was performed using primers designed to span exons 1-2 for *Gapdh* and 12-13 for *Braf*. By adding a fluorescent dye that binds to newly synthesized double stranded DNA, the amplification could be monitored in real time (Morrison, Weis & Wittwer).

In relative quantification, the changes in gene expression of a given sample are measured relative to another sample which is thought to be constant (calibrator) (Pfaffl 2001). In this case, the calibrator sample consisted of the non-treated *Braf*$^{+/+}$ MEFs, which were thought to contain normal levels of *Braf* mRNA. In order to eliminate sample to sample differences, the target gene was expressed as a ratio with a reference gene. The reference gene is characterized by having constant expression under all tested conditions, normally being a house keeping gene such as *β-actin*, *Gapdh* or *rRNA* (Goossens et al. 2005).

The reference gene (*Gapdh*) and the target gene (*Braf*) were amplified in the same plate under the same parameters in order to avoid run-to-run variability. Also, each sample was performed in triplicate to assess variability within samples. The relative expression ratio of Braf was calculated as shown in Section 2.2.2.4. The melting curve showed no primer dimmers or the presence of any non-specific product (Section 2.2.2.4).

As shown in Figure 3.11, similar levels of *Braf* mRNA were observed in the non-infected sample (0) from *Braf*$^{+/+}$ and *Braf*$^{+/LSL\text{-}V600E}$ MEFs. Surprisingly, a reduction in Braf

expression was observed in all AdCre-infected samples from both types of MEFs. Although, the extent of the decrease in *Braf* mRNA was statistically significant in *Braf*^{V600E} MEFs when compared to the correspondent untreated samples (0), no significant decrease in Braf expression was found when comparing similar time points from both types of MEFs. At 96 hours post-AdCre infection, a recovery in *Braf* mRNA levels occurred in *Braf*$^{+/+}$ and *Braf*^{V600E} MEFs suggesting that the cells recovered from the unspecific effect of the AdCre infection at that time point.

3.3.6.2 qRT-PCR analysis of *Craf* expression in *Braf*^{V600E} MEFs

To examine the profile of *Craf* expression over a 96 hour time course in *Braf*$^{+/+}$ and *Braf*^{V600E} MEFs, qRT-PCR analysis was performed using primers spanning exons 2-3 of Craf. For the advance relative quantification, the non-treated sample from *Braf*$^{+/+}$ MEFs was used as the calibrator while *Gapdh* was chosen as the reference gene.

As with Braf, the reference gene (*Gapdh*) and the target gene (C*raf*) were amplified in the same plate under equal parameters. The qRTPCR reactions for each time point were performed in triplicate. The relative expression ratio of Craf was calculated as shown in Section 2.2.2.4. The melting curves showed single peaks, indicating specific cDNA amplification.

As shown in Figure 3.12, *Craf* mRNA levels remained constant in *Braf*$^{+/+}$ MEFs except for the 96 hour time point which shows a slight increase in the mRNA expression of this gene. In the case of *Braf*^{V600E} MEFs, a trend towards a lower level of *Craf* was observed mainly at the 48 and 72 hour time points; however, the reduction was not statistically significant when compared to the correspondent untreated samples (0). Also, no significant difference

Figure 3.11 No difference in *Braf* mRNA expression between *Braf*$^{+/+}$ and *Braf*^{V600E} MEFs. The graph shows the fold of increase or decrease in *Braf* expression of every sample relative to the *Braf* mRNA content from the non-treated sample (0) of *Braf*$^{+/+}$ MEFs. The error bars denote the S.D. of the replicates after applying the Pfaffl formula for the calculation of the final ratio. The graph is the result of four independent experiments using four different MEF lines (Mean ± S.D. One asterisk, P< 0.05).

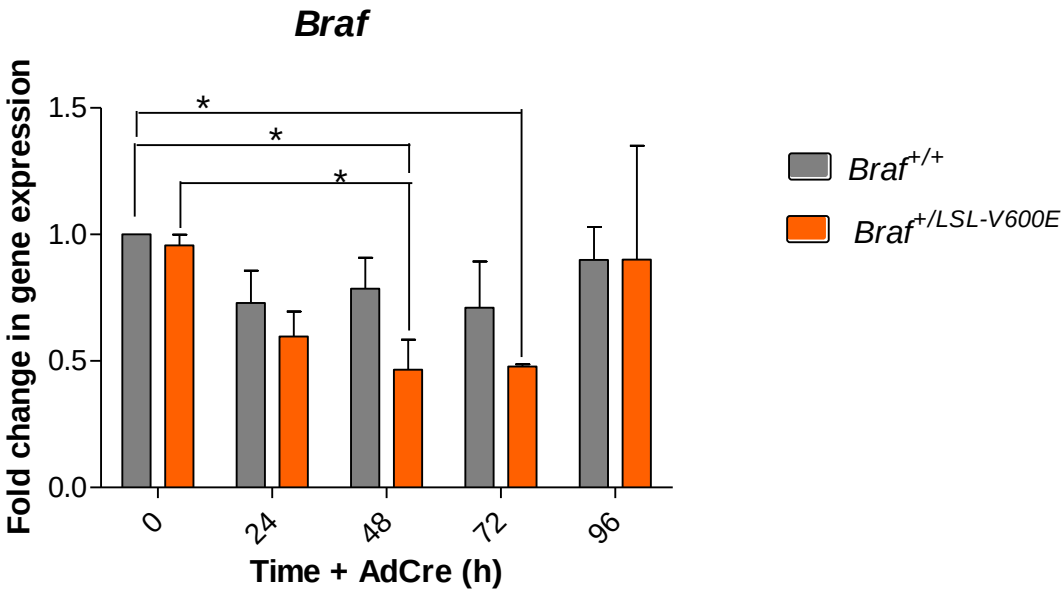

Figure 3.12 *Craf* mRNA levels are unchanged in *Braf*$^{+/+}$ and *Braf*^{V600E} MEFs. The graph shows the fold of increase or decrease in *Craf* expression of every sample relative to the *Craf* mRNA content in the non-treated sample (0) from *Braf*$^{+/+}$ MEFs. The error bars denote the S.D. of the replicates after applying the Pfaffl formula for the calculation of the final ratio. . The graph is the result of four independent experiments using four different MEF lines (Mean ± S.D. One asterisk, P< 0.05).

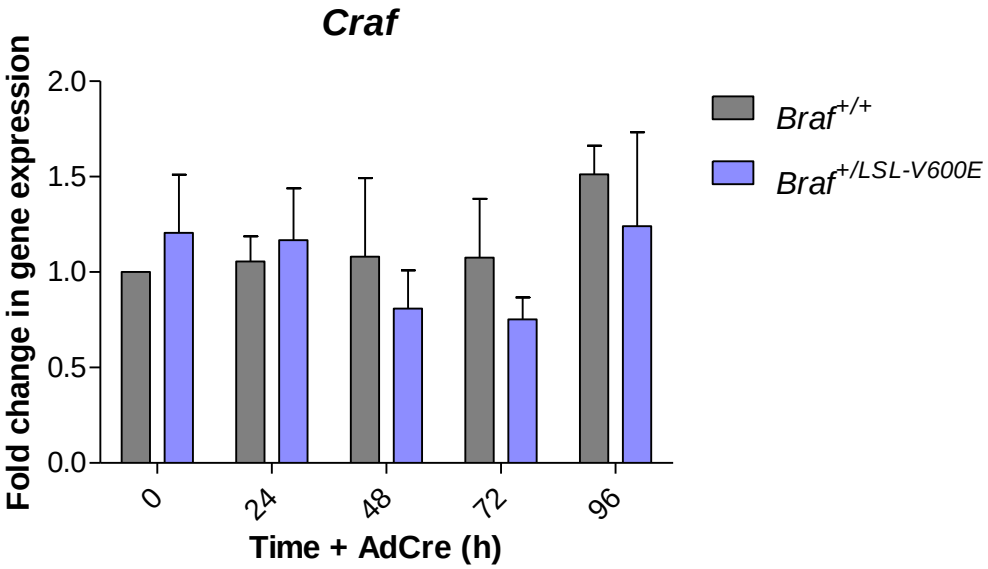

could be determined at any time point when comparing Craf expression in *Braf*$^{+/+}$ and *Braf*^{V600E} MEFs.

Overall data from Figure 3.11 and Figure 3.12 shows no significant difference in *Braf* and *Craf* mRNA levels in *Braf*$^{+/+}$ MEFs compared to *Braf*^{V600E} MEFs confirming that the downregulation in the expression of these proteins does not occur at the transcriptional level.

3.4 Discussion

Mice expressing ^{V600E}Braf in the lung were generated in our laboratory in order to characterize the early development of ^{V600E}Braf-driven tumours in this organ. The appearance of the *Lox-Braf*^{V600E} allele occurred at 3 weeks post-partum and progressively accumulated until the 14 week time point. Within this period, an increase in cell proliferation was observed during the first weeks resulting in the formation of adenomas at the 3 week time point (Figure 3.2). Similar to Dankort et al., these adenomas grew in a time-dependent manner until the 8 week time point after which they entered into a growth arrested state (Figure 3.2) (Dankort et al. 2007). No further progression of the adenomas to adenocarcinomas was observed during the life time of the mice. The growth arrested phase was accompanied by a decrease in staining of Ki67 at 8 weeks post-partum (data not shown). The expression of senescent markers was observed as early as the 6 week time point accompanied by the loss of Erk phosphorylation which remained throughout the time course. Interestingly, before the senescent-related changes begin to appear, an evident reduction in Braf protein levels was observed at the 3 week time point (Figure 3.1).In this chapter, a similar reduction in Braf protein levels was observed in the *LSL-Braf*^{V600E} MEFs after AdCre infection. This drop in Braf expression occurred along with a reduction in Craf protein levels and phospho-Erk levels (Figure 3.7). In contrast to the lung

model, no growth arrest was observed in the MEFs indicating the absence of senescence. Moreover, the cells maintained their transformed phenotype during the suppression of ERK phosphorylation. In 1997, Woods et al. showed by using the BrafER system that low levels of Braf kinase activity caused an increase in the expression and activation of cyclinD1-cdk4 and cyclinE-cdk2 complexes leading to cell cycle progression. By contrast, when Braf activity was elevated, the cells went into a growth arrested state which was associated with an increase expression of the cyclin-dependent kinase inhibitor p21Cip1. Together these data suggested that the kinase activity of the Raf proteins can influence the biological outcome of Erk pathway (Woods et al. 1997). In the context of our results, the decrease in Braf and Craf protein levels could be an attempt of the cells to avoid high Erk signalling allowing them to keep proliferating and consequently escaping from senescence.

Ubiquitylated and unfolded forms of CRAF have been detected in the NP-40 and Triton-X100 insoluble fraction by our lab and other groups (Grbovic et al. 2006, Noble et al. 2008, Schulte, An & Neckers 1997). In order to investigate the processing of BRAF and CRAF proteins in more detail, the NP-40 soluble and insoluble fractions were analysed. When ^{V600E}Braf was expressed in MEFs, an increase in Braf and Craf protein levels was observed in the insoluble fraction simultaneously to the drop in Braf and Craf in the soluble fraction suggesting that ^{V600E}Braf promotes the unfolding or enhanced modification of these proteins by events such as ubiquitylation (Figure 3.9). The fact that Braf and Craf proteins rescued in the soluble fraction appeared as single bands and not as ladder patterns indicative of ubiquitylation, could be explained by the absence of proteasome and deubiquitylase enzymes (DUB´s) inhibitors in the GLB lysis buffer. It is conceivable that the low quantity of Braf and Craf present in the insoluble fraction could be due to a continuous degradation of these proteins. We therefore speculate that ^{V600E}Braf could be

increasing the rate of degradation of Braf recovered in the insoluble fraction or activate alternative pathways of degradation in order to remove the accumulated Braf from this fraction. However to confirm these possibilities, the inhibition of the proteasome and other major pathways for protein degradation is needed. These experiments are presented and discussed in Chapter 4.

Similar to MEFs, ectopic BRAF showed a different partitioning between the soluble and insoluble fraction in Myc-BRAF^{V600E}-expressing cells compared to Myc-BRAF^{WT}-transfected cells (Figure 3.10). In the former cells, lower levels of ectopic BRAF^{V600E} were observed in the soluble fraction while a greater accumulation occurred in the insoluble fraction. Although Myc-BRAF^{WT} and Myc-BRAF^{V600E}-transfected cells showed a similar behaviour in endogenous CRAF expression in the soluble fraction, a further accumulation of this protein was observed in the insoluble fraction from cells overexpressing BRAF^{V600E}. Given these observations, it seems that the severity of the regulatory mechanism, reflected in the reduction and accumulation of the proteins in the different fractions, is proportional to the intensity of the activating signal coming from the RAF proteins. Thus, cells overexpressing ^{V600E}BRAF resulted in a more evident phenotype compared to cells overexpressing ^{WT}BRAF. In terms of phospho-ERK, higher levels were observed in Myc-BRAF^{V600E}-expressing cells compared to Myc-BRAF^{WT}-transfected cells suggesting that the regulation of ectopic BRAF and CRAF expression did not result in a reduction of ERK phosphorylation as in *Braf^{V600E}* MEFs (Figure 3.10). It is possible that the regulatory mechanism controlling ectopic BRAF and endogenous CRAF expression is not enough to decrease the intensity of the signal coming from the overexpressed BRAF^{V600E}. Consistent with this, the biological outcome of the MAPK activation after the reduction in ectopic BRAF and CRAF in Myc-BRAF^{V600E}-transfected cells is different compared to *Braf^{V600E}*

MEFs. The former cells entered into a growth arrested state and showed no change in their morphology.

QRTPCR experiments showed a reduction in *Braf* mRNA from AdCre infected samples in in *Braf*$^{+/+}$ and *Braf*^{V600E} MEFs when compared to uninfected samples (0) (Figure 3.11). This behaviour suggests that the downregulation in *Braf* mRNA expression could be attributed to the Adenoviral-Cre infection. Importantly, the reduction in *Braf* mRNA expression is not related to the Lox-P system as it is also observed in *Braf*$^{+/+}$ MEFs which do not contained any modification in the *Braf* locus. However, the reduction was specific for the *Braf* gene as supported by constant *Craf* mRNA levels (Figure 3.12). This observation is consistent with studies published in the literature that have identified cryptic loxP sites naturally present in mammalian cells (Thyagarajan et al. 2000). The expression of the Cre recombinase in these cells has lead to DNA genome damage in the form of chromosomal aberrations and an increased number of sister chromatid exchanges. Thus, it is possible that Cre recombinase could be recognizing a cryptic Lox P site in the *Braf* locus leading to cleavage of the sequence and subsequent transcriptional downregulation (Loonstra et al. 2001). However, a formal search in the coding and non-coding regions of *Braf* is needed to further support this hypothesis.

In agreement with our results, numerous microarray studies published in the literature have not identified *BRAF* or *CRAF* changes in melanoma or colorectal cancer cells expressing ^{V600E}BRAF after treatment with BRAF or MEK inhibitors (Pratilas et al. 2009, Nazarian et al. 2010, Joseph et al. 2010, Packer et al. 2009). Interestingly, a microarray analysis of immortalized *Braf*$^{+/+}$ and *Braf*^{V600E} MEFs performed by our group showed a reduction in *Braf* and *Craf* mRNA expression (Andreadi et al. 2012). These results contrast with our observations from qRTPCR experiments where no significant decrease in *Braf* and *Craf* mRNA was detected. It is conceivable that transcriptional events occurring in

immortalized MEFs that express ^{V600E}Braf in a permanent manner are absent from primary MEFs were the induction of ^{V600E}Braf just occurred. Thus, the comparison of both cellular systems should be done carefully.

Overall these data showed that a reduction in BRAF and CRAF expression occurs in the presence of ^{V600E}BRAF and that this behaviour could be associated to the increase degradation of these proteins but not to their transcriptional downregulation. The decrease in Braf and Craf protein levels in Braf^{V600E} MEFs was associated to a suppression of phospho-Erk levels while the reduction in ectopic ^{V600E}BRAF and endogenous CRAF in HEK293^{T} did not show a decrease in ERK phosphorylation. The difference in the activation of ERK is reflected in the biological outcome of both cellular systems.

CHAPTER 4 Regulation of BRAF and CRAF stability by ^{V600E}BRAF

4.1 Introduction

The presence of the PEST motif (rich in proline [P], glutamic acid [E], serine [S] and threonine [T]) is considered a signature of short-lived proteins degraded by the ubiquitin-proteasome pathway (Rechsteiner, Rogers 1996). RAF proteins contain PEST motifs and both CRAF and BRAF have been found to be ubiquitylated and degraded by the proteasome (Noble et al. 2008) (Section 1.2.5.5).

The lack of phosphorylation of Ser621 in CRAF has been shown to promote its misfolding, ubiquitylation and subsequent degradation by the proteasome (Noble et al. 2008, Hekman et al. 2004) (Section 3.1). Schulte et al. observed that, after treating NIH 3T3 cells with Geldanamycin (GA), an Hsp90 inhibitor, CRAF was poly-ubiquitylated and subsequently degraded by the proteasome (Schulte, An & Neckers 1997) (Section 1.2.5.5). In 2002, Manenti et al. showed that in the absence of cell adhesion to the extracellular matrix, the ubiquitylation and proteasome-dependent degradation of CRAF was observed (Manenti, Delmas & Darbon 2002). In several studies, the co-expression of CRAF and ubiquitin led to the detection of ubiquitylated forms of CRAF suggesting a ubiquitin-dependent degradation of the protein (Noble et al. 2008, Fueller et al. 2008). In the case of BRAF, a recent study showed the interaction of this protein with the E3 ubiquitin ligase RNF149, which resulted in BRAF ubiquitylation and subsequent degradation by the proteasome (Hong et al. 2012) (Section 1.2.5.6).

A large amount of evidence has been generated in the recent years where the proteasome is related to the regulation of a variety of signaling cascades. This role of the proteasome is achieved through the degradation of specific target proteins that influence the outcome of signaling pathways (Meyer et al. 2011, Nie et al. 2002, Li et al. 2005). In this case,

signals such as phopshorylation, the binding of a small molecule or the binding of another protein partner can specifically promote the recruitment of the ubiquitin ligase leading to ubiquitin attachment (Backues, Klionsky 2011). CRAF protein itself has been found able to promote the phosphorylation of the pro-apoptotic protein BAD resulting in its ubiquitylation and proteasome degradation (Fueller et al. 2008). Another example of regulation associated to the ERK pathway is the proteasome-dependent degradation of BIM_{EL}, which is also a pro-apoptotic protein and whose phosphorylation by ERK flags this protein for ubiquitylation (Ley et al. 2003b).

The other major pathway for protein degradation in eukaryotic cells is autophagy (Clague, Urbe 2010b). This pathway has been thought of as a non-selective degradation process related to nutrient management (Mizushima et al. 2008). However, recent evidence showed that it can specifically remove certain organelles and structures such as mitochondria or protein aggregates contributing to the quality control of the cell (Clague, Urbe 2010b, Kirkin et al. 2009) (Section 1.3.3). A type of “selective autophagy” has been recently proposed based on the recognition of ubiquitin moieties by receptors of the autophagosome membrane (Clague, Urbe 2010b, Kirkin et al. 2009) (Section 1.3.3). Moreover, autophagy has shown to be involved in the regulation of signal transduction in a similar way to the ubiquitin-proteasome pathway (Gao et al. 2010).

Recent evidence showed that autophagy is able to modulate the WNT pathway, whose activation is important in cell proliferation. In the canonical WNT pathway, the binding of the WNT ligand to a receptor from the Frizzled family has been shown to recruit the soluble protein Dishevelled (DVL) to the membrane, causing the release of β-catenin. This protein then migrates to the nucleus and acts as a transcription factor (Reya, Clevers 2005, Clevers 2006). Gao et al. found that autophagy, induced by either starvation or rapamycin, is able to specifically degrade Dvl2, reducing the activation of the Wnt pathway in human

tissue culture cells. This group showed that the ubiquitin E3 ligase, pVHL, binds to Dvl2 promoting its ubiquitylation. The poly-ubiquitylated form of Dvl2 interacts with p62 which facilitates its transport to the autophagosome. The subsequent interaction of Dvl2 with LC3II in the autophagosome outer membrane allows its translocation and subsequent degradation inside the autophagosome (Gao et al. 2010).

Another example of autophagy regulating cell proliferation is through its contribution to senescence establishment. In the model for oncogene-induced senescence (OIS) proposed by Narita et al., the existence of a “transition phase” occurring between the initial burst in proliferation and the senescence phase has been defined. During the “transition phase”, signalling and phenotypic changes such as inactivation of mTORC1 (Jung et al. 2010) and the presence of secretory-associated secretory phenotype (SASP) (Kuilman et al. 2008, Acosta et al. 2008) are observed (Section 1.3.4.1). Importantly, an upregulation in the expression of autophagy-associated genes accompanied by an increase in autophagic activity has also been reported in this phase (Narita, Young & Narita 2009). Narita et al. suggested that autophagy, through the rapid turnover of proteins, contributes to the synthesis of SASP components whose main role is to reinforce senescence through autocrine and paracrine signalling (Narita, Young & Narita 2009) (Section 1.3.4.1).

In 2010, a link between overexpression of ^{V600E}BRAF and the induction of autophagy was proposed by Maddodi et al. Based on the fact that the level of activation of the oncogene influences the outcome of the signaling pathways, leading to growth arrest or proliferation, they found that hyperactivation of ^{V600E}BRAF inhibited cell growth by autophagy-associated cell death (Maddodi et al. 2010). They also showed that the induction of autophagy by overexpression of ^{V600E}BRAF occurred through the blockage of AKT-mTORC1 signaling pathway (Maddodi et al. 2010). In support of these results, Dr. Hong Jin from our lab showed that mice containing conditional knockin mutation of *Braf*^{V600E} developed lung

adenomas that subsequently entered into a senescent state which was accompanied by high levels of autophagic activity (Hong Jin, personal communication). In agreement with Maddodi et al., he observed that the induction of autophagy by endogenous ^{V600E}Braf was associated with the inactivation of mTORC2 resulting in low levels of phosphorylation at Ser473 in Akt.

In this chapter the turnover of BRAF and CRAF was further investigated as well as the role of ^{V600E}BRAF in the induction of autophagy in MEFs and HEK293^{T} cells. Moreover, we show that the autophagy pathway contributes to the regulation of BRAF and CRAF in ^{V600E}BRAF-expressing cells using inhibitor approaches.

4.2 Aims

The aim of this chapter was to determine if the decrease in BRAF and CRAF protein levels in the presence of ^{V600E}BRAF could be explained by a reduction in the stability of these proteins. I was also interested to establish if the proteasome and autophagy degradation pathways were contributing to the drop in the expression of these proteins.

4.3 Results

4.3.1 The stability of ectopic ^{V600E}BRAF and endogenous CRAF is reduced in Myc-BRAF^{V600E}-expressing cells

The half-life of a protein is defined as the length of time necessary for the concentration of that protein to drop to half of its original value. The first order kinetics describes the decay of a protein after the blockage of protein biosynthesis and is represented by Equation 2

(Section 2.3.1.8). An essential characteristic of a first order reaction is that the concentration of the reactant falls by the same percentage over similar intervals of time.

As shown in Section 3.3.5, when ectopic ^{V600E}BRAF was expressed in HEK293^{T} cells, an increased accumulation of the protein was observed in the insoluble fraction compared to Myc-BRAF^{WT}-expressing cells. In addition, a decrease in endogenous CRAF protein levels was evident in the soluble fraction. In order to determine the stability of ectopic ^{V600E}BRAF and endogenous CRAF, the half life values of both proteins in the soluble fraction were compared to those in Myc-BRAF^{WT}-expressing cells.

In order to measure the decay of ectopic BRAF, overall protein biosynthesis was blocked by emetine treatment. It has been shown that emetine inhibits the incorporation of the aminoacyl moiety into a polypeptide bound form in an irreversible manner (Grollman 1968). For this experiment, HEK293^{T} cells were transiently transfected with Myc-BRAF^{WT} or Myc-BRAF^{V600E} expression vectors. The cells were treated with emetine over an 18 hour time course beginning at 48 hours post-transfection. The cells were harvested 5, 10, 14 and 18 hours following emetine treatment with GLB lysis buffer and only the soluble fraction was analysed. The same volume of each sample was loaded onto a SDS-PAGE gel, the proteins were transferred to a membrane and immunoblotted with BRAF and CRAF antibodies. The half-life values were calculated as shown in (Section 2.3.1.8).

Figure 4.1 Reduced stability of ectopic ^{V600E}BRAF and endogenous CRAF in Myc-BRAF^{V600E}-expressing cells. (A) HEK293^{T} cells were transiently transfected with Myc-BRAF^{WT} or Myc-BRAF^{V600E} expression vectors. After 48 hours of transfection, the cells were treated with 0.3 mM emetine over an 18 hour time course and lysed with GLB buffer at each time point. The soluble fraction samples were resolved by SDS-PAGE gel and the expression of BRAF CRAF was analyzed by immunoblotting. ACTIN was used as a loading control in these samples. The X-ray films were scanned and the optical density (O.D.) of the bands was measured using Image J software. **(B)** The graph shows the natural logarithm of BRAF and CRAF concentration (ln [Myc-BRAF] and ln [CRAF]) plotted against time (T). Data are representative of a single experiment.

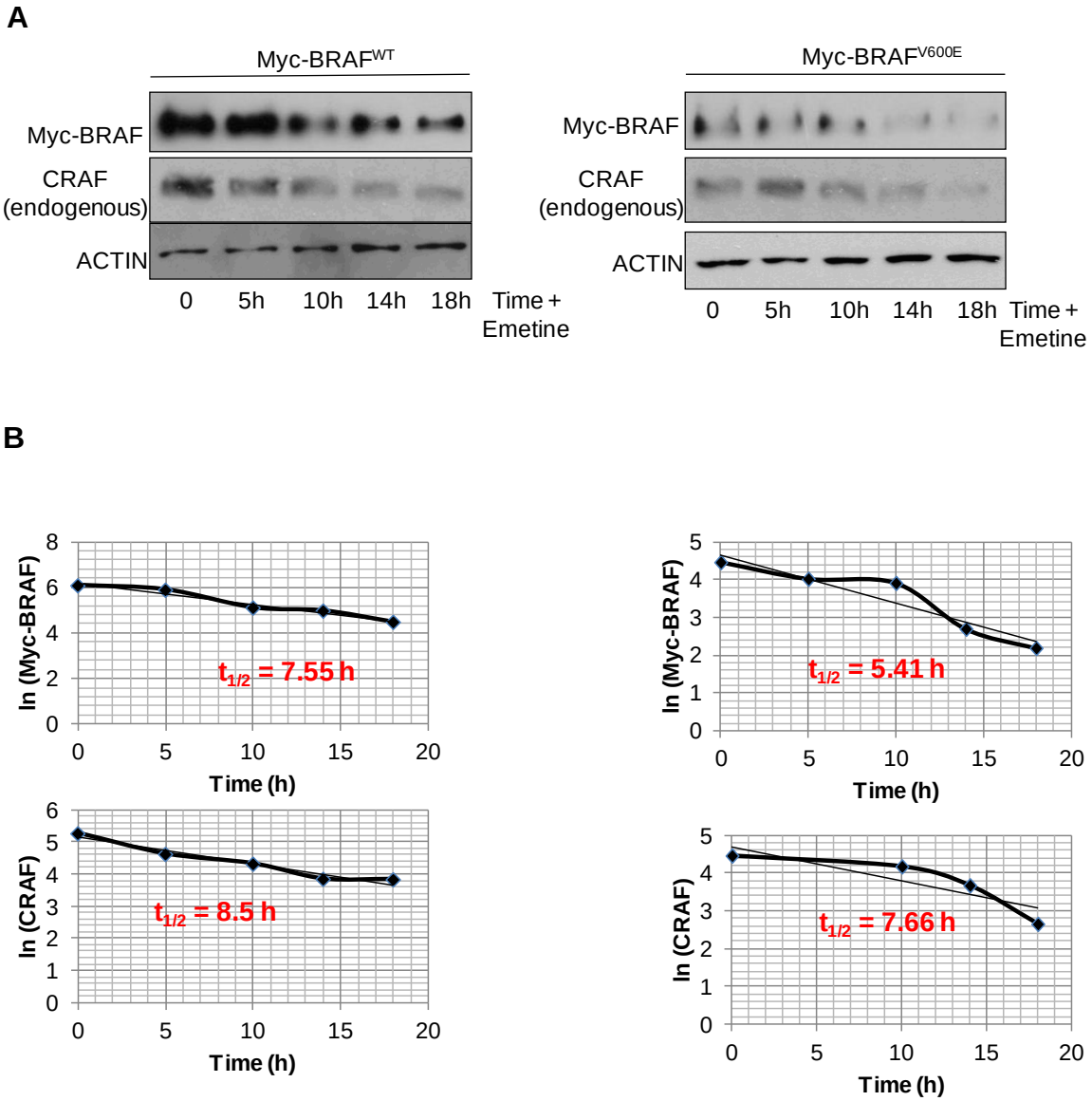

Although the same concentration of Myc-BRAF^{WT} or Myc-BRAF^{V600E} expression vectors were transfected to HEK293^{T} cells, reduced levels of Myc-BRAF^{V600E} were observed in the non-treated sample (0) of these cells (Figure 4.1). Because the half-life value in a first order reaction does not depend upon the initial concentration, the measurement was not affected by this issue. As shown in the plot from Figure 4.1, the concentration of Myc-BRAF^{WT} or Myc-BRAF^{V600E} did not fall by the same extent over similar intervals of time suggesting that the reaction did not behave as an ideal first order reaction. However, when plotting the concentration values of Myc-BRAF^{WT} or Myc-BRAF^{V600E} against time, relatively straight lines could be generated. The analysis of these graphs indicated an approximate 2 hour reduction in the half-life of Myc-BRAF^{V600E} in comparison to Myc-BRAF^{WT} (Figure 4.1). In the case of endogenous CRAF, a progressive decay in its protein levels occurred after emetine treatment in all samples except from the 5 hour time point sample in Myc-BRAF^{V600E}-expressing cells. For calculation purposes, this sample was not included in the analysis. Although the behaviour of CRAF decay did not follow perfect first order kinetics, the extent of the reduction in CRAF protein levels was reasonably constant at all intervals except from the 18 hour time point. Analysis of the graphs showed an approximate 1 hour reduction in the half-life of CRAF in Myc-BRAF^{V600E}-transfected samples in comparison to cells expressing Myc-BRAF^{WT} vector.

Overall, the data from Figure 4.1 shows a reduction in the half-life of Myc-BRAF^{V600E} in comparison to Myc-BRAF^{WT} and a decrease in the stability of endogenous CRAF in the presence of ectopic ^{V600E}BRAF.

4.3.2 Reduced stability of Craf but not Braf in cells expressing endogenous Braf^{V600E}

The half-lives of Braf and Craf proteins were determined in *Braf*^{V600E} MEFs in comparison to *Braf*$^{+/+}$ MEFs. For this experiment, *Braf*$^{+/+}$ and *Braf*$^{+/LSL\text{-}V600E}$ MEFs were infected with AdCre. After 48 hours of AdCre infection, the cells were treated with emetine for 5, 10, 14 and 18 hours. Both types of MEFs were lysed with GLB buffer and the soluble fractions were obtained. The same volume for each sample was loaded onto a SDS-PAGE gel and Braf and Craf expression was examined by immunoblotting. The half-life values were calculated as shown in (Section 2.3.1.8).

As shown in Figure 4.2, a progressive decrease in Braf protein levels was observed in *Braf*$^{+/+}$ and *Braf*^{V600E} MEFs after emetine treatment. Although the reduction in Braf expression during the first 14 hours post-treatment was similar at each interval in both types of MEFs, a marked decrease in Braf content was observed at the 14-18 hour interval.

This could be explained by the high number of apoptotic cells found at the later time point which could influence the amount of Braf. In order to avoid including this error in the estimate of the half-life values, the last time point was omitted from the calculations as shown by the graph (Figure 4.2). When plotting the concentration of Braf [ln Braf] against time [T], the slope of the line showed similar half-life values for Braf in *Braf*$^{+/+}$ and *Braf*^{V600E} MEFs.

The expression of Craf was also analysed in these samples. As shown in Figure 4.2, a time-dependent reduction in Craf protein levels was observed in *Braf*$^{+/+}$ and *Braf*^{V600E} MEFs after emetine treatment. A similar reduction in Craf expression occurred in the first two intervals (0-10 hours) in both types of MEFs. However, a severe decrease in Craf protein levels was observed at the 14 and 18 hour time points, presumably because of the high levels of apoptosis observed at these intervals.

Figure 4.2 Braf stability is not altered in *Braf^{V600E}* MEFs whereas Craf half-life is reduced. *Braf$^{+/+}$* and *Braf$^{+/LSL-V600E}$* MEFs were infected with AdCre. After 48 hours of AdCre infection, the cells were treated with 0.3 mM emetine and harvested at each of the indicated time points. Cells were lysed with GLB buffer and the soluble fraction was obtained. Braf and Craf expression were analyzed by immunoblotting. Actin was used as a loading control in these samples. The X-ray films were scanned and the optical density (O.D.) of the bands was measured using Image J software. **(B)** The graph shows the natural logarithm of Braf and Craf concentration (ln [Braf] and ln [Craf]) plotted against time (T). Data are representative of a single experiment.

A

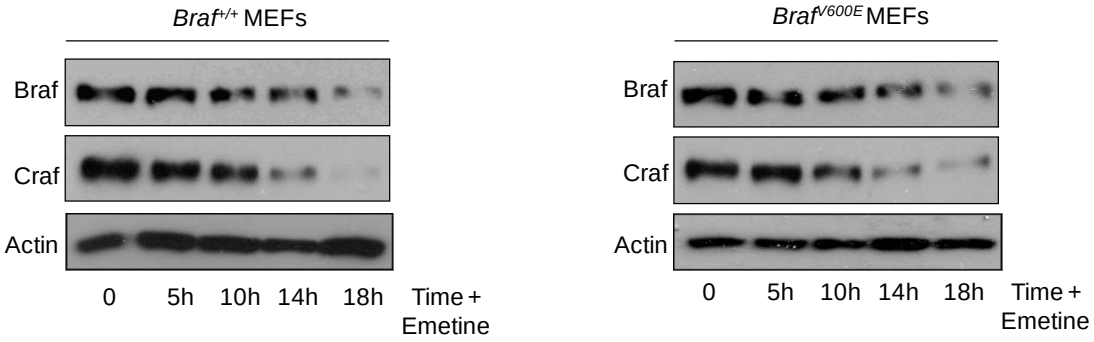

B

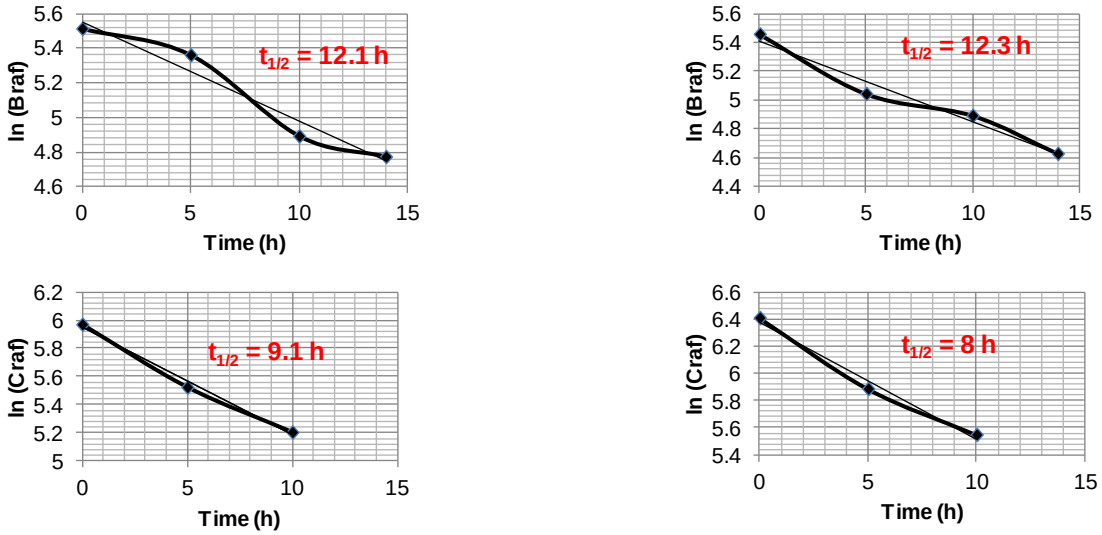

For the calculation of the half-life values, the last two time points were omitted as shown by the graph. When plotting the concentration of Craf [ln Craf] against time [T], the slope of the line showed an approximate 1 hour reduction in the half-life of Craf in *Braf*^{V600E} MEFs compared to *Braf*$^{+/+}$ MEFs.

Overall, the data from Figure 4.2 shows that Craf is less stable in the presence of endogenous ^{V600E}Braf, in agreement with the studies in HEK293^{T} cells. However, in contrast with the data obtained in HEK293^{T} cells, no significant difference in the half-lives of Braf was found in *Braf*$^{+/+}$ and *Braf*^{V600E} MEFs.

4.3.3 Braf and Craf protein levels are rescued after proteasome inhibition in *Braf*^{V600E} MEFs

The results from the previous sections showed that a reduction in the stability of BRAF and CRAF in the presence of ^{V600E}BRAF could be contributing to the decrease in the expression of these proteins. In order to investigate if the proteasome could be involved in this behaviour, its activity was blocked in *Braf*^{V600E} MEFs and Braf/Craf expression was examined. *Braf*$^{+/LSL\text{-}V600E}$ MEFs were infected with AdCre for 96 hours. For the last 5 hours, the cells were treated with the proteasome inhibitors MG132 or epoxomicin. The cells were harvested with GLB lysis buffer and NP-40 soluble and insoluble fractions were obtained as described in section 2.3.1.1. The samples from both fractions were resolved by SDS-PAGE gel, transferred to a membrane and immunoblotted with Braf, Craf, Gapdh and Actin antibodies.

As shown in Figure 4.3, after treatment with both proteasome inhibitors, the major accumulation of Braf and Craf in respect to the correspondent untreated sample was observed in the insoluble fraction. The exposure of *Braf*$^{+/+}$ MEFs to a saturating

concentration of MG132 resulted in approximately a 28-fold increase relative to the untreated sample whereas approximately a 10-fold recovery in Braf protein levels was observed in *Braf*^{V600E} MEFs. Similarly to Braf, a greater accumulation of Craf occurred in the insoluble fraction from *Braf*$^{+/+}$ MEFs (~7.3-fold) compared to *Braf*^{V600E} MEFs (~5-fold). In the case of epoxomicin, a moderate accumulation in Braf expression (~2-fold) was observed in the soluble fraction from *Braf*$^{+/+}$ MEFs; however no recovery in Braf protein levels was observed in the soluble fraction from *Braf*^{V600E} MEFs. In agreement with the behaviour of MG132 treated cells, a greater recovery in Braf protein levels occurred in *Braf*$^{+/+}$ MEFs (~6.8-fold) compared to *Braf*^{V600E} MEFs (~4.4-fold). Surprisingly Craf protein levels remained unchanged in the insoluble fraction from both types of MEFs.

Overall, the data from Figure 4.3 shows that Braf and Craf proteins are accumulated in the insoluble fraction after proteasome inhibitor treatment which suggests that the proteasome could be involved in the turnover of these proteins. In addition, this experiment shows a greater recovery of Braf and Craf in *Braf*$^{+/+}$ MEFs after MG132 and epoxomicin treatment in comparison to *Braf*^{V600E} MEFs which does not agree with the hypothesis of an accelerated degradation of these proteins by the proteasome in *Braf*^{V600E} MEFs.

Figure 4.3 Braf and Craf are degraded by the proteasome in Braf$^{+/+}$ and Braf^{V600E} MEFs. (A) *Braf*$^{+/+}$ and *Braf*$^{+/LSL-V600E}$ MEFs were infected with AdCre for 96 hours and treated with 30 μM MG132 (MG) or 0.5 μM epoxomicin (E) for the final 5 hours. Cells were lysed with GLB buffer and the soluble and insoluble fractions were prepared. Expression of Braf, Craf, Gapdh and Actin was analyzed by immunoblotting. **(B)** The X-ray films were scanned and the optical density (O.D.) of the bands was measured using Image J software. The optical density of the background was subtracted from every sample. The values plotted on the graphs correspond to the Braf/Gapdh or Craf/Gapdh ratio expressed in Arbitrary Units (A.U.) for the soluble fraction while Braf/Actin and Craf/Actin ratios are shown for the insoluble fraction samples. Data are representative of two experiments.

A

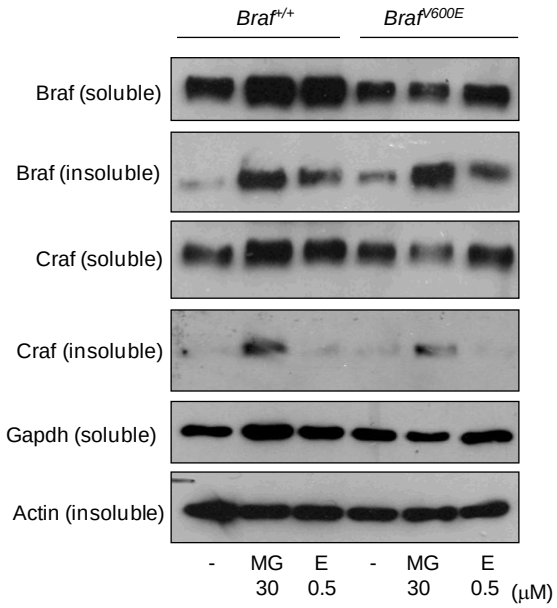

B

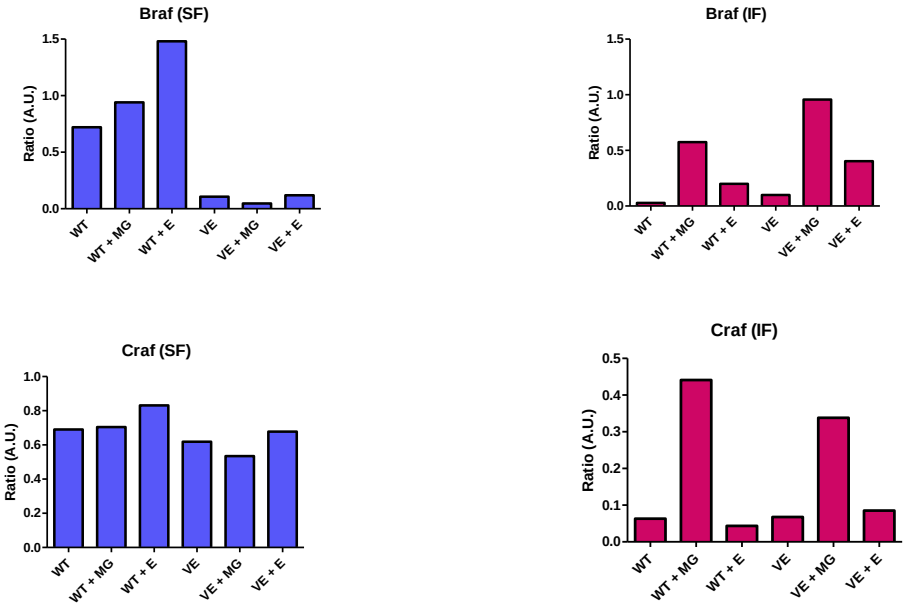

4.3.4 CRAF protein levels are rescued after proteasome inhibition in cells expressing ectopic ^{V600E}BRAF

To examine the role of the proteasome in regulating endogenous CRAF stability in cells containing ectopic ^{V600E}BRAF, HEK293^{T} cells were transiently transfected with Myc-BRAF^{V600E} expression vector. The cells were incubated for 5 hours with the proteasome inhibitor MG132 before being harvested. The cells were lysed with GLB buffer and the soluble and insoluble fractions were obtained. The samples were subjected to western blot with antibodies detecting Myc, CRAF, ERK2 and ACTIN proteins. HEK293^{T} cells that were treated with Lipofectamine 2000 alone were employed as negative controls.

In agreement with previous experiments, a reduction in endogenous CRAF protein levels was observed in the soluble fraction simultaneously to an accumulation of shifted forms of CRAF in the insoluble fraction (Figure 4.4). Similarly to MEFs, the inhibition of the proteasome led to the accumulation of endogenous CRAF in non-transfected cells and cells expressing ectopic ^{V600E}BRAF. Importantly, CRAF was accumulated to a greater extent in the insoluble fraction from Myc-BRAF^{V600E}-transfected cells (~12-fold increase with MG132) in comparison to control samples, where no increase was observed, This behaviour suggests that an increased degradation of endogenous CRAF by the proteasome occurred in the presence of ectopic ^{V600E}BRAF. However, the extent of the recovery of endogenous CRAF in the insoluble fraction must be compared to that in Myc-BRAFWT-transfected sample in order to confirm this observation.

Figure 4.4 Decrease in CRAF protein levels is rescued by proteasome inhibition in the insoluble fraction from HEK293^{T} cells. HEK293^{T} cells were mock transfected (M) or transiently transfected with Myc-BRAF^{V600E} expression vector. For the last 5 hours, cells were treated with DMSO or 30μM MG132 (MG). After 48 hours of transfection, the cells were harvested with GLB buffer and the soluble and insoluble fractions were prepared. Expression of Myc, CRAF, ERK2 and ACTIN was analyzed by immunoblotting. **(B)** The X-ray films were scanned and the optical density (O.D.) of the bands was measured using Image J software. The optical density of the background was subtracted from every sample. The values plotted on the graph correspond to CRAF/ERK2 ratio expressed in Arbitrary Units (A.U.) for the soluble fraction while CRAF/ACTIN ratios are shown for the insoluble fraction samples. Data are representative of two experiments.

A

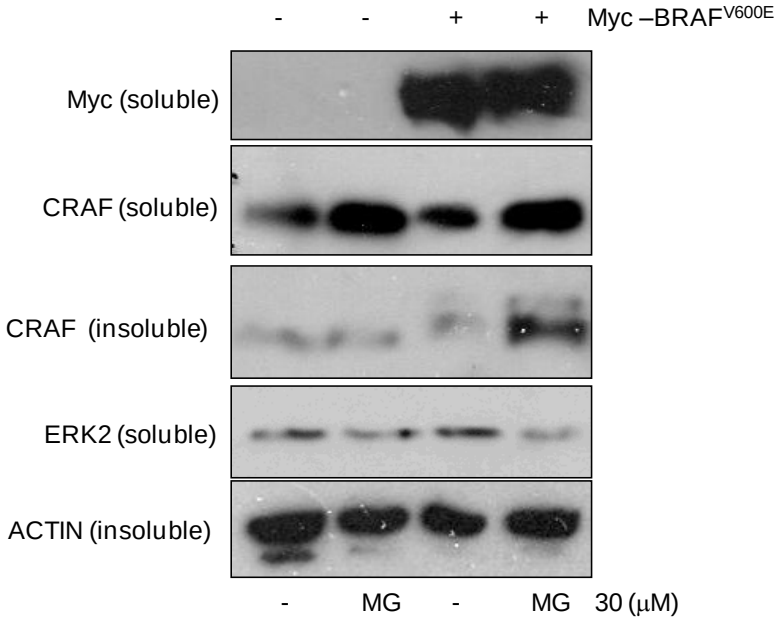

B

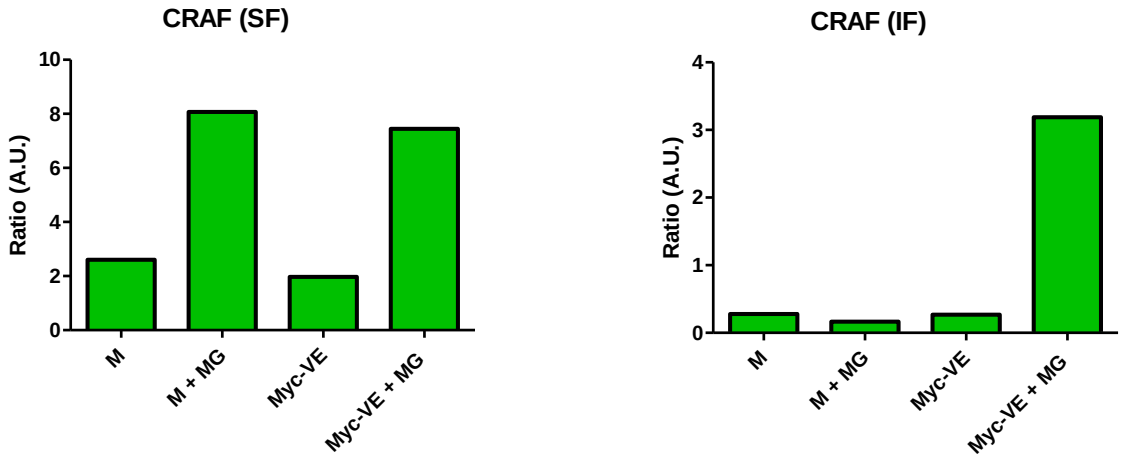

4.3.5 Autophagy is increased in cells expressing ectopic ^{V600E}BRAF

It has been shown that the activation of certain oncogenes is sufficient to upregulate basal autophagy (White 2012). Various studies have reported an increase of autophagy in Ras-driven cancers which is required for mitochondrial function and tumorigenesis (Guo et al. 2011, Lock et al. 2011). As mentioned in section 4.1, Madodi et al., showed that hyperactivation of ^{V600E}BRAF can induce high levels of autophagy resulting in growth inhibition and the suppression of melanoma (Maddodi et al. 2010). To confirm that overexpression of ^{V600E}BRAF induces autophagy as reported by Maddodi et al., immunoblot analysis of the autophagy marker LC3II was performed in cells ectopically expressing ^{V600E}BRAF. HEK293^{T} cells were transfected with Myc-BRAF^{V600E} expression vector. For the last 4 hours, the cells were treated with the lysosomal inhibitor bafilomycin A1 (BFA1). The cells were harvested 48 hours post-transfection with GLB lysis buffer and the soluble fraction was subjected to Western blot analysis. As a positive control for autophagy induction, cells expressing ectopic Myc-BRAF^{V600E} were treated with 0.1 μM rapamycin for the last 4 hours. As a negative control, cells transfected with EGFP expression vector were employed.

Although EGFP-transfected cells showed no LC3II conversion, an accumulation in LC3II protein levels was observed after inhibition of lysosomal activity by BFA1 (Figure 4.5). In contrast, cells expressing ectopic ^{V600E}BRAF showed enhanced LC3II conversion in the basal state and an even further increase in LC3II levels after BFA1 treatment which suggests an augmented autophagic flux in the presence of ^{V600E}BRAF. Intriguingly, the treatment of transfected Myc-BRAF^{V600E} cells with rapamycin did not have any added effect on LC3II accumulation (Figure 4.5).

Figure 4.5 Increased autophagic flux in cells expressing ectopic ^{V600E}BRAF. (A) HEK293^{T} cells were transiently transfected with EGFP or Myc-BRAF^{V600E} expression vectors. The cells were exposed to 0.4 μM bafilomycin A1 (BFA1) for the last 4 hours or to 0.1 μM rapamycin (Rap) for the final 6 hours. After 48 hours of transfection, the cells were harvested with GLB lysis buffer and the soluble fraction was resolved by SDS-PAGE gel. The expression of Myc, LC3 and GAPDH was analyzed by immunoblotting. **(B)** The X-ray films were scanned and the optical density (O.D.) of the bands was measured using Image J software. The optical density of the background was subtracted from every sample. The values plotted on the graph correspond to the LC3II/GAPDH ratio expressed in Arbitrary Units (A.U.). Data are representative of two experiments.

A

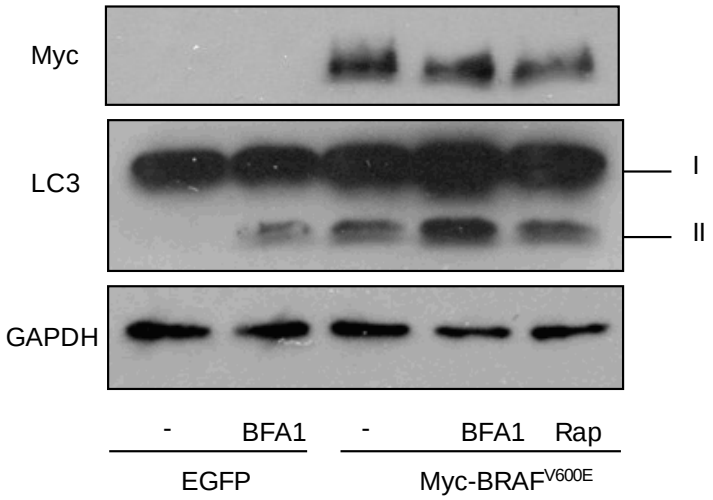

B

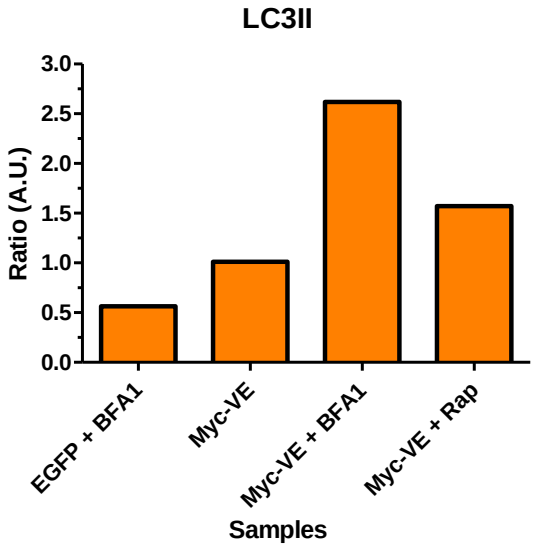

Previously it has been shown that bafilomycin A1 (BFA1) treatment can increase the levels of LC3II even under non-starvation conditions, so the non-specific effect caused by BFA1 exposure, which is represented by the band from lane 2, was subtracted from the LC3II band in lane 4 (Figure 4.5).

These results indicate that, independently from the conditions to which the cells are subjected by transient transfection, the overexpression of ^{V600E}BRAF increases the autophagic activity in the cells.

4.3.6 Autophagy is increased in *Braf^{V600E}* MEFs

As mentioned in section 4.1, Dr. Hong Jin from our lab showed that physiological levels of ^{V600E}Braf are able to induce high levels of autophagy in the lung *in vivo*. In order to examine whether autophagy could be induced by endogenous ^{V600E}Braf in MEFs, the conversion of LC3-I to LC3-II was monitored in these cells. To do this *Braf$^{+/LSL\text{-}V600E}$* MEFs were infected with AdCre over a 96 hour time course. The cells were harvested every 24 hours with GLB lysis buffer and the soluble fraction was subjected to Western Blot analysis. Protein levels of LC3, p70 and Gapdh were assessed by immunoblotting. As negative controls, *Braf$^{+/+}$* MEFs simultaneously infected with AdCre were employed. As positive controls, non-infected *Braf$^{+/+}$* or *Braf$^{+/LSL\text{-}V600E}$* MEFs treated with 0.5 μM rapamycin for the last 6 hours or nutrient-starved for the same length of time were employed. Both samples were harvested at the 96 hour time point. To confirm mTORC1 inhibition by rapamycin, the phosphorylation state of its downstream target p70 S6 kinase was analysed.

As shown in Figure 4.6, the rapamycin treated cells showed increase levels of LC3II indicative of mTOR inhibition and autophagy induction. The efficient inhibition of mTOR by

Figure 4.6 Increased LC3-II conversion in *Braf*^{V600E} MEFs. (A) *Braf*$^{+/+}$ or *Braf*$^{+/LSL-V600E}$ MEFs were infected with AdCre over a 96 hour time course except from the positive controls which were treated with at 0.5 μM rapamycin (Rap) or nutrient-starved (Starv.) for the last 6 hours. Cells were lysed with GLB buffer and the soluble fraction was resolved by SDS-PAGE gel. Expression of LC3, p70 and Gapdh was analyzed by immunoblotting. **(B)** The X-ray films were scanned and the optical density (O.D.) of the bands was measured using Image J software. The optical density of the background was subtracted from every sample. The values plotted on the graph correspond to the LC3II/Gapdh ratio expressed in Arbitrary Units (A.U.). Data are representative of three experiments.

A

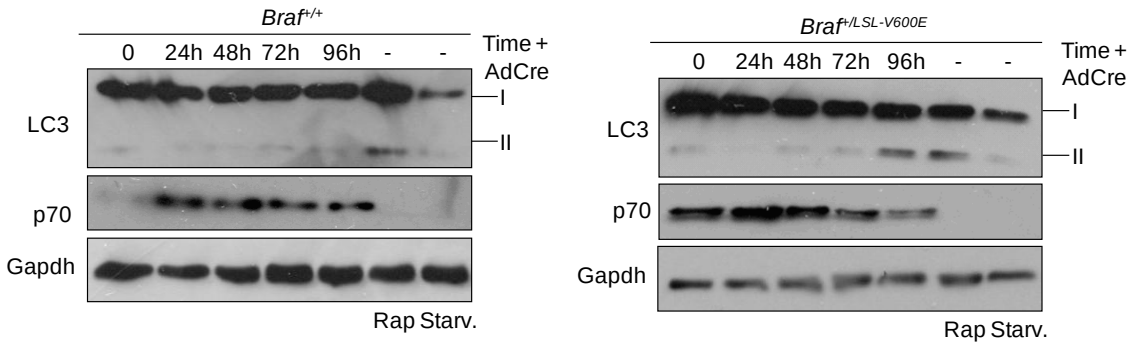

B

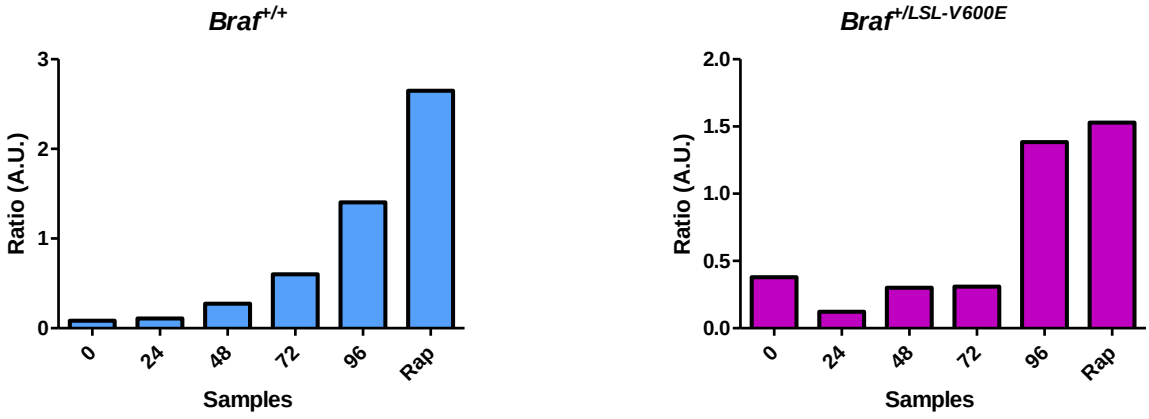

rapamycin was evaluated by the loss of phospho-p70 S6 kinase (Fingar et al. 2002). Interestingly, the cells that were nutrient-starved showed no LC3II accumulation and a reduction in LC3I protein levels. This might be explained by a particularly rapid turnover of LC3II in the autophagolysosome (Klionsky et al. 2008) (Section 1.3.3). In *Braf*$^{+/+}$ MEFs, a slight increase in LC3II conversion was observed at the later time points presumably because of the depletion of some nutrients from the media during the long incubation period (72-96 hours). In contrast, high levels of LC3II protein were detected at 96 hours post-AdCre infection in *Braf*^{V600E} MEFs. The progressive loss of p70 phosphorylation observed in ^{V600E}Braf samples suggests a reduction in mTOR activity at the later time points (Figure 4.6).

These results show that, independently of the incubation conditions for MEFs, the expression of endogenous ^{V600E}Braf results in an enhanced autophagic activity presumably through the modulation of mTOR.

4.3.7 Braf and Craf protein levels are rescued after autophagy inhibition in *Braf*^{V600E} MEFs

Recent evidence has showed that the autophagosome can be involved in the regulated degradation of fully functional proteins that act as part of signalling cascades. To investigate whether autophagy is involved in the degradation of Braf and Craf protein levels in *Braf*^{V600E} MEFs, autolysosome activity was impaired and the expression of these proteins was examined. To do this, *Braf*$^{+/LSL\text{-}V600E}$ MEFs were infected with AdCre for 96 hours. The cells were treated with two different concentrations of the lysosomal inhibitor chloroquine (CQ) for the last 6 hours. The cells were lysed with GLB buffer and the soluble and insoluble fractions were obtained. Samples were resolved by SDS-PAGE gel and immunoblotted for Braf, Craf, LC3, Gapdh and Actin proteins. As positive controls, *Braf*$^{+/+}$

MEFs were subjected to nutrient-starvation simultaneously to CQ treatment for the final 6 hours.

As shown in Figure 4.7, the expression of Braf^{V600E} caused an increase in autophagy levels as indicated by the accumulation of LC3II after CQ treatment. Although there is no accumulation of LC3II in *Braf*$^{+/+}$ MEFs after CQ exposure, a reduction in LC3I levels indicates that an increase in the rate of autophagosome formation and LC3II degradation is happening in these cells under starvation conditions. After *Braf*$^{+/+}$ MEFs were treated with a saturating concentration of CQ (100 μM), Braf protein levels were increased by ~1.23-fold and ~2.6-fold in the soluble and insoluble fraction, respectively. When *Braf*^{V600E} MEFs were treated with 100 μM CQ, approximately a 2.5-fold increase in Braf expression was observed in the soluble fraction while an increase of approximately 5-fold occurred in the insoluble fraction. In the case of Craf, no recovery was observed in any of the fractions for *Braf*$^{+/+}$ MEFs whereas *Braf*^{V600E} MEFs showed an augment of Craf expression in the soluble (~4.7-fold) and insoluble fraction (~2-fold).

Overall the data from Figure 4.7 shows that Braf and Craf can be degraded by starvation-mediated autophagy. Moreover, it shows that the levels of autophagy induced by the expression of endogenous ^{V600E}Braf are enough to contribute in the degradation of Braf and Craf.

4.3.8 Blockage of autophagy rescues CRAF protein levels in cells expressing ectopic ^{V600E}BRAF

In order to investigate whether autophagy is involved in the reduction of endogenous CRAF protein levels in cells expressing ectopic ^{V600E}BRAF, autophagy was blocked in these cells and the expression of BRAF and CRAF was examined. To do this, HEK293^{T}

Figure 4.7 Autophagy inhibition rescues Braf and Craf protein levels in *Braf^{V600E}* MEFs. (A) *Braf$^{+/LSL-V600E}$* MEFs were infected with AdCre for 96 hours. The *Braf^{V600E}* cells were treated with 50 μM or 100 μM chloroquine (CQ) for the final 6 hours whereas *Braf$^{+/+}$* cells were simultaneously nutrient-starved and treated with 50 μM or 100 μM chloroquine (CQ). Cells were lysed with GLB buffer and the soluble and insoluble fractions were prepared. Expression of Braf, Craf, LC3, Gapdh and Actin was analyzed by immunoblotting. **(B)** The X-ray films were scanned and the optical density (O.D.) of the bands was measured using Image J software. The optical density of the background was subtracted from every sample. The values plotted on the graphs correspond to the Braf/Gapdh or Craf/Gapdh ratio expressed in Arbitrary Units (A.U.) for the soluble fraction while Braf/Actin and Craf/Actin ratios are shown for the insoluble fraction samples. Data are representative of two experiments.

A

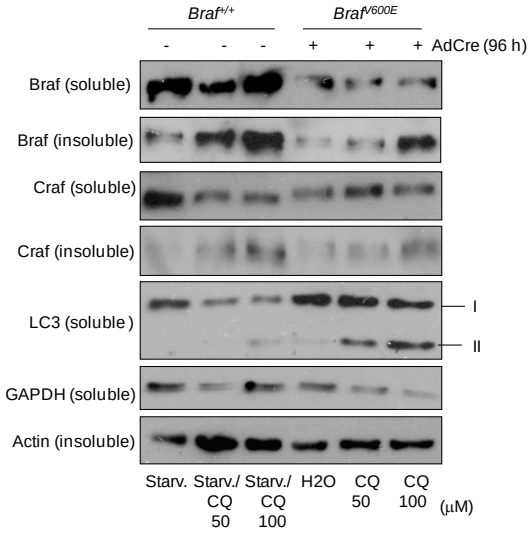

B

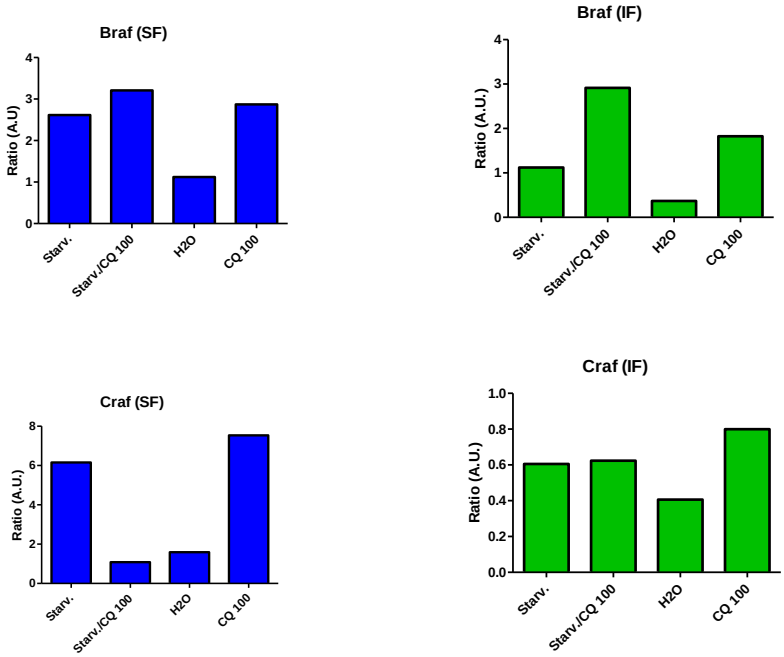

cells were transiently transfected with Myc-BRAF^{V600E} expression vector. Cells were either treated with BFA1 for the final 4 hours or CQ for the last 4 or 6 hours. Transfected HEK293^{T} cells were harvested 48 hours post-transfection. The cells were lysed with GLB buffer and the soluble and insoluble fractions were obtained. Samples were resolved by SDS-PAGE and immunoblotted for CRAF, LC3, GAPDH and ACTIN proteins.

As expected, after treatment with both lysosomal inhibitors, an increase in LC3II protein levels was observed (Figure 4.8). However, autophagy inhibition resulted in a slight accumulation of Myc-BRAF^{V600E} in the soluble (~1.5-fold) and insoluble (~1.5-fold) fractions. In the case of endogenous CRAF, no recovery of this protein was observed in the soluble fraction; however, a ~2-fold increase in its protein levels occurred in the insoluble fraction. All these changes were observed after the cells were treated with 100 μM CQ.

Overall, the data from Figure 4.7 and Figure 4.8 shows that autophagy inhibition causes an marked accumulation of Braf and Craf in *Braf^{V600E}* MEFs and a moderate recovery of ectopic BRAF and endogenous CRAF in HEK293^{T} cells.

4.4 Discussion

The results from the previous Chapter showed that the reduction in Braf and Craf expression in *Braf^{V600E}* MEFs cannot be explained by a down-regulation in the mRNA of these proteins. Thus, in order to examine the stability of BRAF and CRAF in the soluble fraction of ^{V600E}BRAF-expressing cells, the decay of these proteins was measured after the inhibition of general protein synthesis by emetine.

A half-life of approximately 8 hours was determined for Craf in *Braf$^{+/+}$* MEFs and Myc-BRAF^{WT}-transfected cells (Figure 4.1 and Figure 4.2) which agrees with previous reports

Figure 4.8 Ectopic ^{V600E}BRAF but not CRAF protein levels are rescued by autophagy inhibition in HEK293^{T} cells. (A) HEK293^{T} cells were transiently transfected with Myc-BRAF^{V600E} expression vector. For the last 4 hours, cells were treated with 0.4 μM or 0.8 μM bafilomycin A1 (BFA1) or 100 μM chloroquine (CQ) for the final 4 or 6 hours. After 48 hours of transfection, the cells were harvested with GLB lysis buffer and the soluble and insoluble fractions were prepared. Samples were electrophoresed on a SDS-PAGE gel and the protein levels of BRAF, CRAF, LC3, GAPDH and ACTIN were assessed by immunoblotting. **(B)** The X-ray films were scanned and the optical density (O.D.) of the bands was measured using Image J software. The optical density of the background was subtracted from every sample. The values plotted on the graph correspond to BRAF/GAPDH or CRAF/GAPDH ratio expressed in Arbitrary Units (A.U.) for the soluble fraction while BRAF/ACTIN and CRAF/ACTIN ratios are shown for the insoluble fraction samples. Data are representative of two experiments.

A

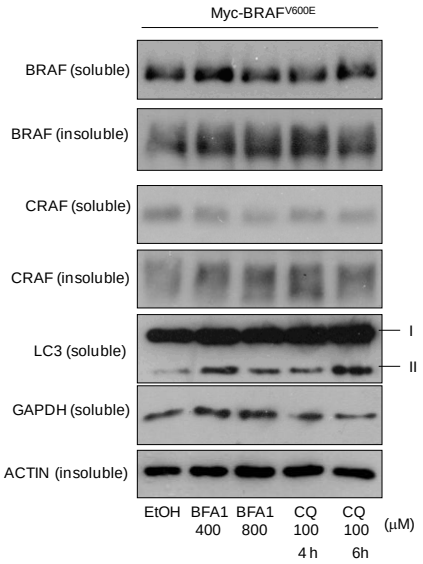

B

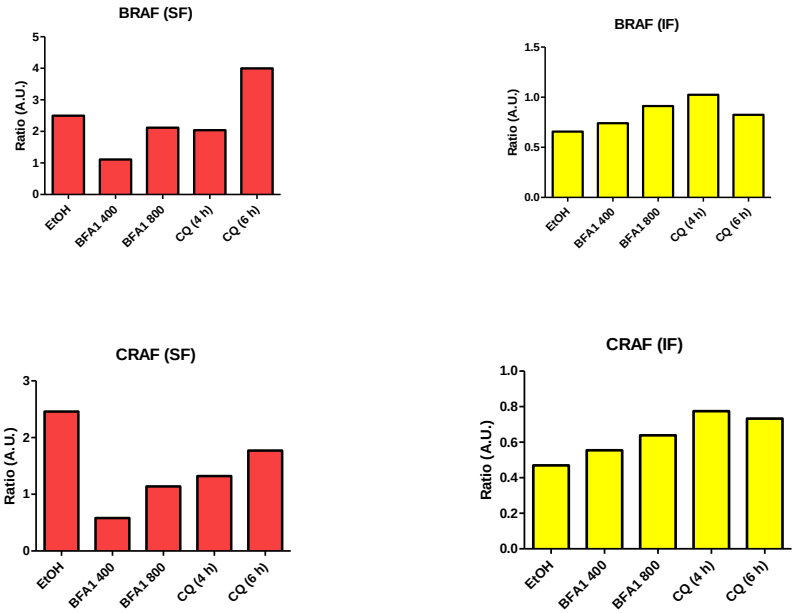

showing similar values (~7-8 hours) (Noble et al. 2008). Importantly, an approximate 2 hour reduction in the half-life of ectopic ^{V600E}BRAF was found in comparison to ectopic ^{WT}BRAF (Figure 4.1) while endogenous CRAF half-life was reduced by approximately 1 hour in cells expressing Myc-BRAF^{V600E} compared to Myc-BRAF^{WT} cells (Figure 4.1).

These results agree with the reduction in BRAF and CRAF protein levels in the soluble fraction from ^{V600E}BRAF-expressing cells observed in previous experiments. The 1 hour difference in the half-life of CRAF detected in HEK293^{T} cells transfected with Myc-BRAF^{V600E} was reproduced in *Braf^{V600E}* MEFs (Figure 4.1 and Figure 4.2). However, no difference in the half-lives of Braf was determined in *Braf$^{+/+}$* and *Braf^{V600E}* MEFs (Figure 4.2).This could be explained by the fact that endogenous Braf in *Braf^{V600E}* MEFs is a 50:50 mix of ^{WT}Braf and ^{V600E}Braf proteins which could increase the value of the half-life. In addition, due to time constraints, I was only able to do experiments once, so it is possible that other variables such as differences in the preparation of the soluble and insoluble fractions could influence the final result.

In the previous Chapter, we showed that the expression of endogenous or ectopic ^{V600E}BRAF caused a decrease in BRAF and CRAF protein levels in the soluble fraction simultaneous to an accumulation of these proteins in the insoluble fraction. Previous reports have shown that the treatment of cells with Hsp90 inhibitors such as Geldanamycin and/or proteasome inhibitors such as MG132 resulted in the accumulation of the target protein in the insoluble fraction. This suggests that the proteins rescued in this fraction could be unfolded and/or ubiquitylated. Based on the previous information, we investigated the possibility that an accelerated degradation of BRAF and CRAF by the proteasome could be the cause of the reduction in the expression of these proteins. For this purpose, the extent of the recovery in Braf and Craf protein levels after proteasome inhibition was compared between both types of MEFs. The results showed a greater accumulation of

Braf and Craf in *Braf*$^{+/+}$ MEFs after proteasome inhibition suggesting that the presence of ^{V600E}Braf does not promote an increase degradation of these proteins. However, it is also conceivable that another degradatory pathway such as autophagy could be involved in the turn-over.

The fact that Craf was only recovered after MG132 treatment but not after epoxomicin treatment in both types of MEFs suggests that a lysosome-based degradatory pathway could play an important role in the degradation of this protein. Studies on MG132 kinetics have revealed that, when this compound is added at the saturating concentration employed in our experiments, it can also inhibit the lysosomal proteases calpains and cathepsins (Letoha et al. 2005). This could also be the reason for the higher accumulation of Braf after MG132 treatment compared to epoxomicin-treated cells.

In agreement with the study by Noble et al. in 2009, the accumulation of Craf was observed in the insoluble fraction after proteasome inhibition. Also according to their observations, the protein was recovered without any sign of polyubiquitylation. This could be explained in both studies by the absence of proteasome and de-ubiquitylated enzymes (DUBs) inhibitors in the lysis buffer. Although the recovery of ubiquitylated ectopic CRAF has been observed in the insoluble fraction when co-transfected with HA-ubiquitin, the accumulation of ubiquitylated forms of endogenous Braf and Craf in this fraction have not been detected. Thus, we proposed that in future experiments aimed to analysed ubiquitylated proteins in an endogenous system such as MEFs, the addition of the previously mentioned inhibitors to the GLB buffer should be done.

In agreement with the study performed by Maddodi et al., we found that ^{V600E}BRAF overexpression increased autophagic flux in HEK293^{T} cells (Maddodi et al. 2010) (Figure 4.5). Moreover, our results showed that physiological levels of ^{V600E}Braf were also capable of increasing autophagic activity in MEFs (Figure 4.6). In order to inhibit autophagic activity,

two different compounds were employed: chloroquine (CQ) which blocks the acidification inside the lysosome and bafilomycin A1 (BafA1) which acts as a PI3K inhibitor. The starvation-mediated autophagy in *Braf*$^{+/+}$ MEFs and its subsequent inhibition resulted in the recovery of Braf and Craf suggesting that autophagy can be involved in the degradation of these proteins. The autophagic activity induced by ^{V600E}Braf expression and its subsequent inhibition also proved to be related to the recovery of Braf and Craf expression. However, in the experiment showed in Figure 4.7, it is no possible to compare the degradation rate of Braf and Craf between starved *Braf*$^{+/+}$ and *Braf*^{V600E} MEFs. The level of autophagy induced by starvation and that caused by the presence of ^{V600E}Braf are not the same. In order to compare the extent of the recovery in Braf and Craf expression after autophagy inhibition in Braf$^{+/+}$ and Braf^{V600E}, the former cells need to be incubated in non-starved conditions. The experts in the autophagy field have shown that LC3II is best solubilized in 1% SDS after heating compared to Triton-X. In base of this information, an increase recovery of the protein was expected in the insoluble fraction after autophagy inhibition. However, the data shows that in some cases the major accumulation can occurred in the soluble fraction. This also could explain the fact that the LC3-I is in a much higher concentration in respect to LC3-II.

A recovery of Myc-BRAF^{V600E} and endogenous CRAF was observed in HEK293^{T} cells after autophagy inhibition; however the extent of the recovery was lower compared to that in *Braf*^{V600E} MEFs. Because of ^{V600E}BRAF overexpression, a greater autophagic activity was expected in these cells compared to MEFs. However, in base of the extent of the recovery, it seems that lower levels of autophagic activity towards the RAF proteins are being induced in cells overexpressing ^{V600E}BRAF. Because the accumulation in ectopic ^{V600E}BRAF and endogenous CRAF after autophagy inhibition is moderate at least another experiment will be needed in order to confirm this recovery.

Overall, the data shows ectopic ^{V600E}BRAF is less stable than ectopic ^{WT}BRAF and that CRAF stability is reduced in the presence of endogenous or ectopic ^{V600E}BRAF. The experiments presented in this Chapter not only confirm the induction of high levels of autophagy by endogenous and ectopic ^{V600E}BRAF expression, but also show the accumulation of Braf and Craf in ^{V600E}Braf-expressing cells after autophagy inhibition. The fact that an increase recovery in Braf and Craf is observed in *Braf*$^{+/+}$ MEFs after proteasome inhibition and that higher levels of autophagy are observed in *Braf*^{V600E} MEFs suggests that autophagy could be the cause of the increased degradation of Braf and Craf in *Braf*^{V600E} MEFs. Although a recovery in these proteins was observed in cells expressing ectopic and endogenous Braf^{V600E}, more specialized experiments showing the interaction between Braf or Craf and the autophagosome components are needed. In the context of the observations generated in these two chapters, we propose that the ubiquitin-proteasome and autophagy pathways are able to downregulate BRAF and CRAF protein levels in order to modulate the activation of the ERK pathway and escape from a growth arrested state as discussed in section 3.4.

CHAPTER 5 Role of the ERK pathway in the regulation of BRAF and CRAF expression

5.1 Introduction

The spatiotemporal regulation of ERK has been recognized as a key issue for normal cellular growth (Lefloch, Pouyssegur & Lenormand 2008). Experimental evidence showing that the ERK pathway is able to regulate the activation of upstream members of the MAPK cascade through direct or indirect feedback loops has been generated (Ritt et al. 2010b, Courtois-Cox et al. 2006a, Dougherty et al. 2005, Brummer et al. 2003) (Section 1.4). In addition, several examples of ERK regulating the expression of proteins through the combined effect of post-translational modifications and the alteration of its transcription have also been found (DaSilva et al. 2006, Fueller et al. 2008, Okazaki, Sagata 1995). Such is the case for the negative regulator SPROUTY 2 (SPRY2). Phosphorylation of SPRY2 at Tyr55 upon EGFR activation has been shown to promote the binding of the E3-ubiquitin ligase c-Cbl resulting in its polyubiquitylation and proteasomal degradation (Fong et al. 2003). However, the phosphorylation of residues Ser112 and Ser121 on SPRY2 by ERK downstream effector, MNK1, have shown to antagonize the effect of Tyr55 phosphorylation, leading to the stabilization and accumulation of the protein (DaSilva et al. 2006). In addition, it has been demonstrated that *SPRY* gene expression is induced as a result of increased levels of phospho-ERK (Hanafusa et al. 2002, Ozaki et al. 2001). These data showed that ERK is not only able to promote SPRY2 accumulation by delaying its proteolytic degradation but also by enhancing its transcription. Another example of simultaneous transcriptional and post-translational control by ERK is the one represented by the transcription factor c-FOS (Murphy et al. 2002, Okazaki, Sagata 1995). It is known that the activation of ERK, leads to an increased expression of *c-FOS* mRNA, besides it

has also been reported that c-FOS can be phosphorylated by ERK and RSK1, resulting in an increased stability of the protein (Chen et al. 1996).

In order to examine if the transcriptional down-regulation of *Braf* and *Craf* (Section 3.3.6) or the partitioning of these proteins to the insoluble fraction (Section 3.3.4) in ^{V600E}Braf-expressing cells could be regulated by the Mek-Erk cascade or by Braf itself, in this chapter, cells were exposed to Mek and Braf inhibitors.

MEK inhibitors belong to a group of compounds identified as non-competitive inhibitors while BRAF inhibitors are ATP-competitive (Tsai et al. 2008a, King et al. 2006, Favata et al. 1998). The non-competitive inhibitors bind to sites different from those occupied by ATP or the correspondent substrate in the target molecule while the ATP-competitive inhibitors bind directly to the ATP pocket (Liu, Gray 2006). The ATP competitive inhibitors are classified into two groups: type I and type II. The difference between both groups is that the type I inhibitors bind to the ATP binding site when the kinase is in its active conformation whereas the type II inhibitors bind to the inactive conformation of the kinase therefore preventing its activation (Liu, Gray 2006).

To inhibit MEK-ERK, we used a potent selective compound: PD184352 (Sebolt-Leopold et al. 1999, Favata et al. 1998) (Section 1.7.1). PD184352 inhibits both MEK1 and MEK2 with an IC_{50} of 72 nM and 58 nM, respectively (Favata et al. 1998). The only known substrates for PD184352 are MEK1, MEK2 and MEK5 (Solit et al. 2006). However, the concentration of PD184352 needed for MEK5 inhibition is 50-fold more than that employed in the experiments presented in this chapter.

Although PLX4720 has been recognized as a highly specific and potent inhibitor of ^{V600E}BRAF (Section 1.7.1), other molecules have also shown promising results in pre-clinical studies (Nissan, Solit 2011b). This is the case for two recently discovered

molecules: SB-590885, which is a well-studied compound belonging to the next-generation of oncogene-specific drugs capable of inhibiting mutant BRAF but not from ^{WT}BRAF and its close analog 885-A (King et al. 2006). In this chapter, the inhibition of BRAF was achieved by treating the cells with 885-A. The small molecule SB-590885 belongs to the triarylimidazole class and has been classified as a type I inhibitor. The co-crystallization experiments of the ^{V600E}BRAF kinase domain and SB-590885 revealed that the indane oxime group of the compound formed strong interactions with the salt bridge of BRAF as well as the formation of hydrogen bonds between the SB-590885 molecule and the backbone amide of the activation loop in BRAF (King et al. 2006). In a study performed by King et al. in 2006, the reduction of ERK activity to its half (EC_{50}) after SB-590885 treatment of cancer cells containing ^{WT}BRAF was achieved with doses between 1.1-11 μM, whereas the EC_{50} value for cancer cell lines expressing ^{V600E}BRAF was within the range of 0.028 to 0.29 μM (King et al. 2006).

5.2 Aims

The aim of this chapter was to determine if the mechanism responsible for the reduction in BRAF and CRAF protein levels in ^{V600E}BRAF-expressing cells was activated by kinases downstream of MEK and whether it is dependent on BRAF kinase activity.

5.3 Results

5.3.1 Braf kinase inhibition increases the overall expression of Braf and accumulates Craf in the insoluble fraction from *Braf^{V600E}* MEFs.

In order to examine if the expression of Braf and Craf is dependent on Braf kinase activity, Braf was inhibited with the compound 885-A. To do this, *Braf$^{+/LSL\text{-}V600E}$* MEFs were infected

with AdCre and subsequently treated with 885-A for the last 24 or 72 hours before being harvested at 96 hours post-AdCre infection. MEFs were lysed with GLB buffer and the soluble and insoluble fractions were obtained. Samples were resolved by SDS-PAGE gel and immunoblotted for Braf, Craf, pErk, Gapdh and Actin proteins. As negative controls, *Braf*^{V600E} MEFs were treated for the last 72 hours with DMSO and harvested at 96 hours post-AdCre infection.

A decrease in Erk phosphorylation, proportional to the length of 885-A treatment, was observed in *Braf*^{V600E} MEFs as indicated by the densitometric analysis from Figure 5.1. A rescue in Braf expression in the soluble fraction occurred after 24 hours or 72 hours of 885-A exposure compared to the untreated sample. An accumulation in Braf protein levels was also observed in the insoluble fraction after 24 hours or 72 hours of 885-A treatment. In the case of Craf, no increase in its expression was observed in the soluble fraction after Braf inhibition; however, a recovery in Craf protein levels in the insoluble fraction was observed after 24 hours of 885-A exposure (Figure 5.1).

Overall, the data shows that the long-term inhibition of Braf in *Braf*^{V600E} MEFs results in the recovery of Braf and Craf expression. The distribution between the soluble and insoluble fractions differs somewhat between the two.

5.3.2 BRAF kinase inhibition rescues ectopic ^{V600E}BRAF and endogenous CRAF protein levels

In order to examine if BRAF kinase inhibition could rescue ectopic ^{V600E}BRAF and endogenous CRAF expression, GFP-BRAF^{V600E}–expressing cells were treated with the BRAF inhibitor, 885-A.

Figure 5.1 Braf kinase inhibition induces a recovery of Braf and Craf in *Braf^{V600E}* MEFs. (A) Schematic representation of the treatment regime with 885-A for *Braf^{V600E}* MEFs. **(B)** *Braf$^{+/LSL-V600E}$* MEFs were infected with AdCre and subsequently treated with 1μM 885-A for the last 24or 72 hours before being harvested at 96 hours post AdCre-infection. The inhibitor was re-added after 12 hours in the 24 hour-treated samples and every 24 hours in the 72 hour-treated samples. Cells were lysed with GLB buffer and the soluble and insoluble fractions were prepared. Expression of Braf, Craf, pErk, Gapdh and Actin was analyzed by immunoblotting. Data represents a single experiment.

A

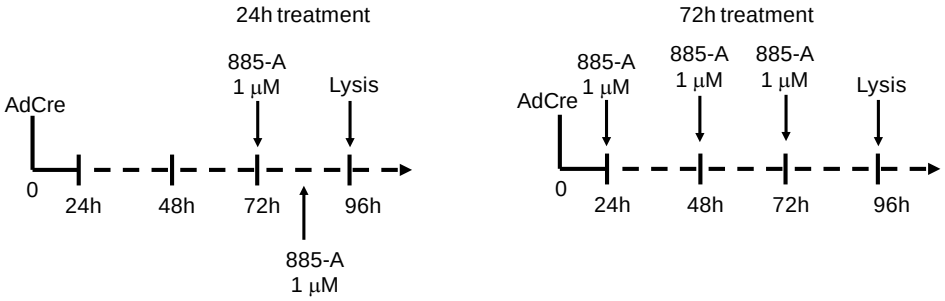

B

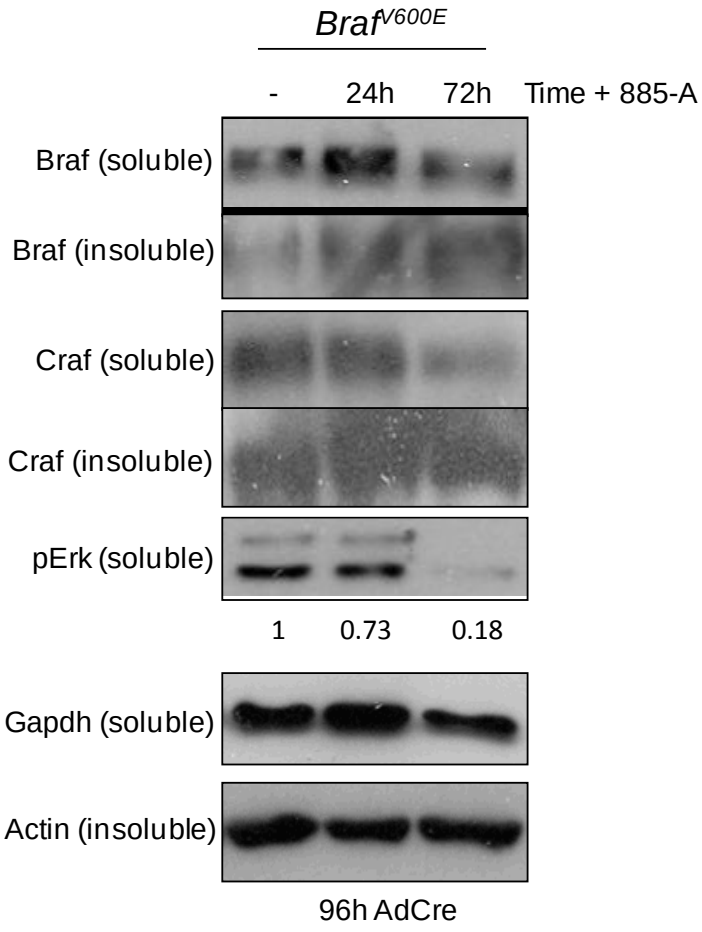

The compound was added to the cells for the last 24 or 36 hours. Cells were harvested 48 hours post-transfection with GLB lysis buffer and the soluble and insoluble fractions were obtained. The samples were subjected to western blot analysis with antibodies detecting BRAF, CRAF, pERK, GAPDH and ACTIN proteins.

The 885-A treatment caused a time-dependent reduction in phospho-ERK levels as indicated by the densitometric analysis in Figure 5.2. In agreement with the results obtained in *Braf*^{V600E} MEFs, an increase in ectopic ^{V600E}BRAF protein levels was observed in the soluble and insoluble fractions after 36 hours of 885-A exposure compared to the untreated cells. An accumulation of endogenous CRAF protein levels was also observed in the soluble fraction and insoluble fraction after 36 hours of 885-A treatment. Interestingly, after the cells were exposed to 885-A, a shift in the GFP-BRAF^{V600E} and endogenous CRAF bands towards a lower molecular weight was observed in the insoluble fraction.

The data from Figure 5.2 suggests that the long-term inhibition of BRAF results in the recovery of ectopic ^{V600E}BRAF and endogenous CRAF expression in both fractions. In addition, BRAF kinase inhibition resulted in a faster migration of ectopic ^{V600E}BRAF and endogenous CRAF indicating its involvement in post-translational events concerning these proteins.

5.3.3 Mek inhibition rescues the expression of Braf and Craf in *Braf*^{V600E} MEFs

In order to investigate if the recovery of Braf and Craf protein levels in *Braf*^{V600E} MEFs is due to the MEK/ERK pathway, *Braf*$^{+/LSL\text{-}V600E}$ MEFs were infected with AdCre and then treated with PD184352.

Figure 5.2 BRAF kinase inhibition accumulates ectopic ^{V600E}BRAF and endogenous CRAF in GFP-BRAF^{V600E}-expressing cells. (A) Schematic representation of the treatment regime with 885-A for GFP-BRAF^{V600E}-expressing cells. **(B)** HEK293^{T} cells were transiently transfected with GFP-BRAF^{V600E} expression vector. For the last 24 or 36 hours, cells were treated with DMSO or 1μM 885-A (885A). The inhibitor was re-added every 12 hours until cells were harvested at 48 hours post-transfection. HEK293^{T} cells were lysed with GLB buffer and the soluble and insoluble fractions were prepared. Expression of BRAF, CRAF, pERK, GAPDH and ACTIN was analyzed by immunoblotting. Data are representative of two experiments.

A

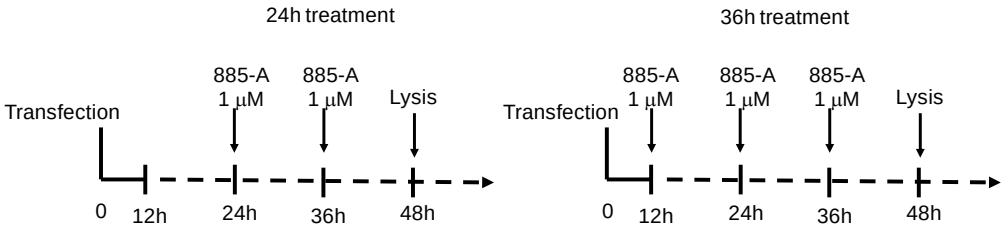

B

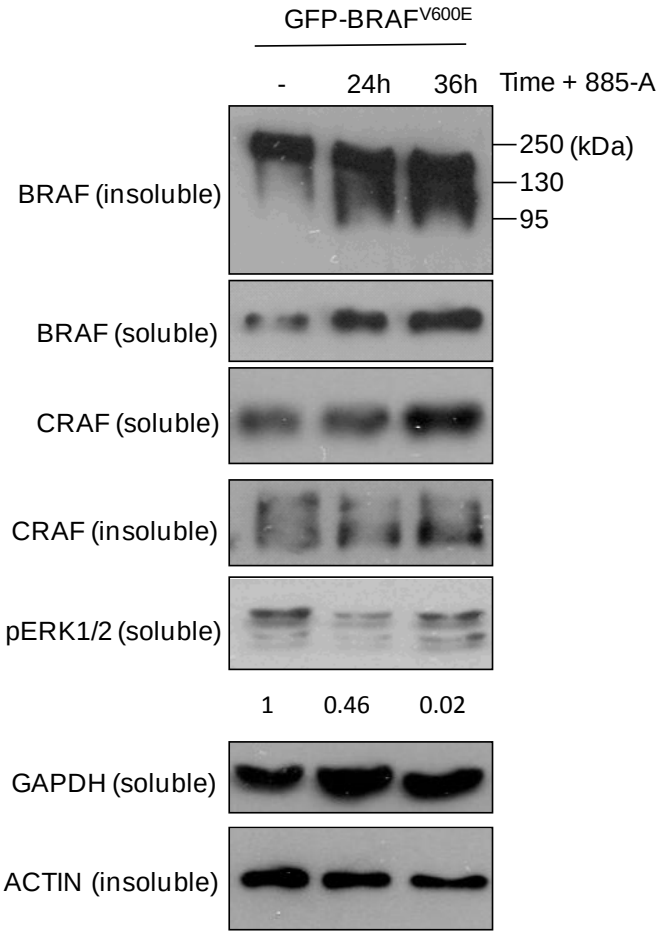

The inhibitor was added to the cells for the last 24 before being harvested at 72 and 96 hours post-AdCre infection. The cells were harvested with GLB lysis buffer and the soluble and insoluble fractions were obtained. The samples from both fractions were resolved by SDS-PAGE gel, transferred to membranes and immunoblotted with Braf, Craf, pErk, Erk2 and Actin antibodies.

As shown in Figure 5.3, Erk phosphorylation was considerably reduced after PD184352 treatment in all samples. An accumulation of Braf protein levels in the soluble fraction was observed after 24 hours of Mek inhibition at 72 and 96 hours post-AdCre infection. Also, an increase in Braf expression occurred in the insoluble fraction after 24 of PD184352 exposure at both time points. In the case of Craf, a reduction in its protein levels was observed in the soluble fraction after 24 hours of PD184352 exposure while a significant accumulation of this protein occurred in the insoluble fraction.

Overall, the data from Figure 5.3 shows that the blockage of the Erk pathway at the level of Mek recovers Braf and Craf protein levels in *Braf*^{V600E} MEFs suggesting that the expression of both proteins in the presence of ^{V600E}Braf is controlled by the ERK pathway. The further reduction of Craf protein levels in the soluble fraction and its accumulation in the insoluble fraction after Erk pathway inhibition, suggest that there might be a slightly different regulatory mechanism for Craf than Braf.

Figure 5.3 Mek inhibition induces the recovery of Braf and Craf in *Braf^{V600E}* MEFs. (A) Schematic representation of the treatment regime with PD184352 for *Braf^{V600E}* MEFs. **(B)** *Braf$^{+/LSL-V600E}$* MEFs were infected with AdCre and treated with 1μM PD184352 for the last 24 or 72 hours before being harvested at 96 hours post AdCre-infection. The inhibitor was re-added after 12 hours in the 24 hour-treated samples and every 24 hours in the 72 hour-treated samples. Cells were lysed with GLB buffer and the soluble and insoluble fractions were prepared. Expression of Braf, Craf, pErk, Erk2 and Actin was analyzed by immunoblotting. Data are representative of two experiments.

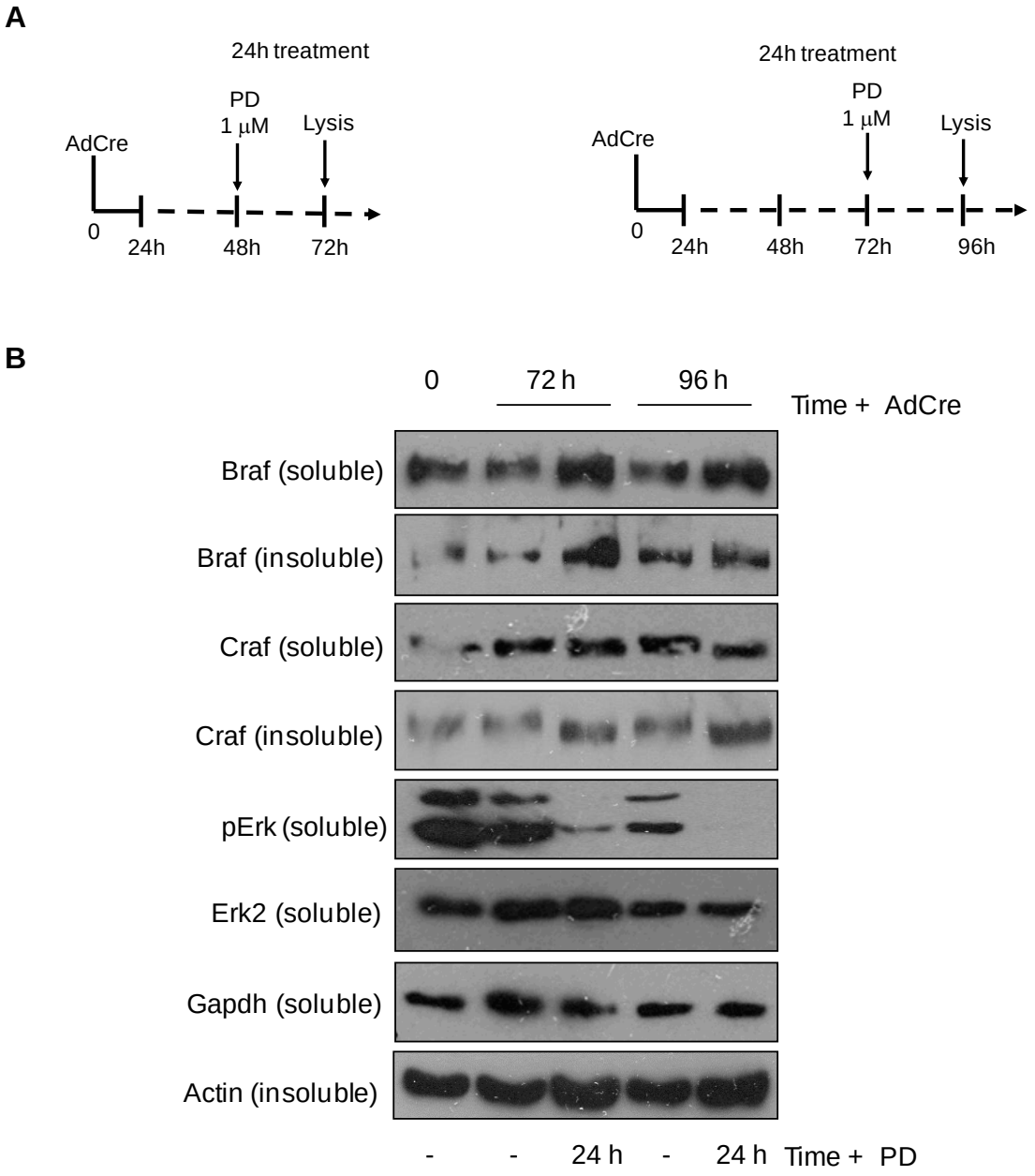

5.3.4 MEK inhibition causes a reduction in ectopic ^{V600E}BRAF and endogenous CRAF protein levels

In order to investigate if the expression of ectopic ^{V600E}BRAF and endogenous CRAF is regulated via the MEK-ERK axis activation, the MEK kinase activity was blocked by PD184352 treatment. HEK293^{T} were transiently transfected with GFP-BRAF^{V600E} expression vector and subsequently treated with PD184352 for the last 24 or 36 hours (Figure 5.4). The cells were harvested 48 hours post-transfection with GLB lysis buffer and the soluble and insoluble fractions were obtained. The samples were subjected to western blot analysis with antibodies detecting BRAF, CRAF, pERK, GAPDH and ACTIN proteins.

As shown in Figure 5.4, an evident reduction in phospho-ERK levels was detected after PD184352 treatment in cells expressing ectopic ^{V600E}BRAF. In contrast to BRAF kinase inhibition, the blockage of MEK resulted in a reduction in ectopic ^{V600E}BRAF protein levels in the soluble and insoluble fractions. The inhibition of MEK also reduced CRAF expression in the soluble fraction after 24 or 72 hours of PD184352 exposure. In addition, a decrease in endogenous CRAF expression occurred in the insoluble fraction after 24 and 72 hours of PD184352 treatment, respectively. In contrast to *Braf*^{V600E} MEFs, no changes in the electrophoretic migration of GFP-BRAF^{V600E} or endogenous CRAF were detected after MEK inhibition.

Overall, the data from Figure 5.4 shows that the inhibition of downstream kinases of MEK results in a further loss of ectopic ^{V600E}BRAF and endogenous CRAF expression in both fractions indicating that the blockage of the ERK pathway at the level of MEK has different effects to those of BRAF kinase inhibition in cells overexpressing ^{V600E}BRAF.

Figure 5.4 MEK inhibition decreases ectopic ^{V600E}BRAF and endogenous CRAF expression in the HEK293^{T} cells. (A) Schematic representation of the treatment regime with PD184352 for GFP-BRAF^{V600E}-expressing cells. **(B)** HEK293^{T} cells were transiently transfected with GFP-BRAF^{V600E} expression vector. For the last 24 or 36 hours, cells were treated with DMSO or 1μM PD (PD184352). The inhibitor was re-added every 12 hours until cells were harvested at 48 hours post-transfection. HEK293^{T} cells were lysed with GLB buffer and the soluble and insoluble fractions were prepared. Expression of BRAF, CRAF, pERK, GAPDH and ACTIN was analyzed by immunoblotting. Data are representative of two experiments.

A

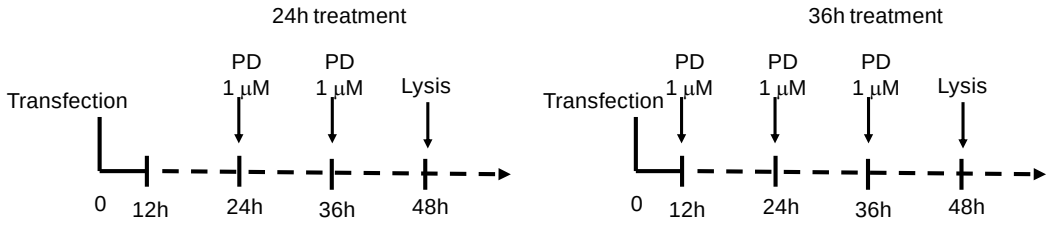

B

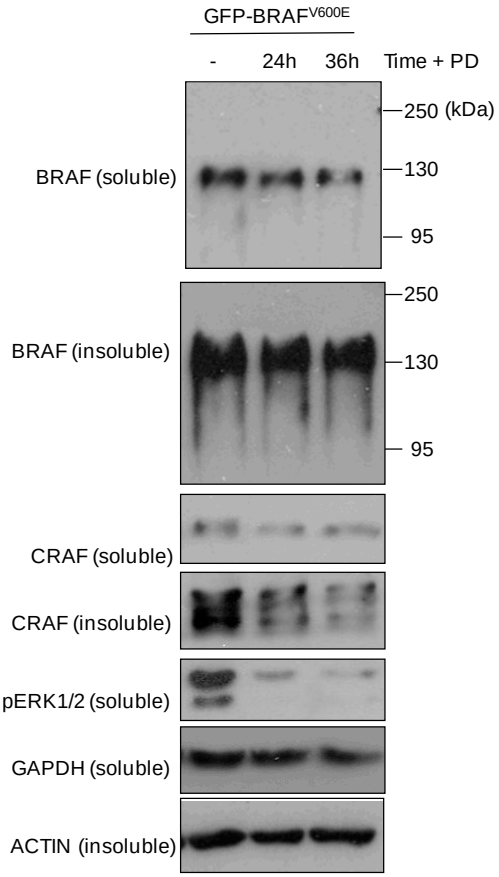

5.4 Discussion

In this Chapter an investigation was performed as to whether the reduction in BRAF and CRAF protein levels in ^{V600E}BRAF-expressing cells depends on BRAF kinase activity or on the activation of the MEK/ERK pathway. To do this, *Braf*^{V600E} MEFs and HEK293^{T} cells expressing ectopic ^{V600E}BRAF were treated with BRAF (885-A) or MEK (PD184352) kinase inhibitors. Results show that the long-term inhibition of Braf kinase activity in both *Braf*^{V600E} MEFs and Myc-BRAF^{V600E} cells rescued BRAF and CRAF expression. There was some variability as to whether the rescue occurred in the soluble or insoluble fractions but overall both proteins were rescued to some extent. In addition, faster electrophoretic migration of BRAF and CRAF was often observed, particularly in the insoluble fraction.

The inhibition of BRAF was not entirely mirrored by the inhibition of Mek. When Mek kinase activity was inhibited in *Braf*^{V600E} MEFs, an accumulation of Braf and Craf was observed (Figure 4.3). However, in the case of Myc-BRAF^{V600E}-transected cells, PD184352 treatment resulted in a decrease in ectopic ^{V600E}BRAF and endogenous CRAF expression in both fractions with no apparent changes in the electrophoretic migration of the proteins (Figure 4.4). The cause of this behavior is not entirely clear; however, it is possible that the intensity of ERK activation resulting from the overexpression of oncogenic BRAF and its subsequent suppression by PD184352 generates a different cellular response to that generated by the level of Erk activity in cells expressing physiological levels of ^{V600E}Braf. It is also conceivable that in cells overexpressing ^{V600E}BRAF, the reduction of ectopic ^{V600E}BRAF and endogenous CRAF depends directly on oncogenic BRAF and not on downstream kinases of MEK. In support of this view, it has been shown that not only MEK but also CRAF can be phosphorylated by BRAF (Garnett et al. 2005a, Alessi et al. 1994a, Papin et al. 1995). Moreover, it has been probed that mutant forms of BRAF bind to CRAF which results in the phosphorylation of residues T491 and S494 in the activation segment

of the latter protein (Rushworth et al. 2006a, Garnett et al. 2005c). Also, Stephens et al. identified some *in vitro* autophosphorylation sites in BRAF which included residues Thr372 and Ser366; however, the phosphorylation of these sites *in vivo* was not proven (Stephens et al. 1992). Thus, it is possible that the direct phosphorylation of CRAF by BRAF or any identified BRAF autophosphorylation sites could play a role in the protein processing of CRAF/BRAF as observed here. This is investigated further in chapter 6.

The fact that Braf or Mek inhibition in *Braf*^{V600E} MEFs had the same effect in Braf and Craf expression agrees with the results of various microarray studies addressing transcriptional changes in ^{V600E}BRAF melanoma cells after the exposure to BRAF or MEK inhibitors (Pratilas et al. 2009, Nazarian et al. 2010, Joseph et al. 2010, Packer et al. 2009). In these studies, ^{V600E}BRAF melanoma cells were exposed to these inhibitors for short term (2 hours) or long term (24 hours) treatments. Microarray analysis of gene expression of the treated cells showed that the blockage of BRAF or MEK resulted in similar transcriptional profiles in cells expressing physiological levels of ^{V600E}BRAF (Joseph et al. 2010, Packer et al. 2009) indicating that transcriptional control by ^{V600E}BRAF is mediated solely by the MEK/ERK pathway. These groups observed that short-term inhibition of BRAF or MEK mainly caused the down-regulation of genes that belong to negative feedback responses such as DUSP6, SPRY2 and SPRY4 whereas the long-term inhibition of these kinases, resulted in the decreased expression of transcription factors or co-activators such as EGR1, ETV1, ETV5, IER3 and FOSL1 (Joseph et al. 2010, Packer et al. 2009).

The results presented in this Chapter showed another difference between *Braf*^{V600E} MEFs and cells expressing ectopic ^{V600E}BRAF in response to BRAF/MEK inhibitors: the pattern of accumulation of Craf. The fact that Craf recovery was observed only in the insoluble fraction but not in the soluble fraction of *Braf*^{V600E} MEFs after Braf/Mek inhibition may suggest that the regulation of Craf in these cells may be slightly different compared to

Myc-BRAF^{V600E}-transfected cells. It is possible that the blockage of the ERK pathway activation could inhibit Braf and Craf degradation which depending on their ubiquitylated or autophagosome-bounded state, accumulates preferentially in the soluble or insoluble fraction.

Overall, the data presented in this Chapter shows that the inhibition of the Erk pathway at the level of Braf or Mek in *Braf^{V600E}* MEFs rescues Braf and Craf protein levels indicating that the control of the expression of these proteins by ^{V600E}Braf is mediated by the Mek/Erk pathway. However, due to differences in the distribution of Braf and Craf between the soluble and insoluble fractions after Braf or Mek inhibition, the mechanism regulating the expression of Braf and Craf may vary. In the case of cells over-expressing ectopic ^{V600E}BRAF, the inhibition of BRAF or MEK has different effects suggesting that ^{V600E}BRAF may regulate its own expression and that of endogenous CRAF through MEK-independent pathways.

CHAPTER 6 Analysis of post-translational modifications in ^{V600E}BRAF and CRAF

6.1 Introduction

Multiple consensus motifs for serine/threonine and tyrosine kinases have been localized in the RAF proteins. The phosphorylation of these residues can lead to the activation or inhibition of the RAF isoforms (Guan et al. 2000, Ritt et al. 2010b, Dougherty et al. 2005, Brummer et al. 2003). Although some of these residues are conserved among the three RAF isoforms, it has been shown that the great majority are unique to one of the RAF proteins. Such is the case of the negative regulation of BRAF and CRAF by AKT. The latter has been shown to phosphorylate BRAF on Ser365 and CRAF on Ser259, which is the equivalent residue to Ser365 in BRAF (Zimmermann, Moelling 1999, Guan et al. 2000). However, AKT has also been found to phosphorylate BRAF at Ser428, a site which is unique to BRAF (Guan et al. 2000)(Guan et al. 2000). The phosphorylation of either Ser365 or Ser428 results in a similar reduction of BRAF kinase activity (Guan et al. 2000). Other example of a non-conserved regulatory phosphorylation particular to a RAF isoform is Ser499 in CRAF. This residue, which is conserved in CRAF and BRAF but not in ARAF, has been found phosphorylated only in CRAF by PKCα (Kolch et al. 1993). The phosphorylation of Ser499 has been shown to increase the kinase activity of this protein (Kolch et al. 1993).

The regulation of BRAF or CRAF activation by ERK has been shown to occur through the phosphorylation of non-equivalent residues in both proteins (Ritt et al. 2010b, Dougherty et al. 2005, Brummer et al. 2003). In BRAF, the phosphorylation of residues Ser151, Thr401, Ser750 and Ser753 by ERK prevents the interaction of BRAF with RAS resulting in the inactivation of the protein, while in CRAF, the phosphorylation of Ser29, Ser43, Ser289,

Ser296, Ser301 and Ser642 by ERK leads to the same effect (Ritt et al. 2010b, Dougherty et al. 2005).

The addition of a phosphate group to a serine, threonine or tyrosine residue can also have indirect consequences on the stability of a target protein. Many examples of proteins whose accumulation or degradation has been found to be regulated by single or multiple phosphorylations have been reported (Fueller et al. 2008, Okazaki, Sagata 1995, Su et al. 2011b, Ley et al. 2003a). It has been demonstrated that the phosphorylated residues within the PEST motifs offer a binding site to the SH2 domain of the E3-ubiquitin ligase. The association of the E3-ubiquitin ligase to its substrate allows the transference of ubiquitin moieties from an E2-ubiquitin conjugating enzyme (Fuchs, Spiegelman & Kumar 2004b, Wong et al. 2001). Importantly, the creation of an E3-ligase binding site through phosphorylation can also occur outside of the PEST motif (Hershko, Ciechanover 1998). An example of a protein whose phosphorylation enhances its interaction with an E3 ligase is AKT, in which the phosphorylation of Thr308 by PDK1 and Ser473 by mTORC2, expose a potential recognition motif for the E3-ubiquitin ligase CHIP (Su et al. 2011a)(Su et al. 2011a).

To investigate the possibility that BRAF and CRAF expression could be regulated by a mechanism involving its phosphorylation and ubiquitylation, qualitative mass spectrometry analysis using liquid chromatography (LC-MS/MS) was performed. Because of the low cellular abundance of most of the RAF kinases, ^{V600E}BRAF and CRAF had to be overexpressed and then enriched through immunoprecipitation techniques in order to reach the analytical sensitivity needed for mass spectra detection. For this purpose, the GFP-tagged version of the proteins was transiently expressed in HEK293^{T} cells and subsequently isolated by using the GFP-trap system (Section 2.3.2.1).

6.2 Aims

The aim of this chapter was to determine by LC-MS/MS the phosphorylations and ubiquitylations in ^{V600E}BRAF and CRAF when co-expressed with Myc-BRAF^{V600E}. We were also interested to examine whether the partitioning of ^{V600E}BRAF and CRAF between the soluble and insoluble fractions was associated with specific post-translational events.

6.3 Results

6.3.1 Increased accumulation of ectopic ^{WT}CRAF in the insoluble fraction when co-expressed with ectopic ^{V600E}BRAF

In order to confirm that the overexpression of CRAF and ^{V600E}BRAF leads to the same phenotype as observed with endogenous CRAF, HEK293^{T} cells were transiently co-transfected with Myc-BRAF^{V600E} and GFP-CRAF^{WT}. After 48 hours of transfection, cells were lysed with GLB buffer and the soluble and insoluble fractions were obtained. Samples were resolved by SDS-PAGE and immunoblotted for Myc, CRAF, GAPDH and ACTIN proteins.

As shown in Figure 6.1, the overexpression of ^{V600E}BRAF or ^{WT}CRAF alone resulted in the accumulation of both proteins in the insoluble fraction. Although the co-expression of ectopic ^{V600E}BRAF and ^{WT}CRAF did not show a reduction in GFP-CRAF^{WT} protein levels in the soluble fraction, a greater accumulation of GFP-CRAF^{WT} protein was observed in the insoluble fraction compared to cells transfected only with GFP-CRAF^{WT}. Low and high-molecular-weight forms of ectopic ^{WT}CRAF were observed in the insoluble fraction of both samples; however, a larger amount of these forms of ectopic ^{WT}CRAF were found in the sample co-transfected with Myc-BRAF^{V600E} and GFP-CRAF^{WT}.

.

Figure 6.1 Co-expression of Myc-BRAF^{V600E} and GFP-CRAF^{WT} induces the accumulation of ectopic ^{WT}CRAF in the insoluble fraction. HEK293^{T} cells were transfected with Myc-BRAF^{V600E} or GFP-CRAF^{WT} or both expression vectors. The cells were harvested 48 hours post-transfection with GLB buffer and the soluble and insoluble fractions were obtained. Expression of Myc, CRAF, GAPDH and ACTIN was analyzed by immunoblotting.

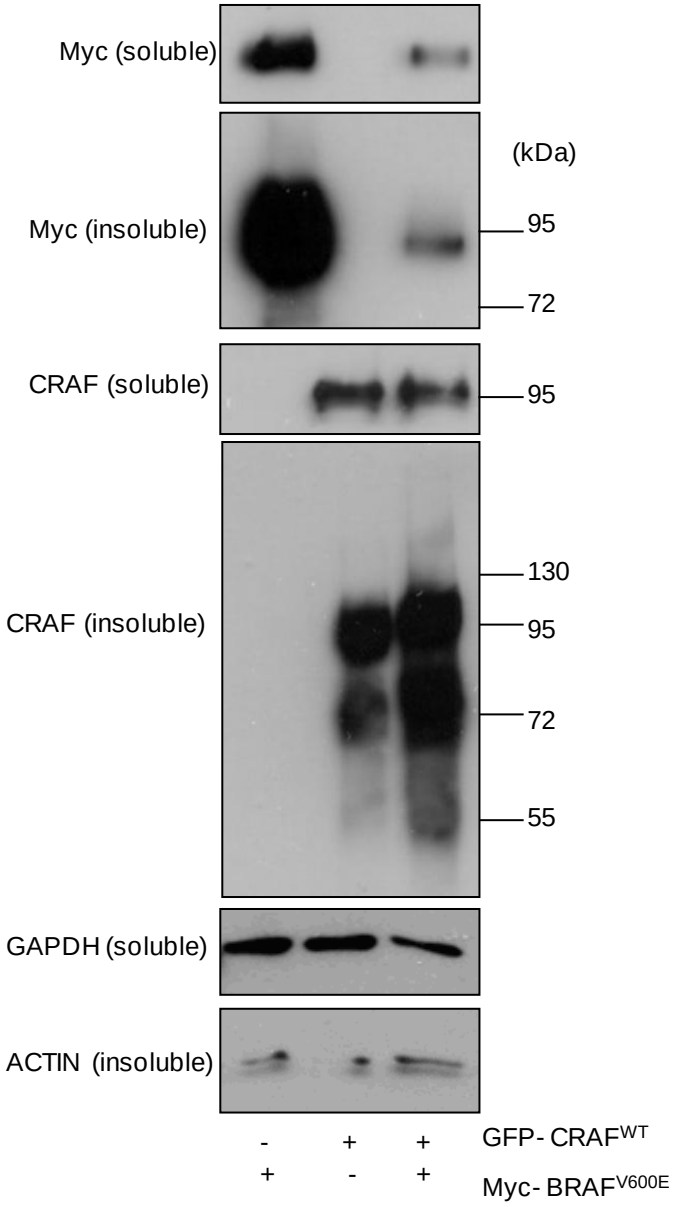

Overall, the data from Figure 6.1 shows that, in the presence of ectopic ^{V600E}BRAF, an increased accumulation of ectopic ^{WT}CRAF is observed in the insoluble fraction occurs. The presence of ectopic ^{WT}CRAF in this fraction is presumably linked with its post-translational modification and degradation as indicated by the high and low-molecular-weight-products.

6.3.2 LC-MS/MS strategy

In order to identify the post-translational modifications that characterised ectopic ^{V600E}BRAF and ^{WT}CRAF, liquid chromatography-mass spectrometry analysis (LC-MS/MS) was performed. Cells expressing only GFP-BRAF^{V600E}, GFP-CRAF^{WT} or co-expressing Myc-BRAF^{V600E} and GFP-CRAF^{WT}, were lysed 48 hours post-transfection with GLB buffer and the soluble and insoluble fractions were obtained. Each fraction was incubated with agarose beads coupled to GFP antibodies. After the fused GFP proteins were bound to the GFP-antibodies, the beads were centrifuged and subsequently boiled under denaturing conditions. The eluted GFP-fused proteins were electrophoresed on a SDS-PAGE gel and stained with Coomassie blue (Figure 6.2). The areas of the gel corresponding to the molecular weight of GFP-BRAF^{V600E} or GFP-CRAF^{WT} (~130 and 105 kDa, respectively) were excised from the gel as indicated by the red dotted lines (Figure 6.2). Importantly, an upper area of approximately 80 kDa was included when the main bands were cut out from the gels; however, the region below the main band, which contained the low molecular weight products, was not excised and therefore not included in the LC-MS/MS analysis. The gel fragments were digested with trypsin or GluC/LysC proteases. The resulting peptides were analyzed by LC-MS/MS with precursor of 79 scanning as described in section 2.3.2.3. The raw MS/MS data from the mixture of peptides was compared against amino acid sequence databases using the MASCOT algorithm.

Figure 6.2 Purification of ectopic ^{V600E}BRAF and ^{WT}CRAF for LC-MS/MS analysis HEK293^{T} cells were transfected with GFP-BRAF^{V600E}, GFP-CRAF^{WT} or both expression vectors. After 48 hours of transfection, the cells were lysed with GLB buffer and the soluble and insoluble fractions were obtained. Each fraction was incubated with GFP-coupled beads in order to isolate the fused GFP proteins. After the elution of the GFP fused proteins from the beads, the proteins were separated by SDS-PAGE gel and analyzed by western blot. The excision of the sections in the gel corresponding to the molecular weight of GFP-BRAF^{V600E} and GFP-CRAF^{WT} was followed by in-gel digestion with the correspondent protease. The resulting peptides were separated by liquid chromatography and analyzed by mass spectrometry.

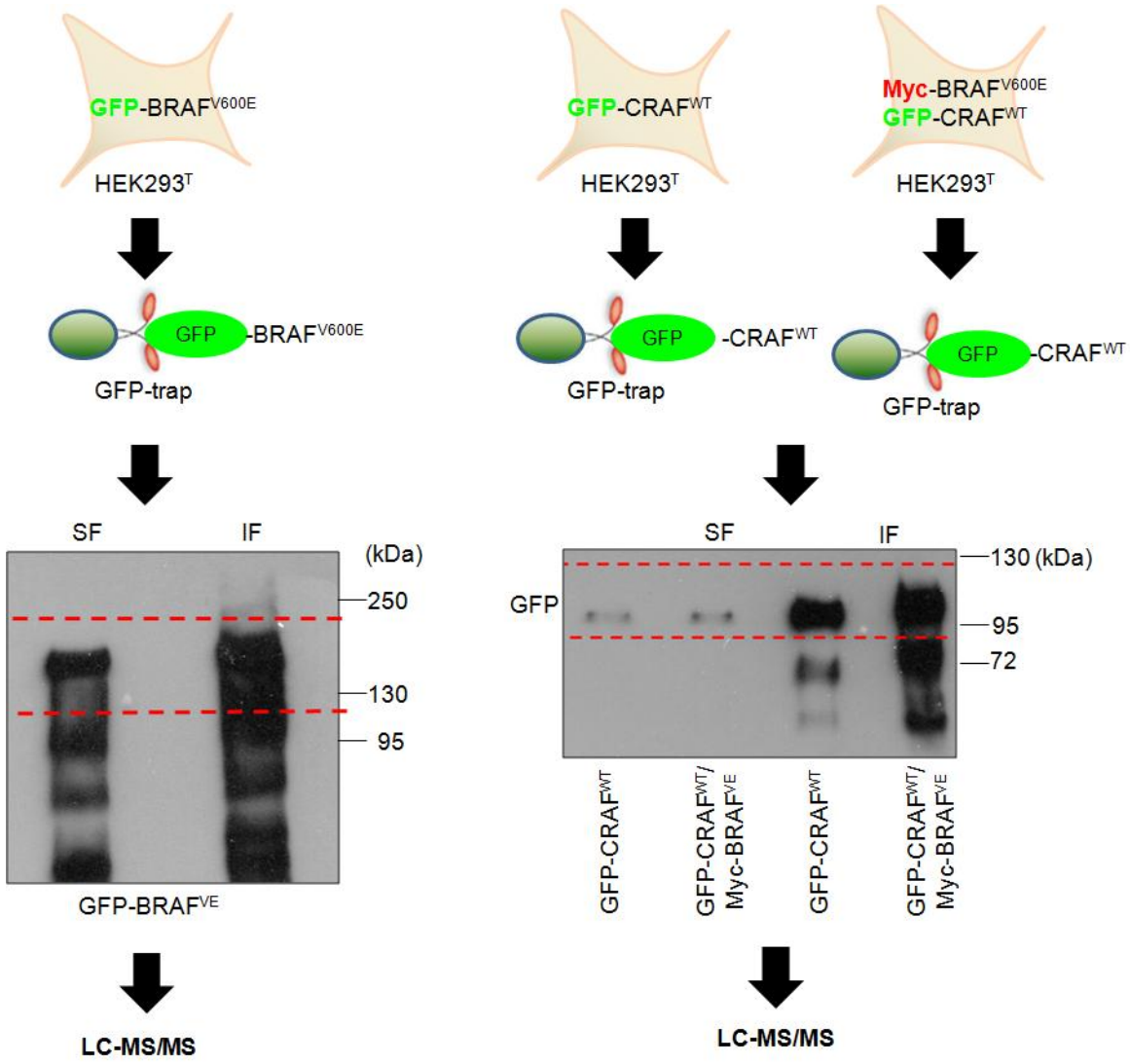

6.3.3 Identification of phosphorylated residues in ectopic ^{V600E}BRAF

Trypsin is a protease frequently employed in mass spectrometry analysis to convert protein mixtures into peptide populations. This enzyme is known to specifically cleave at the carboxyl side of arginine and lysine residues (Steen et al. 2006). In order to generate the short peptides for LC-MS/MS analysis, in-gel trypsin digestion was performed.

As shown in Figure 6.3, the trypsin digestion of GFP-BRAF^{V600E} showed a sequence coverage of approximately 44%. In order to improve the sequence coverage, the bands excised from the gel were digested in a second experiment with two other proteases: GluC and LysC. The cleavage of GFP-BRAF^{V600E} with GluC, which recognizes the glutamyl bonds, and LysC which detects Lys-Pro and Lys-Glu residues, resulted in a sequence coverage of approximately 45%. Although this value is very similar to that obtained after trypsin digestion, after combining the data generated in both experiments, a final coverage of 60% was achieved (Figure 6.3).

As shown in the table from Figure 6.4, the same phospho-sites that were detected in ectopic ^{V600E}BRAF isolated from the soluble fraction were present in ectopic ^{V600E}BRAF isolated from the insoluble fraction with the exception of a single phospho-site (Ser675) exclusive to the GFP-BRAF^{V600E} (IF) sample. Among the sites that were found phosphorylated in ectopic ^{V600E}BRAF, previously identified essential regulatory sites were observed. Such is the case of residues Ser446 and Ser447 of the N-region, in which phosphorylation is related to the maximal kinase activity of BRAF when compared with the other RAF isoforms (Mason et al. 1999a, Carey et al. 2003). The Ser729, that when phosphorylated is known to act as a 14-3-3 binding site playing an essential role in the modulation of BRAF catalytic activity, was also found phosphorylated (Fischer et al. 2009). The Ser151, T401, S750 and Ser753 have been found to be phosphorylated by ERK as part of its negative feedback on BRAF. The phosphorylation of these residues leads to the

Figure 6.3 Coverage of BRAF sequence after Trypsin and LysC/GluC digestion. (A) The regions of the BRAF sequence highlighted in yellow represent the peptides detected by the Orbitrap-Velos mass spectrometer after Trypsin or GluC/LysC digestion. The amino acids highlighted in green represent the modifications found in the protein such as phospho-serines, phospho-threonine, phospho-tyrosines, carbamidomethyl (C) and oxidised methionine (M). **(B)** The combination of the sequence coverage obtained after Trypsin and GluC/LysC digestion is also shown. The coverage is expressed as a percent of the total sequence.

A

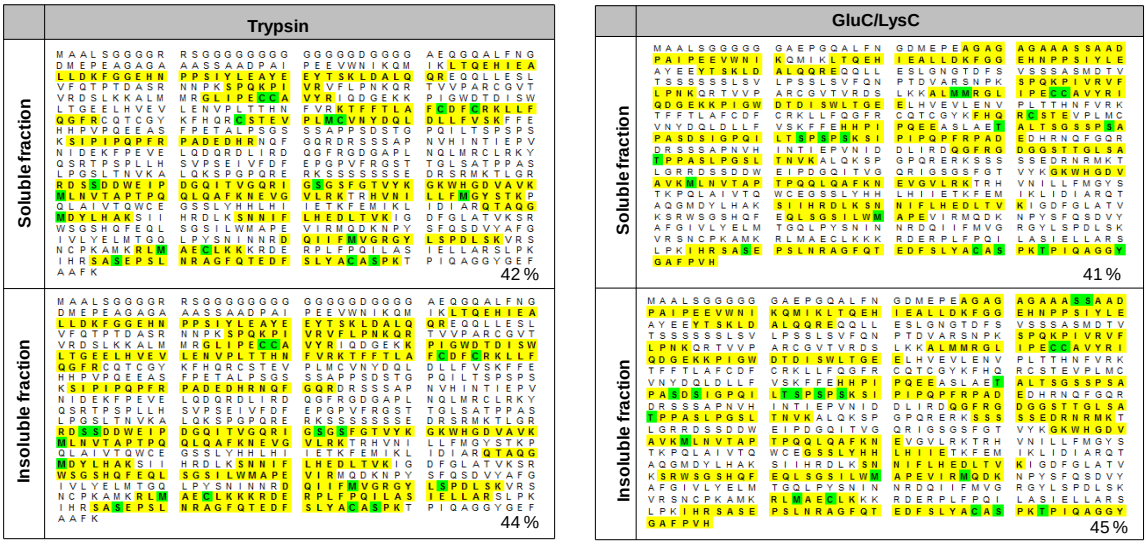

B

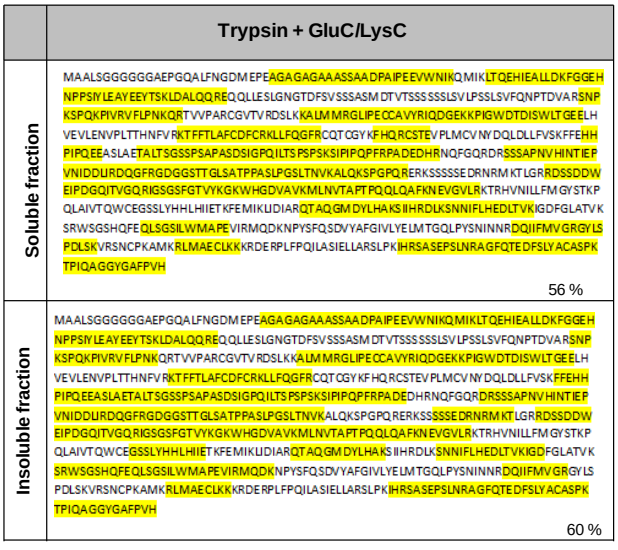

disruption of 14-3-3 and RAS binding to BRAF resulting in the inactivation of the latter. However, ^{V600E}BRAF has demonstrated to be resistant to this feedback as this protein is permanently active and not activated by RAS. Other phospho-sites such as Ser333, Ser335 and Ser399 have been reported in previous mass spectrometry analysis; however, the effect of the phosphorylation of these residues on BRAF activity is still unknown (Dephoure et al. 2008).

The phosphorylation of other important regulatory sites such as Ser599, Ser602 and Ser365 could not be verified because they were not included in the peptides generated after trypsin or GluC/LysC digestion (Zhang, Guan 2000, Fischer et al. 2009). As shown in the ribbon structure of ^{V600E}BRAF kinase domain (Figure 6.4) (Hatzivassiliou et al. 2010), the residue Ser675 is located at the C´terminus of the CR3 domain and apparently it is not located within interacting distance of any residues belonging to a key regulatory segment.

Overall, the data from Figure 6.4 shows that, although a large part of the BRAF sequence was not covered, many important positive and negative regulatory sites were found to be phosphorylated, which is indicative of the activity of the ^{V600E}BRAF protein. The data also shows that is the first time that the phosphorylation of Ser675 in ^{V600E}BRAF has been related to the partitioning of the protein to the insoluble fraction.

6.3.4 Identification of phospho-residues in ectopic ^{WT}CRAF

As shown in Figure 6.5, sequence coverage of approximately 80% was achieved after in-gel trypsin digestion of GFP-CRAF^{WT}. The presence of multiple phospho-sites in all samples was observed; however, an increased amount of post-translational modifications in GFP-CRAF^{WT} purified from the insoluble fractions was detected.

Figure 6.4 Phospho-sites detected by LC-MS/MS in GFP-BRAF^{V600E} isolated from the soluble and insoluble fractions. (A) Table showing the phosphorylated residues detected by LC-MS/MS analysis of GFP-BRAF^{V600E}. **(B)** Ion chromatograms showing the phosphorylation status of Ser675 in GFP-BRAF^{V600E} isolated from the soluble and insoluble fractions. The phosphorylated serine is indicated by a blue asterisk. **(C)** Ribbon diagram of the ^{V600E}BRAF kinase domain (449-720). The N-region is indicated in yellow; the glycine rich-loop is in blue; the activation segment, is shown in green and the catalytic loop is in red. The position of the residue Ser675 is shown in pink.

A

Residues	GFP-BRAF^{V600E} (SF)	GFP-BRAF^{V600E} (IF)
S151	P	P
S333	P	P
S335	P	P
S399	P	P
T401	P	P
S446	P	P
S447	P	P
S465	P	P
S675	Not P	P
S729	P	P
S750	P	P

P, phosphorylated residue; Not P, non-phopshorylated residue.

B

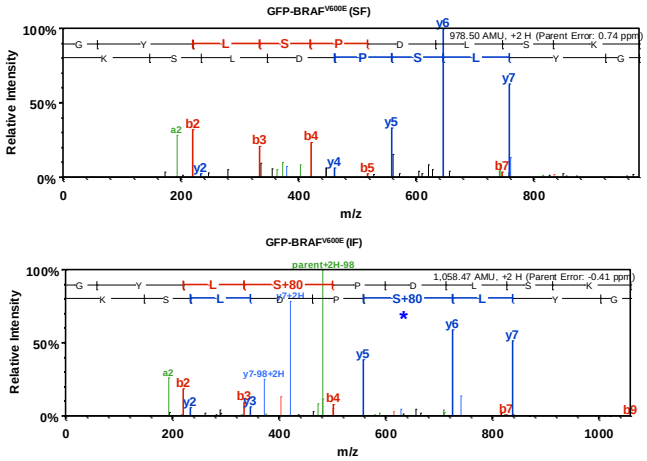

C

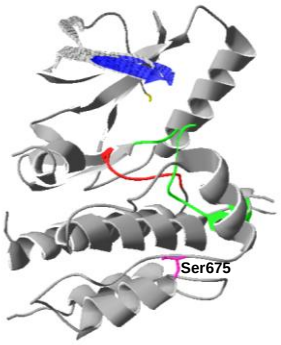

As shown in the table from Figure 6.6, the phospho-residues detected in GFP-CRAF^{WT} by our LC-MS/MS study can be classified in three different groups: i) Residues that were found phosphorylated in some samples but in others their phosphorylation status remained uncertain; ii) Residues that were found phosphorylated in all of the samples and iii) Residues that were found phosphorylated exclusively GFP-CRAF^{WT} isolated from the insoluble fraction.

The first group included residues Ser43 and Ser642 which were found phosphorylated in GFP-CRAF$^{WT/}$Myc-BRAF^{V600E} (SF), GFP-CRAF$^{WT/}$Myc-BRAF^{V600E} (IF) and in GFP-CRAF^{WT} (IF) samples; however, no conclusion could be obtained for the GFP-CRAF^{WT} (SF) sample. Although a phosphate group was detected in the peptides including Ser43 and Ser642 in the GFP-CRAF^{WT} (SF) sample, it was not possible for the software to localize the precise serine, threonine or tyrosine that was phosphorylated. This meant that all phosphorylatable residues within the peptides had the same probability of being phosphorylated. In a similar case, residues Ser296, Ser257 and Thr260 were found phosphorylated in some samples; however, the precise serine, threonine or tyrosine containing the phosphate group could not be determined. All residues included in this group (Ser43, Ser257, Thr260, Ser296 and Ser642) were not taken into account for future analysis because of the uncertainty related to their phosphorylation status.

The second group was integrated by phospho-residues Ser244, Ser301 and Ser621 which were detected in all samples suggesting that their phosphorylation is important for the kinase activity of CRAF. Although the role of Ser244 in CRAF activity has not been elucidated yet, this residue has been found phosphorylated during mitosis progression whereas Ser301 is one of the Erk-dependent feedback phosphorylation sites contributing to the down-regulation of CRAF signaling. The residue Ser621 has been shown to be phosphorylated by PKACα and CRAF itself acting as a binding site for the 14-3-3 protein

Figure 6.5 Coverage of CRAF sequence after trypsin digestion. The regions of the CRAF sequence highlighted in yellow represent the peptides detected by the Orbitrap-Velos mass spectrometer after trypsin digestion. The amino acids highlighted in green represent the modifications found in the protein such as phospho-serines, phospho-threonine, phospho-tyrosines, carbamidomethyl (C) and oxidised methionine (M). The coverage is expressed as a percent of the total sequence.

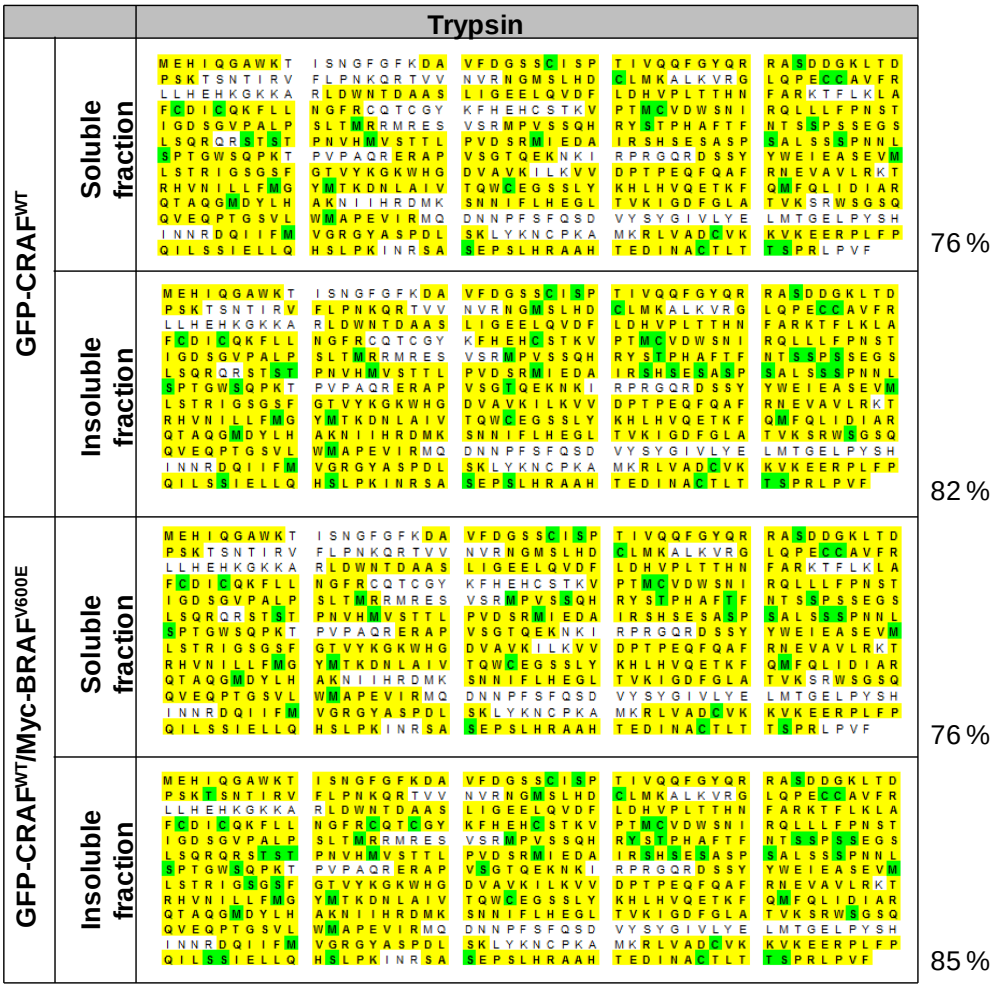

and ensuring CRAF correct folding (Dhillon et al. 2002a, Noble et al. 2008, Hekman et al. 2004).

The last group included residues Ser246, Ser247, Ser322, Ser357, Ser359 and Ser612 that were found phosphorylated only in GFP-CRAF^{WT} when isolated from the insoluble fraction suggesting that these post-translational modifications are required for the partitioning of the protein to the insoluble fraction. Importantly, the phosphorylation of Ser357 and Ser359 was exclusively found in the GFP-CRAF$^{WT/}$Myc-BRAF^{V600E} (IF) sample, which directly linked the phosphorylation of these residues to the presence of oncogenic BRAF. The effect that the phosphorylation of these residues has on CRAF activity has not been investigated. Previous reports in the literature have shown that Ser357 and Ser612 have been found phosphorylated in response to the T cell receptor (TCR) activation in Jurkat T cell leukemia cell line (Mayya et al. 2009) while the mutation of Ser257 and Thr260 has been shown to disrupt the binding of the 14-3-3 protein to CRAF resulting in the hyperactivation of the latter in Noonan syndrome (Molzan et al. 2010). In the case of Ser246, Ser247, Ser322 and Ser359, it is the first time that these residues have been found phosphorylated in a LC-MS/MS analysis.

Two particular cases were those represented by phospho-residues Thr54 and Ser29. The former residue was found phosphorylated in the GFP-CRAF^{WT}/Myc-BRAF^{V600E} (IF) sample; however, the peptide containing this residue was lost in the other samples and consequently no information could be obtained about its phosphorylation status. In the case of Ser29, it was found phosphorylated in all samples except in the GFP-CRAF^{WT} (SF) sample suggesting that the phopshorylation of this residue is not related to the partitioning of ectopic ^{WT}CRAF or to the presence of ectopic ^{V600E}BRAF.

Finally, our LC-MS/MS study showed that key regulatory residues in which phosphorylation depends CRAF activity such as Ser338 and Tyr341 within the N-region,

were not phosphorylated in any of the samples (Fabian, Daar & Morrison 1993, Mason et al. 1999a). The phosphorylation in residue Thr491, which is localized in the catalytic domain, was also missing in all the samples and the phosphorylation of residue Ser494, which was covered only in the GFP-CRAF^{WT} (IF) and GFP-CRAF^{WT}/Myc-BRAF^{V600E} (IF) samples, was found non-phosphorylated in these samples. These last two phospho-sites have also proved to be essential for CRAF activation (Wan et al. 2004a, Cutler et al. 1998, Tran, Wu & Frost 2005).(Hatzivassiliou et al. 2010)

The crystal structure of the CRAF kinase domain is shown in Figure 6.6 (Hatzivassiliou et al. 2010). However, because the structure of the CR1 and CR2 domains has not been resolved, only the phospho-residues localized within the CR3 domain were identified in the ribbon diagram. The residues Ser357 and Ser359 are localized inside the ATP pocket while Ser612 seem not to be localized within an interacting distance from any of the key regulatory segments.

Overall, the data from Figure 6.6 shows that well known inhibitory and activating phosphorylations in CRAF were detected by our LC-MS/MS study. The data also shows that the phosphorylation of residues Ser246, Ser247, Ser322, Ser357, Ser359 and Ser612 was exclusively observed in ectopic ^{WT}CRAF isolated from the insoluble fraction and therefore could be related to the partitioning of this protein in this fraction. Of these phospho-residues, only Ser357 and Ser359 were unique to ectopic ^{WT}CRAF isolated from the insoluble fraction when co-expressed with ectopic ^{V600E}BRAF.

Figure 6.6 Phospho-sites detected in GFP-CRAF^{WT} when co-expressed with Myc-BRAF^{V600E}. (A) Table showing the phosphorylated residues detected by LC-MS/MS analysis in GFP-CRAF^{WT} when expressed alone or co-expressed with Myc-BRAF^{V600E}. **(B)** Ribbon diagram of the CRAF kinase domain (Tyr340-Lys615). The N-region is indicated in yellow; the glycine rich-loop is in blue; the activation segment is shown in green and the catalytic loop is in red. The position of the residue Ser357, Ser359 and Ser612 are shown in pink.

A

Residues	GFP-CRAF^{WT} (SF)	GFP-CRAF^{WT} (IF)	GFP-CRAF^{WT}/Myc-BRAF^{V600E} (SF)	GFP-CRAF^{WT}/Myc-BRAF^{V600E} (IF)
S29	Not P	P	P	P
S43	Inconclusive	P	P	P
T54	Not covered	Not covered	Not covered	P
S244	P	P	P	P
S246	Not P	Inconclusive	Not P	P
S247	Not P	Inconclusive	Not P	P
S257	P	Inconclusive	Inconclusive	Inconclusive
T260	Inconclusive	Inconclusive	Inconclusive	P
S296	P	Inconclusive	P	Inconclusive
S301	P	P	P	P
S322	Not P	Inconclusive	Not P	P
S357	Not P	Not P	Not P	P
S359	Not P	Not P	Not P	P
S612	Not P	P	Not P	P
S621	P	P	P	P
S642	Inconclusive	P	P	P

Inconclusive, phosphorylation that could not be allocated to a specific serine, threonine or tyrosine within the peptide; Not covered, residue that was not included in any of the peptides generated after trypsin digestion; P, phosphorylated residue; Not P, non-phopshorylated residue.

B

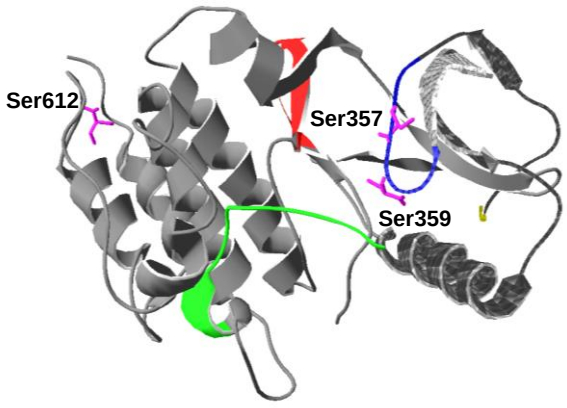

6.3.5 Predicted consensus sequences in ectopic ^{V600E}BRAF and ^{WT}CRAF

Consensus phosphorylation motifs are helpful for predicting phosphorylation sites for specific protein kinases within a potential substrate (Kennelly, Krebs 1991). By using the post-translational modification data base PHOSIDA (Gnad, Gunawardena & Mann 2011), a list of kinases that could phosphorylate the identified residues in GFP-BRAF^{V600E} and GFP-CRAF^{WT} was generated.

The table from Figure 6.7 shows that the Ser675 in ^{V600E}BRAF was recognized as part of a GSK3 consensus motif (Fiol et al. 1990). The Ser29, Ser246, Ser247 and Ser357 residues in CRAF were located within motifs recognized and phosphorylated by the kinase CK1 (Flotow et al. 1990). The amino acid sequence surrounding Ser246 in ectopic CRAF also matched with the GSK3 consensus phosphorylation site. The sequence surrounding

Ser612 in ectopic CRAF was compatible with the consensus phosphorylation motif of NEK6 (O'Regan, Fry 2009, Kang et al. 2011) while the motifs containing residues Thr54 and Ser359 in ectopic CRAF, were not identified as part of any consensus phosphorylation site known.

Overall, the data from Figure 6.7 shows that it is conceivable that an intermediary kinase such as GSK3 or CK1 could be responsible for phosphorylating ^{V600E}BRAF and CRAF and consequently play a role in the degradation of these proteins.

6.3.6 Identification of ubiquitylated sites in ectopic ^{V600E}BRAF

The trypsin mediated proteolysis of ubiquitylated proteins yields peptides with internal lysine residues harbouring a diglycine tag (GlyGly) derived from the C´-terminus of ubiquitin. This approach makes possible the identification of ubiquitylated sites by LC-MS/MS (Kirkpatrick, Denison & Gygi 2005).

Figure 6.7 Kinase prediction based on the consensus motif analysis surrounding the differential phospho-residues. In accordance to the PHOSIDA database, a prediction of the kinases that might be responsible for phosphorylating the differential phospho-residues was performed. The results were verified using the NetPhorest database.

	Residue	Kinase	Full name	Consensus phosphosite
CRAF	S29	CK1	Casein kinase-1	(S-X-X-**S/T**, S/T-X-X-X-**S**)
	T54	-	-	-
	S246	CK1	Casein kinase-1	(S-X-X-**S/T**, S/T-X-X-X-**S**)
		GSK3	Glycogen synthase kinase-3	(**S**-X-X-X-S)
	S247	CK1	Casein kinase-1	(S-X-X-**S/T**, S/T-X-X-X-**S**)
	S322	-	-	-
	S357	CK1	Casein kinase-1	(S-X-X-**S/T**, S/T-X-X-X-**S**)
	S359	-	-	
	S612	NEK6	NIMA (never in mitosis gene a)-related kinase 6	(L-X-X-**S/T**)
BRAF	S675	GSK3	Glycogen synthase kinase-3	(**S**-X-X-X-S)

A ubiquitylated residue was found in GFP-BRAF^{V600E} rescued from the insoluble fraction. In contrast, no ubiquitylated residues were detected in ectopic ^{V600E}BRAF purified from the soluble fraction. The ribbon structure of ^{V600E}BRAF kinase domain (Bollag et al. 2010) shows that Lys499 residue is located in the CR3 domain and apparently it is not located within interacting distance from any residues belonging to a key regulatory segment or predicted PEST sequences.

6.3.7 Identification of ubiquitylated residues in ectopic ^{WT}CRAF

In samples where ^{WT}CRAF was ectopically expressed, ubiquitylated residues were also detected (Figure 6.9). In agreement with GFP-BRAF^{V600E} ubiquitylation (Figure 6.8) and previous reports from other groups, the ubiquitylated form of CRAF was found in the insoluble fraction but not in the soluble fraction (Noble et al. 2008, Schulte, An & Neckers 1997). Interestingly, 12 lysine residues were detected as being ubiquitylated in GFP-CRAF^{WT}. From these residues, only four were exclusive to GFP-CRAF^{WT} when co-expressed with ectopic ^{V600E}BRAF (Lys439, Lys470, Lys483 and Lys493). As shown in the ribbon structure of the CRAF kinase domain (Figure 6.9) (Hatzivassiliou et al. 2010), the residues Lys470, Lys483 and Lys493 are facing the ATP pocket while residues Lys439 is located on the surface of the protein and consequently are more exposed to E3 ligases.

Overall, the data from Figure 6.9 shows that several lysine residues are ubiquitylated specifically in CRAF when isolated from the insoluble fraction; however, there are additional sites that become ubiquitylated in the presence of ^{V600E}BRAF.

Figure 6.8 Ubiquitylated residue detected in ectopic ^{V600E}BRAF. Ribbon diagram of the ^{V600E}BRAF kinase domain. The N-region is indicated in yellow; the glycine rich-loop is in blue; the activation segment is shown in green and the catalytic loop is in red. The position of the residue Lys499 is shown in pink.

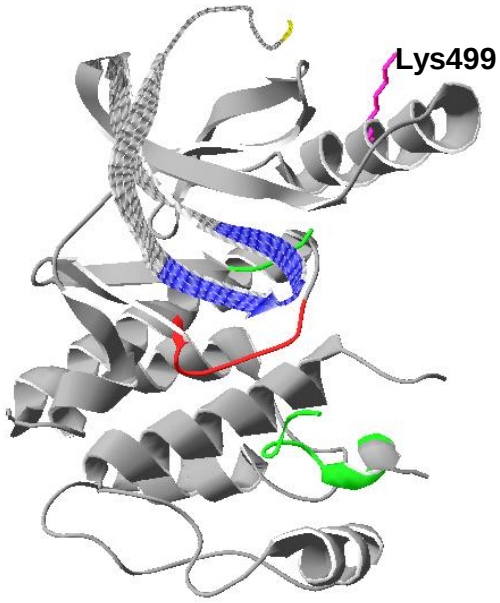

Figure 6.9 Ubiquitylated sites detected in GFP-CRAF^{WT} when co-expressed or not with Myc-BRAF^{V600E}. (A) Venn diagram showing the ubiquitylated residues found in GFP-CRAF^{WT} when expressed with or without ectopic ^{V600E}BRAF (yellow). In the green area are indicated those residues exclusively detected in GFP-CRAF^{WT} when co-expressed with ectopic ^{V600E}BRAF **(B)** Ribbon diagram of the CRAF kinase domain (Tyr340-Lys615). The N-region is indicated in yellow; the glycine rich-loop is in blue; the activation segment is shown in green and the catalytic loop is in red. The position of the residues Lys439, Lys470, Lys483 and Lys493 is shown in pink.

A

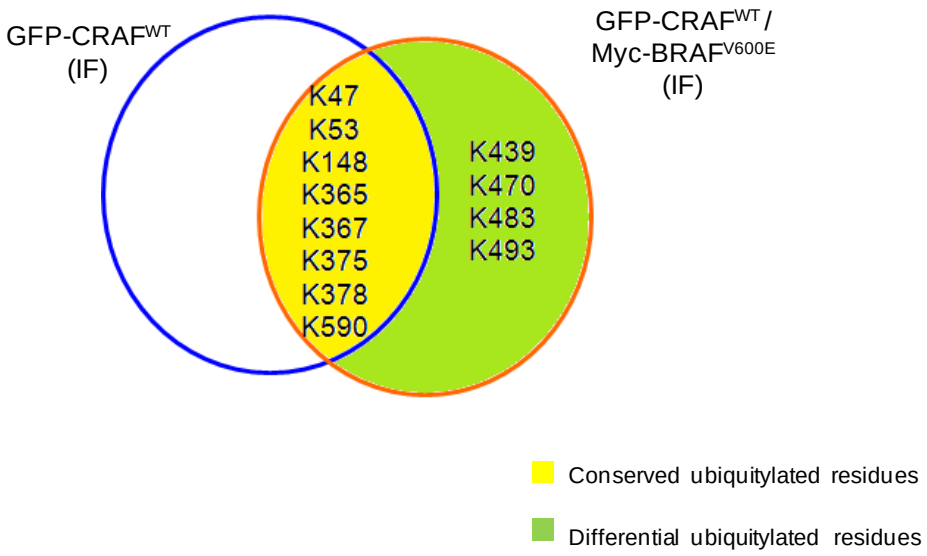

B

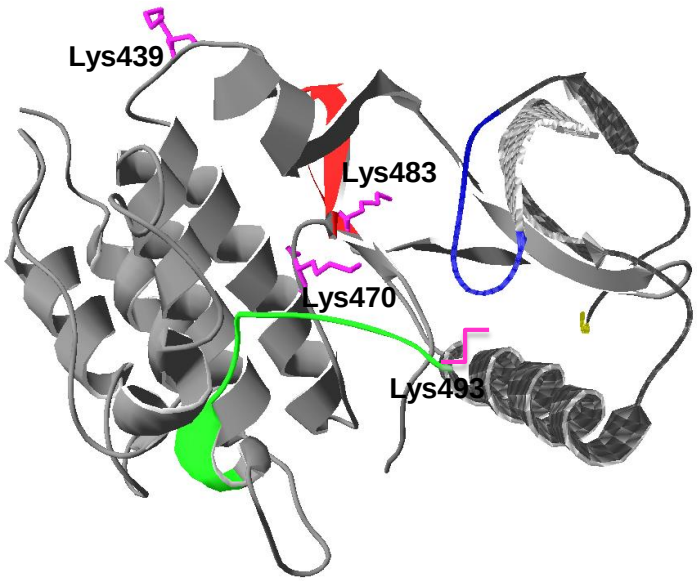

6.3.8 Conservation of phosphorylated and ubiquitylated residues among the RAF isoforms

In order to analyse if the phosphorylated and ubiquitylated sites found in ectopic ^{V600E}BRAF and ectopic ^{WT}CRAF were conserved between the RAF isoforms or were exclusive to each protein, the sequence alignment of human ARAF, BRAF and CRAF was performed. As shown in Figure 6.10, the residue S675 that was found phosphorylated in ^{V600E}BRAF is conserved in ARAF (Ser528) and CRAF (Ser567). In the case of the phospho-residues detected in CRAF, only Ser322, Ser359 and Ser612 are conserved among the three RAF isoforms. The residue Ser357 is conserved in BRAF but not in ARAF while the rest of the

residues are equivalent to non-phosphorylatable residues in BRAF and ARAF isoforms (Figure 6.10). The Lys499 residue that was found ubiquitylated in ^{V600E}BRAF is conserved in CRAF but not in ARAF. In the case of the lysine residues that were found ubiquitylated in CRAF when co-expressed with Myc-BRAF^{V600E}, all of them are conserved among the three RAF isoforms with the exception of Lys439, which is present in BRAF but not in ARAF.

Overall the data shows that among the residues found phosphorylated and ubiquitylated in ^{V600E}BRAF and ^{WT}CRAF, there is a mix of conserved and unique residues.

6.3.9 Mutation of the phosphorylation site found in ectopic ^{V600E}BRAF

According to the data shown in section 6.3.3, the differential phosphorylation of ectopic ^{V600E}BRAF could be related to the partitioning of this protein to the insoluble fraction. In order to investigate if this is related to phopshorylation of Ser675, this residue was mutated to a non-phosphorylatable alanine. The construct of GFP-BRAF^{V600E} (S675A),

Figure 6.10 Schematic representation of human RAF isoforms. The alignment of the protein sequences of human RAF isoforms was done using the Clustal programme. The phospho-residue detected in ^{V600E}BRAF (blue) and the phospho-residues identified in CRAF when co-expressed with ^{V600E}BRAF (red) are indicated in the sequence. Also, the ubiquitylated lysines found in ^{V600E}BRAF (green) and ^{WT}CRAF when co-expressed with ^{V600E}BRAF (magenta) are shown. The three conserved regions are highlighted by grey dotted lines.

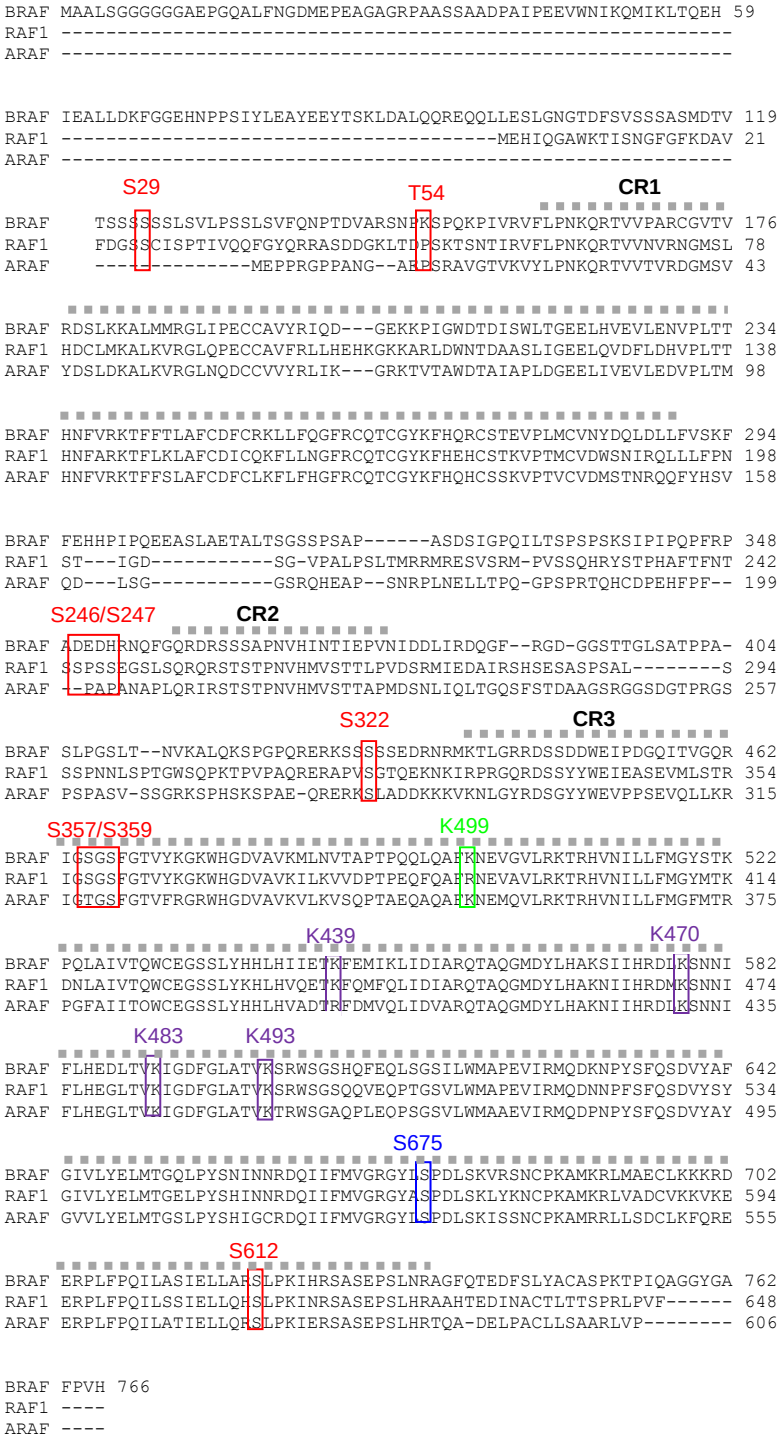

was generated by PCR site-directed mutagenesis (Section 2.2.2.5). HEK293^{T} cells were transiently transfected with Myc-BRAF^{WT}, GFP-BRAF^{V600E} or GFP-BRAF^{V600E} (S675A) expression vectors. The cells were harvested 48 hours post-transfection with GLB lysis buffer and the soluble and insoluble fractions were obtained. The samples were subjected to western blot with antibodies detecting BRAF, pERK, GAPDH and ACTIN proteins. HEK293^{T} cells that were treated with Lipofectamine 2000 alone were employed as negative controls (MOCK). In order to eliminate the error related to the different uptake of the BRAF vector in each sample, the total protein in each lane (100%) was considered as the addition of BRAF optical density from the soluble and insoluble fraction (Figure 6.11).

As shown in Figure 6.11, a decrease in ectopic BRAF protein levels was observed in the soluble fraction of GFP-BRAF^{V600E} and GFP-BRAF^{V600E} (S675A)-transfected cells compared to Myc-BRAF^{WT}-expressing cells. In agreement with previous experiments, simultaneous to this drop in the soluble fraction, a greater accumulation of ectopic BRAF occurred in the insoluble fraction compared to Myc-BRAF^{WT}-transfected cells. Although ectopic BRAF^{WT} is fused to a myc-tag while ectopic BRAF^{V600E} and ectopic BRAF^{V600E} (S675A) are bound to a GFP-tag and this could potentially influence the synthesis or stability of these proteins, previous experiments have shown that myc-tagged BRAF^{WT} and myc-tagged BRAF^{V600E} showed the same behavior in its expression (Figure 3.10). The mutation of the serine to alanine in position 675 did not rescue ectopic BRAF expression in the soluble fraction compared to the GFP-BRAF^{V600E}-transfected sample. No changes were observed in BRAF expression in the insoluble fraction from GFP-BRAF^{V600E} (S6745A) compared to GFP-BRAF^{V600E}-expressing cells. In the case of phospho-ERK, higher levels (~1.8-fold) were detected when ectopic ^{V600E}BRAF was expressed compared to Myc-BRAF^{WT}-transfected cells. Interestingly, the sample expressing GFP-BRAF^{V600E} (S6745A) showed a slight reduction in ERK phosphorylation in comparison to cells expressing

Figure 6.11 Mutation of the phospho-residue in ectopic ^{V600E}BRAF. (A) HEK293^{T} cells were transiently transfected with Myc-BRAF^{WT}, GFP-BRAF^{V600E} or GFP-BRAF^{V600E} (S675A) expression vectors. After 48 hours of transfection, the cells were harvested with GLB buffer and the soluble and insoluble fractions were prepared. Expression of BRAF, pERK, ACTIN and GAPDH was analyzed by immunoblotting. For the densitometric analysis of pERK, the X-ray films were scanned and the optical density (O.D.) of the bands was measured using Image J software. The optical density of the background was subtracted from every sample. The values representing the level of ERK phosphorylation correspond to the pERK/GAPDH ratio expressed as a percentage of phospho-ERK in the Myc-BRAF^{WT} sample. **(B)** The values plotted on the graph correspond to normalized BRAF in the soluble fraction (BRAF/GAPDH) and normalized BRAF in the insoluble fraction (BRAF/ACTIN) expressed as a percentage of total BRAF. Data is representative of a single experiment.

A

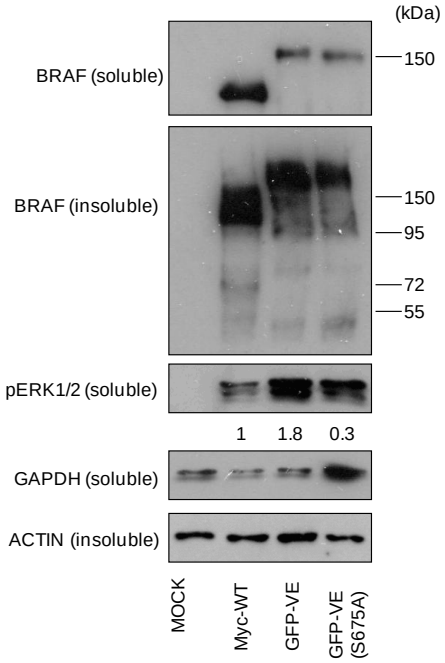

B

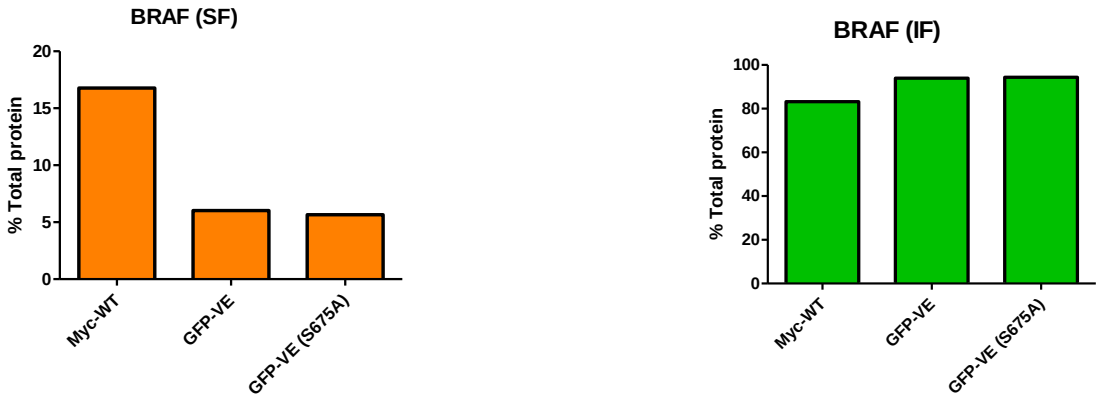

ectopic ^{V600E}BRAF. This could be explained by the slight decrease in ^{V600E}BRAF protein levels in the soluble fraction from this sample. However, the reproducibility of these results has to be verified by performing similar experiments.

Overall the data from Figure 6.11 showed that the mutation of Ser675 to alanine in ectopic ^{V600E}BRAF did not alter the distribution of the protein between the soluble and insoluble fractions.

6.3.10 Mutation of differential phosphorylation sites found in ectopic ^{WT}CRAF

In order to examine if the phosphorylations detected in ectopic ^{WT}CRAF isolated from the insoluble fraction were related to its accumulation in this fraction, the residues were mutated to non-phosphorylatable alanines and the expression of ectopic ^{WT}CRAF was analysed. To do this, individual mutations of residues Thr54A, Ser246A, Ser247A Ser357A and Ser359A as well as the 3A (Thr54A, Ser246A and Ser247A) and 5A (Thr54A, Ser246A, Ser247A Ser357A and Ser359A) mutants were performed. All mutants were generated by Bipin Patel using PCR site-directed mutagenesis (Section 2.2.2.5). All CRAF mutants were co-transfected with ectopic ^{V600E}BRAF into HEK293^{T} cells. These cells were lysed 48 hours post-transfection with GLB buffer and the soluble and insoluble fractions were obtained. The samples were subjected to western blot with antibodies detecting BRAF, CRAF, pERK and GAPDH proteins. GFP-CRAF^{WT} transfected alone was employed as positive control whereas GFP-CRAF^{WT} co-expressed with GFP-BRAF^{V600E} was used as negative control. In order to eliminate the error related to the different uptake of the CRAF vector in each sample, the total protein in each lane (100%) was considered as the addition of CRAF optical density from the soluble and insoluble fraction (Figure 6.12).

As shown in Figure 6.12, ectopic CRAF protein levels were rescued in the soluble fraction when the 3A mutant was expressed. Also, an increase in the expression of this protein was observed when the 5A mutant was transfected; however the extent of the recovery was lower than that obtained with the 3A mutant. Interestingly, simultaneous to the accumulation of ectopic mutant CRAF in the soluble fraction, a reduction in the expression of this protein was observed in the insoluble fraction. The concomitant alteration of mutant CRAF distribution in both fractions suggests that the reduction of the protein in the soluble fraction is not caused by a decrease in the synthesis of the mutant protein but due to an alteration in its partitioning The fact that the 3A and 5A mutants showed the same pattern of CRAF expression in the soluble and insoluble fraction indicates that the lack of phosphorylation in residues T54, S246 and S247 might be related with the shift of the protein to the insoluble fraction.

Interestingly, a slight reduction in ERK phosphorylation (~30%) compared to the GFP-CRAF^{WT}/GFP-BRAF^{V600E} sample was shown when most of the CRAF mutants were expressed. However, a 67% and 73% decrease in phospho-ERK levels was detected in the samples expressing the S357A and S359A mutants, respectively. This behaviour could be explained by the low levels of ectopic CRAF expression in the soluble fraction of the samples expressing these mutants.

Overall, the data from figure 6.12 shows that the mutation of single residues did not prevent the accumulation of ectopic CRAF in the insoluble fraction. However, when 3 or 5 residues were mutated simultaneously, an evident decrease in CRAF expression occurred in this fraction. The expression of the 3A or 5A mutants also resulted in a reduction in phospho-ERK levels.

Figure 6.12 Mutation of the phospho-residues detected in ectopic ^{WT}CRAF rescued from the insoluble fraction. (A) GFP-CRAF phosphorylation site mutants were transiently co-transfected with GFP-BRAF^{V600E} expression vector. After 48 hours of transfection, the cells were harvested with GLB buffer and the soluble and insoluble fractions were prepared. Expression of BRAF, CRAF, Perk and GAPDH was analyzed by immunoblotting. For the densitometric analysis of pERK, the X-ray films were scanned and the optical density (O.D.) of the bands was measured using Image J software. The optical density of the background was subtracted from every sample. The values representing the level of ERK phosphorylation correspond to the pERK/GAPDH ratio expressed as a percentage of phospho-ERK from the GFP-CRAF^{WT}/GFP-BRAF^{V600E} sample. **(B)** The values plotted on the graph correspond to normalized CRAF in the soluble fraction (CRAF/GAPDH) and normalized CRAF in the insoluble fraction (CRAF/ACTIN) expressed as a percentage of total CRAF. Data is representative of two experiments.

A

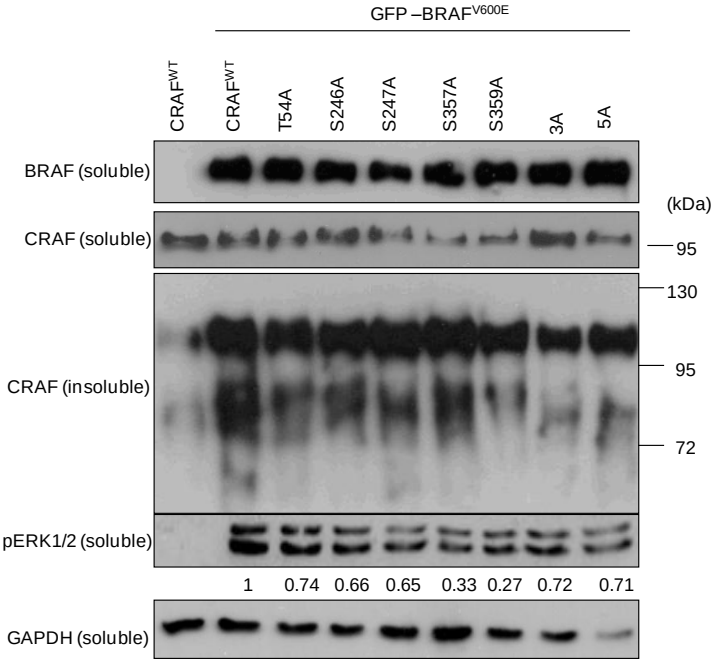

B

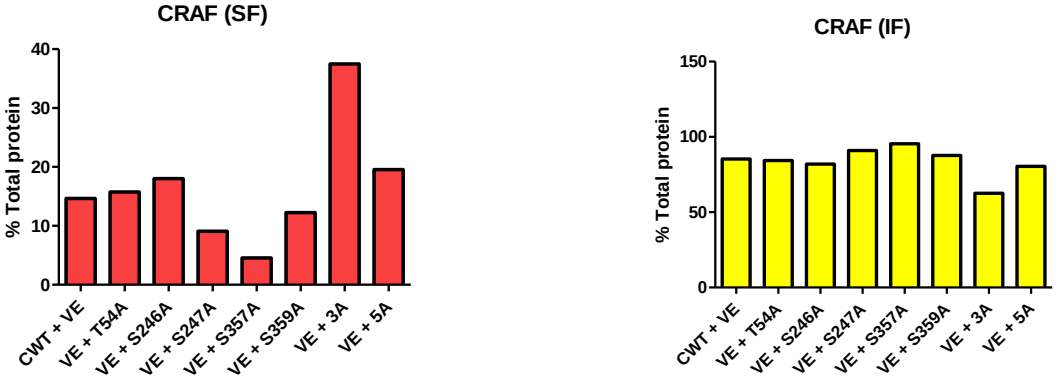

6.4 Discussion

The non-ionic detergents such as Triton and NP-40 are employed in the extraction of membrane-bound proteins, cytoskeletal-bound proteins and free cytosolic proteins. The ionic detergents such as SDS are considered to be the harshest of all and have been found able to disrupt membranes and protein-protein interactions which results in the liberation of proteins from aggregates or high molecular complexes (Schulte, An & Neckers 1997, Luckett et al. 2000).

In order to investigate more about the nature of ^{V600E}BRAF and ^{WT}CRAF rescued from the insoluble fraction or SDS-soluble fraction, the detection of post-translational modifications was carried out by mass spectrometry. The presence of post-translational events was anticipated by the electrophoretic migration pattern observed in ^{V600E}BRAF and ^{WT}CRAF in the insoluble fraction.

The fact that the LC-MS/MS analysis was not quantitative, meaning that the samples were not normalized in respect to an unchangeable ion current (Previs et al. 2008), indicates that it is possible that the phosphor-residues detected in the insoluble fraction but not in the soluble fraction could be explained by a variation in the amount of starting material and not because these residues are not being phosphorylated. Also, when employing non-quantitative LC-MS/MS, it is not possible to know which portion of total BRAF and CRAF proteins are being phosphorylated in the differential residues which in terms of the impact of this regulatory mechanism, would be important. In order to confirm the authenticity of the phospho-sites proposed in Chapter 6, a more specialized version of the mass spectrometry technique such as IMAC/MS will be needed as well as repeating the experiment (n=3) in order to assess the consistency of the phospho-sites detected.

Important inhibitory and stimulatory sites of BRAF activity were found phosphorylated in ectopic ^{V600E}BRAF isolated from the soluble or insoluble fractions (Figure 6.4). Interestingly, the phospho-sites detected in ectopic ^{V600E}BRAF purified from the soluble fraction were exactly the same residues that were found phosphorylated in ectopic ^{V600E}BRAF rescued from the insoluble fraction suggesting that the protein accumulated in the insoluble fraction is still active or was active at some point. Only one differential phosphorylation (Ser675) was found in GFP-BRAF^{V600E} purified from the insoluble fraction in comparison to the protein isolated from the soluble fraction (Figure 6.4). It is the first time that the Ser675 residue, which is located in the kinase domain of BRAF but not within any key regulatory segment, has been found phosphorylated in a LC-MS/MS study. The Ser675 is not localized within the PEST motif in BRAF or near to the ubiquitylated lysine detected in this study, which makes unlikely the possibility that the phosphorylation of Ser675 could be creating a binding site for an E3 ligase which potentially could add ubiquitin moieties to the protein leading to its degradation (Figure 6.4) (Hershko, Ciechanover 1998, Fuchs, Spiegelman & Kumar 2004a) . The Ser675 residue, which is conserved in CRAF and ARAF, has not been found phosphorylated in CRAF (Ser567) but it has been detected as a phospho-residue in ARAF (Ser526) (Baljuls et al. 2008) (Figure 6.10).

Mutagenesis experiments showed that the prevention of Ser675 phosphorylation did not altered the partitioning of ^{V600E}BRAF to the insoluble fraction suggesting that this residue is not involved in the accumulation of ^{V600E}BRAF in this fraction (Figure 6.11). It is possible that the phosphorylation of other residues that were not detected by our study, could be promoting the shift of ^{V600E}BRAF to the insoluble fraction. It is worth mentioning that approximately 40% of the BRAF sequence was left out of the LC-MS/MS analysis due to the poor coverage after trypsin or LysC/GluC digestion (Figure 6.3). In agreement with previous studies showing the ubiquitylation and proteasomal degradation of BRAF

(Grbovic et al. 2006), a differential ubiquitylated lysine residue (Lys499) was also found in ectopic ^{V600E}BRAF isolated from the insoluble fraction. The Lys499 residue is located in the kinase domain of BRAF but outside any key regulatory segment (Figure 6.8). The role of this residue in the processing of BRAF is not clear.

In the case of CRAF, the same well known regulatory phospho-residues such as ERK or AKT phosphorylation sites were detected when the protein was isolated from the soluble and insoluble fractions, confirming that the partitioning of CRAF between both fractions is not related to the activity of the protein (Zimmermann, Moelling 1999, Dougherty et al. 2005) (Figure 6.6). The lack of phosphorylation of key residues belonging to the N-region and activation segment in ectopic ^{WT}CRAF could be explained by the nature of the qualitative LC-MS/MS analysis. The peptides retained by the mass spectrometer are not always representative of the entire population of GFP-CRAF^{WT} present in the sample and it is possible that other peptides with a different phosphorylation pattern were lost during different steps of the process (Previs et al. 2008). Interestingly, 6 residues (Ser246, Ser247, Ser322, Ser612, Ser357 and Ser359) were found phosphorylated exclusively in GFP-CRAF^{WT} isolated from the insoluble fraction (Figure 6.6). Specifically, the residues Ser357 and Ser359 were detected as being phosphorylated in this fraction only when ectopic ^{WT}CRAF was co-expressed with Myc-BRAF^{V600E}.

Mutagenesis experiments showed that only the simultaneous mutation of all residues to non-phosphorylatable alanines was able to reverse the partitioning of CRAF to the insoluble fraction leading instead to an accumulation of this protein in the soluble fraction (Figure 6.12). Clearly, the mutation of individual residues in some cases had the opposite effect to what was expected or simply resulted in the reduction of the general expression of RAF (Figure 6.12). It is possible that the arrangement of the phospho-residues in the 3-dimensional structure of CRAF could influence CRAF conformation making it compatible

with the insoluble fraction. However; because the crystal structure of CR1 and CR2 domains has not been resolved, a pattern of distribution between the phosphorylated residues was not elucidated (Figure 6.6). The fact that most of the residues found phosphorylated in CRAF were not conserved among the other RAF isoforms suggests that this mechanism of regulation could be particular for CRAF (Figure 6.10). Importantly, none of the phosphorylated residues detected in ectopic ^{WT}CRAF isolated from the insoluble fraction are located within the potential PEST motifs in CRAF. The ubiquitylated lysines found in GFP-CRAF^{WT} when co-expressed with Myc-BRAF^{V600E} and isolated from the insoluble fraction were localized within the catalytic loop (Figure 6.9). It is possible that the presence of ubiquitin chains in this location could cause spatial restrictions affecting the binding of the ATP molecule to the protein.

CHAPTER 7 Discussion

7.1 BRAF and CRAF are regulated at the post-translational level in ^{V600E}BRAF-expressing cells

This study shows that the expression of endogenous ^{V600E}Braf or ectopic ^{V600E}BRAF results in a decrease in total BRAF and CRAF protein levels in the NP-40 soluble fraction. I also showed that, simultaneous to the drop in protein expression, an accumulation of BRAF and CRAF occurs in the NP-40 insoluble fraction of both cellular systems (Figure 7.1).

QRT-PCR experiments showed little effect of the presence of endogenous Braf^{V600E} on *Braf* and *Craf* mRNA expression. However, experiments measuring the half-lives of Braf and Craf showed a reduction in the stability of these proteins when extracted from the soluble fraction of ^{V600E}BRAF-expressing cells. Consistent with previous studies by Noble et al., which showed that unfolded and ubiquitylated Craf$^{DA/DA}$ accumulates in the insoluble fraction after the proteasome activity is inhibited (Noble et al. 2008), our mass spectrometry analysis of ectopic ^{V600E}BRAF and ^{WT}CRAF rescued from the soluble and insoluble fractions shows the presence of ubiquitylated forms of these proteins exclusively in the insoluble fraction.

The involvement of the proteasome and autophagy pathways in the degradation of specific members belonging to different signaling cascades has been shown by several studies (Gao et al. 2010, Su et al. 2011a, Xu, Kim & Gumbiner 2009). In this study I showed that Braf and Craf protein levels were rescued in both types of MEFs after proteasome inhibition. However, from the results obtained in those experiments, it was not possible to conclude if an accelerated degradation of Braf and Craf was taking place in the presence of Braf^{V600E} compared to *Braf*$^{+/+}$ MEFs. In order to address this question, other types of

Figure 7.1 A proposed model for the control of BRAF and CRAF protein levels by ^{V600E}BRAF. The expression of ^{V600E}BRAF results in the hyperactivation of the MEK-ERK axis which leads to the post-translational downregulation of BRAF and CRAF. This is reflected by a reduction in the expression of BRAF and CRAF in the NP-40 soluble fraction and their simultaneous accumulation in the NP-40 insoluble fraction. The inhibition of MEK as well as the inactivation of the autophagy pathway rescued the expression of BRAF and CRAF suggesting the involvement of these elements in the degradation of BRAF and CRAF in ^{V600E}BRAF-expressing cells.

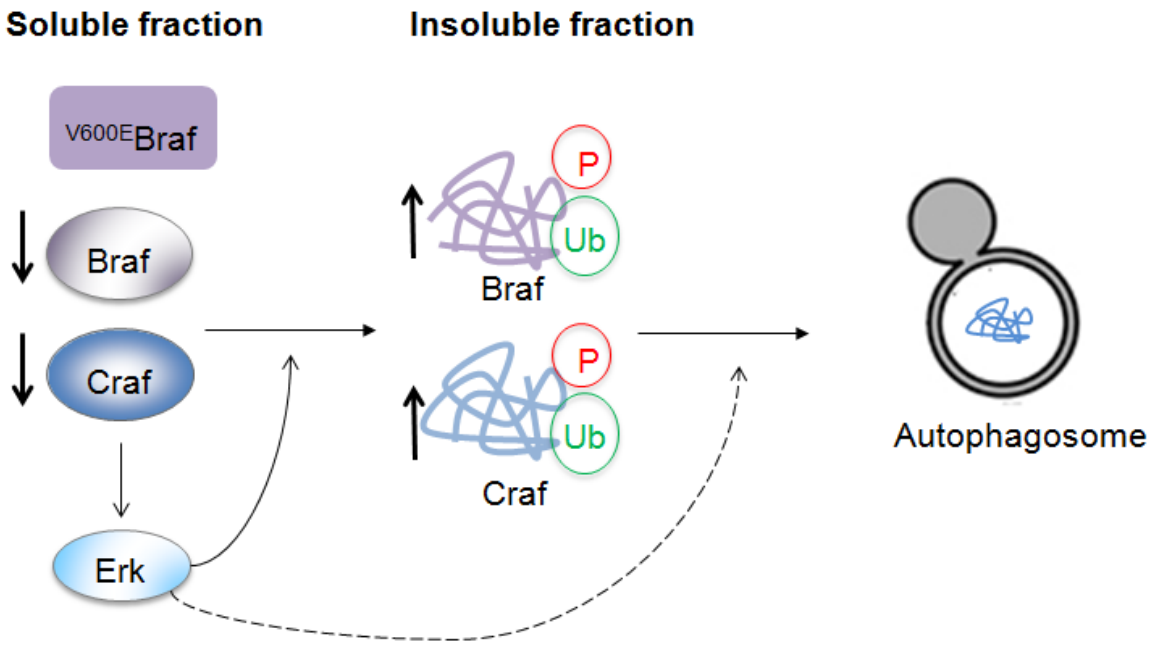

experiments such as the co-transfection of Myc-tagged expression vectors for ^{V600E}BRAF, ^{WT}BRAF or ^{WT}CRAF and HA-ubiquitin should be performed. In the case that the degradation of BRAF and CRAF by the proteasome is increased in cells expressing ectopic BRAF^{V600E}, an increased amount of ubiquitylated BRAF and CRAF should be observed in these cells compared to cells expressing Myc-BRAF^{WT}.

Madodi et al. in 2010 showed that hyperactivation of ^{V600E}BRAF can induce high levels of autophagy in melanoma cells (Maddodi et al. 2010). In agreement with these results and previous reports from our lab, our data show that the expression of ectopic or endogenous ^{V600E}Braf results in an increase in LC3I to LC3II conversion compared to Braf$^{+/+}$ cells. Moreover, the use of compounds that inhibit autophagolysosome formation and function indicated that autophagy was functional in these cells. The induction of autophagy by starvation in Braf$^{+/+}$ MEFs and the subsequent inhibition of the degradatory activity of the autophagolysosome resulted in the accumulation of Braf in the insoluble fraction suggesting that autophagy can be related to the processing of Braf. This was confirmed by treating Braf^{V600E} MEFs, which already showed high levels of autophagy, with chloroquine (CQ). However, experts in the autophagy field recommend the use of multiple assays for testing autophagy activity instead of relying on a single method (Klionsky et al. 2008). Thus, in order to conclude that Braf and Craf are being degraded by autophagy, more specialized experiments that show the engulfment of these proteins by the autophagosome must be performed (Mizushima, Yoshimori & Levine 2010). In 2010, Gao et al. showed that, under starvation conditions, autophagy promotes the degradation of Dishevelled (Dvl) which results in the degradation of β-catenin (Gao et al. 2010). Although they showed that Dvl2 is also degraded by the proteasome, their experiments also proved that autophagy plays a significant role in the turn-over of this protein. Another example of autophagic downregulation of signaling is that involving the degradation of the ubiquitin

ligase Hiw (Shen, Ganetzky 2009). Based on this information, it is conceivable that due to the resistance showed by $Braf^{V600E}$ to ERK-dependent inhibitory phosphorylation (Ritt et al. 2010a) and to negative feedback regulators (Tsavachidou et al. 2004, Brady et al. 2009), an alternative mechanism for regulating the activity of oncogenic BRAF has been developed by the cells.

7.2 A possible mechanism for the regulation of BRAF and CRAF protein levels in ^{V600E}BRAF-expressing cells

In order to investigate if the differential phospho-sites found in ectopic ^{V600E}BRAF and CRAF rescued in the insoluble fraction were related to the accumulation of these proteins in the insoluble fraction, the residues were mutated. The mutation of the S675 phospho-residue detected in ectopic ^{V600E}BRAF did not alter the partitioning of the protein between the soluble and insoluble fractions; however, the mutation of three of the five phospho-sites detected in CRAF as well as the 5A mutant showed a recovery of ectopic CRAF protein levels in the soluble fraction and the decrease of this protein in the insoluble fraction. There are various examples in the literature where the phosphorylation of specific residues has been related to the degradation of certain proteins by creating a binding site for an E3 ligase (Su et al. 2011a, Patrick et al. 1998). Such is the case of β-catenin and Snail which contain the "DSGxxS/TxxxS/T destruction motif (Yook et al. 2005). In this sequence, the serine residue from the DSG has to be phosphorylated in order for the β-Trcp (E3 ligase) to bind (Fuchs, Spiegelman & Kumar 2004a). Also the phosphorylation of the first serine or threonine from the S/TxxxS/T sequence by Gsk3β and the phosphorylation of the second serine or threonine by an unknown kinase, are needed (Doble, Woodgett 2003). As a result, the β-Trcp binds and conjugates ubiquitin moieties to

lysine residues in position 9-13 upstream from the destruction motif (Fuchs, Spiegelman & Kumar 2004a). Although some E3 ligases have been proposed to be involved in the degradation of BRAF and CRAF such as Ring Finger Protein 149 (Hong et al. 2012) and CHIP (Demand et al. 2001a), it has been shown that other as yet unidentified E3 ligases are playing a role in this process for CRAF (Noble et al. 2008). From the data obtained by mass spectrometry analysis, is not possible to determine a relation between the phospho-sites and the ubiquitylated residues detected in ectopic ^{V600E}BRAF and CRAF because each family of E3 ligases have different requirements for binding to their substrates (Weissman 2001).

ERK has been shown to promote the degradation of various proteins by phosphorylation which leads to their ubiquitylation and subsequent degradation (Yang et al. 2008, Fueller et al. 2008, Ley et al. 2003a). Thus, I investigated whether ERK or downstream substrates of ERK were involved in the regulation of BRAF and CRAF expression. After Braf^{V600E} MEFs were treated with MEK inhibitor, Braf protein levels were rescued in the soluble and insoluble fraction whereas Craf protein levels were rescued only in the insoluble fraction. These results suggest that ERK or downstream targets of ERK could be implicated in the phosphorylation of BRAF and CRAF leading to their subsequent ubiquitylation (Figure 7.1). It is also conceivable that ERK can be directly regulating the transcription or activity of the E3 ligase responsible for the degradation of BRAF and CRAF. Thus, when ERK is inhibited, the downregulation of the E3 ligase could result in the accumulation of the BRAF and CRAF in the insoluble fraction (Ries et al. 2000). An increasing number of studies have suggested the involvement of ERK in the modulation of autophagy (Shinojima et al. 2007, Aoki et al. 2007, Zhu et al. 2007). In these studies, the stimulation of the ERK pathway by different activators such as TNF (Sivaprasad, Basu 2008) or the natural product curcumin (diferuloylmethane) (Aoki et al. 2007) has shown to increase autophagic

activity. Although the mechanism by which ERK promotes autophagy is not clear yet, a recent study by Shinojima et al. in 2007 showed that ERK increases autophagy in starved cells by down-regulating AKT/mTOR/S6K pathway (Shinojima et al. 2007). Another study proposing a non-canonical MEK/ERK signaling that regulates autophagy by regulating Beclin-1 expression has also been published (Wang et al. 2009). However, further studies will be needed in order to validate these theories.

7.3 The intensity of the signal by BRAF^{V600E} influences the biological outcome of the ERK pathway

The fact that the drop in Braf protein levels and the reduction in ERK phosphorylation in ^{V600E}Braf lung adenomas were detected in the senescent phase suggests that these changes are required for the cells to enter into a growth arrested state (Dr. Hong Jin personal communication). In contrast, the results in this study showed that the decrease in Braf and Craf expression and the reduction in Erk phosphorylation in *Braf*^{V600E} MEFs, did not stop the cells from proliferating or altered their transformation. In agreement with these observations, a recent study by Andreadi et al. showed that *Braf*^{V600E} MEFs did not become senescent when cultivated *in vitro* (Andreadi et al. 2012). Moreover, they showed that proliferating *Braf*^{V600E} MEFs contained reduced levels of phospho-Erk, similar to those showed by ^{L597V}Braf MEFs, which express an intermediate activity mutant of Braf. These data suggests that although the *in vivo* and *in vitro* systems show a reduction in BRAF protein levels and phospho-ERK, the intensity of the activating signal received by ERK must be different in both systems which results in a different outcome of the pathway. It is important to consider that the level of ERK phosphorylation not only would depend on the amount of cellular BRAF and CRAF but can also be regulated by DUSPs and the

expression of DUSPs has been shown to increase with the activation of the ERK pathway (Owens, Keyse 2007). For this reason, various studies have suggested the use of phospho-MEK as a marker of the activation of the ERK pathway instead of phospho-ERK (Pratilas et al. 2009). They also suggested that, in order to confirm the activation of the pathway, the phopshorylation status of ERK downstream substrates must be assessed (Pratilas et al. 2009).

7.4 Endogenous and Ectopic ^{V600E}BRAF expression: two different responses

The intensity of the activating signal by ectopic ^{V600E}Braf or endogenous ^{V600E}BRAF is expected to differ greatly because of the increase amount of protein contained in transfected cells. Although Myc-BRAF^{V600E}-expressing cells showed a downregulation of ectopic BRAF^{V600E} and endogenous CRAF protein levels in the soluble fraction concomitantly to an accumulation of these proteins in the insoluble fraction, key differences were found between both cellular systems. In the Myc-BRAF^{V600E} cells, the drop in endogenous CRAF expression did not result in a reduction of ERK phosphorylation. Moreover, the examination of these cells by light microscopy showed an arrest in the proliferation of the cells. These observations agree with the results published by Madodi et al. in 2010 when they observed high levels of phospho-ERK and growth arrest in melanoma cell lines overexpressing ^{V600E}BRAF (Maddodi et al. 2010). High levels of BRAF activity in artificial systems have been shown to induce cell cycle arrest through the up-regulation of p21 transcription (Woods et al. 1997). In this context, is possible that the high kinase activity of ectopic ^{V600E}BRAF could be inducing early senescence in HEK293^{T} cells.

A real breakthrough in the treatment of metastatic melanoma came with the development of PLX4032 (Vemurafenib) (Tsai et al. 2008a). Based on the accumulated information from phase I, II and III studies, it was shown that an overall benefit of 13.2 vs 9.6 months compared to the chemotherapeutic agent dacarbizine was reached after Vemurafenib treatment (Chapman et al. 2011). However, the development of resistance by the tumour which was associated with the reactivation of the MAPK pathway was also shown (Su et al. 2012). Various studies have proposed that the molecular basis of this resistance relies on negative feedbacks that act on the ERK pathway (Flaherty et al. 2012). A recent study by Lito et al. showed that ERK inhibition by Vemurafenib, relieves the negative feedbacks that depend on ERK which results in the induction of RAS activation and the activation of the downstream targets by RAF heterodimers (Lito et al. 2012). This study gives a rational basis for the concomitant use of MEK and RAF inhibitors. In this study we propose an alternative mechanism for the regulation of the RAF proteins signaling in ^{V600E}BRAF expressing cells, which could contribute to the understanding of the adaptation mechanisms of the tumour in response to inhibitors such as Vemurafenib.

7.5 Future work

It would be important to confirm the involvement of ERK or downstream kinases of ERK in the reduced stability of BRAF and CRAF in the soluble fraction of ^{V600E}BRAF-expressing cells. A possible experiment to determine this would be to measure the half-life of BRAF and CRAF after MEK inhibition which presumably should increase or to determine if the autophagy induced in BrafV600E MEFs is responsive to MEK inhibition.

It would be important to perform another study of mass spectrometry to confirm the phosphorylation of the residues detected by our first experiment. However this time, a

mass spectrometry analysis specialized in the detection of phospho-residues such as that coupled to an immobilized metal affinity chromatography (IMAC) should be done.

It would be desirable to identify the potential intermediary kinase or kinases involved in the phosphorylation of ectopic ^{V600E}BRAF and ^{WT}CRAF rescued in the insoluble fraction. It would be useful to confirm the list of candidate kinases shown in Chapter 6 after the results of the new mass spectrometry studies are obtained. The inhibition of the kinase activity of these candidate proteins and the subsequent alteration of the phenotype, could be a first step in elucidating their involvement in the post-translational regulation of BRAF and CRAF.

It would be important to show that Braf^{V600E} and Craf are being degraded by the autophagosome. A potential experiment to determine this would be to use fluorescence microscopy in order to show the co-localization of these proteins and LC3 or to do immunoprecipitation of ^{V600E}BRAF and LC3 to show their interaction in the autophagosome.

References

Abraham, D., Podar, K., Pacher, M., Kubicek, M., Welzel, N., Hemmings, B.A., Dilworth, S.M., Mischak, H., Kolch, W. & Baccarini, M. 2000, "Raf-1-associated protein phosphatase 2A as a positive regulator of kinase activation.", *Journal of Biological Chemistry,* vol. 275, no. 29, pp. 22300-22304.

Acosta, J.C., O'Loghlen, A., Banito, A., Guijarro, M.V., Augert, A., Raguz, S., Fumagalli, M., Da Costa, M., Brown, C., Popov, N., Takatsu, Y., Melamed, J., d'Adda di Fagagna, F., Bernard, D., Hernando, E. & Gil, J. 2008, "Chemokine signaling via the CXCR2 receptor reinforces senescence.", *Cell,* vol. 133, no. 6, pp. 1006-1018.

Adachi, M., Fukuda, M. & Nishida, E. 1999, "Two co-existing mechanisms for nuclear import of MAP kinase: passive diffusion of a monomer and active transport of a dimer.", *EMBO Journal,* vol. 18, no. 19, pp. 5347-5358.

Adnane, L., Trail, P.A., Taylor, I. & Wilhelm, S.M. 2006, "Sorafenib (BAY 43-9006, Nexavar), a dual-action inhibitor that targets RAF/MEK/ERK pathway in tumor cells and tyrosine kinases VEGFR/PDGFR in tumor vasculature.", *Methods in enzymology,* vol. 407, pp. 597-612.

Aebersold, D.M., Shaul, Y.D., Yung, Y., Yarom, N., Yao, Z., Hanoch, T. & Seger, R. 2004, "Extracellular signal-regulated kinase 1c (ERK1c), a novel 42-kilodalton ERK, demonstrates unique modes of regulation, localization, and function.", *Molecular & Cellular Biology,* vol. 24, no. 22, pp. 10000-10015.

Aglipay, J.A., Martin, S.A., Tawara, H., Lee, S.W. & Ouchi, T. 2006, "ATM activation by ionizing radiation requires BRCA1-associated BAAT1.", *Journal of Biological Chemistry,* vol. 281, no. 14, pp. 9710-9718.

Aguirre, A.J., Bardeesy, N., Sinha, M., Lopez, L., Tuveson, D.A., Horner, J., Redston, M.S. & DePinho, R.A. 2003, "Activated Kras and Ink4a/Arf deficiency cooperate to produce metastatic pancreatic ductal adenocarcinoma.", *Genes & development,* vol. 17, no. 24, pp. 3112-3126.

Aitken, A. 2006, "14-3-3 proteins: a historic overview", *Seminars in cancer biology,* vol. 16, no. 3, pp. 162-172.

Albanese, C., Johnson, J., Watanabe, G., Eklund, N., Vu, D., Arnold, A. & Pestell, R.G. 1995, "Transforming p21ras mutants and c-Ets-2 activate the cyclin D1 promoter through distinguishable regions.", *Journal of Biological Chemistry,* vol. 270, no. 40, pp. 23589-23597.

Alessi, D.R., Saito, Y., Campbell, D.G., Cohen, P., Sithanandam, G., Rapp, U., Ashworth, A., Marshall, C.J. & Cowley, S. 1994a, "Identification of the sites in MAP kinase kinase-1 phosphorylated by p74raf-1.", *EMBO Journal,* vol. 13, no. 7, pp. 1610-1619.

Alessi, D.R., Saito, Y., Campbell, D.G., Cohen, P., Sithanandam, G., Rapp, U., Ashworth, A., Marshall, C.J. & Cowley, S. 1994b, "Identification of the sites in MAP

kinase kinase-1 phosphorylated by p74raf-1.", *EMBO Journal,* vol. 13, no. 7, pp. 1610-1619.

Ali, M.M., Roe, S.M., Vaughan, C.K., Meyer, P., Panaretou, B., Piper, P.W., Prodromou, C. & Pearl, L.H. 2006, "Crystal structure of an Hsp90-nucleotide-p23/Sba1 closed chaperone complex.", *Nature,* vol. 440, no. 7087, pp. 1013-1017.

Almoguera, C., Shibata, D., Forrester, K., Martin, J., Arnheim, N. & Perucho, M. 1988, "Most human carcinomas of the exocrine pancreas contain mutant c-K-ras genes.", *Cell,* vol. 53, no. 4, pp. 549-554.

Andreadi, C., Cheung, L.K., Giblett, S., Patel, B., Jin, H., Mercer, K., Kamata, T., Lee, P., Williams, A., McMahon, M., Marais, R. & Pritchard, C. 2012, "The intermediate-activity (L597V)BRAF mutant acts as an epistatic modifier of oncogenic RAS by enhancing signaling through the RAF/MEK/ERK pathway.", *Genes & development,* vol. 26, no. 17, pp. 1945-1958.

Angel, P. & Karin, M. 1991, "The role of Jun, Fos and the AP-1 complex in cell-proliferation and transformation", *Biochimica et biophysica acta,* vol. 1072, no. 2-3, pp. 129-157.

Aoki, H., Takada, Y., Kondo, S., Sawaya, R., Aggarwal, B.B. & Kondo, Y. 2007, "Evidence that curcumin suppresses the growth of malignant gliomas in vitro and in vivo through induction of autophagy: role of Akt and extracellular signal-regulated kinase signaling pathways.", *Molecular pharmacology,* vol. 72, no. 1, pp. 29-39.

Apolloni, A., Prior, I.A., Lindsay, M., Parton, R.G. & Hancock, J.F. 2000, "H-ras but not K-ras traffics to the plasma membrane through the exocytic pathway.", *Molecular & Cellular Biology,* vol. 20, no. 7, pp. 2475-2487.

Ascierto, P.A., De Maio, E., Bertuzzi, S., Palmieri, G., Halaban, R., Hendrix, M., Kashani-sabet, M., Ferrone, S., Wang, E., Cochran, A., Rivoltini, L., Lee, P.P., Fox, B.A., Kirkwood, J.M., Ullmann, C.D., Lehmann, F.F., Sznol, M., Schwartzentruber, D.J., Maio, M., Flaherty, K., Galon, J., Ribas, A., Yang, J., Stroncek, D.F., Mozzillo, N. & Marincola, F.M. 2011, "Future perspectives in melanoma research. Meeting report from the "Melanoma Research: a bridge Naples-USA. Naples, December 6th-7th 2010".", *Journal of Translational Medicine,* vol. 9, pp. 32.

Ashkenazi, A. 2002, "Targeting death and decoy receptors of the tumour-necrosis factor superfamily", *Nature Reviews.Cancer,* vol. 2, no. 6, pp. 420-430.

Ayer, D.E. & Eisenman, R.N. 1993, "A switch from Myc:Max to Mad:Max heterocomplexes accompanies monocyte/macrophage differentiation.", *Genes & development,* vol. 7, no. 11, pp. 2110-2119.

Baccarini, M. 2002, "An old kinase on a new path: Raf and apoptosis", *Cell Death & Differentiation,* vol. 9, no. 8, pp. 783-785.

Backues, S.K. & Klionsky, D.J. 2011, "Autophagy gets in on the regulatory act.", *Journal Of Molecular Cell Biology,* vol. 3, no. 2, pp. 76-77.

Bakkenist, C.J. & Kastan, M.B. 2004, "Initiating cellular stress responses", *Cell,* vol. 118, no. 1, pp. 9-17.

Bakkenist, C.J. & Kastan, M.B. 2003, "DNA damage activates ATM through intermolecular autophosphorylation and dimer dissociation.", *Nature,* vol. 421, no. 6922, pp. 499-506.

Baljuls, A., Schmitz, W., Mueller, T., Zahedi, R.P., Sickmann, A., Hekman, M. & Rapp, U.R. 2008, "Positive regulation of A-RAF by phosphorylation of isoform-specific hinge segment and identification of novel phosphorylation sites.", *Journal of Biological Chemistry,* vol. 283, no. 40, pp. 27239-27254.

Balmanno, K. & Cook, S.J. 2009, "Tumour cell survival signalling by the ERK1/2 pathway", *Cell Death & Differentiation,* vol. 16, no. 3, pp. 368-377.

Barbacid, M. 1987, "ras genes", *Annual Review of Biochemistry,* vol. 56, pp. 779-827.

Bardwell, L. 2006, "Mechanisms of MAPK signalling specificity.", *Biochemical Society transactions,* vol. 34, no. Pt 5, pp. 837-841.

Barnier, J.V., Papin, C., Eychene, A., Lecoq, O. & Calothy, G. 1995, "The mouse B-raf gene encodes multiple protein isoforms with tissue-specific expression.", *Journal of Biological Chemistry,* vol. 270, no. 40, pp. 23381-23389.

Baumeister, W., Walz, J., Zuhl, F. & Seemuller, E. 1998, "The proteasome: paradigm of a self-compartmentalizing protease", *Cell,* vol. 92, no. 3, pp. 367-380.

Beck, T.W., Huleihel, M., Gunnell, M., Bonner, T.I. & Rapp, U.R. 1987, "The complete coding sequence of the human A-raf-1 oncogene and transforming activity of a human A-raf carrying retrovirus.", *Nucleic acids research,* vol. 15, no. 2, pp. 595-609.

Bennett, D.C. 2003, "Human melanocyte senescence and melanoma susceptibility genes", *Oncogene,* vol. 22, no. 20, pp. 3063-3069.

Berg, T.O., Fengsrud, M., Stromhaug, P.E., Berg, T. & Seglen, P.O. 1998, "Isolation and characterization of rat liver amphisomes. Evidence for fusion of autophagosomes with both early and late endosomes.", *Journal of Biological Chemistry,* vol. 273, no. 34, pp. 21883-21892.

Bivona, T.G., Perez De Castro, I., Ahearn, I.M., Grana, T.M., Chiu, V.K., Lockyer, P.J., Cullen, P.J., Pellicer, A., Cox, A.D. & Philips, M.R. 2003, "Phospholipase Cgamma activates Ras on the Golgi apparatus by means of RasGRP1.", *Nature,* vol. 424, no. 6949, pp. 694-698.

Blasco, R.B., Francoz, S., Santamaria, D., Canamero, M., Dubus, P., Charron, J., Baccarini, M. & Barbacid, M. 2011, "c-Raf, but not B-Raf, is essential for development of K-Ras oncogene-driven non-small cell lung carcinoma.", *Cancer Cell,* vol. 19, no. 5, pp. 652-663.

Bloethner, S., Chen, B., Hemminki, K., Muller-Berghaus, J., Ugurel, S., Schadendorf, D. & Kumar, R. 2005, "Effect of common B-RAF and N-RAS mutations on global gene expression in melanoma cell lines.", *Carcinogenesis,* vol. 26, no. 7, pp. 1224-1232.

Bodnar, A.G., Ouellette, M., Frolkis, M., Holt, S.E., Chiu, C.P., Morin, G.B., Harley, C.B., Shay, J.W., Lichtsteiner, S. & Wright, W.E. 1998, "Extension of life-span by introduction of telomerase into normal human cells.", *Science,* vol. 279, no. 5349, pp. 349-352.

Bollag, G., Hirth, P., Tsai, J., Zhang, J., Ibrahim, P.N., Cho, H., Spevak, W., Zhang, C., Zhang, Y., Habets, G., Burton, E.A., Wong, B., Tsang, G., West, B.L., Powell, B., Shellooe, R., Marimuthu, A., Nguyen, H., Zhang, K.Y., Artis, D.R., Schlessinger, J., Su, F., Higgins, B., Iyer, R., D'Andrea, K., Koehler, A., Stumm, M., Lin, P.S., Lee, R.J., Grippo, J., Puzanov, I., Kim, K.B., Ribas, A., McArthur, G.A., Sosman, J.A., Chapman, P.B., Flaherty, K.T., Xu, X., Nathanson, K.L. & Nolop, K. 2010, "Clinical efficacy of a RAF inhibitor needs broad target blockade in BRAF-mutant melanoma.", *Nature,* vol. 467, no. 7315, pp. 596-599.

Bonni, A., Brunet, A., West, A.E., Datta, S.R., Takasu, M.A. & Greenberg, M.E. 1999, "Cell survival promoted by the Ras-MAPK signaling pathway by transcription-dependent and -independent mechanisms.", *Science,* vol. 286, no. 5443, pp. 1358-1362.

Bos, J.L., Fearon, E.R., Hamilton, S.R., Verlaan-de Vries, M., van Boom, J.H., van der Eb, A.J. & Vogelstein, B. 1987, "Prevalence of ras gene mutations in human colorectal cancers.", *Nature,* vol. 327, no. 6120, pp. 293-297.

Bouyain, S., Longo, P.A., Li, S., Ferguson, K.M. & Leahy, D.J. 2005, "The extracellular region of ErbB4 adopts a tethered conformation in the absence of ligand.", *Proceedings of the National Academy of Sciences of the United States of America,* vol. 102, no. 42, pp. 15024-15029.

Bowtell, D., Fu, P., Simon, M. & Senior, P. 1992, "Identification of murine homologues of the Drosophila son of sevenless gene: potential activators of ras.", *Proceedings of the National Academy of Sciences of the United States of America,* vol. 89, no. 14, pp. 6511-6515.

Brady, S.C., Coleman, M.L., Munro, J., Feller, S.M., Morrice, N.A. & Olson, M.F. 2009, "Sprouty2 association with B-Raf is regulated by phosphorylation and kinase conformation.", *Cancer research,* vol. 69, no. 17, pp. 6773-6781.

Brannigan, J.A., Dodson, G., Duggleby, H.J., Moody, P.C., Smith, J.L., Tomchick, D.R. & Murzin, A.G. 1995, "A protein catalytic framework with an N-terminal nucleophile is capable of self-activation", *Nature,* vol. 378, no. 6555, pp. 416-419.

Brehm, A., Miska, E.A., McCance, D.J., Reid, J.L., Bannister, A.J. & Kouzarides, T. 1998, "Retinoblastoma protein recruits histone deacetylase to repress transcription.", *Nature,* vol. 391, no. 6667, pp. 597-601.

Brondello, J.M., Pouyssegur, J. & McKenzie, F.R. 1999, "Reduced MAP kinase phosphatase-1 degradation after p42/p44MAPK-dependent phosphorylation.", *Science,* vol. 286, no. 5449, pp. 2514-2517.

Brose, M.S., Volpe, P., Feldman, M., Kumar, M., Rishi, I., Gerrero, R., Einhorn, E., Herlyn, M., Minna, J., Nicholson, A., Roth, J.A., Albelda, S.M., Davies, H., Cox, C., Brignell, G., Stephens, P., Futreal, P.A., Wooster, R., Stratton, M.R. & Weber, B.L. 2002, "BRAF and RAS mutations in human lung cancer and melanoma.", *Cancer research,* vol. 62, no. 23, pp. 6997-7000.

Brummer, T., Naegele, H., Reth, M. & Misawa, Y. 2003, "Identification of novel ERK-mediated feedback phosphorylation sites at the C-terminus of B-Raf.", *Oncogene,* vol. 22, no. 55, pp. 8823-8834.

Brummer, T., Shaw, P.E., Reth, M. & Misawa, Y. 2002, "Inducible gene deletion reveals different roles for B-Raf and Raf-1 in B-cell antigen receptor signalling.", *EMBO Journal,* vol. 21, no. 21, pp. 5611-5622.

Bundschu, K., Walter, U. & Schuh, K. 2007, "Getting a first clue about SPRED functions", *Bioessays,* vol. 29, no. 9, pp. 897-907.

Burgess, A.W., Cho, H.S., Eigenbrot, C., Ferguson, K.M., Garrett, T.P., Leahy, D.J., Lemmon, M.A., Sliwkowski, M.X., Ward, C.W. & Yokoyama, S. 2003, "An open-and-shut case? Recent insights into the activation of EGF/ErbB receptors", *Molecular cell,* vol. 12, no. 3, pp. 541-552.

Burma, S., Chen, B.P., Murphy, M., Kurimasa, A. & Chen, D.J. 2001, "ATM phosphorylates histone H2AX in response to DNA double-strand breaks.", *Journal of Biological Chemistry,* vol. 276, no. 45, pp. 42462-42467.

Buschmann, T., Potapova, O., Bar-Shira, A., Ivanov, V.N., Fuchs, S.Y., Henderson, S., Fried, V.A., Minamoto, T., Alarcon-Vargas, D., Pincus, M.R., Gaarde, W.A., Holbrook, N.J., Shiloh, Y. & Ronai, Z. 2001, "Jun NH2-terminal kinase phosphorylation of p53 on Thr-81 is important for p53 stabilization and transcriptional activities in response to stress.", *Molecular & Cellular Biology,* vol. 21, no. 8, pp. 2743-2754.

Butch, E.R. & Guan, K.L. 1996, "Characterization of ERK1 activation site mutants and the effect on recognition by MEK1 and MEK2.", *Journal of Biological Chemistry,* vol. 271, no. 8, pp. 4230-4235.

Cagnol, S. & Chambard, J.C. 2010, "ERK and cell death: mechanisms of ERK-induced cell death--apoptosis, autophagy and senescence", *FEBS Journal,* vol. 277, no. 1, pp. 2-21.

Cagnol, S., Van Obberghen-Schilling, E. & Chambard, J.C. 2006, "Prolonged activation of ERK1,2 induces FADD-independent caspase 8 activation and cell death.", *Apoptosis,* vol. 11, no. 3, pp. 337-346.

Callaway, K., Rainey, M.A. & Dalby, K.N. 2005, "Quantifying ERK2-protein interactions by fluorescence anisotropy: PEA-15 inhibits ERK2 by blocking the binding of DEJL domains", *Biochimica et biophysica acta,* vol. 1754, no. 1-2, pp. 316-323.

Calogeraki, I., Barnier, J.V., Eychene, A., Felder, M.P., Calothy, G. & Marx, M. 1993, "Genomic organization and nucleotide sequence of the coding region of the chicken c-Rmil(B-raf-1) proto-oncogene.", *Biochemical & Biophysical Research Communications,* vol. 193, no. 3, pp. 1324-1331.

Campisi, J. 2005, "Senescent cells, tumor suppression, and organismal aging: good citizens, bad neighbors", *Cell,* vol. 120, no. 4, pp. 513-522.

Carey, K.D., Watson, R.T., Pessin, J.E. & Stork, P.J. 2003, "The requirement of specific membrane domains for Raf-1 phosphorylation and activation.", *Journal of Biological Chemistry,* vol. 278, no. 5, pp. 3185-3196.

Cargnello, M. & Roux, P.P. 2011a, "Activation and function of the MAPKs and their substrates, the MAPK-activated protein kinases", *Microbiology & Molecular Biology Reviews,* vol. 75, no. 1, pp. 50-83.

Carragher, L.A., Snell, K.R., Giblett, S.M., Aldridge, V.S., Patel, B., Cook, S.J., Winton, D.J., Marais, R. & Pritchard, C.A. 2010a, "V600EBraf induces gastrointestinal crypt senescence and promotes tumour progression through enhanced CpG methylation of p16INK4a.", *EMBO molecular medicine,* vol. 2, no. 11, pp. 458-471.

Carrier, F., Georgel, P.T., Pourquier, P., Blake, M., Kontny, H.U., Antinore, M.J., Gariboldi, M., Myers, T.G., Weinstein, J.N., Pommier, Y. & Fornace, A.J.,Jr 1999, "Gadd45, a p53-responsive stress protein, modifies DNA accessibility on damaged chromatin.", *Molecular & Cellular Biology,* vol. 19, no. 3, pp. 1673-1685.

Carriere, A., Cargnello, M., Julien, L.A., Gao, H., Bonneil, E., Thibault, P. & Roux, P.P. 2008, "Oncogenic MAPK signaling stimulates mTORC1 activity by promoting RSK-mediated raptor phosphorylation.", *Current Biology,* vol. 18, no. 17, pp. 1269-1277.

Carriere, A., Romeo, Y., Acosta-Jaquez, H.A., Moreau, J., Bonneil, E., Thibault, P., Fingar, D.C. & Roux, P.P. 2011, "ERK1/2 phosphorylate Raptor to promote Ras-dependent activation of mTOR complex 1 (mTORC1).", *Journal of Biological Chemistry,* vol. 286, no. 1, pp. 567-577.

Carvalho, I., Milanezi, F., Martins, A., Reis, R.M. & Schmitt, F. 2005, "Overexpression of platelet-derived growth factor receptor alpha in breast cancer is associated with tumour progression.", *Breast Cancer Research,* vol. 7, no. 5, pp. R788-95.

Casey, P.J. & Seabra, M.C. 1996, "Protein prenyltransferases", *Journal of Biological Chemistry,* vol. 271, no. 10, pp. 5289-5292.

Catalanotti, F., Reyes, G., Jesenberger, V., Galabova-Kovacs, G., de Matos Simoes, R., Carugo, O. & Baccarini, M. 2009, "A Mek1-Mek2 heterodimer determines the

strength and duration of the Erk signal.", *Nature Structural & Molecular Biology,* vol. 16, no. 3, pp. 294-303.

Caunt, C.J., Armstrong, S.P., Rivers, C.A., Norman, M.R. & McArdle, C.A. 2008, "Spatiotemporal regulation of ERK2 by dual specificity phosphatases.", *Journal of Biological Chemistry,* vol. 283, no. 39, pp. 26612-26623.

Cebollero, E. & Reggiori, F. 2009, "Regulation of autophagy in yeast Saccharomyces cerevisiae", *Biochimica et biophysica acta,* vol. 1793, no. 9, pp. 1413-1421.

Chainiaux, F., Magalhaes, J.P., Eliaers, F., Remacle, J. & Toussaint, O. 2002, "UVB-induced premature senescence of human diploid skin fibroblasts.", *International Journal of Biochemistry & Cell Biology,* vol. 34, no. 11, pp. 1331-1339.

Chambard, J.C., Lefloch, R., Pouyssegur, J. & Lenormand, P. 2007, "ERK implication in cell cycle regulation", *Biochimica et biophysica acta,* vol. 1773, no. 8, pp. 1299-1310.

Chan, E.Y., Kir, S. & Tooze, S.A. 2007, "siRNA screening of the kinome identifies ULK1 as a multidomain modulator of autophagy.", *Journal of Biological Chemistry,* vol. 282, no. 35, pp. 25464-25474.

Chang, C.I., Xu, B.E., Akella, R., Cobb, M.H. & Goldsmith, E.J. 2002, "Crystal structures of MAP kinase p38 complexed to the docking sites on its nuclear substrate MEF2A and activator MKK3b.", *Molecular cell,* vol. 9, no. 6, pp. 1241-1249.

Chapman, P.B., Hauschild, A., Robert, C., Haanen, J.B., Ascierto, P., Larkin, J., Dummer, R., Garbe, C., Testori, A., Maio, M., Hogg, D., Lorigan, P., Lebbe, C., Jouary, T., Schadendorf, D., Ribas, A., O'Day, S.J., Sosman, J.A., Kirkwood, J.M., Eggermont, A.M., Dreno, B., Nolop, K., Li, J., Nelson, B., Hou, J., Lee, R.J., Flaherty, K.T., McArthur, G.A. & BRIM-3 Study, G. 2011, "Improved survival with vemurafenib in melanoma with BRAF V600E mutation.", *New England Journal of Medicine,* vol. 364, no. 26, pp. 2507-2516.

Chehab, N.H., Malikzay, A., Appel, M. & Halazonetis, T.D. 2000a, "Chk2/hCds1 functions as a DNA damage checkpoint in G(1) by stabilizing p53.", *Genes & development,* vol. 14, no. 3, pp. 278-288.

Chen, P.L., Scully, P., Shew, J.Y., Wang, J.Y. & Lee, W.H. 1989, "Phosphorylation of the retinoblastoma gene product is modulated during the cell cycle and cellular differentiation.", *Cell,* vol. 58, no. 6, pp. 1193-1198.

Chen, R.H., Juo, P.C., Curran, T. & Blenis, J. 1996, "Phosphorylation of c-Fos at the C-terminus enhances its transforming activity.", *Oncogene,* vol. 12, no. 7, pp. 1493-1502.

Chen, T.T. & Wang, J.Y. 2000, "Establishment of irreversible growth arrest in myogenic differentiation requires the RB LXCXE-binding function.", *Molecular & Cellular Biology,* vol. 20, no. 15, pp. 5571-5580.

Chiu, V.K., Bivona, T., Hach, A., Sajous, J.B., Silletti, J., Wiener, H., Johnson, R.L.,2nd, Cox, A.D. & Philips, M.R. 2002, "Ras signalling on the endoplasmic reticulum and the Golgi.", *Nature cell biology,* vol. 4, no. 5, pp. 343-350.

Choy, E., Chiu, V.K., Silletti, J., Feoktistov, M., Morimoto, T., Michaelson, D., Ivanov, I.E. & Philips, M.R. 1999, "Endomembrane trafficking of ras: the CAAX motif targets proteins to the ER and Golgi.", *Cell,* vol. 98, no. 1, pp. 69-80.

Ciechanover, A. 1998, "The ubiquitin-proteasome pathway: on protein death and cell life", *EMBO Journal,* vol. 17, no. 24, pp. 7151-7160.

Clague, M.J. & Urbe, S. 2010a, "Ubiquitin: same molecule, different degradation pathways", *Cell,* vol. 143, no. 5, pp. 682-685.

Clarke, S. 1992, "Protein isoprenylation and methylation at carboxyl-terminal cysteine residues", *Annual Review of Biochemistry,* vol. 61, pp. 355-386.

Clarke, S., Vogel, J.P., Deschenes, R.J. & Stock, J. 1988, "Posttranslational modification of the Ha-ras oncogene protein: evidence for a third class of protein carboxyl methyltransferases", *Proceedings of the National Academy of Sciences of the United States of America,* vol. 85, no. 13, pp. 4643-4647.

Classon, M. & Dyson, N. 2001, "p107 and p130: versatile proteins with interesting pockets", *Experimental cell research,* vol. 264, no. 1, pp. 135-147.

Clayton, A.L. & Mahadevan, L.C. 2003, "MAP kinase-mediated phosphoacetylation of histone H3 and inducible gene regulation", *FEBS letters,* vol. 546, no. 1, pp. 51-58.

Clevers, H. 2006, "Wnt/beta-catenin signaling in development and disease", *Cell,* vol. 127, no. 3, pp. 469-480.

Cobb, M.H., Boulton, T.G. & Robbins, D.J. 1991, "Extracellular signal-regulated kinases: ERKs in progress", *Cell regulation,* vol. 2, no. 12, pp. 965-978.

Colicelli, J. 2004, "Human RAS superfamily proteins and related GTPases", *Science's Stke [Electronic Resource]: Signal Transduction Knowledge Environment,* vol. 2004, no. 250, pp. RE13.

Collado, M., Gil, J., Efeyan, A., Guerra, C., Schuhmacher, A.J., Barradas, M., Benguria, A., Zaballos, A., Flores, J.M., Barbacid, M., Beach, D. & Serrano, M. 2005, "Tumour biology: senescence in premalignant tumours.", *Nature,* vol. 436, no. 7051, pp. 642.

Connell, P., Ballinger, C.A., Jiang, J., Wu, Y., Thompson, L.J., Hohfeld, J. & Patterson, C. 2001, "The co-chaperone CHIP regulates protein triage decisions mediated by heat-shock proteins.", *Nature cell biology,* vol. 3, no. 1, pp. 93-96.

Cory, S. & Adams, J.M. 2002a, "The Bcl2 family: regulators of the cellular life-or-death switch", *Nature Reviews.Cancer,* vol. 2, no. 9, pp. 647-656.

Courtois-Cox, S., Genther Williams, S.M., Reczek, E.E., Johnson, B.W., McGillicuddy, L.T., Johannessen, C.M., Hollstein, P.E., MacCollin, M. & Cichowski, K. 2006a, "A negative feedback signaling network underlies oncogene-induced senescence", *Cancer Cell,* vol. 10, no. 6, pp. 459-472.

Coux, O., Tanaka, K. & Goldberg, A.L. 1996, "Structure and functions of the 20S and 26S proteasomes", *Annual Review of Biochemistry,* vol. 65, pp. 801-847.

Cutler, R.E.,Jr, Stephens, R.M., Saracino, M.R. & Morrison, D.K. 1998, "Autoregulation of the Raf-1 serine/threonine kinase.", *Proceedings of the National Academy of Sciences of the United States of America,* vol. 95, no. 16, pp. 9214-9219.

Dalby, K.N., Morrice, N., Caudwell, F.B., Avruch, J. & Cohen, P. 1998, "Identification of regulatory phosphorylation sites in mitogen-activated protein kinase (MAPK)-activated protein kinase-1a/p90rsk that are inducible by MAPK.", *Journal of Biological Chemistry,* vol. 273, no. 3, pp. 1496-1505.

Danielian, P.S., Muccino, D., Rowitch, D.H., Michael, S.K. & McMahon, A.P. 1998, "Modification of gene activity in mouse embryos in utero by a tamoxifen-inducible form of Cre recombinase.", *Current Biology,* vol. 8, no. 24, pp. 1323-1326.

Danielian, P.S., White, R., Hoare, S.A., Fawell, S.E. & Parker, M.G. 1993, "Identification of residues in the estrogen receptor that confer differential sensitivity to estrogen and hydroxytamoxifen.", *Molecular Endocrinology,* vol. 7, no. 2, pp. 232-240.

Dankort, D., Filenova, E., Collado, M., Serrano, M., Jones, K. & McMahon, M. 2007, "A new mouse model to explore the initiation, progression, and therapy of BRAFV600E-induced lung tumors.", *Genes & development,* vol. 21, no. 4, pp. 379-384.

DaSilva, J., Xu, L., Kim, H.J., Miller, W.T. & Bar-Sagi, D. 2006, "Regulation of sprouty stability by Mnk1-dependent phosphorylation.", *Molecular & Cellular Biology,* vol. 26, no. 5, pp. 1898-1907.

Davie, J.R. & Spencer, V.A. 1999, "Control of histone modifications", *Journal of cellular biochemistry,* , no. Suppl 32-33, pp. 141-148.

Davies, H., Bignell, G.R., Cox, C., Stephens, P., Edkins, S., Clegg, S., Teague, J., Woffendin, H., Garnett, M.J., Bottomley, W., Davis, N., Dicks, E., Ewing, R., Floyd, Y., Gray, K., Hall, S., Hawes, R., Hughes, J., Kosmidou, V., Menzies, A., Mould, C., Parker, A., Stevens, C., Watt, S., Hooper, S., Wilson, R., Jayatilake, H., Gusterson, B.A., Cooper, C., Shipley, J., Hargrave, D., Pritchard-Jones, K., Maitland, N., Chenevix-Trench, G., Riggins, G.J., Bigner, D.D., Palmieri, G., Cossu, A., Flanagan, A., Nicholson, A., Ho, J.W., Leung, S.Y., Yuen, S.T., Weber, B.L., Seigler, H.F., Darrow, T.L., Paterson, H., Marais, R., Marshall, C.J., Wooster, R., Stratton, M.R. & Futreal, P.A. 2002, "Mutations of the BRAF gene in human cancer.", *Nature,* vol. 417, no. 6892, pp. 949-954.

Davis, I.J., Hazel, T.G., Chen, R.H., Blenis, J. & Lau, L.F. 1993, "Functional domains and phosphorylation of the orphan receptor Nur77.", *Molecular Endocrinology,* vol. 7, no. 8, pp. 953-964.

De Vries, L., Zheng, B., Fischer, T., Elenko, E. & Farquhar, M.G. 2000, "The regulator of G protein signaling family", *Annual Review of Pharmacology & Toxicology,* vol. 40, pp. 235-271.

Deak, M., Clifton, A.D., Lucocq, L.M. & Alessi, D.R. 1998, "Mitogen- and stress-activated protein kinase-1 (MSK1) is directly activated by MAPK and SAPK2/p38, and may mediate activation of CREB.", *EMBO Journal,* vol. 17, no. 15, pp. 4426-4441.

DeHaan, R.D., Yazlovitskaya, E.M. & Persons, D.L. 2001, "Regulation of p53 target gene expression by cisplatin-induced extracellular signal-regulated kinase.", *Cancer Chemotherapy & Pharmacology,* vol. 48, no. 5, pp. 383-388.

Demand, J., Alberti, S., Patterson, C. & Hohfeld, J. 2001a, "Cooperation of a ubiquitin domain protein and an E3 ubiquitin ligase during chaperone/proteasome coupling", *Current Biology,* vol. 11, no. 20, pp. 1569-1577.

Dephoure, N., Zhou, C., Villen, J., Beausoleil, S.A., Bakalarski, C.E., Elledge, S.J. & Gygi, S.P. 2008, "A quantitative atlas of mitotic phosphorylation.", *Proceedings of the National Academy of Sciences of the United States of America,* vol. 105, no. 31, pp. 10762-10767.

Dhillon, A.S., Hagan, S., Rath, O. & Kolch, W. 2007, "MAP kinase signalling pathways in cancer", *Oncogene,* vol. 26, no. 22, pp. 3279-3290.

Dhillon, A.S., Meikle, S., Yazici, Z., Eulitz, M. & Kolch, W. 2002a, "Regulation of Raf-1 activation and signalling by dephosphorylation.", *EMBO Journal,* vol. 21, no. 1-2, pp. 64-71.

Dhomen, N., Da Rocha Dias, S., Hayward, R., Ogilvie, L., Hedley, D., Delmas, V., McCarthy, A., Henderson, D., Springer, C.J., Pritchard, C., Larue, L. & Marais, R. 2010, "Inducible expression of (V600E) Braf using tyrosinase-driven Cre recombinase results in embryonic lethality", *Pigment Cell & Melanoma Research,* vol. 23, no. 1, pp. 112-120.

Dhomen, N., Reis-Filho, J.S., da Rocha Dias, S., Hayward, R., Savage, K., Delmas, V., Larue, L., Pritchard, C. & Marais, R. 2009, "Oncogenic Braf induces melanocyte senescence and melanoma in mice.", *Cancer Cell,* vol. 15, no. 4, pp. 294-303.

Di Leonardo, A., Linke, S.P., Clarkin, K. & Wahl, G.M. 1994, "DNA damage triggers a prolonged p53-dependent G1 arrest and long-term induction of Cip1 in normal human fibroblasts.", *Genes & development,* vol. 8, no. 21, pp. 2540-2551.

Dimitri, C.A., Dowdle, W., MacKeigan, J.P., Blenis, J. & Murphy, L.O. 2005, "Spatially separate docking sites on ERK2 regulate distinct signaling events in vivo.", *Current Biology,* vol. 15, no. 14, pp. 1319-1324.

Dimri, G.P., Lee, X., Basile, G., Acosta, M., Scott, G., Roskelley, C., Medrano, E.E., Linskens, M., Rubelj, I. & Pereira-Smith, O. 1995a, "A biomarker that identifies senescent human cells in culture and in aging skin in vivo.", *Proceedings of the National Academy of Sciences of the United States of America,* vol. 92, no. 20, pp. 9363-9367.

Doble, B.W. & Woodgett, J.R. 2003, "GSK-3: tricks of the trade for a multi-tasking kinase", *Journal of cell science,* vol. 116, no. Pt 7, pp. 1175-1186.

Dougherty, M.K., Muller, J., Ritt, D.A., Zhou, M., Zhou, X.Z., Copeland, T.D., Conrads, T.P., Veenstra, T.D., Lu, K.P. & Morrison, D.K. 2005, "Regulation of Raf-1 by direct feedback phosphorylation.", *Molecular cell,* vol. 17, no. 2, pp. 215-224.

Downward, J. 2003, "Targeting RAS signalling pathways in cancer therapy", *Nature Reviews.Cancer,* vol. 3, no. 1, pp. 11-22.

Drosopoulos, K.G., Roberts, M.L., Cermak, L., Sasazuki, T., Shirasawa, S., Andera, L. & Pintzas, A. 2005, "Transformation by oncogenic RAS sensitizes human colon cells to TRAIL-induced apoptosis by up-regulating death receptor 4 and death receptor 5 through a MEK-dependent pathway.", *Journal of Biological Chemistry,* vol. 280, no. 24, pp. 22856-22867.

Dumaz, N., Hayward, R., Martin, J., Ogilvie, L., Hedley, D., Curtin, J.A., Bastian, B.C., Springer, C. & Marais, R. 2006, "In melanoma, RAS mutations are accompanied by switching signaling from BRAF to CRAF and disrupted cyclic AMP signaling.", *Cancer research,* vol. 66, no. 19, pp. 9483-9491.

Dye, B.T. & Schulman, B.A. 2007, "Structural mechanisms underlying posttranslational modification by ubiquitin-like proteins.", *Annual Review of Biophysics & Biomolecular Structure,* vol. 36, pp. 131-150.

Eblen, S.T., Slack-Davis, J.K., Tarcsafalvi, A., Parsons, J.T., Weber, M.J. & Catling, A.D. 2004, "Mitogen-activated protein kinase feedback phosphorylation regulates MEK1 complex formation and activation during cellular adhesion.", *Molecular & Cellular Biology,* vol. 24, no. 6, pp. 2308-2317.

Ehrenreiter, K., Kern, F., Velamoor, V., Meissl, K., Galabova-Kovacs, G., Sibilia, M. & Baccarini, M. 2009, "Raf-1 addiction in Ras-induced skin carcinogenesis.", *Cancer Cell,* vol. 16, no. 2, pp. 149-160.

Ekerot, M., Stavridis, M.P., Delavaine, L., Mitchell, M.P., Staples, C., Owens, D.M., Keenan, I.D., Dickinson, R.J., Storey, K.G. & Keyse, S.M. 2008, "Negative-feedback regulation of FGF signalling by DUSP6/MKP-3 is driven by ERK1/2 and mediated by Ets factor binding to a conserved site within the DUSP6/MKP-3 gene promoter.", *Biochemical Journal,* vol. 412, no. 2, pp. 287-298.

Emuss, V., Garnett, M., Mason, C. & Marais, R. 2005, "Mutations of C-RAF are rare in human cancer because C-RAF has a low basal kinase activity compared with B-RAF.", *Cancer research,* vol. 65, no. 21, pp. 9719-9726.

Ewings, K.E., Hadfield-Moorhouse, K., Wiggins, C.M., Wickenden, J.A., Balmanno, K., Gilley, R., Degenhardt, K., White, E. & Cook, S.J. 2007, "ERK1/2-dependent phosphorylation of BimEL promotes its rapid dissociation from Mcl-1 and Bcl-xL.", *EMBO Journal,* vol. 26, no. 12, pp. 2856-2867.

Ezhevsky, S.A., Nagahara, H., Vocero-Akbani, A.M., Gius, D.R., Wei, M.C. & Dowdy, S.F. 1997, "Hypo-phosphorylation of the retinoblastoma protein (pRb) by cyclin D:Cdk4/6 complexes results in active pRb.", *Proceedings of the National Academy of Sciences of the United States of America,* vol. 94, no. 20, pp. 10699-10704.

Fabian, J.R., Daar, I.O. & Morrison, D.K. 1993, "Critical tyrosine residues regulate the enzymatic and biological activity of Raf-1 kinase.", *Molecular & Cellular Biology,* vol. 13, no. 11, pp. 7170-7179.

Falck, J., Mailand, N., Syljuasen, R.G., Bartek, J. & Lukas, J. 2001, "The ATM-Chk2-Cdc25A checkpoint pathway guards against radioresistant DNA synthesis.", *Nature,* vol. 410, no. 6830, pp. 842-847.

Favata, M.F., Horiuchi, K.Y., Manos, E.J., Daulerio, A.J., Stradley, D.A., Feeser, W.S., Van Dyk, D.E., Pitts, W.J., Earl, R.A., Hobbs, F., Copeland, R.A., Magolda, R.L., Scherle, P.A. & Trzaskos, J.M. 1998, "Identification of a novel inhibitor of mitogen-activated protein kinase kinase.", *Journal of Biological Chemistry,* vol. 273, no. 29, pp. 18623-18632.

Fawell, S.E., Lees, J.A., White, R. & Parker, M.G. 1990, "Characterization and colocalization of steroid binding and dimerization activities in the mouse estrogen receptor.", *Cell,* vol. 60, no. 6, pp. 953-962.

Ferguson, C.A. & Kidson, S.H. 1997, "The regulation of tyrosinase gene transcription", *Pigment Cell Research,* vol. 10, no. 3, pp. 127-138.

Fingar, D.C., Salama, S., Tsou, C., Harlow, E. & Blenis, J. 2002, "Mammalian cell size is controlled by mTOR and its downstream targets S6K1 and 4EBP1/eIF4E.", *Genes & development,* vol. 16, no. 12, pp. 1472-1487.

Fiol, C.J., Wang, A., Roeske, R.W. & Roach, P.J. 1990, "Ordered multisite protein phosphorylation. Analysis of glycogen synthase kinase 3 action using model peptide substrates.", *Journal of Biological Chemistry,* vol. 265, no. 11, pp. 6061-6065.

Fischer, A., Baljuls, A., Reinders, J., Nekhoroshkova, E., Sibilski, C., Metz, R., Albert, S., Rajalingam, K., Hekman, M. & Rapp, U.R. 2009, "Regulation of RAF activity by 14-3-3 proteins: RAF kinases associate functionally with both homo- and heterodimeric forms of 14-3-3 proteins.", *Journal of Biological Chemistry,* vol. 284, no. 5, pp. 3183-3194.

Fischmann, T.O., Smith, C.K., Mayhood, T.W., Myers, J.E., Reichert, P., Mannarino, A., Carr, D., Zhu, H., Wong, J., Yang, R.S., Le, H.V. & Madison, V.S. 2009, "Crystal structures of MEK1 binary and ternary complexes with nucleotides and inhibitors.", *Biochemistry,* vol. 48, no. 12, pp. 2661-2674.

Flaherty, K.T., Infante, J.R., Daud, A., Gonzalez, R., Kefford, R.F., Sosman, J., Hamid, O., Schuchter, L., Cebon, J., Ibrahim, N., Kudchadkar, R., Burris, H.A.,3rd, Falchook, G., Algazi, A., Lewis, K., Long, G.V., Puzanov, I., Lebowitz, P., Singh, A., Little, S., Sun, P., Allred, A., Ouellet, D., Kim, K.B., Patel, K. & Weber, J. 2012, "Combined BRAF and MEK inhibition in melanoma with BRAF V600 mutations.", *New England Journal of Medicine,* vol. 367, no. 18, pp. 1694-1703.

Flaherty, K.T., Puzanov, I., Kim, K.B., Ribas, A., McArthur, G.A., Sosman, J.A., O'Dwyer, P.J., Lee, R.J., Grippo, J.F., Nolop, K. & Chapman, P.B. 2010, "Inhibition of mutated, activated BRAF in metastatic melanoma.", *New England Journal of Medicine,* vol. 363, no. 9, pp. 809-819.

Flotow, H., Graves, P.R., Wang, A.Q., Fiol, C.J., Roeske, R.W. & Roach, P.J. 1990, "Phosphate groups as substrate determinants for casein kinase I action.", *Journal of Biological Chemistry,* vol. 265, no. 24, pp. 14264-14269.

Fong, C.W., Chua, M.S., McKie, A.B., Ling, S.H., Mason, V., Li, R., Yusoff, P., Lo, T.L., Leung, H.Y., So, S.K. & Guy, G.R. 2006, "Sprouty 2, an inhibitor of mitogen-activated protein kinase signaling, is down-regulated in hepatocellular carcinoma.", *Cancer research,* vol. 66, no. 4, pp. 2048-2058.

Fong, C.W., Leong, H.F., Wong, E.S., Lim, J., Yusoff, P. & Guy, G.R. 2003, "Tyrosine phosphorylation of Sprouty2 enhances its interaction with c-Cbl and is crucial for its function.", *Journal of Biological Chemistry,* vol. 278, no. 35, pp. 33456-33464.

Foster, K.G. & Fingar, D.C. 2010, "Mammalian target of rapamycin (mTOR): conducting the cellular signaling symphony", *Journal of Biological Chemistry,* vol. 285, no. 19, pp. 14071-14077.

Frodin, M., Jensen, C.J., Merienne, K. & Gammeltoft, S. 2000, "A phosphoserine-regulated docking site in the protein kinase RSK2 that recruits and activates PDK1.", *EMBO Journal,* vol. 19, no. 12, pp. 2924-2934.

Fuchs, S.Y., Spiegelman, V.S. & Kumar, K.G. 2004a, "The many faces of beta-TrCP E3 ubiquitin ligases: reflections in the magic mirror of cancer", *Oncogene,* vol. 23, no. 11, pp. 2028-2036.

Fueller, J., Becker, M., Sienerth, A.R., Fischer, A., Hotz, C. & Galmiche, A. 2008, "C-RAF activation promotes BAD poly-ubiquitylation and turn-over by the proteasome.", *Biochemical & Biophysical Research Communications,* vol. 370, no. 4, pp. 552-556.

Furukawa, T., Yatsuoka, T., Youssef, E.M., Abe, T., Yokoyama, T., Fukushige, S., Soeda, E., Hoshi, M., Hayashi, Y., Sunamura, M., Kobari, M. & Horii, A. 1998, "Genomic analysis of DUSP6, a dual specificity MAP kinase phosphatase, in pancreatic cancer.", *Cytogenetics & Cell Genetics,* vol. 82, no. 3-4, pp. 156-159.

Galanis, A., Yang, S.H. & Sharrocks, A.D. 2001, "Selective targeting of MAPKs to the ETS domain transcription factor SAP-1.", *Journal of Biological Chemistry,* vol. 276, no. 2, pp. 965-973.

Galibert, F., Dupont de Dinechin, S., Righi, M. & Stehelin, D. 1984, "The second oncogene mil of avian retrovirus MH2 is related to the src gene family.", *EMBO Journal,* vol. 3, no. 6, pp. 1333-1338.

Ganley, I.G., Lam du, H., Wang, J., Ding, X., Chen, S. & Jiang, X. 2009, "ULK1.ATG13.FIP200 complex mediates mTOR signaling and is essential for autophagy.", *Journal of Biological Chemistry,* vol. 284, no. 18, pp. 12297-12305.

Gao, C., Cao, W., Bao, L., Zuo, W., Xie, G., Cai, T., Fu, W., Zhang, J., Wu, W., Zhang, X. & Chen, Y.G. 2010, "Autophagy negatively regulates Wnt signalling by promoting Dishevelled degradation.", *Nature cell biology,* vol. 12, no. 8, pp. 781-790.

Garnett, M.J. & Marais, R. 2004, "Guilty as charged: B-RAF is a human oncogene", *Cancer Cell,* vol. 6, no. 4, pp. 313-319.

Garnett, M.J., Rana, S., Paterson, H., Barford, D. & Marais, R. 2005a, "Wild-type and mutant B-RAF activate C-RAF through distinct mechanisms involving heterodimerization.", *Molecular cell,* vol. 20, no. 6, pp. 963-969.

Garrett, T.P., McKern, N.M., Lou, M., Elleman, T.C., Adams, T.E., Lovrecz, G.O., Zhu, H.J., Walker, F., Frenkel, M.J., Hoyne, P.A., Jorissen, R.N., Nice, E.C., Burgess, A.W. & Ward, C.W. 2002, "Crystal structure of a truncated epidermal growth factor receptor extracellular domain bound to transforming growth factor alpha.", *Cell,* vol. 110, no. 6, pp. 763-773.

Gilmartin, A.G., Bleam, M.R., Groy, A., Moss, K.G., Minthorn, E.A., Kulkarni, S.G., Rominger, C.M., Erskine, S., Fisher, K.E., Yang, J., Zappacosta, F., Annan, R., Sutton, D. & Laquerre, S.G. 2011, "GSK1120212 (JTP-74057) is an inhibitor of MEK activity and activation with favorable pharmacokinetic properties for sustained in vivo pathway inhibition.", *Clinical Cancer Research,* vol. 17, no. 5, pp. 989-1000.

Ginty, D.D., Bonni, A. & Greenberg, M.E. 1994, "Nerve growth factor activates a Ras-dependent protein kinase that stimulates c-fos transcription via phosphorylation of CREB.", *Cell,* vol. 77, no. 5, pp. 713-725.

Gluck, U., Kwiatkowski, D.J. & Ben-Ze'ev, A. 1993, "Suppression of tumorigenicity in simian virus 40-transformed 3T3 cells transfected with alpha-actinin cDNA.", *Proceedings of the National Academy of Sciences of the United States of America,* vol. 90, no. 2, pp. 383-387.

Gnad, F., Gunawardena, J. & Mann, M. 2011, "PHOSIDA 2011: the posttranslational modification database.", *Nucleic acids research,* vol. 39, no. Database issue, pp. 253-260.

Gonzalez, F.A., Seth, A., Raden, D.L., Bowman, D.S., Fay, F.S. & Davis, R.J. 1993, "Serum-induced translocation of mitogen-activated protein kinase to the cell surface ruffling membrane and the nucleus.", *Journal of Cell Biology,* vol. 122, no. 5, pp. 1089-1101.

Goossens, K., Van Poucke, M., Van Soom, A., Vandesompele, J., Van Zeveren, A. & Peelman, L.J. 2005, "Selection of reference genes for quantitative real-time PCR in bovine preimplantation embryos.", *BMC Developmental Biology,* vol. 5, pp. 27.

Gopalbhai, K., Jansen, G., Beauregard, G., Whiteway, M., Dumas, F., Wu, C. & Meloche, S. 2003, "Negative regulation of MAPKK by phosphorylation of a conserved serine residue equivalent to Ser212 of MEK1.", *Journal of Biological Chemistry,* vol. 278, no. 10, pp. 8118-8125.

Grandis, J.R. & Sok, J.C. 2004, "Signaling through the epidermal growth factor receptor during the development of malignancy", *Pharmacology & therapeutics,* vol. 102, no. 1, pp. 37-46.

Gray-Schopfer, V., Wellbrock, C. & Marais, R. 2007, "Melanoma biology and new targeted therapy", *Nature,* vol. 445, no. 7130, pp. 851-857.

Grbovic, O.M., Basso, A.D., Sawai, A., Ye, Q., Friedlander, P., Solit, D. & Rosen, N. 2006, "V600E B-Raf requires the Hsp90 chaperone for stability and is degraded in response to Hsp90 inhibitors.", *Proceedings of the National Academy of Sciences of the United States of America,* vol. 103, no. 1, pp. 57-62.

Grollman, A.P. 1968, "Inhibitors of protein biosynthesis. V. Effects of emetine on protein and nucleic acid biosynthesis in HeLa cells.", *Journal of Biological Chemistry,* vol. 243, no. 15, pp. 4089-4094.

Guan, K.L., Figueroa, C., Brtva, T.R., Zhu, T., Taylor, J., Barber, T.D. & Vojtek, A.B. 2000, "Negative regulation of the serine/threonine kinase B-Raf by Akt.", *Journal of Biological Chemistry,* vol. 275, no. 35, pp. 27354-27359.

Guo, J.Y., Chen, H.Y., Mathew, R., Fan, J., Strohecker, A.M., Karsli-Uzunbas, G., Kamphorst, J.J., Chen, G., Lemons, J.M., Karantza, V., Coller, H.A., Dipaola, R.S., Gelinas, C., Rabinowitz, J.D. & White, E. 2011, "Activated Ras requires autophagy to maintain oxidative metabolism and tumorigenesis.", *Genes & development,* vol. 25, no. 5, pp. 460-470.

Guy, G.R., Jackson, R.A., Yusoff, P. & Chow, S.Y. 2009, "Sprouty proteins: modified modulators, matchmakers or missing links?", *Journal of Endocrinology,* vol. 203, no. 2, pp. 191-202.

Guy, G.R., Wong, E.S., Yusoff, P., Chandramouli, S., Lo, T.L., Lim, J. & Fong, C.W. 2003, "Sprouty: how does the branch manager work?", *Journal of cell science,* vol. 116, no. Pt 15, pp. 3061-3068.

Gwinn, D.M., Shackelford, D.B., Egan, D.F., Mihaylova, M.M., Mery, A., Vasquez, D.S., Turk, B.E. & Shaw, R.J. 2008, "AMPK phosphorylation of raptor mediates a metabolic checkpoint.", *Molecular cell,* vol. 30, no. 2, pp. 214-226.

Hacohen, N., Kramer, S., Sutherland, D., Hiromi, Y. & Krasnow, M.A. 1998, "sprouty encodes a novel antagonist of FGF signaling that patterns apical branching of the Drosophila airways.", *Cell,* vol. 92, no. 2, pp. 253-263.

Halilovic, E., She, Q.B., Ye, Q., Pagliarini, R., Sellers, W.R., Solit, D.B. & Rosen, N. 2010, "PIK3CA mutation uncouples tumor growth and cyclin D1 regulation from MEK/ERK and mutant KRAS signaling.", *Cancer research,* vol. 70, no. 17, pp. 6804-6814.

Hamilton, D.L. & Abremski, K. 1984, "Site-specific recombination by the bacteriophage P1 lox-Cre system. Cre-mediated synapsis of two lox sites.", *Journal of Molecular Biology,* vol. 178, no. 2, pp. 481-486.

Hanafusa, H., Torii, S., Yasunaga, T. & Nishida, E. 2002, "Sprouty1 and Sprouty2 provide a control mechanism for the Ras/MAPK signalling pathway.", *Nature cell biology,* vol. 4, no. 11, pp. 850-858.

Hanahan, D. & Weinberg, R.A. 2000, "The hallmarks of cancer", *Cell,* vol. 100, no. 1, pp. 57-70.

Hancock, J.F. & Parton, R.G. 2005, "Ras plasma membrane signalling platforms", *Biochemical Journal,* vol. 389, no. Pt 1, pp. 1-11.

Hardie, D.G. 2007, "AMP-activated/SNF1 protein kinases: conserved guardians of cellular energy", *Nature Reviews Molecular Cell Biology,* vol. 8, no. 10, pp. 774-785.

Harley, C.B., Futcher, A.B. & Greider, C.W. 1990, "Telomeres shorten during ageing of human fibroblasts.", *Nature,* vol. 345, no. 6274, pp. 458-460.

Harper, J.W., Adami, G.R., Wei, N., Keyomarsi, K. & Elledge, S.J. 1993, "The p21 Cdk-interacting protein Cip1 is a potent inhibitor of G1 cyclin-dependent kinases.", *Cell,* vol. 75, no. 4, pp. 805-816.

Harris, K., Lamson, R.E., Nelson, B., Hughes, T.R., Marton, M.J., Roberts, C.J., Boone, C. & Pryciak, P.M. 2001, "Role of scaffolds in MAP kinase pathway specificity revealed by custom design of pathway-dedicated signaling proteins.", *Current Biology,* vol. 11, no. 23, pp. 1815-1824.

Harrison, R.E. & Turley, E.A. 2001, "Active erk regulates microtubule stability in H-ras-transformed cells.", *Neoplasia (New York),* vol. 3, no. 5, pp. 385-394.

Hartl, F.U. & Hayer-Hartl, M. 2009a, "Converging concepts of protein folding in vitro and in vivo", *Nature Structural & Molecular Biology,* vol. 16, no. 6, pp. 574-581.

Hartl, F.U. & Hayer-Hartl, M. 2009b, "Converging concepts of protein folding in vitro and in vivo", *Nature Structural & Molecular Biology,* vol. 16, no. 6, pp. 574-581.

Harvey, J.J. 1964, "AN UNIDENTIFIED VIRUS WHICH CAUSES THE RAPID PRODUCTION OF TUMOURS IN MICE.", *Nature,* vol. 204, pp. 1104-1105.

Hatzivassiliou, G., Song, K., Yen, I., Brandhuber, B.J., Anderson, D.J., Alvarado, R., Ludlam, M.J., Stokoe, D., Gloor, S.L., Vigers, G., Morales, T., Aliagas, I., Liu, B., Sideris, S., Hoeflich, K.P., Jaiswal, B.S., Seshagiri, S., Koeppen, H., Belvin, M.,

Friedman, L.S. & Malek, S. 2010, "RAF inhibitors prime wild-type RAF to activate the MAPK pathway and enhance growth.", *Nature,* vol. 464, no. 7287, pp. 431-435.

Hayflick, L. & Moorhead, P.S. 1961, "The serial cultivation of human diploid cell strains.", *Experimental cell research,* vol. 25, pp. 585-621.

Heidorn, S.J., Milagre, C., Whittaker, S., Nourry, A., Niculescu-Duvas, I., Dhomen, N., Hussain, J., Reis-Filho, J.S., Springer, C.J., Pritchard, C. & Marais, R. 2010, "Kinase-dead BRAF and oncogenic RAS cooperate to drive tumor progression through CRAF.", *Cell,* vol. 140, no. 2, pp. 209-221.

Hekman, M., Wiese, S., Metz, R., Albert, S., Troppmair, J., Nickel, J., Sendtner, M. & Rapp, U.R. 2004, "Dynamic changes in C-Raf phosphorylation and 14-3-3 protein binding in response to growth factor stimulation: differential roles of 14-3-3 protein binding sites.", *Journal of Biological Chemistry,* vol. 279, no. 14, pp. 14074-14086.

Henriksen, R., Funa, K., Wilander, E., Backstrom, T., Ridderheim, M. & Oberg, K. 1993, "Expression and prognostic significance of platelet-derived growth factor and its receptors in epithelial ovarian neoplasms.", *Cancer research,* vol. 53, no. 19, pp. 4550-4554.

Heo, Y.S., Kim, S.K., Seo, C.I., Kim, Y.K., Sung, B.J., Lee, H.S., Lee, J.I., Park, S.Y., Kim, J.H., Hwang, K.Y., Hyun, Y.L., Jeon, Y.H., Ro, S., Cho, J.M., Lee, T.G. & Yang, C.H. 2004, "Structural basis for the selective inhibition of JNK1 by the scaffolding protein JIP1 and SP600125.", *EMBO Journal,* vol. 23, no. 11, pp. 2185-2195.

Herbig, U. & Sedivy, J.M. 2006, "Regulation of growth arrest in senescence: telomere damage is not the end of the story", *Mechanisms of Ageing & Development,* vol. 127, no. 1, pp. 16-24.

Hermeking, H., Lengauer, C., Polyak, K., He, T.C., Zhang, L., Thiagalingam, S., Kinzler, K.W. & Vogelstein, B. 1997, "14-3-3 sigma is a p53-regulated inhibitor of G2/M progression.", *Molecular cell,* vol. 1, no. 1, pp. 3-11.

Hershko, A. 1997, "Roles of ubiquitin-mediated proteolysis in cell cycle control", *Current opinion in cell biology,* vol. 9, no. 6, pp. 788-799.

Hershko, A. & Ciechanover, A. 1998, "The ubiquitin system", *Annual Review of Biochemistry,* vol. 67, pp. 425-479.

Hinds, P.W., Mittnacht, S., Dulic, V., Arnold, A., Reed, S.I. & Weinberg, R.A. 1992, "Regulation of retinoblastoma protein functions by ectopic expression of human cyclins.", *Cell,* vol. 70, no. 6, pp. 993-1006.

Hingorani, S.R., Petricoin, E.F., Maitra, A., Rajapakse, V., King, C., Jacobetz, M.A., Ross, S., Conrads, T.P., Veenstra, T.D., Hitt, B.A., Kawaguchi, Y., Johann, D., Liotta, L.A., Crawford, H.C., Putt, M.E., Jacks, T., Wright, C.V., Hruban, R.H., Lowy, A.M. & Tuveson, D.A. 2003, "Preinvasive and invasive ductal pancreatic cancer and its early detection in the mouse.", *Cancer Cell,* vol. 4, no. 6, pp. 437-450.

Hofer, M.D., Fecko, A., Shen, R., Setlur, S.R., Pienta, K.G., Tomlins, S.A., Chinnaiyan, A.M. & Rubin, M.A. 2004, "Expression of the platelet-derived growth factor receptor in prostate cancer and treatment implications with tyrosine kinase inhibitors.", *Neoplasia (New York),* vol. 6, no. 5, pp. 503-512.

Honda, R. & Yasuda, H. 1999, "Association of p19(ARF) with Mdm2 inhibits ubiquitin ligase activity of Mdm2 for tumor suppressor p53.", *EMBO Journal,* vol. 18, no. 1, pp. 22-27.

Hong, S.W., Jin, D.H., Shin, J.S., Moon, J.H., Na, Y.S., Jung, K.A., Kim, S.M., Kim, J.C., Kim, K.P., Hong, Y.S., Lee, J.L., Choi, E.K., Lee, J.S. & Kim, T.W. 2012, "Ring finger protein 149 is an E3 ubiquitin ligase active on wild-type v-Raf murine sarcoma viral oncogene homolog B1 (BRAF).", *Journal of Biological Chemistry,* vol. 287, no. 28, pp. 24017-24025.

Hosokawa, N., Hara, T., Kaizuka, T., Kishi, C., Takamura, A., Miura, Y., Iemura, S., Natsume, T., Takehana, K., Yamada, N., Guan, J.L., Oshiro, N. & Mizushima, N. 2009a, "Nutrient-dependent mTORC1 association with the ULK1-Atg13-FIP200 complex required for autophagy.", *Molecular biology of the cell,* vol. 20, no. 7, pp. 1981-1991.

Hosokawa, N., Sasaki, T., Iemura, S., Natsume, T., Hara, T. & Mizushima, N. 2009b, "Atg101, a novel mammalian autophagy protein interacting with Atg13.", *Autophagy,* vol. 5, no. 7, pp. 973-979.

Hu, L.F., Wang, L.P., Ju, L.W., Huang, L.H., Li, X.L., Li, X.Z. & Gu, J.R. 1986, "Expression of N-ras gene in human primary hepatocarcinoma.", *Scientia Sinica - Series B, Chemical, Biological, Agricultural, Medical & Earth Sciences,* vol. 29, no. 2, pp. 181-186.

Hubbard, S.R. 2004, "Juxtamembrane autoinhibition in receptor tyrosine kinases", *Nature Reviews Molecular Cell Biology,* vol. 5, no. 6, pp. 464-471.

Huleihel, M., Goldsborough, M., Cleveland, J., Gunnell, M., Bonner, T. & Rapp, U.R. 1986, "Characterization of murine A-raf, a new oncogene related to the v-raf oncogene.", *Molecular & Cellular Biology,* vol. 6, no. 7, pp. 2655-2662.

Hunter, T. 2009, "Tyrosine phosphorylation: thirty years and counting", *Current opinion in cell biology,* vol. 21, no. 2, pp. 140-146.

Hunter, T. & Marais, R. 2010, "Genetic and cellular mechanisms of oncogenesis.", *Current opinion in genetics & development,* vol. 20, no. 1, pp. 1-3.

Ikawa, S., Fukui, M., Ueyama, Y., Tamaoki, N., Yamamoto, T. & Toyoshima, K. 1988, "B-raf, a new member of the raf family, is activated by DNA rearrangement.", *Molecular & Cellular Biology,* vol. 8, no. 6, pp. 2651-2654.

Indra, A.K., Warot, X., Brocard, J., Bornert, J.M., Xiao, J.H., Chambon, P. & Metzger, D. 1999, "Temporally-controlled site-specific mutagenesis in the basal layer of the epidermis: comparison of the recombinase activity of the tamoxifen-inducible Cre-

ER(T) and Cre-ER(T2) recombinases.", *Nucleic acids research,* vol. 27, no. 22, pp. 4324-4327.

noki, K., Li, Y., Xu, T. & Guan, K.L. 2003, "Rheb GTPase is a direct target of TSC2 GAP activity and regulates mTOR signaling.", *Genes & development,* vol. 17, no. 15, pp. 1829-1834.

Inoki, K., Zhu, T. & Guan, K.L. 2003, "TSC2 mediates cellular energy response to control cell growth and survival.", *Cell,* vol. 115, no. 5, pp. 577-590.

Ip, Y.T. & Davis, R.J. 1998, "Signal transduction by the c-Jun N-terminal kinase (JNK)--from inflammation to development", *Current opinion in cell biology,* vol. 10, no. 2, pp. 205-219.

Ishibe, S., Joly, D., Zhu, X. & Cantley, L.G. 2003, "Phosphorylation-dependent paxillin-ERK association mediates hepatocyte growth factor-stimulated epithelial morphogenesis.", *Molecular cell,* vol. 12, no. 5, pp. 1275-1285.

Itoh, S., Itoh, F., Goumans, M.J. & Ten Dijke, P. 2000, "Signaling of transforming growth factor-beta family members through Smad proteins", *European Journal of Biochemistry,* vol. 267, no. 24, pp. 6954-6967.

Iwabuchi, K., Li, B., Massa, H.F., Trask, B.J., Date, T. & Fields, S. 1998, "Stimulation of p53-mediated transcriptional activation by the p53-binding proteins, 53BP1 and 53BP2.", *Journal of Biological Chemistry,* vol. 273, no. 40, pp. 26061-26068.

Jacobs, D., Glossip, D., Xing, H., Muslin, A.J. & Kornfeld, K. 1999, "Multiple docking sites on substrate proteins form a modular system that mediates recognition by ERK MAP kinase.", *Genes & development,* vol. 13, no. 2, pp. 163-175.

Jansen, H.W. & Bister, K. 1985, "Nucleotide sequence analysis of the chicken gene c-mil, the progenitor of the retroviral oncogene v-mil.", *Virology,* vol. 143, no. 2, pp. 359-367.

Jeffrey, K.L., Camps, M., Rommel, C. & Mackay, C.R. 2007, "Targeting dual-specificity phosphatases: manipulating MAP kinase signalling and immune responses", *Nature Reviews.Drug Discovery,* vol. 6, no. 5, pp. 391-403.

Jo, S.K., Cho, W.Y., Sung, S.A., Kim, H.K. & Won, N.H. 2005, "MEK inhibitor, U0126, attenuates cisplatin-induced renal injury by decreasing inflammation and apoptosis.", *Kidney international,* vol. 67, no. 2, pp. 458-466.

Joel, P.B., Smith, J., Sturgill, T.W., Fisher, T.L., Blenis, J. & Lannigan, D.A. 1998, "pp90rsk1 regulates estrogen receptor-mediated transcription through phosphorylation of Ser-167.", *Molecular & Cellular Biology,* vol. 18, no. 4, pp. 1978-1984.

Johannessen, C.M., Boehm, J.S., Kim, S.Y., Thomas, S.R., Wardwell, L., Johnson, L.A., Emery, C.M., Stransky, N., Cogdill, A.P., Barretina, J., Caponigro, G., Hieronymus, H., Murray, R.R., Salehi-Ashtiani, K., Hill, D.E., Vidal, M., Zhao, J.J.,

Yang, X., Alkan, O., Kim, S., Harris, J.L., Wilson, C.J., Myer, V.E., Finan, P.M., Root, D.E., Roberts, T.M., Golub, T., Flaherty, K.T., Dummer, R., Weber, B.L., Sellers, W.R., Schlegel, R., Wargo, J.A., Hahn, W.C. & Garraway, L.A. 2010, "COT drives resistance to RAF inhibition through MAP kinase pathway reactivation.", *Nature,* vol. 468, no. 7326, pp. 968-972.

Johnson, L., Mercer, K., Greenbaum, D., Bronson, R.T., Crowley, D., Tuveson, D.A. & Jacks, T. 2001, "Somatic activation of the K-ras oncogene causes early onset lung cancer in mice.", *Nature,* vol. 410, no. 6832, pp. 1111-1116.

Johnson, L.N., Lowe, E.D., Noble, M.E. & Owen, D.J. 1998, "The Eleventh Datta Lecture. The structural basis for substrate recognition and control by protein kinases", *FEBS letters,* vol. 430, no. 1-2, pp. 1-11.

Joseph, E.W., Pratilas, C.A., Poulikakos, P.I., Tadi, M., Wang, W., Taylor, B.S., Halilovic, E., Persaud, Y., Xing, F., Viale, A., Tsai, J., Chapman, P.B., Bollag, G., Solit, D.B. & Rosen, N. 2010, "The RAF inhibitor PLX4032 inhibits ERK signaling and tumor cell proliferation in a V600E BRAF-selective manner.", *Proceedings of the National Academy of Sciences of the United States of America,* vol. 107, no. 33, pp. 14903-14908.

Jung, C.H., Ro, S.H., Cao, J., Otto, N.M. & Kim, D.H. 2010, "mTOR regulation of autophagy", *FEBS letters,* vol. 584, no. 7, pp. 1287-1295.

Kamata, T., Hussain, J., Giblett, S., Hayward, R., Marais, R. & Pritchard, C. 2010, "BRAF inactivation drives aneuploidy by deregulating CRAF.", *Cancer research,* vol. 70, no. 21, pp. 8475-8486.

Kang, J., Goodman, B., Zheng, Y. & Tantin, D. 2011, "Dynamic regulation of Oct1 during mitosis by phosphorylation and ubiquitination.", *PLoS ONE [Electronic Resource],* vol. 6, no. 8, pp. e23872.

Karantza-Wadsworth, V., Patel, S., Kravchuk, O., Chen, G., Mathew, R., Jin, S. & White, E. 2007, "Autophagy mitigates metabolic stress and genome damage in mammary tumorigenesis.", *Genes & development,* vol. 21, no. 13, pp. 1621-1635.

Karapetis, C.S., Khambata-Ford, S., Jonker, D.J., O'Callaghan, C.J., Tu, D., Tebbutt, N.C., Simes, R.J., Chalchal, H., Shapiro, J.D., Robitaille, S., Price, T.J., Shepherd, L., Au, H.J., Langer, C., Moore, M.J. & Zalcberg, J.R. 2008, "K-ras mutations and benefit from cetuximab in advanced colorectal cancer.", *New England Journal of Medicine,* vol. 359, no. 17, pp. 1757-1765.

Karreth, F.A., DeNicola, G.M., Winter, S.P. & Tuveson, D.A. 2009, "C-Raf inhibits MAPK activation and transformation by B-Raf(V600E).", *Molecular cell,* vol. 36, no. 3, pp. 477-486.

Karreth, F.A. & Tuveson, D.A. 2009, "Modelling oncogenic Ras/Raf signalling in the mouse", *Current opinion in genetics & development,* vol. 19, no. 1, pp. 4-11.

Keenan, S.M., Bellone, C. & Baldassare, J.J. 2001, "Cyclin-dependent kinase 2 nucleocytoplasmic translocation is regulated by extracellular regulated kinase.", *Journal of Biological Chemistry,* vol. 276, no. 25, pp. 22404-22409.

Kemp, R., Ireland, H., Clayton, E., Houghton, C., Howard, L. & Winton, D.J. 2004, "Elimination of background recombination: somatic induction of Cre by combined transcriptional regulation and hormone binding affinity.", *Nucleic acids research,* vol. 32, no. 11, pp. e92.

Kennelly, P.J. & Krebs, E.G. 1991, "Consensus sequences as substrate specificity determinants for protein kinases and protein phosphatases.", *Journal of Biological Chemistry,* vol. 266, no. 24, pp. 15555-15558.

Kim, E., Ambroziak, P., Otto, J.C., Taylor, B., Ashby, M., Shannon, K., Casey, P.J. & Young, S.G. 1999, "Disruption of the mouse Rce1 gene results in defective Ras processing and mislocalization of Ras within cells.", *Journal of Biological Chemistry,* vol. 274, no. 13, pp. 8383-8390.

Kim, J., Kundu, M., Viollet, B. & Guan, K.L. 2011, "AMPK and mTOR regulate autophagy through direct phosphorylation of Ulk1.", *Nature cell biology,* vol. 13, no. 2, pp. 132-141.

King, A.J., Patrick, D.R., Batorsky, R.S., Ho, M.L., Do, H.T., Zhang, S.Y., Kumar, R., Rusnak, D.W., Takle, A.K., Wilson, D.M., Hugger, E., Wang, L., Karreth, F., Lougheed, J.C., Lee, J., Chau, D., Stout, T.J., May, E.W., Rominger, C.M., Schaber, M.D., Luo, L., Lakdawala, A.S., Adams, J.L., Contractor, R.G., Smalley, K.S., Herlyn, M., Morrissey, M.M., Tuveson, D.A. & Huang, P.S. 2006, "Demonstration of a genetic therapeutic index for tumors expressing oncogenic BRAF by the kinase inhibitor SB-590885.", *Cancer research,* vol. 66, no. 23, pp. 11100-11105.

Kirkin, V., McEwan, D.G., Novak, I. & Dikic, I. 2009, "A role for ubiquitin in selective autophagy", *Molecular cell,* vol. 34, no. 3, pp. 259-269.

Kirkpatrick, D.S., Denison, C. & Gygi, S.P. 2005, "Weighing in on ubiquitin: the expanding role of mass-spectrometry-based proteomics", *Nature cell biology,* vol. 7, no. 8, pp. 750-757.

Klionsky, D.J., Abeliovich, H., Agostinis, P., Agrawal, D.K., Aliev, G., Askew, D.S., Baba, M., Baehrecke, E.H., Bahr, B.A., Ballabio, A., Bamber, B.A., Bassham, D.C., Bergamini, E., Bi, X., Biard-Piechaczyk, M., Blum, J.S., Bredesen, D.E., Brodsky, J.L., Brumell, J.H., Brunk, U.T., Bursch, W., Camougrand, N., Cebollero, E., Cecconi, F., Chen, Y., Chin, L.S., Choi, A., Chu, C.T., Chung, J., Clarke, P.G., Clark, R.S., Clarke, S.G., Clave, C., Cleveland, J.L., Codogno, P., Colombo, M.I., Coto-Montes, A., Cregg, J.M., Cuervo, A.M., Debnath, J., Demarchi, F., Dennis, P.B., Dennis, P.A., Deretic, V., Devenish, R.J., Di Sano, F., Dice, J.F., Difiglia, M., Dinesh-Kumar, S., Distelhorst, C.W., Djavaheri-Mergny, M., Dorsey, F.C., Droge, W., Dron, M., Dunn, W.A.,Jr, Duszenko, M., Eissa, N.T., Elazar, Z., Esclatine, A., Eskelinen, E.L., Fesus, L., Finley, K.D., Fuentes, J.M., Fueyo, J., Fujisaki, K., Galliot, B., Gao, F.B., Gewirtz, D.A., Gibson, S.B., Gohla, A., Goldberg, A.L., Gonzalez, R., Gonzalez-Estevez, C., Gorski, S., Gottlieb, R.A., Haussinger, D., He, Y.W., Heidenreich, K., Hill, J.A., Hoyer-Hansen,

M., Hu, X., Huang, W.P., Iwasaki, A., Jaattela, M., Jackson, W.T., Jiang, X., Jin, S., Johansen, T., Jung, J.U., Kadowaki, M., Kang, C., Kelekar, A., Kessel, D.H., Kiel, J.A., Kim, H.P., Kimchi, A., Kinsella, T.J., Kiselyov, K., Kitamoto, K., Knecht, E., Komatsu, M., Kominami, E., Kondo, S., Kovacs, A.L., Kroemer, G., Kuan, C.Y., Kumar, R., Kundu, M., Landry, J., Laporte, M., Le, W., Lei, H.Y., Lenardo, M.J., Levine, B., Lieberman, A., Lim, K.L., Lin, F.C., Liou, W., Liu, L.F., Lopez-Berestein, G., Lopez-Otin, C., Lu, B., Macleod, K.F., Malorni, W., Martinet, W., Matsuoka, K., Mautner, J., Meijer, A.J., Melendez, A., Michels, P., Miotto, G., Mistiaen, W.P., Mizushima, N., Mograbi, B., Monastyrska, I., Moore, M.N., Moreira, P.I., Moriyasu, Y., Motyl, T., Munz, C., Murphy, L.O., Naqvi, N.I., Neufeld, T.P., Nishino, I., Nixon, R.A., Noda, T., Nurnberg, B., Ogawa, M., Oleinick, N.L., Olsen, L.J., Ozpolat, B., Paglin, S., Palmer, G.E., Papassideri, I., Parkes, M., Perlmutter, D.H., Perry, G., Piacentini, M., Pinkas-Kramarski, R., Prescott, M., Proikas-Cezanne, T., Raben, N., Rami, A., Reggiori, F., Rohrer, B., Rubinsztein, D.C., Ryan, K.M., Sadoshima, J., Sakagami, H., Sakai, Y., Sandri, M., Sasakawa, C., Sass, M., Schneider, C., Seglen, P.O., Seleverstov, O., Settleman, J., Shacka, J.J., Shapiro, I.M., Sibirny, A., Silva-Zacarin, E.C., Simon, H.U., Simone, C., Simonsen, A., Smith, M.A., Spanel-Borowski, K., Srinivas, V., Steeves, M., Stenmark, H., Stromhaug, P.E., Subauste, C.S., Sugimoto, S., Sulzer, D., Suzuki, T., Swanson, M.S., Tabas, I., Takeshita, F., Talbot, N.J., Talloczy, Z., Tanaka, K., Tanaka, K., Tanida, I., Taylor, G.S., Taylor, J.P., Terman, A., Tettamanti, G., Thompson, C.B., Thumm, M., Tolkovsky, A.M., Tooze, S.A., Truant, R., Tumanovska, L.V., Uchiyama, Y., Ueno, T., Uzcategui, N.L., van der Klei, I., Vaquero, E.C., Vellai, T., Vogel, M.W., Wang, H.G., Webster, P., Wiley, J.W., Xi, Z., Xiao, G., Yahalom, J., Yang, J.M., Yap, G., Yin, X.M., Yoshimori, T., Yu, L., Yue, Z., Yuzaki, M., Zabirnyk, O., Zheng, X., Zhu, X. & Deter, R.L. 2008, "Guidelines for the use and interpretation of assays for monitoring autophagy in higher eukaryotes", *Autophagy,* vol. 4, no. 2, pp. 151-175.

Koff, A., Giordano, A., Desai, D., Yamashita, K., Harper, J.W., Elledge, S., Nishimoto, T., Morgan, D.O., Franza, B.R. & Roberts, J.M. 1992, "Formation and activation of a cyclin E-cdk2 complex during the G1 phase of the human cell cycle.", *Science,* vol. 257, no. 5077, pp. 1689-1694.

Kolch, W. 2005, "Coordinating ERK/MAPK signalling through scaffolds and inhibitors", *Nature Reviews Molecular Cell Biology,* vol. 6, no. 11, pp. 827-837.

Kolch, W., Heidecker, G., Kochs, G., Hummel, R., Vahidi, H., Mischak, H., Finkenzeller, G., Marme, D. & Rapp, U.R. 1993, "Protein kinase C alpha activates RAF-1 by direct phosphorylation.", *Nature,* vol. 364, no. 6434, pp. 249-252.

Kretzschmar, M., Doody, J., Timokhina, I. & Massague, J. 1999, "A mechanism of repression of TGFbeta/ Smad signaling by oncogenic Ras.", *Genes & development,* vol. 13, no. 7, pp. 804-816.

Kuilman, T., Michaloglou, C., Mooi, W.J. & Peeper, D.S. 2010a, "The essence of senescence", *Genes & development,* vol. 24, no. 22, pp. 2463-2479.

Kuilman, T., Michaloglou, C., Vredeveld, L.C., Douma, S., van Doorn, R., Desmet, C.J., Aarden, L.A., Mooi, W.J. & Peeper, D.S. 2008, "Oncogene-induced senescence

relayed by an interleukin-dependent inflammatory network.", *Cell,* vol. 133, no. 6, pp. 1019-1031.

Kwak, E.L., Jankowski, J., Thayer, S.P., Lauwers, G.Y., Brannigan, B.W., Harris, P.L., Okimoto, R.A., Haserlat, S.M., Driscoll, D.R., Ferry, D., Muir, B., Settleman, J., Fuchs, C.S., Kulke, M.H., Ryan, D.P., Clark, J.W., Sgroi, D.C., Haber, D.A. & Bell, D.W. 2006, "Epidermal growth factor receptor kinase domain mutations in esophageal and pancreatic adenocarcinomas.", *Clinical Cancer Research,* vol. 12, no. 14 Pt 1, pp. 4283-4287.

La Thangue, N.B. 1994, "DRTF1/E2F: an expanding family of heterodimeric transcription factors implicated in cell-cycle control", *Trends in biochemical sciences,* vol. 19, no. 3, pp. 108-114.

Laplante, M. & Sabatini, D.M. 2009, "mTOR signaling at a glance", *Journal of cell science,* vol. 122, no. Pt 20, pp. 3589-3594.

Lee, C.C., Putnam, A.J., Miranti, C.K., Gustafson, M., Wang, L.M., Vande Woude, G.F. & Gao, C.F. 2004, "Overexpression of sprouty 2 inhibits HGF/SF-mediated cell growth, invasion, migration, and cytokinesis.", *Oncogene,* vol. 23, no. 30, pp. 5193-5202.

Lee, J., Lee, I., Han, B., Park, J.O., Jang, J., Park, C. & Kang, W.K. 2011, "Effect of simvastatin on cetuximab resistance in human colorectal cancer with KRAS mutations.", *Journal of the National Cancer Institute,* vol. 103, no. 8, pp. 674-688.

Lee, J.H. & Paull, T.T. 2005, "ATM activation by DNA double-strand breaks through the Mre11-Rad50-Nbs1 complex", *Science,* vol. 308, no. 5721, pp. 551-554.

Lee, T., Hoofnagle, A.N., Kabuyama, Y., Stroud, J., Min, X., Goldsmith, E.J., Chen, L., Resing, K.A. & Ahn, N.G. 2004, "Docking motif interactions in MAP kinases revealed by hydrogen exchange mass spectrometry.", *Molecular cell,* vol. 14, no. 1, pp. 43-55.

Lefloch, R., Pouyssegur, J. & Lenormand, P. 2008, "Single and combined silencing of ERK1 and ERK2 reveals their positive contribution to growth signaling depending on their expression levels.", *Molecular & Cellular Biology,* vol. 28, no. 1, pp. 511-527.

Lemmon, M.A. & Schlessinger, J. 2010, "Cell signaling by receptor tyrosine kinases", *Cell,* vol. 141, no. 7, pp. 1117-1134.

Lents, N.H., Keenan, S.M., Bellone, C. & Baldassare, J.J. 2002, "Stimulation of the Raf/MEK/ERK cascade is necessary and sufficient for activation and Thr-160 phosphorylation of a nuclear-targeted CDK2.", *Journal of Biological Chemistry,* vol. 277, no. 49, pp. 47469-47475.

Letoha, T., Somlai, C., Takacs, T., Szabolcs, A., Rakonczay, Z.,Jr, Jarmay, K., Szalontai, T., Varga, I., Kaszaki, J., Boros, I., Duda, E., Hackler, L., Kurucz, I. & Penke, B. 2005, "The proteasome inhibitor MG132 protects against acute pancreatitis.", *Free radical biology & medicine,* vol. 39, no. 9, pp. 1142-1151.

Levine, A.J. 1997, "p53, the cellular gatekeeper for growth and division", *Cell,* vol. 88, no. 3, pp. 323-331.

Levine, B. & Kroemer, G. 2008, "Autophagy in the pathogenesis of disease", *Cell,* vol. 132, no. 1, pp. 27-42.

Ley, R., Balmanno, K., Hadfield, K., Weston, C. & Cook, S.J. 2003a, "Activation of the ERK1/2 signaling pathway promotes phosphorylation and proteasome-dependent degradation of the BH3-only protein, Bim.", *Journal of Biological Chemistry,* vol. 278, no. 21, pp. 18811-18816.

Ley, R., Balmanno, K., Hadfield, K., Weston, C. & Cook, S.J. 2003b, "Activation of the ERK1/2 signaling pathway promotes phosphorylation and proteasome-dependent degradation of the BH3-only protein, Bim.", *Journal of Biological Chemistry,* vol. 278, no. 21, pp. 18811-18816.

Li, H., Wang, X., Li, N., Qiu, J., Zhang, Y. & Cao, X. 2007, "hPEBP4 resists TRAIL-induced apoptosis of human prostate cancer cells by activating Akt and deactivating ERK1/2 pathways.", *Journal of Biological Chemistry,* vol. 282, no. 7, pp. 4943-4950.

Li, H., Zhu, H., Xu, C.J. & Yuan, J. 1998, "Cleavage of BID by caspase 8 mediates the mitochondrial damage in the Fas pathway of apoptosis.", *Cell,* vol. 94, no. 4, pp. 491-501.

Li, P., Nijhawan, D., Budihardjo, I., Srinivasula, S.M., Ahmad, M., Alnemri, E.S. & Wang, X. 1997, "Cytochrome c and dATP-dependent formation of Apaf-1/caspase-9 complex initiates an apoptotic protease cascade.", *Cell,* vol. 91, no. 4, pp. 479-489.

Li, X., Brunton, V.G., Burgar, H.R., Wheldon, L.M. & Heath, J.K. 2004, "FRS2-dependent SRC activation is required for fibroblast growth factor receptor-induced phosphorylation of Sprouty and suppression of ERK activity.", *Journal of cell science,* vol. 117, no. Pt 25, pp. 6007-6017.

Li, Z., Wang, D., Messing, E.M. & Wu, G. 2005, "VHL protein-interacting deubiquitinating enzyme 2 deubiquitinates and stabilizes HIF-1alpha.", *EMBO reports,* vol. 6, no. 4, pp. 373-378.

Lin, A.W., Barradas, M., Stone, J.C., van Aelst, L., Serrano, M. & Lowe, S.W. 1998, "Premature senescence involving p53 and p16 is activated in response to constitutive MEK/MAPK mitogenic signaling.", *Genes & development,* vol. 12, no. 19, pp. 3008-3019.

Liou, W., Geuze, H.J., Geelen, M.J. & Slot, J.W. 1997, "The autophagic and endocytic pathways converge at the nascent autophagic vacuoles.", *Journal of Cell Biology,* vol. 136, no. 1, pp. 61-70.

Littlewood, T.D., Hancock, D.C., Danielian, P.S., Parker, M.G. & Evan, G.I. 1995, "A modified oestrogen receptor ligand-binding domain as an improved switch for the regulation of heterologous proteins.", *Nucleic acids research,* vol. 23, no. 10, pp. 1686-1690.

Liu, J., Mao, W., Ding, B. & Liang, C.S. 2008, "ERKs/p53 signal transduction pathway is involved in doxorubicin-induced apoptosis in H9c2 cells and cardiomyocytes.", *American Journal of Physiology - Heart & Circulatory Physiology,* vol. 295, no. 5, pp. H1956-65.

Liu, Y. & Gray, N.S. 2006, "Rational design of inhibitors that bind to inactive kinase conformations.", *Nature Chemical Biology,* vol. 2, no. 7, pp. 358-364.

Lock, R., Roy, S., Kenific, C.M., Su, J.S., Salas, E., Ronen, S.M. & Debnath, J. 2011, "Autophagy facilitates glycolysis during Ras-mediated oncogenic transformation.", *Molecular biology of the cell,* vol. 22, no. 2, pp. 165-178.

Loonstra, A., Vooijs, M., Beverloo, H.B., Allak, B.A., van Drunen, E., Kanaar, R., Berns, A. & Jonkers, J. 2001, "Growth inhibition and DNA damage induced by Cre recombinase in mammalian cells.", *Proceedings of the National Academy of Sciences of the United States of America,* vol. 98, no. 16, pp. 9209-9214.

Lowe, S.W., Cepero, E. & Evan, G. 2004, "Intrinsic tumour suppression", *Nature,* vol. 432, no. 7015, pp. 307-315.

Lowy, D.R. & Willumsen, B.M. 1993, "Function and regulation of ras", *Annual Review of Biochemistry,* vol. 62, pp. 851-891.

Luckett, J.C., Huser, M.B., Giagtzoglou, N., Brown, J.E. & Pritchard, C.A. 2000, "Expression of the A-raf proto-oncogene in the normal adult and embryonic mouse.", *Cell Growth & Differentiation,* vol. 11, no. 3, pp. 163-171.

Lundberg, A.S. & Weinberg, R.A. 1998, "Functional inactivation of the retinoblastoma protein requires sequential modification by at least two distinct cyclin-cdk complexes.", *Molecular & Cellular Biology,* vol. 18, no. 2, pp. 753-761.

Lunn, C.L., Chrivia, J.C. & Baldassare, J.J. 2010, "Activation of Cdk2/Cyclin E complexes is dependent on the origin of replication licensing factor Cdc6 in mammalian cells.", *Cell Cycle,* vol. 9, no. 22, pp. 4533-4541.

Luo, R.X., Postigo, A.A. & Dean, D.C. 1998, "Rb interacts with histone deacetylase to repress transcription.", *Cell,* vol. 92, no. 4, pp. 463-473.

Ma, L., Chen, Z., Erdjument-Bromage, H., Tempst, P. & Pandolfi, P.P. 2005, "Phosphorylation and functional inactivation of TSC2 by Erk implications for tuberous sclerosis and cancer pathogenesis.", *Cell,* vol. 121, no. 2, pp. 179-193.

Maddodi, N., Huang, W., Havighurst, T., Kim, K., Longley, B.J. & Setaluri, V. 2010, "Induction of autophagy and inhibition of melanoma growth in vitro and in vivo by hyperactivation of oncogenic BRAF.", *Journal of Investigative Dermatology,* vol. 130, no. 6, pp. 1657-1667.

Madesh, M., Antonsson, B., Srinivasula, S.M., Alnemri, E.S. & Hajnoczky, G. 2002, "Rapid kinetics of tBid-induced cytochrome c and Smac/DIABLO release and

mitochondrial depolarization.", *Journal of Biological Chemistry,* vol. 277, no. 7, pp. 5651-5659.

Magnaghi-Jaulin, L., Groisman, R., Naguibneva, I., Robin, P., Lorain, S., Le Villain, J.P., Troalen, F., Trouche, D. & Harel-Bellan, A. 1998, "Retinoblastoma protein represses transcription by recruiting a histone deacetylase.", *Nature,* vol. 391, no. 6667, pp. 601-605.

Maloney, A. & Workman, P. 2002, "HSP90 as a new therapeutic target for cancer therapy: the story unfolds", *Expert Opinion on Biological Therapy,* vol. 2, no. 1, pp. 3-24.

Mammucari, C., Milan, G., Romanello, V., Masiero, E., Rudolf, R., Del Piccolo, P., Burden, S.J., Di Lisi, R., Sandri, C., Zhao, J., Goldberg, A.L., Schiaffino, S. & Sandri, M. 2007, "FoxO3 controls autophagy in skeletal muscle in vivo.", *Cell Metabolism,* vol. 6, no. 6, pp. 458-471.

Manenti, S., Delmas, C. & Darbon, J.M. 2002, "Cell adhesion protects c-Raf-1 against ubiquitin-dependent degradation by the proteasome.", *Biochemical & Biophysical Research Communications,* vol. 294, no. 5, pp. 976-980.

Martin, M.C., Allan, L.A., Mancini, E.J. & Clarke, P.R. 2008, "The docking interaction of caspase-9 with ERK2 provides a mechanism for the selective inhibitory phosphorylation of caspase-9 at threonine 125.", *Journal of Biological Chemistry,* vol. 283, no. 7, pp. 3854-3865.

Marx, M., Eychene, A., Laugier, D., Bechade, C., Crisanti, P., Dezelee, P., Pessac, B. & Calothy, G. 1988, "A novel oncogene related to c-mil is transduced in chicken neuroretina cells induced to proliferate by infection with an avian lymphomatosis virus.", *EMBO Journal,* vol. 7, no. 11, pp. 3369-3373.

Mason, C.S., Springer, C.J., Cooper, R.G., Superti-Furga, G., Marshall, C.J. & Marais, R. 1999a, "Serine and tyrosine phosphorylations cooperate in Raf-1, but not B-Raf activation.", *EMBO Journal,* vol. 18, no. 8, pp. 2137-2148.

Mason, J.M., Morrison, D.J., Basson, M.A. & Licht, J.D. 2006, "Sprouty proteins: multifaceted negative-feedback regulators of receptor tyrosine kinase signaling", *Trends in cell biology,* vol. 16, no. 1, pp. 45-54.

Mathew, R., Kongara, S., Beaudoin, B., Karp, C.M., Bray, K., Degenhardt, K., Chen, G., Jin, S. & White, E. 2007, "Autophagy suppresses tumor progression by limiting chromosomal instability", *Genes & development,* vol. 21, no. 11, pp. 1367-1381.

Mayya, V., Lundgren, D.H., Hwang, S.I., Rezaul, K., Wu, L., Eng, J.K., Rodionov, V. & Han, D.K. 2009, "Quantitative phosphoproteomic analysis of T cell receptor signaling reveals system-wide modulation of protein-protein interactions.", *Science Signaling [Electronic Resource],* vol. 2, no. 84, pp. ra46.

McCormick, F. 1993, "Signal transduction. How receptors turn Ras on.", *Nature,* vol. 363, no. 6424, pp. 15-16.

McCoy, C.E., macdonald, A., Morrice, N.A., Campbell, D.G., Deak, M., Toth, R., McIlrath, J. & Arthur, J.S. 2007, "Identification of novel phosphorylation sites in MSK1 by precursor ion scanning MS.", *Biochemical Journal,* vol. 402, no. 3, pp. 491-501.

McGary, E.C., Weber, K., Mills, L., Doucet, M., Lewis, V., Lev, D.C., Fidler, I.J. & Bar-Eli, M. 2002, "Inhibition of platelet-derived growth factor-mediated proliferation of osteosarcoma cells by the novel tyrosine kinase inhibitor STI571.", *Clinical Cancer Research,* vol. 8, no. 11, pp. 3584-3591.

Meijer, W.H., van der Klei, I.J., Veenhuis, M. & Kiel, J.A. 2007, "ATG genes involved in non-selective autophagy are conserved from yeast to man, but the selective Cvt and pexophagy pathways also require organism-specific genes.", *Autophagy,* vol. 3, no. 2, pp. 106-116.

Mendoza, M.C., Er, E.E. & Blenis, J. 2011, "The Ras-ERK and PI3K-mTOR pathways: cross-talk and compensation", *Trends in biochemical sciences,* vol. 36, no. 6, pp. 320-328.

Mercer, K., Giblett, S., Green, S., Lloyd, D., DaRocha Dias, S., Plumb, M., Marais, R. & Pritchard, C. 2005, "Expression of endogenous oncogenic V600EB-raf induces proliferation and developmental defects in mice and transformation of primary fibroblasts.", *Cancer research,* vol. 65, no. 24, pp. 11493-11500.

Mercer, K.E. & Pritchard, C.A. 2003a, "Raf proteins and cancer: B-Raf is identified as a mutational target", *Biochimica et biophysica acta,* vol. 1653, no. 1, pp. 25-40.

Meyer, R.D., Srinivasan, S., Singh, A.J., Mahoney, J.E., Gharahassanlou, K.R. & Rahimi, N. 2011, "PEST motif serine and tyrosine phosphorylation controls vascular endothelial growth factor receptor 2 stability and downregulation.", *Molecular & Cellular Biology,* vol. 31, no. 10, pp. 2010-2025.

Meyne, J., Ratliff, R.L. & Moyzis, R.K. 1989, "Conservation of the human telomere sequence (TTAGGG)n among vertebrates.", *Proceedings of the National Academy of Sciences of the United States of America,* vol. 86, no. 18, pp. 7049-7053.

Michaloglou, C., Vredeveld, L.C., Soengas, M.S., Denoyelle, C., Kuilman, T., van der Horst, C.M., Majoor, D.M., Shay, J.W., Mooi, W.J. & Peeper, D.S. 2005a, "BRAFE600-associated senescence-like cell cycle arrest of human naevi", *Nature,* vol. 436, no. 7051, pp. 720-724.

Miyoshi, K., Wakioka, T., Nishinakamura, H., Kamio, M., Yang, L., Inoue, M., Hasegawa, M., Yonemitsu, Y., Komiya, S. & Yoshimura, A. 2004, "The Sprouty-related protein, Spred, inhibits cell motility, metastasis, and Rho-mediated actin reorganization.", *Oncogene,* vol. 23, no. 33, pp. 5567-5576.

Mizushima, N. 2010, "The role of the Atg1/ULK1 complex in autophagy regulation", *Current opinion in cell biology,* vol. 22, no. 2, pp. 132-139.

Mizushima, N., Levine, B., Cuervo, A.M. & Klionsky, D.J. 2008, "Autophagy fights disease through cellular self-digestion", *Nature,* vol. 451, no. 7182, pp. 1069-1075.

Mizushima, N., Yoshimori, T. & Levine, B. 2010, "Methods in mammalian autophagy research.", *Cell,* vol. 140, no. 3, pp. 313-326.

Molzan, M., Schumacher, B., Ottmann, C., Baljuls, A., Polzien, L., Weyand, M., Thiel, P., Rose, R., Rose, M., Kuhenne, P., Kaiser, M., Rapp, U.R., Kuhlmann, J. & Ottmann, C. 2010, "Impaired binding of 14-3-3 to C-RAF in Noonan syndrome suggests new approaches in diseases with increased Ras signaling.", *Molecular & Cellular Biology,* vol. 30, no. 19, pp. 4698-4711.

Montagut, C., Sharma, S.V., Shioda, T., McDermott, U., Ulman, M., Ulkus, L.E., Dias-Santagata, D., Stubbs, H., Lee, D.Y., Singh, A., Drew, L., Haber, D.A. & Settleman, J. 2008, "Elevated CRAF as a potential mechanism of acquired resistance to BRAF inhibition in melanoma.", *Cancer research,* vol. 68, no. 12, pp. 4853-4861.

Mooi, W.J. & Peeper, D.S. 2006, "Oncogene-induced cell senescence--halting on the road to cancer", *New England Journal of Medicine,* vol. 355, no. 10, pp. 1037-1046.

Morrison, D.K. 2001, "KSR: a MAPK scaffold of the Ras pathway?", *Journal of cell science,* vol. 114, no. Pt 9, pp. 1609-1612.

Morrison, D.K. & Davis, R.J. 2003, "Regulation of MAP kinase signaling modules by scaffold proteins in mammals", *Annual Review of Cell & Developmental Biology,* vol. 19, pp. 91-118.

Morrison, T.B., Weis, J.J. & Wittwer, C.T. *Quantification of low-copy transcripts by continuous SYBR Green I monitoring during amplification*.

Mott, H.R., Carpenter, J.W., Zhong, S., Ghosh, S., Bell, R.M. & Campbell, S.L. 1996, "The solution structure of the Raf-1 cysteine-rich domain: a novel ras and phospholipid binding site.", *Proceedings of the National Academy of Sciences of the United States of America,* vol. 93, no. 16, pp. 8312-8317.

Muller, J., Ory, S., Copeland, T., Piwnica-Worms, H. & Morrison, D.K. 2001, "C-TAK1 regulates Ras signaling by phosphorylating the MAPK scaffold, KSR1.", *Molecular cell,* vol. 8, no. 5, pp. 983-993.

Murphy, L.O., Smith, S., Chen, R.H., Fingar, D.C. & Blenis, J. 2002, "Molecular interpretation of ERK signal duration by immediate early gene products.", *Nature cell biology,* vol. 4, no. 8, pp. 556-564.

Nagy, A. 2000, "Cre recombinase: the universal reagent for genome tailoring", *Genesis: the Journal of Genetics & Development,* vol. 26, no. 2, pp. 99-109.

Nakamura, A.J., Redon, C.E., Bonner, W.M. & Sedelnikova, O.A. 2009, "Telomere-dependent and telomere-independent origins of endogenous DNA damage in tumor cells.", *Aging,* vol. 1, no. 2, pp. 212-218.

Nakatogawa, H., Suzuki, K., Kamada, Y. & Ohsumi, Y. 2009, "Dynamics and diversity in autophagy mechanisms: lessons from yeast", *Nature Reviews Molecular Cell Biology,* vol. 10, no. 7, pp. 458-467.

Narita, M., Nunez, S., Heard, E., Narita, M., Lin, A.W., Hearn, S.A., Spector, D.L., Hannon, G.J. & Lowe, S.W. 2003a, "Rb-mediated heterochromatin formation and silencing of E2F target genes during cellular senescence.", *Cell,* vol. 113, no. 6, pp. 703-716.

Narita, M., Young, A.R. & Narita, M. 2009, "Autophagy facilitates oncogene-induced senescence.", *Autophagy,* vol. 5, no. 7, pp. 1046-1047.

Nazarian, R., Shi, H., Wang, Q., Kong, X., Koya, R.C., Lee, H., Chen, Z., Lee, M.K., Attar, N., Sazegar, H., Chodon, T., Nelson, S.F., McArthur, G., Sosman, J.A., Ribas, A. & Lo, R.S. 2010, "Melanomas acquire resistance to B-RAF(V600E) inhibition by RTK or N-RAS upregulation.", *Nature,* vol. 468, no. 7326, pp. 973-977.

Niault, T.S. & Baccarini, M. 2010, "Targets of Raf in tumorigenesis", *Carcinogenesis,* vol. 31, no. 7, pp. 1165-1174.

Nie, J., McGill, M.A., Dermer, M., Dho, S.E., Wolting, C.D. & McGlade, C.J. 2002, "LNX functions as a RING type E3 ubiquitin ligase that targets the cell fate determinant Numb for ubiquitin-dependent degradation.", *EMBO Journal,* vol. 21, no. 1-2, pp. 93-102.

Nishio, K., Inoue, A., Qiao, S., Kondo, H. & Mimura, A. 2001, "Senescence and cytoskeleton: overproduction of vimentin induces senescent-like morphology in human fibroblasts.", *Histochemistry & Cell Biology,* vol. 116, no. 4, pp. 321-327.

Nissan, M.H. & Solit, D.B. 2011a, "The "SWOT" of BRAF inhibition in melanoma: RAF inhibitors, MEK inhibitors or both?", *Current oncology reports,* vol. 13, no. 6, pp. 479-487.

Nissan, M.H. & Solit, D.B. 2011b, "The "SWOT" of BRAF inhibition in melanoma: RAF inhibitors, MEK inhibitors or both?", *Current oncology reports,* vol. 13, no. 6, pp. 479-487.

Noble, C., Mercer, K., Hussain, J., Carragher, L., Giblett, S., Hayward, R., Patterson, C., Marais, R. & Pritchard, C.A. 2008, "CRAF autophosphorylation of serine 621 is required to prevent its proteasome-mediated degradation.", *Molecular cell,* vol. 31, no. 6, pp. 862-872.

Ogier-Denis, E., Pattingre, S., El Benna, J. & Codogno, P. 2000, "Erk1/2-dependent phosphorylation of Galpha-interacting protein stimulates its GTPase accelerating activity and autophagy in human colon cancer cells.", *Journal of Biological Chemistry,* vol. 275, no. 50, pp. 39090-39095.

Ogier-Denis, E., Petiot, A., Bauvy, C. & Codogno, P. 1997, "Control of the expression and activity of the Galpha-interacting protein (GAIP) in human intestinal cells.", *Journal of Biological Chemistry,* vol. 272, no. 39, pp. 24599-24603.

Okazaki, K. & Sagata, N. 1995, "The Mos/MAP kinase pathway stabilizes c-Fos by phosphorylation and augments its transforming activity in NIH 3T3 cells.", *EMBO Journal,* vol. 14, no. 20, pp. 5048-5059.

Oltvai, Z.N., Milliman, C.L. & Korsmeyer, S.J. 1993, "Bcl-2 heterodimerizes in vivo with a conserved homolog, Bax, that accelerates programmed cell death.", *Cell,* vol. 74, no. 4, pp. 609-619.

O'Regan, L. & Fry, A.M. 2009, "The Nek6 and Nek7 protein kinases are required for robust mitotic spindle formation and cytokinesis.", *Molecular & Cellular Biology,* vol. 29, no. 14, pp. 3975-3990.

Owens, D.M. & Keyse, S.M. 2007, "Differential regulation of MAP kinase signalling by dual-specificity protein phosphatases", *Oncogene,* vol. 26, no. 22, pp. 3203-3213.

Ozaki, K., Kadomoto, R., Asato, K., Tanimura, S., Itoh, N. & Kohno, M. 2001, "ERK pathway positively regulates the expression of Sprouty genes.", *Biochemical & Biophysical Research Communications,* vol. 285, no. 5, pp. 1084-1088.

Ozaki, K., Miyazaki, S., Tanimura, S. & Kohno, M. 2005, "Efficient suppression of FGF-2-induced ERK activation by the cooperative interaction among mammalian Sprouty isoforms.", *Journal of cell science,* vol. 118, no. Pt 24, pp. 5861-5871.

Packer, L.M., East, P., Reis-Filho, J.S. & Marais, R. 2009, "Identification of direct transcriptional targets of (V600E)BRAF/MEK signalling in melanoma.", *Pigment Cell & Melanoma Research,* vol. 22, no. 6, pp. 785-798.

Pagano, M., Pepperkok, R., Lukas, J., Baldin, V., Ansorge, W., Bartek, J. & Draetta, G. 1993, "Regulation of the cell cycle by the cdk2 protein kinase in cultured human fibroblasts.", *Journal of Cell Biology,* vol. 121, no. 1, pp. 101-111.

Papin, C., Denouel, A., Calothy, G. & Eychene, A. 1996, "Identification of signalling proteins interacting with B-Raf in the yeast two-hybrid system.", *Oncogene,* vol. 12, no. 10, pp. 2213-2221.

Papin, C., Denouel-Galy, A., Laugier, D., Calothy, G. & Eychene, A. 1998, "Modulation of kinase activity and oncogenic properties by alternative splicing reveals a novel regulatory mechanism for B-Raf.", *Journal of Biological Chemistry,* vol. 273, no. 38, pp. 24939-24947.

Papin, C., Eychene, A., Brunet, A., Pages, G., Pouyssegur, J., Calothy, G. & Barnier, J.V. 1995, "B-Raf protein isoforms interact with and phosphorylate Mek-1 on serine residues 218 and 222.", *Oncogene,* vol. 10, no. 8, pp. 1647-1651.

Park, H.Y. & Gilchrest, B.A. 2002, "More on MITF", *Journal of Investigative Dermatology,* vol. 119, no. 6, pp. 1218-1219.

Park, S.H., Zarrinpar, A. & Lim, W.A. 2003, "Rewiring MAP kinase pathways using alternative scaffold assembly mechanisms.", *Science,* vol. 299, no. 5609, pp. 1061-1064.

Parrinello, S., Samper, E., Krtolica, A., Goldstein, J., Melov, S. & Campisi, J. 2003, "Oxygen sensitivity severely limits the replicative lifespan of murine fibroblasts", *Nature cell biology,* vol. 5, no. 8, pp. 741-747.

Patrick, G.N., Zhou, P., Kwon, Y.T., Howley, P.M. & Tsai, L.H. 1998, "p35, the neuronal-specific activator of cyclin-dependent kinase 5 (Cdk5) is degraded by the ubiquitin-proteasome pathway.", *Journal of Biological Chemistry,* vol. 273, no. 37, pp. 24057-24064.

Pattingre, S., Bauvy, C. & Codogno, P. 2003, "Amino acids interfere with the ERK1/2-dependent control of macroautophagy by controlling the activation of Raf-1 in human colon cancer HT-29 cells.", *Journal of Biological Chemistry,* vol. 278, no. 19, pp. 16667-16674.

Pavey, S., Johansson, P., Packer, L., Taylor, J., Stark, M., Pollock, P.M., Walker, G.J., Boyle, G.M., Harper, U., Cozzi, S.J., Hansen, K., Yudt, L., Schmidt, C., Hersey, P., Ellem, K.A., O'Rourke, M.G., Parsons, P.G., Meltzer, P., Ringner, M. & Hayward, N.K. 2004, "Microarray expression profiling in melanoma reveals a BRAF mutation signature.", *Oncogene,* vol. 23, no. 23, pp. 4060-4067.

Pawson, T. 2004, "Specificity in signal transduction: from phosphotyrosine-SH2 domain interactions to complex cellular systems", *Cell,* vol. 116, no. 2, pp. 191-203.

Pearson, G., Robinson, F., Beers Gibson, T., Xu, B.E., Karandikar, M., Berman, K. & Cobb, M.H. 2001, "Mitogen-activated protein (MAP) kinase pathways: regulation and physiological functions", *Endocrine reviews,* vol. 22, no. 2, pp. 153-183.

Pelicci, G., Lanfrancone, L., Grignani, F., McGlade, J., Cavallo, F., Forni, G., Nicoletti, I., Grignani, F., Pawson, T. & Pelicci, P.G. 1992, "A novel transforming protein (SHC) with an SH2 domain is implicated in mitogenic signal transduction.", *Cell,* vol. 70, no. 1, pp. 93-104.

Pellecchia, M., Montgomery, D.L., Stevens, S.Y., Vander Kooi, C.W., Feng, H.P., Gierasch, L.M. & Zuiderweg, E.R. 2000, "Structural insights into substrate binding by the molecular chaperone DnaK.", *Nature structural biology,* vol. 7, no. 4, pp. 298-303.

Perez de Castro, I., Bivona, T.G., Philips, M.R. & Pellicer, A. 2004, "Ras activation in Jurkat T cells following low-grade stimulation of the T-cell receptor is specific to N-Ras and occurs only on the Golgi apparatus.", *Molecular & Cellular Biology,* vol. 24, no. 8, pp. 3485-3496.

Petros, A.M., Medek, A., Nettesheim, D.G., Kim, D.H., Yoon, H.S., Swift, K., Matayoshi, E.D., Oltersdorf, T. & Fesik, S.W. 2001, "Solution structure of the antiapoptotic protein bcl-2.", *Proceedings of the National Academy of Sciences of the United States of America,* vol. 98, no. 6, pp. 3012-3017.

Pfaffl, M.W. 2001, "A new mathematical model for relative quantification in real-time RT-PCR.", *Nucleic acids research,* vol. 29, no. 9, pp. e45.

Philips, M.R. 2004, "Sef: a MEK/ERK catcher on the Golgi.", *Molecular cell,* vol. 15, no. 2, pp. 168-169.

Pickart, C.M. 2001, "Mechanisms underlying ubiquitination", *Annual Review of Biochemistry,* vol. 70, pp. 503-533.

Platz, A., Egyhazi, S., Ringborg, U. & Hansson, J. 2008, "Human cutaneous melanoma; a review of NRAS and BRAF mutation frequencies in relation to histogenetic subclass and body site.", *Molecular Oncology,* vol. 1, no. 4, pp. 395-405.

Pollock, P.M., Harper, U.L., Hansen, K.S., Yudt, L.M., Stark, M., Robbins, C.M., Moses, T.Y., Hostetter, G., Wagner, U., Kakareka, J., Salem, G., Pohida, T., Heenan, P., Duray, P., Kallioniemi, O., Hayward, N.K., Trent, J.M. & Meltzer, P.S. 2003a, "High frequency of BRAF mutations in nevi.", *Nature genetics,* vol. 33, no. 1, pp. 19-20.

Porfiri, E. & McCormick, F. 1996, "Regulation of epidermal growth factor receptor signaling by phosphorylation of the ras exchange factor hSOS1.", *Journal of Biological Chemistry,* vol. 271, no. 10, pp. 5871-5877.

Porter, A.G. & Janicke, R.U. 1999, "Emerging roles of caspase-3 in apoptosis", *Cell Death & Differentiation,* vol. 6, no. 2, pp. 99-104.

Poulikakos, P.I., Persaud, Y., Janakiraman, M., Kong, X., Ng, C., Moriceau, G., Shi, H., Atefi, M., Titz, B., Gabay, M.T., Salton, M., Dahlman, K.B., Tadi, M., Wargo, J.A., Flaherty, K.T., Kelley, M.C., Misteli, T., Chapman, P.B., Sosman, J.A., Graeber, T.G., Ribas, A., Lo, R.S., Rosen, N. & Solit, D.B. 2011, "RAF inhibitor resistance is mediated by dimerization of aberrantly spliced BRAF(V600E).", *Nature,* vol. 480, no. 7377, pp. 387-390.

Poulikakos, P.I., Zhang, C., Bollag, G., Shokat, K.M. & Rosen, N. 2010, "RAF inhibitors transactivate RAF dimers and ERK signalling in cells with wild-type BRAF.", *Nature,* vol. 464, no. 7287, pp. 427-430.

Pouyssegur, J., Volmat, V. & Lenormand, P. 2002, "Fidelity and spatio-temporal control in MAP kinase (ERKs) signalling", *Biochemical pharmacology,* vol. 64, no. 5-6, pp. 755-763.

Powers, M.V. & Workman, P. 2006, "Targeting of multiple signalling pathways by heat shock protein 90 molecular chaperone inhibitors", *Endocrine-related cancer,* vol. 13, no. Suppl 1, pp. S125-35.

Pratilas, C.A., Hanrahan, A.J., Halilovic, E., Persaud, Y., Soh, J., Chitale, D., Shigematsu, H., Yamamoto, H., Sawai, A., Janakiraman, M., Taylor, B.S., Pao, W., Toyooka, S., Ladanyi, M., Gazdar, A., Rosen, N. & Solit, D.B. 2008, "Genetic predictors of MEK dependence in non-small cell lung cancer.", *Cancer research,* vol. 68, no. 22, pp. 9375-9383.

Pratilas, C.A., Taylor, B.S., Ye, Q., Viale, A., Sander, C., Solit, D.B. & Rosen, N. 2009, "(V600E)BRAF is associated with disabled feedback inhibition of RAF-MEK signaling and elevated transcriptional output of the pathway.", *Proceedings of the National Academy of Sciences of the United States of America,* vol. 106, no. 11, pp. 4519-4524.

Previs, M.J., VanBuren, P., Begin, K.J., Vigoreaux, J.O., LeWinter, M.M. & Matthews, D.E. 2008, "Quantification of protein phosphorylation by liquid chromatography-mass spectrometry.", *Analytical Chemistry,* vol. 80, no. 15, pp. 5864-5872.

Pritchard, C.A., Samuels, M.L., Bosch, E. & McMahon, M. 1995, "Conditionally oncogenic forms of the A-Raf and B-Raf protein kinases display different biological and biochemical properties in NIH 3T3 cells.", *Molecular & Cellular Biology,* vol. 15, no. 11, pp. 6430-6442.

Prive, G.G., Milburn, M.V., Tong, L., de Vos, A.M., Yamaizumi, Z., Nishimura, S. & Kim, S.H. 1992, "X-ray crystal structures of transforming p21 ras mutants suggest a transition-state stabilization mechanism for GTP hydrolysis.", *Proceedings of the National Academy of Sciences of the United States of America,* vol. 89, no. 8, pp. 3649-3653.

Puthalakath, H. & Strasser, A. 2002, "Keeping killers on a tight leash: transcriptional and post-translational control of the pro-apoptotic activity of BH3-only proteins", *Cell Death & Differentiation,* vol. 9, no. 5, pp. 505-512.

Rabinowitz, J.D. & White, E. 2010, "Autophagy and metabolism", *Science,* vol. 330, no. 6009, pp. 1344-1348.

Ramirez, R.D., Morales, C.P., Herbert, B.S., Rohde, J.M., Passons, C., Shay, J.W. & Wright, W.E. 2001, "Putative telomere-independent mechanisms of replicative aging reflect inadequate growth conditions.", *Genes & development,* vol. 15, no. 4, pp. 398-403.

Ranganathan, A., Pearson, G.W., Chrestensen, C.A., Sturgill, T.W. & Cobb, M.H. 2006, "The MAP kinase ERK5 binds to and phosphorylates p90 RSK.", *Archives of Biochemistry & Biophysics,* vol. 449, no. 1-2, pp. 8-16.

Rapp, U.R., Goldsborough, M.D., Mark, G.E., Bonner, T.I., Groffen, J., Reynolds, F.H.,Jr & Stephenson, J.R. 1983, "Structure and biological activity of v-raf, a unique oncogene transduced by a retrovirus.", *Proceedings of the National Academy of Sciences of the United States of America,* vol. 80, no. 14, pp. 4218-4222.

Rayman, J.B., Takahashi, Y., Indjeian, V.B., Dannenberg, J.H., Catchpole, S., Watson, R.J., te Riele, H. & Dynlacht, B.D. 2002, "E2F mediates cell cycle-dependent transcriptional repression in vivo by recruitment of an HDAC1/mSin3B corepressor complex.", *Genes & development,* vol. 16, no. 8, pp. 933-947.

Rebollo, A., Perez-Sala, D. & Martinez-A, C. 1999, "Bcl-2 differentially targets K-, N-, and H-Ras to mitochondria in IL-2 supplemented or deprived cells: implications in prevention of apoptosis.", *Oncogene,* vol. 18, no. 35, pp. 4930-4939.

Rechsteiner, M. & Rogers, S.W. 1996, "PEST sequences and regulation by proteolysis", *Trends in biochemical sciences,* vol. 21, no. 7, pp. 267-271.

Reddy, E.P., Reynolds, R.K., Santos, E. & Barbacid, M. 1982, "A point mutation is responsible for the acquisition of transforming properties by the T24 human bladder carcinoma oncogene.", *Nature,* vol. 300, no. 5888, pp. 149-152.

Reya, T. & Clevers, H. 2005, "Wnt signalling in stem cells and cancer", *Nature,* vol. 434, no. 7035, pp. 843-850.

Rhee, S.G. 1991, "Inositol phospholipids-specific phospholipase C: interaction of the gamma 1 isoform with tyrosine kinase", *Trends in biochemical sciences,* vol. 16, no. 8, pp. 297-301.

Ries, S., Biederer, C., Woods, D., Shifman, O., Shirasawa, S., Sasazuki, T., McMahon, M., Oren, M. & McCormick, F. 2000, "Opposing effects of Ras on p53: transcriptional activation of mdm2 and induction of p19ARF.", *Cell,* vol. 103, no. 2, pp. 321-330.

Rikova, K., Guo, A., Zeng, Q., Possemato, A., Yu, J., Haack, H., Nardone, J., Lee, K., Reeves, C., Li, Y., Hu, Y., Tan, Z., Stokes, M., Sullivan, L., Mitchell, J., Wetzel, R., Macneill, J., Ren, J.M., Yuan, J., Bakalarski, C.E., Villen, J., Kornhauser, J.M., Smith, B., Li, D., Zhou, X., Gygi, S.P., Gu, T.L., Polakiewicz, R.D., Rush, J. & Comb, M.J. 2007, "Global survey of phosphotyrosine signaling identifies oncogenic kinases in lung cancer.", *Cell,* vol. 131, no. 6, pp. 1190-1203.

Ritt, D.A., Monson, D.M., Specht, S.I. & Morrison, D.K. 2010a, "Impact of feedback phosphorylation and Raf heterodimerization on normal and mutant B-Raf signaling.", *Molecular & Cellular Biology,* vol. 30, no. 3, pp. 806-819.

Rivera, V.M., Miranti, C.K., Misra, R.P., Ginty, D.D., Chen, R.H., Blenis, J. & Greenberg, M.E. 1993, "A growth factor-induced kinase phosphorylates the serum response factor at a site that regulates its DNA-binding activity.", *Molecular & Cellular Biology,* vol. 13, no. 10, pp. 6260-6273.

Rivett, A.J. & Gardner, R.C. 2000, "Proteasome inhibitors: from in vitro uses to clinical trials", *Journal of Peptide Science,* vol. 6, no. 9, pp. 478-488.

Robbins, D.J., Zhen, E., Owaki, H., Vanderbilt, C.A., Ebert, D., Geppert, T.D. & Cobb, M.H. 1993, "Regulation and properties of extracellular signal-regulated protein kinases 1 and 2 in vitro.", *Journal of Biological Chemistry,* vol. 268, no. 7, pp. 5097-5106.

Robinson, D.R., Wu, Y.M. & Lin, S.F. 2000, "The protein tyrosine kinase family of the human genome", *Oncogene,* vol. 19, no. 49, pp. 5548-5557.

Robinson, M.J. & Cobb, M.H. 1997, "Mitogen-activated protein kinase pathways", *Current opinion in cell biology,* vol. 9, no. 2, pp. 180-186.

Rocks, O., Peyker, A., Kahms, M., Verveer, P.J., Koerner, C., Lumbierres, M., Kuhlmann, J., Waldmann, H., Wittinghofer, A. & Bastiaens, P.I. 2005, "An acylation cycle regulates localization and activity of palmitoylated Ras isoforms.", *Science,* vol. 307, no. 5716, pp. 1746-1752.

Rodenhuis, S., van de Wetering, M.L., Mooi, W.J., Evers, S.G., van Zandwijk, N. & Bos, J.L. 1987, "Mutational activation of the K-ras oncogene. A possible pathogenetic factor in adenocarcinoma of the lung.", *New England Journal of Medicine,* vol. 317, no. 15, pp. 929-935.

Rodier, F. & Campisi, J. 2011, "Four faces of cellular senescence", *Journal of Cell Biology,* vol. 192, no. 4, pp. 547-556.

Rodier, F., Coppe, J.P., Patil, C.K., Hoeijmakers, W.A., Munoz, D.P., Raza, S.R., Freund, A., Campeau, E., Davalos, A.R. & Campisi, J. 2009, "Persistent DNA damage signalling triggers senescence-associated inflammatory cytokine secretion", *Nature cell biology,* vol. 11, no. 8, pp. 973-979.

Rodriguez Fernandez, J.L., Geiger, B., Salomon, D., Sabanay, I., Zoller, M. & Ben-Ze'ev, A. 1992, "Suppression of tumorigenicity in transformed cells after transfection with vinculin cDNA.", *Journal of Cell Biology,* vol. 119, no. 2, pp. 427-438.

Roe, S.M., Ali, M.M., Meyer, P., Vaughan, C.K., Panaretou, B., Piper, P.W., Prodromou, C. & Pearl, L.H. 2004, "The Mechanism of Hsp90 regulation by the protein kinase-specific cochaperone p50(cdc37).", *Cell,* vol. 116, no. 1, pp. 87-98.

Rogakou, E.P., Pilch, D.R., Orr, A.H., Ivanova, V.S. & Bonner, W.M. 1998, "DNA double-stranded breaks induce histone H2AX phosphorylation on serine 139.", *Journal of Biological Chemistry,* vol. 273, no. 10, pp. 5858-5868.

Roskoski, R.,Jr 2012, "MEK1/2 dual-specificity protein kinases: structure and regulation", *Biochemical & Biophysical Research Communications,* vol. 417, no. 1, pp. 5-10.

Rossomando, A.J., Dent, P., Sturgill, T.W. & Marshak, D.R. 1994, "Mitogen-activated protein kinase kinase 1 (MKK1) is negatively regulated by threonine phosphorylation.", *Molecular & Cellular Biology,* vol. 14, no. 3, pp. 1594-1602.

Roux, P.P., Ballif, B.A., Anjum, R., Gygi, S.P. & Blenis, J. 2004, "Tumor-promoting phorbol esters and activated Ras inactivate the tuberous sclerosis tumor suppressor complex via p90 ribosomal S6 kinase.", *Proceedings of the National Academy of Sciences of the United States of America,* vol. 101, no. 37, pp. 13489-13494.

Rudiger, S., Buchberger, A. & Bukau, B. 1997, "Interaction of Hsp70 chaperones with substrates", *Nature structural biology,* vol. 4, no. 5, pp. 342-349.

Rusch, V., Baselga, J., Cordon-Cardo, C., Orazem, J., Zaman, M., Hoda, S., McIntosh, J., Kurie, J. & Dmitrovsky, E. 1993, "Differential expression of the epidermal growth factor receptor and its ligands in primary non-small cell lung cancers and adjacent benign lung.", *Cancer research,* vol. 53, no. 10 Suppl, pp. 2379-2385.

Rushworth, L.K., Hindley, A.D., O'Neill, E. & Kolch, W. 2006a, "Regulation and role of Raf-1/B-Raf heterodimerization.", *Molecular & Cellular Biology,* vol. 26, no. 6, pp. 2262-2272.

Russo, A.A., Jeffrey, P.D., Patten, A.K., Massague, J. & Pavletich, N.P. 1996, "Crystal structure of the p27Kip1 cyclin-dependent-kinase inhibitor bound to the cyclin A-Cdk2 complex.", *Nature,* vol. 382, no. 6589, pp. 325-331.

Russo, A.A., Tong, L., Lee, J.O., Jeffrey, P.D. & Pavletich, N.P. 1998, "Structural basis for inhibition of the cyclin-dependent kinase Cdk6 by the tumour suppressor p16INK4a.", *Nature,* vol. 395, no. 6699, pp. 237-243.

Sansom, O.J., Meniel, V., Wilkins, J.A., Cole, A.M., Oien, K.A., Marsh, V., Jamieson, T.J., Guerra, C., Ashton, G.H., Barbacid, M. & Clarke, A.R. 2006, "Loss of Apc allows phenotypic manifestation of the transforming properties of an endogenous K-ras oncogene in vivo.", *Proceedings of the National Academy of Sciences of the United States of America,* vol. 103, no. 38, pp. 14122-14127.

Sarkisian, C.J., Keister, B.A., Stairs, D.B., Boxer, R.B., Moody, S.E. & Chodosh, L.A. 2007, "Dose-dependent oncogene-induced senescence in vivo and its evasion during mammary tumorigenesis.", *Nature cell biology,* vol. 9, no. 5, pp. 493-505.

Sasaki, A., Taketomi, T., Kato, R., Saeki, K., Nonami, A., Sasaki, M., Kuriyama, M., Saito, N., Shibuya, M. & Yoshimura, A. 2003, "Mammalian Sprouty4 suppresses Ras-independent ERK activation by binding to Raf1", *Cell Cycle,* vol. 2, no. 4, pp. 281-282.

Sasaki, A., Taketomi, T., Wakioka, T., Kato, R. & Yoshimura, A. 2001, "Identification of a dominant negative mutant of Sprouty that potentiates fibroblast growth factor- but not epidermal growth factor-induced ERK activation.", *Journal of Biological Chemistry,* vol. 276, no. 39, pp. 36804-36808.

Schaeffer, H.J., Catling, A.D., Eblen, S.T., Collier, L.S., Krauss, A. & Weber, M.J. 1998, "MP1: a MEK binding partner that enhances enzymatic activation of the MAP kinase cascade.", *Science,* vol. 281, no. 5383, pp. 1668-1671.

Scheffler, J.E., Waugh, D.S., Bekesi, E., Kiefer, S.E., LoSardo, J.E., Neri, A., Prinzo, K.M., Tsao, K.L., Wegrzynski, B. & Emerson, S.D. 1994, "Characterization of a 78-residue fragment of c-Raf-1 that comprises a minimal binding domain for the interaction with Ras-GTP.", *Journal of Biological Chemistry,* vol. 269, no. 35, pp. 22340-22346.

Scheffzek, K., Ahmadian, M.R., Kabsch, W., Wiesmuller, L., Lautwein, A., Schmitz, F. & Wittinghofer, A. 1997, "The Ras-RasGAP complex: structural basis for GTPase activation and its loss in oncogenic Ras mutants.", *Science,* vol. 277, no. 5324, pp. 333-338.

Schlessinger, J. 2000, "Cell signaling by receptor tyrosine kinases", *Cell,* vol. 103, no. 2, pp. 211-225.

Schlessinger, J. & Lemmon, M.A. 2003, "SH2 and PTB domains in tyrosine kinase signaling", *Science's Stke [Electronic Resource]: Signal Transduction Knowledge Environment,* vol. 2003, no. 191, pp. RE12.

Schulte, T.W., An, W.G. & Neckers, L.M. 1997, "Geldanamycin-induced destabilization of Raf-1 involves the proteasome.", *Biochemical & Biophysical Research Communications,* vol. 239, no. 3, pp. 655-659.

Schulte, T.W., Blagosklonny, M.V., Ingui, C. & Neckers, L. 1995, "Disruption of the Raf-1-Hsp90 molecular complex results in destabilization of Raf-1 and loss of Raf-1-Ras association.", *Journal of Biological Chemistry,* vol. 270, no. 41, pp. 24585-24588.

Schwartzberg, P.L., Goff, S.P. & Robertson, E.J. 1989, "Germ-line transmission of a c-abl mutation produced by targeted gene disruption in ES cells.", *Science,* vol. 246, no. 4931, pp. 799-803.

Sears, R., Nuckolls, F., Haura, E., Taya, Y., Tamai, K. & Nevins, J.R. 2000, "Multiple Ras-dependent phosphorylation pathways regulate Myc protein stability.", *Genes & development,* vol. 14, no. 19, pp. 2501-2514.

Sebolt-Leopold, J.S., Dudley, D.T., Herrera, R., Van Becelaere, K., Wiland, A., Gowan, R.C., Tecle, H., Barrett, S.D., Bridges, A., Przybranowski, S., Leopold, W.R. & Saltiel, A.R. 1999, "Blockade of the MAP kinase pathway suppresses growth of colon tumors in vivo.", *Nature medicine,* vol. 5, no. 7, pp. 810-816.

Sedelnikova, O.A., Horikawa, I., Zimonjic, D.B., Popescu, N.C., Bonner, W.M. & Barrett, J.C. 2004, "Senescing human cells and ageing mice accumulate DNA lesions with unrepairable double-strand breaks.", *Nature cell biology,* vol. 6, no. 2, pp. 168-170.

Seeburg, P.H., Colby, W.W., Capon, D.J., Goeddel, D.V. & Levinson, A.D. 1984, "Biological properties of human c-Ha-ras1 genes mutated at codon 12.", *Nature,* vol. 312, no. 5989, pp. 71-75.

Seet, B.T., Dikic, I., Zhou, M.M. & Pawson, T. 2006, "Reading protein modifications with interaction domains", *Nature Reviews Molecular Cell Biology,* vol. 7, no. 7, pp. 473-483.

Sengupta, S., Peterson, T.R. & Sabatini, D.M. 2010, "Regulation of the mTOR complex 1 pathway by nutrients, growth factors, and stress", *Molecular cell,* vol. 40, no. 2, pp. 310-322.

Seoane, J., Pouponnot, C., Staller, P., Schader, M., Eilers, M. & Massague, J. 2001, "TGFbeta influences Myc, Miz-1 and Smad to control the CDK inhibitor p15INK4b.", *Nature cell biology,* vol. 3, no. 4, pp. 400-408.

Serrano, M., Lin, A.W., McCurrach, M.E., Beach, D. & Lowe, S.W. 1997, "Oncogenic ras provokes premature cell senescence associated with accumulation of p53 and p16INK4a.", *Cell,* vol. 88, no. 5, pp. 593-602.

Shapiro, P.S. & Ahn, N.G. 1998, "Feedback regulation of Raf-1 and mitogen-activated protein kinase (MAP) kinase kinases 1 and 2 by MAP kinase phosphatase-1 (MKP-1).", *Journal of Biological Chemistry,* vol. 273, no. 3, pp. 1788-1793.

Sharp, S. & Workman, P. 2006, "Inhibitors of the HSP90 molecular chaperone: current status", *Advances in Cancer Research,* vol. 95, pp. 323-348.

Sharpless, N.E. & DePinho, R.A. 2005, "Cancer: crime and punishment.", *Nature,* vol. 436, no. 7051, pp. 636-637.

Sharrocks, A.D., Yang, S.H. & Galanis, A. 2000, "Docking domains and substrate-specificity determination for MAP kinases", *Trends in biochemical sciences,* vol. 25, no. 9, pp. 448-453.

Shaw, A.T., Meissner, A., Dowdle, J.A., Crowley, D., Magendantz, M., Ouyang, C., Parisi, T., Rajagopal, J., Blank, L.J., Bronson, R.T., Stone, J.R., Tuveson, D.A., Jaenisch, R. & Jacks, T. 2007, "Sprouty-2 regulates oncogenic K-ras in lung development and tumorigenesis", *Genes & development,* vol. 21, no. 6, pp. 694-707.

Shay, J.W., Pereira-Smith, O.M. & Wright, W.E. 1991, "A role for both RB and p53 in the regulation of human cellular senescence.", *Experimental cell research,* vol. 196, no. 1, pp. 33-39.

Shen, W. & Ganetzky, B. 2009, "Autophagy promotes synapse development in Drosophila.", *Journal of Cell Biology,* vol. 187, no. 1, pp. 71-79.

Shenoy, K., Wu, Y. & Pervaiz, S. 2009, "LY303511 enhances TRAIL sensitivity of SHEP-1 neuroblastoma cells via hydrogen peroxide-mediated mitogen-activated protein kinase activation and up-regulation of death receptors.", *Cancer research,* vol. 69, no. 5, pp. 1941-1950.

Sherr, C.J. 1994, "Growth factor-regulated G1 cyclins", *Stem cells,* vol. 12, no. Suppl 1, pp. 47-55.

Sherr, C.J., Kato, J., Quelle, D.E., Matsuoka, M. & Roussel, M.F. 1994, "D-type cyclins and their cyclin-dependent kinases: G1 phase integrators of the mitogenic response", *Cold Spring Harbor symposia on quantitative biology,* vol. 59, pp. 11-19.

Sherr, C.J. & Roberts, J.M. 1999, "CDK inhibitors: positive and negative regulators of G1-phase progression", *Genes & development,* vol. 13, no. 12, pp. 1501-1512.

Shimamura, A., Ballif, B.A., Richards, S.A. & Blenis, J. 2000, "Rsk1 mediates a MEK-MAP kinase cell survival signal.", *Current Biology,* vol. 10, no. 3, pp. 127-135.

Shimizu, K., Goldfarb, M., Perucho, M. & Wigler, M. 1983, "Isolation and preliminary characterization of the transforming gene of a human neuroblastoma cell line.", *Proceedings of the National Academy of Sciences of the United States of America,* vol. 80, no. 2, pp. 383-387.

Shinojima, N., Yokoyama, T., Kondo, Y. & Kondo, S. 2007, "Roles of the Akt/mTOR/p70S6K and ERK1/2 signaling pathways in curcumin-induced autophagy.", *Autophagy,* vol. 3, no. 6, pp. 635-637.

Sivaprasad, U. & Basu, A. 2008, "Inhibition of ERK attenuates autophagy and potentiates tumour necrosis factor-alpha-induced cell death in MCF-7 cells.", *Journal of Cellular & Molecular Medicine,* vol. 12, no. 4, pp. 1265-1271.

Skolnik, E.Y., Lee, C.H., Batzer, A., Vicentini, L.M., Zhou, M., Daly, R., Myers, M.J.,Jr, Backer, J.M., Ullrich, A. & White, M.F. 1993, "The SH2/SH3 domain-containing protein GRB2 interacts with tyrosine-phosphorylated IRS1 and Shc: implications for insulin control of ras signalling.", *EMBO Journal,* vol. 12, no. 5, pp. 1929-1936.

Smit, V.T., Boot, A.J., Smits, A.M., Fleuren, G.J., Cornelisse, C.J. & Bos, J.L. 1988, "KRAS codon 12 mutations occur very frequently in pancreatic adenocarcinomas.", *Nucleic acids research,* vol. 16, no. 16, pp. 7773-7782.

Sobering, A.K., Romeo, M.J., Vay, H.A. & Levin, D.E. 2003, "A novel Ras inhibitor, Eri1, engages yeast Ras at the endoplasmic reticulum.", *Molecular & Cellular Biology,* vol. 23, no. 14, pp. 4983-4990.

Solit, D.B., Garraway, L.A., Pratilas, C.A., Sawai, A., Getz, G., Basso, A., Ye, Q., Lobo, J.M., She, Y., Osman, I., Golub, T.R., Sebolt-Leopold, J., Sellers, W.R. & Rosen, N. 2006, "BRAF mutation predicts sensitivity to MEK inhibition.", *Nature,* vol. 439, no. 7074, pp. 358-362.

Soloaga, A., Thomson, S., Wiggin, G.R., Rampersaud, N., Dyson, M.H., Hazzalin, C.A., Mahadevan, L.C. & Arthur, J.S. 2003, "MSK2 and MSK1 mediate the mitogen- and stress-induced phosphorylation of histone H3 and HMG-14.", *EMBO Journal,* vol. 22, no. 11, pp. 2788-2797.

Steen, H., Jebanathirajah, J.A., Rush, J., Morrice, N. & Kirschner, M.W. 2006, "Phosphorylation analysis by mass spectrometry: myths, facts, and the consequences for qualitative and quantitative measurements.", *Molecular & Cellular Proteomics,* vol. 5, no. 1, pp. 172-181.

Stennicke, H.R., Jurgensmeier, J.M., Shin, H., Deveraux, Q., Wolf, B.B., Yang, X., Zhou, Q., Ellerby, H.M., Ellerby, L.M., Bredesen, D., Green, D.R., Reed, J.C., Froelich, C.J. & Salvesen, G.S. 1998, "Pro-caspase-3 is a major physiologic target of caspase-8.", *Journal of Biological Chemistry,* vol. 273, no. 42, pp. 27084-27090.

Stephens, R.M., Sithanandam, G., Copeland, T.D., Kaplan, D.R., Rapp, U.R. & Morrison, D.K. 1992, "95-kilodalton B-Raf serine/threonine kinase: identification of the protein and its major autophosphorylation site.", *Molecular & Cellular Biology,* vol. 12, no. 9, pp. 3733-3742.

Storm, S.M., Cleveland, J.L. & Rapp, U.R. 1990, "Expression of raf family proto-oncogenes in normal mouse tissues.", *Oncogene,* vol. 5, no. 3, pp. 345-351.

Su, C.H., Wang, C.Y., Lan, K.H., Li, C.P., Chao, Y., Lin, H.C., Lee, S.D. & Lee, W.P. 2011a, "Akt phosphorylation at Thr308 and Ser473 is required for CHIP-mediated ubiquitination of the kinase.", *Cellular signalling,* vol. 23, no. 11, pp. 1824-1830.

Su, F., Viros, A., Milagre, C., Trunzer, K., Bollag, G., Spleiss, O., Reis-Filho, J.S., Kong, X., Koya, R.C., Flaherty, K.T., Chapman, P.B., Kim, M.J., Hayward, R., Martin, M., Yang, H., Wang, Q., Hilton, H., Hang, J.S., Noe, J., Lambros, M., Geyer, F., Dhomen, N., Niculescu-Duvaz, I., Zambon, A., Niculescu-Duvaz, D., Preece, N., Robert, L., Otte, N.J., Mok, S., Kee, D., Ma, Y., Zhang, C., Habets, G., Burton, E.A.,

Wong, B., Nguyen, H., Kockx, M., Andries, L., Lestini, B., Nolop, K.B., Lee, R.J., Joe, A.K., Troy, J.L., Gonzalez, R., Hutson, T.E., Puzanov, I., Chmielowski, B., Springer, C.J., McArthur, G.A., Sosman, J.A., Lo, R.S., Ribas, A. & Marais, R. 2012, "RAS mutations in cutaneous squamous-cell carcinomas in patients treated with BRAF inhibitors.", *New England Journal of Medicine,* vol. 366, no. 3, pp. 207-215.

Sun, Y., Jiang, X., Chen, S., Fernandes, N. & Price, B.D. 2005, "A role for the Tip60 histone acetyltransferase in the acetylation and activation of ATM.", *Proceedings of the National Academy of Sciences of the United States of America,* vol. 102, no. 37, pp. 13182-13187.

Suzuki, K., Kirisako, T., Kamada, Y., Mizushima, N., Noda, T. & Ohsumi, Y. 2001, "The pre-autophagosomal structure organized by concerted functions of APG genes is essential for autophagosome formation.", *EMBO Journal,* vol. 20, no. 21, pp. 5971-5981.

Suzuki, K. & Ohsumi, Y. 2010, "Current knowledge of the pre-autophagosomal structure (PAS)", *FEBS letters,* vol. 584, no. 7, pp. 1280-1286.

Suzuki, K. & Ohsumi, Y. 2007, "Molecular machinery of autophagosome formation in yeast, Saccharomyces cerevisiae.", *FEBS letters,* vol. 581, no. 11, pp. 2156-2161.

Takahashi, T., Yamaguchi, S., Chida, K. & Shibuya, M. 2001, "A single autophosphorylation site on KDR/Flk-1 is essential for VEGF-A-dependent activation of PLC-gamma and DNA synthesis in vascular endothelial cells.", *EMBO Journal,* vol. 20, no. 11, pp. 2768-2778.

Takai, H., Naka, K., Okada, Y., Watanabe, M., Harada, N., Saito, S., Anderson, C.W., Appella, E., Nakanishi, M., Suzuki, H., Nagashima, K., Sawa, H., Ikeda, K. & Motoyama, N. 2002, "Chk2-deficient mice exhibit radioresistance and defective p53-mediated transcription.", *EMBO Journal,* vol. 21, no. 19, pp. 5195-5205.

Takeshige, K., Baba, M., Tsuboi, S., Noda, T. & Ohsumi, Y. 1992, "Autophagy in yeast demonstrated with proteinase-deficient mutants and conditions for its induction.", *Journal of Cell Biology,* vol. 119, no. 2, pp. 301-311.

Takezawa, K., Okamoto, I., Yonesaka, K., Hatashita, E., Yamada, Y., Fukuoka, M. & Nakagawa, K. 2009, "Sorafenib inhibits non-small cell lung cancer cell growth by targeting B-RAF in KRAS wild-type cells and C-RAF in KRAS mutant cells.", *Cancer research,* vol. 69, no. 16, pp. 6515-6521.

Tang, D., Wu, D., Hirao, A., Lahti, J.M., Liu, L., Mazza, B., Kidd, V.J., Mak, T.W. & Ingram, A.J. 2002, "ERK activation mediates cell cycle arrest and apoptosis after DNA damage independently of p53.", *Journal of Biological Chemistry,* vol. 277, no. 15, pp. 12710-12717.

Taniguchi, K., Kohno, R., Ayada, T., Kato, R., Ichiyama, K., Morisada, T., Oike, Y., Yonemitsu, Y., Maehara, Y. & Yoshimura, A. 2007, "Spreds are essential for embryonic lymphangiogenesis by regulating vascular endothelial growth factor receptor 3 signaling.", *Molecular & Cellular Biology,* vol. 27, no. 12, pp. 4541-4550.

Tanoue, T., Adachi, M., Moriguchi, T. & Nishida, E. 2000, "A conserved docking motif in MAP kinases common to substrates, activators and regulators.", *Nature cell biology,* vol. 2, no. 2, pp. 110-116.

Teis, D., Wunderlich, W. & Huber, L.A. 2002, "Localization of the MP1-MAPK scaffold complex to endosomes is mediated by p14 and required for signal transduction.", *Developmental Cell,* vol. 3, no. 6, pp. 803-814.

Terasawa, K., Minami, M. & Minami, Y. 2005, "Constantly updated knowledge of Hsp90", *Journal of Biochemistry,* vol. 137, no. 4, pp. 443-447.

Tewari, R., Sharma, V., Koul, N. & Sen, E. 2008, "Involvement of miltefosine-mediated ERK activation in glioma cell apoptosis through Fas regulation.", *Journal of neurochemistry,* vol. 107, no. 3, pp. 616-627.

Thyagarajan, B., Guimaraes, M.J., Groth, A.C. & Calos, M.P. 2000, "Mammalian genomes contain active recombinase recognition sites.", *Gene,* vol. 244, no. 1-2, pp. 47-54.

Tian, T., Harding, A., Inder, K., Plowman, S., Parton, R.G. & Hancock, J.F. 2007, "Plasma membrane nanoswitches generate high-fidelity Ras signal transduction.", *Nature cell biology,* vol. 9, no. 8, pp. 905-914.

Tompers, D.M. & Labosky, P.A. 2004, "Electroporation of murine embryonic stem cells: a step-by-step guide", *Stem cells,* vol. 22, no. 3, pp. 243-249.

Tran, N.H., Wu, X. & Frost, J.A. 2005, "B-Raf and Raf-1 are regulated by distinct autoregulatory mechanisms.", *Journal of Biological Chemistry,* vol. 280, no. 16, pp. 16244-16253.

Tsai, J., Lee, J.T., Wang, W., Zhang, J., Cho, H., Mamo, S., Bremer, R., Gillette, S., Kong, J., Haass, N.K., Sproesser, K., Li, L., Smalley, K.S., Fong, D., Zhu, Y.L., Marimuthu, A., Nguyen, H., Lam, B., Liu, J., Cheung, I., Rice, J., Suzuki, Y., Luu, C., Settachatgul, C., Shellooe, R., Cantwell, J., Kim, S.H., Schlessinger, J., Zhang, K.Y., West, B.L., Powell, B., Habets, G., Zhang, C., Ibrahim, P.N., Hirth, P., Artis, D.R., Herlyn, M. & Bollag, G. 2008a, "Discovery of a selective inhibitor of oncogenic B-Raf kinase with potent antimelanoma activity.", *Proceedings of the National Academy of Sciences of the United States of America,* vol. 105, no. 8, pp. 3041-3046.

Tsavachidou, D., Coleman, M.L., Athanasiadis, G., Li, S., Licht, J.D., Olson, M.F. & Weber, B.L. 2004, "SPRY2 is an inhibitor of the ras/extracellular signal-regulated kinase pathway in melanocytes and melanoma cells with wild-type BRAF but not with the V599E mutant.", *Cancer research,* vol. 64, no. 16, pp. 5556-5559.

Tuveson, D.A., Shaw, A.T., Willis, N.A., Silver, D.P., Jackson, E.L., Chang, S., Mercer, K.L., Grochow, R., Hock, H., Crowley, D., Hingorani, S.R., Zaks, T., King, C., Jacobetz, M.A., Wang, L., Bronson, R.T., Orkin, S.H., DePinho, R.A. & Jacks, T. 2004, "Endogenous oncogenic K-ras(G12D) stimulates proliferation and widespread neoplastic and developmental defects.", *Cancer Cell,* vol. 5, no. 4, pp. 375-387.

Ulisse, S., Cinque, B., Silvano, G., Rucci, N., Biordi, L., Cifone, M.G. & D'Armiento, M. 2000, "Erk-dependent cytosolic phospholipase A2 activity is induced by CD95 ligand cross-linking in the mouse derived Sertoli cell line TM4 and is required to trigger apoptosis in CD95 bearing cells.", *Cell Death & Differentiation,* vol. 7, no. 10, pp. 916-924.

Vakkila, J. & Lotze, M.T. 2004, "Inflammation and necrosis promote tumour growth.", *Nature Reviews.Immunology,* vol. 4, no. 8, pp. 641-648.

Vetter, I.R. & Wittinghofer, A. 2001, "The guanine nucleotide-binding switch in three dimensions", *Science,* vol. 294, no. 5545, pp. 1299-1304.

Vik, T.A. & Ryder, J.W. 1997, "Identification of serine 380 as the major site of autophosphorylation of Xenopus pp90rsk.", *Biochemical & Biophysical Research Communications,* vol. 235, no. 2, pp. 398-402.

Villanueva, J., Vultur, A., Lee, J.T., Somasundaram, R., Fukunaga-Kalabis, M., Cipolla, A.K., Wubbenhorst, B., Xu, X., Gimotty, P.A., Kee, D., Santiago-Walker, A.E., Letrero, R., D'Andrea, K., Pushparajan, A., Hayden, J.E., Brown, K.D., Laquerre, S., McArthur, G.A., Sosman, J.A., Nathanson, K.L. & Herlyn, M. 2010, "Acquired resistance to BRAF inhibitors mediated by a RAF kinase switch in melanoma can be overcome by cotargeting MEK and IGF-1R/PI3K.", *Cancer Cell,* vol. 18, no. 6, pp. 683-695.

Voice, J.K., Klemke, R.L., Le, A. & Jackson, J.H. 1999, "Four human ras homologs differ in their abilities to activate Raf-1, induce transformation, and stimulate cell motility.", *Journal of Biological Chemistry,* vol. 274, no. 24, pp. 17164-17170.

von Kriegsheim, A., Pitt, A., Grindlay, G.J., Kolch, W. & Dhillon, A.S. 2006, "Regulation of the Raf-MEK-ERK pathway by protein phosphatase 5.", *Nature cell biology,* vol. 8, no. 9, pp. 1011-1016.

Vousden, K.H. & Prives, C. 2009, "Blinded by the Light: The Growing Complexity of p53", *Cell,* vol. 137, no. 3, pp. 413-431.

Voziyanov, Y., Pathania, S. & Jayaram, M. 1999, "A general model for site-specific recombination by the integrase family recombinases.", *Nucleic acids research,* vol. 27, no. 4, pp. 930-941.

Wagle, N., Emery, C., Berger, M.F., Davis, M.J., Sawyer, A., Pochanard, P., Kehoe, S.M., Johannessen, C.M., Macconaill, L.E., Hahn, W.C., Meyerson, M. & Garraway, L.A. 2011, "Dissecting therapeutic resistance to RAF inhibition in melanoma by tumor genomic profiling.", *Journal of Clinical Oncology,* vol. 29, no. 22, pp. 3085-3096.

Wakioka, T., Sasaki, A., Kato, R., Shouda, T., Matsumoto, A., Miyoshi, K., Tsuneoka, M., Komiya, S., Baron, R. & Yoshimura, A. 2001, "Spred is a Sprouty-related suppressor of Ras signalling.", *Nature,* vol. 412, no. 6847, pp. 647-651.

Wan, P.T., Garnett, M.J., Roe, S.M., Lee, S., Niculescu-Duvaz, D., Good, V.M., Jones, C.M., Marshall, C.J., Springer, C.J., Barford, D., Marais, R. & Cancer Genome,

P. 2004a, "Mechanism of activation of the RAF-ERK signaling pathway by oncogenic mutations of B-RAF.", *Cell,* vol. 116, no. 6, pp. 855-867.

Wandinger, S.K., Richter, K. & Buchner, J. 2008, "The Hsp90 chaperone machinery", *Journal of Biological Chemistry,* vol. 283, no. 27, pp. 18473-18477.

Wang, J., Whiteman, M.W., Lian, H., Wang, G., Singh, A., Huang, D. & Denmark, T. 2009, "A non-canonical MEK/ERK signaling pathway regulates autophagy via regulating Beclin 1.", *Journal of Biological Chemistry,* vol. 284, no. 32, pp. 21412-21424.

Wang, S. & Shi, X. 2001, "Mechanisms of Cr(VI)-induced p53 activation: the role of phosphorylation, mdm2 and ERK.", *Carcinogenesis,* vol. 22, no. 5, pp. 757-762.

Ward, I.M., Minn, K., van Deursen, J. & Chen, J. 2003, "p53 Binding protein 53BP1 is required for DNA damage responses and tumor suppression in mice.", *Molecular & Cellular Biology,* vol. 23, no. 7, pp. 2556-2563.

Wei, M.C., Lindsten, T., Mootha, V.K., Weiler, S., Gross, A., Ashiya, M., Thompson, C.B. & Korsmeyer, S.J. 2000, "tBID, a membrane-targeted death ligand, oligomerizes BAK to release cytochrome c.", *Genes & development,* vol. 14, no. 16, pp. 2060-2071.

Wei, W., Mosteller, R.D., Sanyal, P., Gonzales, E., McKinney, D., Dasgupta, C., Li, P., Liu, B.X. & Broek, D. 1992, "Identification of a mammalian gene structurally and functionally related to the CDC25 gene of Saccharomyces cerevisiae.", *Proceedings of the National Academy of Sciences of the United States of America,* vol. 89, no. 15, pp. 7100-7104.

Weintraub, S.J., Chow, K.N., Luo, R.X., Zhang, S.H., He, S. & Dean, D.C. 1995, "Mechanism of active transcriptional repression by the retinoblastoma protein.", *Nature,* vol. 375, no. 6534, pp. 812-815.

Weissman, A.M. 2001, "Themes and variations on ubiquitylation", *Nature Reviews Molecular Cell Biology,* vol. 2, no. 3, pp. 169-178.

Wellbrock, C., Karasarides, M. & Marais, R. 2004, "The RAF proteins take centre stage", *Nature Reviews Molecular Cell Biology,* vol. 5, no. 11, pp. 875-885.

Wellbrock, C., Ogilvie, L., Hedley, D., Karasarides, M., Martin, J., Niculescu-Duvaz, D., Springer, C.J. & Marais, R. 2004, "V599EB-RAF is an oncogene in melanocytes.", *Cancer research,* vol. 64, no. 7, pp. 2338-2342.

Weston, C.R., Balmanno, K., Chalmers, C., Hadfield, K., Molton, S.A., Ley, R., Wagner, E.F. & Cook, S.J. 2003, "Activation of ERK1/2 by deltaRaf-1:ER* represses Bim expression independently of the JNK or PI3K pathways.", *Oncogene,* vol. 22, no. 9, pp. 1281-1293.

Whitesell, L. & Lindquist, S.L. 2005, "HSP90 and the chaperoning of cancer", *Nature Reviews.Cancer,* vol. 5, no. 10, pp. 761-772.

Whitmarsh, A.J., Shore, P., Sharrocks, A.D. & Davis, R.J. 1995, "Integration of MAP kinase signal transduction pathways at the serum response element.", *Science,* vol. 269, no. 5222, pp. 403-407.

Widmann, C., Gibson, S., Jarpe, M.B. & Johnson, G.L. 1999, "Mitogen-activated protein kinase: conservation of a three-kinase module from yeast to human", *Physiological Reviews,* vol. 79, no. 1, pp. 143-180.

Willmore-Payne, C., Holden, J.A. & Layfield, L.J. 2006, "Detection of EGFR- and HER2-activating mutations in squamous cell carcinoma involving the head and neck.", *Modern Pathology,* vol. 19, no. 5, pp. 634-640.

Winter, S., Simboeck, E., Fischle, W., Zupkovitz, G., Dohnal, I., Mechtler, K., Ammerer, G. & Seiser, C. 2008, "14-3-3 proteins recognize a histone code at histone H3 and are required for transcriptional activation.", *EMBO Journal,* vol. 27, no. 1, pp. 88-99.

Wong, E.S., Lim, J., Low, B.C., Chen, Q. & Guy, G.R. 2001, "Evidence for direct interaction between Sprouty and Cbl.", *Journal of Biological Chemistry,* vol. 276, no. 8, pp. 5866-5875.

Woods, D., Parry, D., Cherwinski, H., Bosch, E., Lees, E. & McMahon, M. 1997, "Raf-induced proliferation or cell cycle arrest is determined by the level of Raf activity with arrest mediated by p21Cip1.", *Molecular & Cellular Biology,* vol. 17, no. 9, pp. 5598-5611.

Wright, W.E., Piatyszek, M.A., Rainey, W.E., Byrd, W. & Shay, J.W. 1996, "Telomerase activity in human germline and embryonic tissues and cells.", *Developmental genetics,* vol. 18, no. 2, pp. 173-179.

Wu, J. & Janknecht, R. 2002, "Regulation of the ETS transcription factor ER81 by the 90-kDa ribosomal S6 kinase 1 and protein kinase A.", *Journal of Biological Chemistry,* vol. 277, no. 45, pp. 42669-42679.

Wu, S., Cetinkaya, C., Munoz-Alonso, M.J., von der Lehr, N., Bahram, F., Beuger, V., Eilers, M., Leon, J. & Larsson, L.G. 2003, "Myc represses differentiation-induced p21CIP1 expression via Miz-1-dependent interaction with the p21 core promoter.", *Oncogene,* vol. 22, no. 3, pp. 351-360.

Wullschleger, S., Loewith, R. & Hall, M.N. 2006, "TOR signaling in growth and metabolism", *Cell,* vol. 124, no. 3, pp. 471-484.

Xiong, Y., Hannon, G.J., Zhang, H., Casso, D., Kobayashi, R. & Beach, D. 1993, "p21 is a universal inhibitor of cyclin kinases.", *Nature,* vol. 366, no. 6456, pp. 701-704.

Xu, C., Kim, N.G. & Gumbiner, B.M. 2009, "Regulation of protein stability by GSK3 mediated phosphorylation.", *Cell Cycle,* vol. 8, no. 24, pp. 4032-4039.

Xue, W., Zender, L., Miething, C., Dickins, R.A., Hernando, E., Krizhanovsky, V., Cordon-Cardo, C. & Lowe, S.W. 2007, "Senescence and tumour clearance is

triggered by p53 restoration in murine liver carcinomas", *Nature,* vol. 445, no. 7128, pp. 656-660.

Yang, J.Y., Zong, C.S., Xia, W., Yamaguchi, H., Ding, Q., Xie, X., Lang, J.Y., Lai, C.C., Chang, C.J., Huang, W.C., Huang, H., Kuo, H.P., Lee, D.F., Li, L.Y., Lien, H.C., Cheng, X., Chang, K.J., Hsiao, C.D., Tsai, F.J., Tsai, C.H., Sahin, A.A., Muller, W.J., Mills, G.B., Yu, D., Hortobagyi, G.N. & Hung, M.C. 2008, "ERK promotes tumorigenesis by inhibiting FOXO3a via MDM2-mediated degradation", *Nature cell biology,* vol. 10, no. 2, pp. 138-148.

Yook, J.I., Li, X.Y., Ota, I., Fearon, E.R. & Weiss, S.J. 2005, "Wnt-dependent regulation of the E-cadherin repressor snail.", *Journal of Biological Chemistry,* vol. 280, no. 12, pp. 11740-11748.

Yoon, S. & Seger, R. 2006, "The extracellular signal-regulated kinase: multiple substrates regulate diverse cellular functions", *Growth Factors,* vol. 24, no. 1, pp. 21-44.

Young, A.R., Chan, E.Y., Hu, X.W., Kochl, R., Crawshaw, S.G., High, S., Hailey, D.W., Lippincott-Schwartz, J. & Tooze, S.A. 2006, "Starvation and ULK1-dependent cycling of mammalian Atg9 between the TGN and endosomes.", *Journal of cell science,* vol. 119, no. Pt 18, pp. 3888-3900.

Young, A.R., Narita, M., Ferreira, M., Kirschner, K., Sadaie, M., Darot, J.F., Tavare, S., Arakawa, S., Shimizu, S., Watt, F.M. & Narita, M. 2009, "Autophagy mediates the mitotic senescence transition.", *Genes & development,* vol. 23, no. 7, pp. 798-803.

Young, K., Minchom, A. & Larkin, J. 2012, "BRIM-1, -2 and -3 trials: improved survival with vemurafenib in metastatic melanoma patients with a BRAF(V600E) mutation.", *Future Oncology,* vol. 8, no. 5, pp. 499-507.

Zeh, H.J.,3rd & Lotze, M.T. 2005, "Addicted to death: invasive cancer and the immune response to unscheduled cell death", *Journal of Immunotherapy,* vol. 28, no. 1, pp. 1-9.

Zehorai, E., Yao, Z., Plotnikov, A. & Seger, R. 2010, "The subcellular localization of MEK and ERK--a novel nuclear translocation signal (NTS) paves a way to the nucleus", *Molecular & Cellular Endocrinology,* vol. 314, no. 2, pp. 213-220.

Zhang, B.H. & Guan, K.L. 2000, "Activation of B-Raf kinase requires phosphorylation of the conserved residues Thr598 and Ser601.", *EMBO Journal,* vol. 19, no. 20, pp. 5429-5439.

Zhang, B.H., Tang, E.D., Zhu, T., Greenberg, M.E., Vojtek, A.B. & Guan, K.L. 2001, "Serum- and glucocorticoid-inducible kinase SGK phosphorylates and negatively regulates B-Raf.", *Journal of Biological Chemistry,* vol. 276, no. 34, pp. 31620-31626.

Zhang, F.L. & Casey, P.J. 1996, "Protein prenylation: molecular mechanisms and functional consequences", *Annual Review of Biochemistry,* vol. 65, pp. 241-269.

Zhang, Z., Kobayashi, S., Borczuk, A.C., Leidner, R.S., Laframboise, T., Levine, A.D. & Halmos, B. 2010, "Dual specificity phosphatase 6 (DUSP6) is an ETS-regulated negative feedback mediator of oncogenic ERK signaling in lung cancer cells.", *Carcinogenesis,* vol. 31, no. 4, pp. 577-586.

Zheng, C.F. & Guan, K.L. 1994, "Activation of MEK family kinases requires phosphorylation of two conserved Ser/Thr residues.", *EMBO Journal,* vol. 13, no. 5, pp. 1123-1131.

Zhou, G., Bao, Z.Q. & Dixon, J.E. 1995, "Components of a new human protein kinase signal transduction pathway.", *Journal of Biological Chemistry,* vol. 270, no. 21, pp. 12665-12669.

Zhou, T., Sun, L., Humphreys, J. & Goldsmith, E.J. 2006, "Docking interactions induce exposure of activation loop in the MAP kinase ERK2.", *Structure,* vol. 14, no. 6, pp. 1011-1019.

Zhu, J.H., Horbinski, C., Guo, F., Watkins, S., Uchiyama, Y. & Chu, C.T. 2007, "Regulation of autophagy by extracellular signal-regulated protein kinases during 1-methyl-4-phenylpyridinium-induced cell death.", *American Journal of Pathology,* vol. 170, no. 1, pp. 75-86.

Zimmermann, S. & Moelling, K. 1999, "Phosphorylation and regulation of Raf by Akt (protein kinase B).", *Science,* vol. 286, no. 5445, pp. 1741-1744.

Zoncu, R., Efeyan, A. & Sabatini, D.M. 2011, "mTOR: from growth signal integration to cancer, diabetes and ageing", *Nature Reviews Molecular Cell Biology,* vol. 12, no. 1, pp. 21-35.

Zuniga, A., Torres, J., Ubeda, J. & Pulido, R. 1999, "Interaction of mitogen-activated protein kinases with the kinase interaction motif of the tyrosine phosphatase PTP-SL provides substrate specificity and retains ERK2 in the cytoplasm.", *Journal of Biological Chemistry,* vol. 274, no. 31, pp. 21900-21907.